Spatial control of nucleoporin condensation by Fragile X-related proteins

Arantxa Agote Arán

UNIVERSITÉ DE STRASBOURG

ÉCOLE DOCTORALE 414 – Sciences de la vie et de la santé

Institut de Génétique et de Biologie Moléculaire et Cellulaire

CNRS UMR 7104 – INSERM U 964

THÈSE

présentée par:

Arantxa AGOTE ARÁN

Soutenue le: **06 novembre 2020**

Pour obtenir le grade de:

Docteur de l'université de Strasbourg

Discipline / Spécialité : Aspects moléculaires et cellulaires de la biologie

Spatial control of nucleoporin condensation by Fragile X-related proteins

THÈSE dirigée par :

Mme SUMARA Izabela, PhD — Directeur de recherche (DR2), CNRS

RAPPORTEURS:

Mme OLIFERENKO Snezhana, PhD — Professor of Evolutionary Cell Biology, King's College London

M PINTARD Lionel, PhD — Directeur de recherche (DR1), CNRS

AUTRES MEMBRES DU JURY:

M BARRAL Yves, PhD — Full Professor of Biochemistry, ETH Zurich

M CHARLET-BERGUERAND Nicolas, PhD — Directeur de recherche (DR2), INSERM

Acknowledgments

I was told to write the acknowledgments before the whole manuscript. I was warned and here I am the, 'printing eve', trying to put memories and thoughts together to extract the non-data side I of this beautiful PhD journey. I can only be grateful for all the help that I have received from so many people during these years.

I will start by thanking the jury members Yves Barral, Nicolas Charlet-Berguerand, Snezhana Oliferenko and Lionel Pintard for taking the time to read this thesis and come to the defense (or sit in front of the screen, who knows) to evaluate and discuss my work. I would also like to thank Manuel Mendoza and Monica Gotta for their involvement and advice during my thesis follow-up committees during these years.

A owe a big thank you to you Iza, for the courage to follow new observations that can end up in beautiful adventures such as nucleoporins and FXR happily swimming in an ubiquitin and mitosis lab. I am very thankful for the opportunity to do my PhD in your lab and for the freedom and trust with which I could learn to do science. I admit it was a scary freedom many times, but it also taught me that I was allowed to ask my own questions and look for their answers. Thank you for the contagious enthusiastic scientific talks when my PhD project and myself needed them. And a big thank you for probably the most important lesson of these years: "no matter how big the elephant is, you just need to chop it into pieces". I believe I feel a bit more ready for the next elephant to come.

I would like to thank all past and present members of Sumara lab (Stephane, Charlotte, Katka, Sushil, Eva, Yongrong, Paulo, Lucile, Aurore, Ines and Jeeyun) for the everyday help, exchange and advice, it has been a fascinating combo of so different people. Thank you Stephane for launching this project and setting the ground for my PhD. Thank you Charlotte for taking care of us, making sure everything is in order and for those cheering up coffees that made my day (not so much for the countdown together with Lucile though :p). A special thank you goes to you Katka, for being my "lab mum", for your patience when teaching me from the very beginning (remember when you showed me a shiny mitotic cell at the microscope of the cell culture room?) until the very end (and this is not finished I'm afraid…). Thank you for the exciting scientific discussions and for being also there beyond the bench to help me.

I would also like to thank Romeo Ricci and his present and past team members for the useful discussions during our lab meetings, the helpful exchange of reagents and for the nice moments shared during our lab retreats.

Thank you to all the platforms at IGBMC for facilitating my work, especially the cell culture facility, the microscopy facility (thanks a lot for your patience Erwand and Elvire!) and the flow cytometry facility.

Miles de gracias a vosotros los Embajadores (Bea, Jordi, Laia, Pau, Rafa, Raquel, Roberto y Xènia). Por las frustraciones, aventuras, cenas, noches y viajes compartidos, que han dado a esta experiencia un toque de hogar. Y para ti un gracias especial Bea, porque cuatro años de matrimonio no son algo que pase desapercibido (y yo que pensé que nunca me casaría!). Todos los matrimonios tienen sus momentos, por los que te debo tantas gracias como disculpas. Muchas gracias por toda la ayuda y el apoyo; en los momentos duros del doctorado y en los alegres que ha sido un placer compartir. Tenemos una larga colección de pasajes de tontómetro que me guardo para rememorar cuando nos crucemos, quién sabe dónde, y brindemos con otra pinta más en el idioma que toque.

Te agradezco mucho Irene los paseos improvisados que me han enseñado que es importante y necesario tomarse un tiempo cuando el tiempo falta. Gracias por la ayuda, la ausencia de juicio y la opinión sincera.

Et à vous, Alexia et Vincent, je vous écris dans la langue que je vous dois. Alexia, merci beaucoup pour ces conversations sur les canapés du deuxième étage, pour m'avoir appris le français et pour avoir trouvé les moments nécessaires dans ton agenda chargé pour voyager ou prendre une bière. Vincent, ça a été un grand plaisir de partager l'escalade (et la lutte pour voir qui commence la voie !), les cafés à l'IGBMC, la montagne et les conversations à vélo avec toi. Merci beaucoup de partager ton enthousiasme!

I am grateful to all the people that have shared climbing, hiking, running and dancing with me in Strasbourg (Alba, Alastair, Andrea, Carlos B., Carlos G., Daniel, Elena, Marina, Merce, Paulo, Rocío, Sandrine and many others). Special thanks belong to Matej, for juggling with anything plus science in every conversation, and always being willing to help.

Gracias a los del Goya por no marcharse, y a los bioquímicos de Madrid que nunca se sienten lejos.

Te debo tantas gracias, Pablo, que siempre se quedan cortas. Gracias por enseñarme constantemente ciencias, letras y humor; que también han llenado este doctorado. Por contagiarme tu manera de descubrir y contar historias. Y por poder compartir.

Muchas gracias a la familia, Alba y Bea, por la constancia y la paciencia. Milesker Julen, Ramon eta Miren, Agote umorea gustora partekatzeagatik. Gracias mamá, por el interés en mi ciencia y por enseñarme la de otros. Mil gracias por el apoyo, la calma y la montaña.

Table of contents

Summary (French) - Résumé

Introduction

Les pores nucléaires (NPCs) sont de grands complexes protéiques incrustés dans l'enveloppe nucléaire (EN) et constituent les canaux de transport contrôlant l'échange de protéines et d'ARNm entre le noyau et le cytoplasme. Ils sont constitués d'environ 30 nucléoporines différentes (Nups), chacune étant présente en plusieurs copies dans les NPCs. Les Nups présentes dans le canal central des NPCs contiennent des éléments désordonnés caractérisés par la présence de répétitions de phénylalanine-glycine (FG), appelées FG-Nups. Les FG-Nups ont la capacité de former des hydrogels qui constituent une barrière sélective et perméable pour les cargaisons transportées à travers les NPCs. Les FG- et non-FG-Nups peuvent également former des agrégats dans les cellules car elles sont séquestrées dans les granules de stress et dans divers agrégats pathologiques dans le noyau et dans le cytoplasme. Cela indique que les Nups ont une capacité intrinsèque à s'assembler de manière aberrante, ce qui suggère que des mécanismes de protection doivent exister pour empêcher ce phénomène dans la cellule. En effet, dans les embryons de drosophile, un excès de Nups solubles a été reporté. Dans les cellules, les Nups sont synthétisées sous forme de protéines cytosolubles. On ne sait pas encore comment l'équilibre entre les Nups solubles et leur assemblage localisé dans les NPCs est régulé.

Les protéines apparentées au X fragile (FXR) (FXR1, FXR2 et Fragile X mental retardation protein (FMRP)) forment une famille de protéines de liaison à l'ARN présentant un degré élevé de similarité de séquence et de structure et jouant un rôle important dans la régulation de la traduction des protéines. La mise sous silence du gène FMR1 qui code pour la protéine FMRP conduit au syndrome de l'X fragile (SXF), la forme la plus courante de déficience intellectuelle humaine héréditaire dans le monde, pour laquelle il n'existe, à ce jour, aucune thérapie efficace.

Au cours de mon doctorat, j'ai identifié un rôle inattendu de la famille des protéines FXR et de la protéine motrice dynéine dans la régulation spatiale de la condensation des Nups.

Résultats

FXR1 interagit avec les Nups mais ne régule pas leur expression

Des expériences d'immunoprécipitation (IP) avec la protéine GFP-FXR1 exprimée de manière stable dans les cellules HeLa suivies d'une analyse par spectrométrie de masse, ont identifié plusieurs Nups comme des interactants potentiels de FXR1. Les interactions de FXR1 avec Nup133 et Nup85 ont été confirmées par Western blot. Il est important de noter que FXR1 ne module pas le niveau d'expression des Nups puisque nous n'avons pas observé de changements de quantités de protéines et d'ARNm de plusieurs Nups lorsque FXR1 est déplété. Nous avons

également observé que FXR1 est localisé au niveau de l'enveloppe nucléaire (où résident les NPCs) et également occasionnellement dans de petits foci cytoplasmiques avec les Nups.
Dans l'ensemble, FXR1 interagit avec les Nups et peut se situer à la fois à l'enveloppe nucléaire et dans les foci cytoplasmiques contenant des Nups.

FXR1 inhibe la condensation aberrante des Nups cytoplasmiques et régule la morphologie nucléaire pendant la phase G1 du cycle cellulaire

Pour évaluer la fonction biologique des interactions FXR1-Nup, nous avons inhibé l'expression du gène FXR1 en utilisant des oligonucléotides (siARN). La régulation négative de FXR1 conduit à la formation de noyaux irréguliers ainsi qu'à une accumulation de plusieurs types de Nups dans le cytoplasme sous forme de granules irrégulières. Les deux phénotypes peuvent être corrigés par l'expression ectopique de la protéine GFP-FXR1. La régulation négative de FXR1 réduit également modérément la localisation de plusieurs Nups au niveau de l'EN. Afin de mieux caractériser l'effet de FXR1 sur la localisation des Nups, nous avons filmé nos cellules en direct. Ces essais ont révélé que les défauts de morphologie nucléaire et les granules de nucléoporines cytoplasmiques dans les cellules déficientes en FXR1 pouvaient être détectés au début de la phase G1.
Afin de mieux comprendre la nature de ces granules, nous avons traité les cellules déficientes en FXR1 avec du 1,6-Hexanediol pour distinguer les hydrogels de Nups (qui peuvent être dissous par les hexanediols) et les fibres amyloïdes de Nups (qui sont résistantes aux hexanediols). Le 1,6-Hexanediol a conduit à la dispersion des granules cytoplasmiques de Nups observées lors de la régulation négative de FXR1.
Ainsi, la perte de FXR1 induit des défauts de morphologie nucléaire et des agrégats de Nups inappropriés dans le cytoplasme au début de la phase G1.

FXR1 inhibe la formation d'agrégats de Nups par le transport dépendant des microtubules et de la dynéine

Nous avons identifié la protéine motrice cytoplasmique dynéine et sa protéine adaptatrice BICD2 comme étant capables d'interagir avec la GFP-FXR1. Il est intéressant de noter que l'inhibition de la dynéine et de BICD2 ainsi que la dépolymérisation des microtubules conduisent également à l'accumulation des granules de Nups cytoplasmiques et à l'irrégularité morphologique du noyau.
Dans des expériences de vidéo en direct utilisant des lignées cellulaires rapporteurs GFP-Nup, les agrégats de Nups montrent un comportement dynamique avec des événements de fusion et de fission. Fait important, en l'absence de FXR1 ou de dynéine, les aggrégats de Nups sont

retenus dans le cytoplasme et ces événements de fusion/fission sont plus importants, tandis que dans les conditions contrôles, on observe un mouvement de ces granules vers l'EN et une fusion avec celle-ci. Ces observations suggèrent que le transport par le complexe FXR1-dynéine sur les microtubules peut diminuer les concentrations locales de Nups cytoplasmiques, empêchant ainsi leur assemblage aberrant en agrégats.

Les anomalies de localisation des Nups peuvent être liées au syndrome de l'X fragile

Tous les membres de la famille des protéines FXR partagent-ils des rôles analogues dans le contrôle spatial de la localisation des Nups ? Nous avons observé que FXR2 et FMRP peuvent également être localisées à l'EN. Il est intéressant de noter que la déplétion de chacun des trois membres de cette famille de protéines conduit à la même condensation cytoplasmique des Nups et à une morphologie nucléaire anormale dans les cellules HeLa. De même, différents modèles du syndrome de l'X fragile (fibroblastes primaires, iPSC et Fmr1 KO MEF) ont également montré une accumulation de granules cytoplasmiques de Nups. Cela suggère que les trois protéines FXR partagent ce rôle de régulation de la localisation des Nups.

FXR1 régule l'exportation des protéines et la progression du cycle cellulaire

Pour comprendre si la condensation ectopique des Nups au début de la phase G1 dans les cellules déficientes en FXR affecte la fonction des pores nucléaires, nous avons analysé les taux d'importation/exportation nucléocytoplasmique d'une GFP ectopique lors de l'absence de FXR1. Cette absence ne semble pas affecter l'importation nucléaire alors qu'elle impacte négativement le taux d'exportation uniquement au début de la phase G1.

En ce qui concerne la progression du cycle cellulaire, la régulation négative de FXR1 entraîne une augmentation du pourcentage de cellules en phase S et une diminution du pourcentage de cellules en phase G1, ce qui suggère qu'en l'absence de FXR1, les cellules s'accumulent en phase S.

En conclusion, ces données indiquent que l'absence de FXR1 entraîne des défauts d'exportation de protéines pendant la phase G1 et une perturbation de la progression du cycle cellulaire.

L'absence de RanBP2 annule la condensation cytoplasmique aberrante des Nups induite par l'inhibition de FXR1

Des publications récentes suggèrent que la Nup RanBP2 est une Nup clé dans la biogenèse des NPC par la voie des *Annulate lamellae*. Nous avons cherché à savoir si FXR1 pouvait réguler spécifiquement les niveaux et/ou la localisation de RanBP2 et donc induire une condensation incorrecte des nucléoporines. Nous avons découvert que FXR1 et RanBP2 se régulent

mutuellement à la fois en matière s'expression mais également de localisation subcellulaire. Il est intéressant de noter que la déplétion de RanBP2 abolit la condensation aberrante des Nups induite par régulation à la baisse de FXR1, la dynéine ou la dépolymérisation des microtubules.

Discussion

Nos données suggèrent un modèle où les protéines FXR et la dynéine co-régulent la relocalisation d'un pool cytoplasmique de Nups vers l'EN au début de la phase G1. L'absence de protéines FXR ou l'inhibition du transport médié par dynéine conduisent à la formation de granules de Nups ectopiques non caractérisées auparavant. Nous supposons que la voie FXR-dynéine régule le pool de nucléoporines solubles soit restant dans le cytoplasme après l'assemblage post-mitotique des NPCs, soit étant traduites en interphase précoce, ce qui est important pour les fonctions d'exportation, une forme nucléaire normale et pour la progression du cycle cellulaire.

Les résultats précédents d'autres équipes sont conformes à notre modèle de dispersion des Nups par le complexe dynéine-FXR. Il a été démontré que FMRP forme un complexe avec la protéine motrice dynéine et avec sa protéine adaptatrice BICD2 dans les neurones. Nos données sont cohérentes avec ces résultats et montrent l'interaction de la dynéine et de BICD2 avec la protéine paralogue de FMRP, FXR1 dans des cellules cancéreuses humaines en culture. Des interactions moléculaires entre les Nups et les complexes dynéine-BICD2 ont également été démontrées lors de l'entrée en mitose. Nous supposons que la formation de ces complexes et leur transport disperseraient les Nups cytoplasmiques, inhibant ainsi leur agrégation cytoplasmique. Il serait intéressant d'étudier si ces granules de Nups cytoplasmiques peuvent séquestrer d'autres protéines cohésives.

Nous n'avons pas observé d'augmentation de co-localisation de FXR1 endogène et des Nups en l'absence de dyneine/BICD2. Nous supposons que soit les trois composants sont nécessaires pour former les complexes de transport dans le cytoplasme, soit la formation du complexe FXR-Nups est transitoire et est nécessaire pour le transport des Nups solubles qui sont plus difficiles à visualiser dans le cytoplasme. Les granules cytoplasmiques de Nups que nous observons seraient le résultat de l'absence de ce mécanisme de transport et de l'augmentation locale des niveaux de Nups qui en résulte, entraînant la formation aberrante de granules de Nups plus grosses (faciles à visualiser) qui ne contiennent pas nécessairement FXR1.

Nous n'avons pu détecter aucun changement de quantité de protéines de plusieurs Nups analysées ou du niveau et de la stabilité de leurs ARNm. Cependant, étant donné que la régulation traductionnelle représente l'un des rôles les mieux étudiés de la famille des protéines

FXR, on ne peut pas formellement exclure que l'expression d'autres Nups ou facteurs associés aux Nups, encore à identifier, soit régulée par les protéines FXR.

Nos données suggèrent que la voie FXR-dynéine est importante pour le maintien de la forme du noyau au début de la phase G1. Nous pensons qu'un retard modéré dans l'exportation en G1 pourrait (par un mécanisme inconnu) conduire à des défauts de morphologie nucléaire. Alternativement, la taille et la forme du noyau pourraient être liées aux rôles structurels établis des Nups, indépendamment de leurs fonctions dans le transport des protéines et de l'ARN. En effet, des changements de forme nucléaire dans des cellules déficientes en Nups ont été documentés dans divers organismes. Il est intéressant de noter qu'il a été démontré auparavant que les Nups étaient impliquées dans la progression G1/S en régulant l'exportation d'ARNm de gènes spécifiques, clés du cycle cellulaire. En outre, chez la levure, il a été reporté que la modulation des NPCs retardait leur entrée dans le cycle cellulaire des cellules filles. Une étude précédente sur les myoblastes a proposé un rôle pour FXR1 dans la progression du cycle cellulaire, la délétion de cette protéine entraînant une phase G1 plus longue, une phase S plus courte et une sortie mitotique prématurée. Nos résultats démontrent une phase G1 plus courte, des phases S plus longues et aucun défaut dans la progression mitotique en l'absence de FXR1, ce qui suggère une autre fonction de FXR1 dans les cellules cancéreuses.

Il est intéressant de noter que des anomalies transitoires d'exportation des protéines ont été observées dans les cellules déficientes en FXR1, en particulier au début de la phase G1. Il est plausible que dans des conditions de stress ou dans les cellules à division rapide d'un embryon en développement, cette légère diminution du taux d'exportation de protéines affecte de manière significative l'homéostasie cellulaire et la division asymétrique. Une autre explication serait que les agrégats cytoplasmiques de Nups aient des effets cytotoxiques en séquestrant des facteurs encore inconnus, importants pour la forme du noyau et la progression du cycle cellulaire.

Bien que des études futures soient nécessaires pour comprendre le mécanisme précis de l'axe FXR-dynein-Nup et le rôle de RanBP2 dans la condensation des Nups, nous pouvons supposer que les défauts de ces voies perturbent de façon significative l'homéostasie cellulaire et contribuent à la pathologie du syndrome du X fragile. Collectivement, nos données démontrent un rôle inattendu des protéines FXR et de la dynéine dans la régulation spatiale des Nups solubles, et fournissent un exemple de mécanisme régulant la formation localisée de condensats protéiques.

Summary (English)

Introduction

Nuclear pore complexes (NPCs) are large, multisubunit protein complexes spanning the nuclear envelope (NE) that constitute the transport channels controlling the exchange of proteins and mRNAs between the nucleus and the cytoplasm. They are built from roughly 30 different nucleoporins (Nups) each present in multiple copies in the NPCs. Nups in the central channel contain disordered elements characterized by the presence of phenylalanine-glycine (FG) repeats, the so-called FG-Nups. The FG-Nups have the ability to phase separate into sieve-like hydrogels that constitute a selective and permeable barrier for transported cargos through the NPCs. The FG- and non-FG-Nups can also form condensates in cells as they are sequestered in the stress granules and in various pathological aggregates in the nucleus and in the cytoplasm. This indicates that Nups have an intrinsic capacity to aberrantly assemble, suggesting that protective mechanisms may exist to prevent it in the cell. Indeed, in *Drosophila* embryos a large excess of soluble Nups has been reported and in cells Nups are synthesized as soluble proteins in the cytoplasm. How the balance of soluble Nups and their localized assembly in NPCs is currently unknown.

The Fragile X related (FXR) proteins (FXR1, FXR2 and Fragile X mental retardation protein (FMRP)) are a family of RNA-binding proteins displaying a high degree of sequence and structural similarity and playing important roles in regulating protein translation. Silencing of the *FMR1* gene that encodes the FMRP protein leads to Fragile X syndrome (FXS), the most common form of inherited intellectual human disability worldwide, for which no efficient therapy exists to date.

During my PhD I identified an unexpected role for the FXR protein family and the motor protein dynein in the spatial regulation of Nup condensation.

Results

FXR1 interacts with Nups but does not regulate their levels

Immunoprecipitation experiments (IPs) of stably expressed GFP-FXR1 protein in HeLa cells followed by mass spectrometry analysis identified several Nups as potential FXR1 interactors, and FXR1 interactions with Nup133 and Nup85 were confirmed by Western blot. Importantly, FXR1 does not modulate Nups levels since we did not observe changes in protein and mRNA levels of several analyzed Nups upon depletion of FXR1. We also observed that FXR1 localizes to the NE (where NPCs reside) and also occasionally to small cytoplasmic foci labelled by Nups. Altogether, FXR1 interacts with Nups and can localize to both the NE and to cytoplasmic foci containing Nups.

FXR1 inhibits aberrant condensation of cytoplasmic Nups and regulates nuclear morphology during G1 cell cycle phase

To assess the biological function of the FXR1-Nup interaction, we silenced the FXR1 gene using siRNA oligonucleotides. Downregulation of FXR1 led to irregular nuclei together with an accumulation of several types of Nups in the cytoplasm in the form of irregular granules. Both phenotypes could be rescued by ectopic expression of GFP-FXR1. FXR1 downregulation also moderately reduced the NE localization of several Nups. To further characterize this effect of FXR1 in Nup localization, we carried out live video microscopy experiments. These assays revealed that nuclear morphology defects and cytoplasmic Nup granules in FXR1-deficient cells could be detected at the beginning of G1 phase.

In order to get insight regarding the nature of these granules, we treated FXR1 deficient cells with 1,6-Hexanediol to distinguish between Nup hydrogels (which can be dissolved by hexanediols) and Nup amyloid fibers (which are resistant to hexanediols). 1,6-Hexanediol led to the dispersion of the cytoplasmic Nup granules observed upon FXR1 downregulation.

Thus, loss of FXR1 induces nuclear shape defects and inappropriate Nups condensates in the cytoplasm in early G1 phase.

FXR1 inhibits Nup condensate formation by dynein-based microtubule-dependent transport

We identified cytoplasmic motor protein Dynein and its adaptor protein BICD2 as GFP-FXR1 interactors. Interestingly, downregulation of both dynein and BICD2 and microtubule depolymerization also led to the accumulation of the cytoplasmic Nup granules and to the irregular nuclei.

In live video experiments using GFP-Nup reporter cell lines, Nup aggregates showed dynamic behavior with both fusion and splitting events. Importantly, in the absence of FXR1 or dynein Nups granules were retained in the cytoplasm and these fusion/fission events were increased, while in control cells NE-directed movement of Nup granules and fusion with the NE were observed. These observations suggest that microtubule-based transport by the FXR1-dynein complex can decrease local concentrations of cytoplasmic Nups thereby preventing their assembly into condensates.

Nup localization defects can be linked to FXS

Do all members of the FXR protein family share analogous roles in the spatial control of Nup localization? We observed that FXR2 and FMRP can also localize at the NE. Interestingly, depletion of each of the three members of this protein family led to the condensation of

cytoplasmic Nups and to nuclear morphology defects in HeLa cells. Likewise, different FXS models (primary fibroblasts, iPSC and Fmr1 KO MEFs) also displayed accumulation of cytoplasmic Nup granules. This suggests that the three FXR proteins share the role in regulating Nup localization.

FXR1 regulates protein export and cell cycle progression

To understand if ectopic Nup condensation during early G1 in FXR-deficient cells affects the function of the nuclear pores, we analyzed the rates of nucleocytoplasmic import/export of an ectopic GFP upon FXR1 downregulation. The absence of FXR1 did not affect nuclear import while it reduced the export rate solely in early G1.

Regarding cell cycle progression, downregulation of FXR1 led to an increased percentage of cells in S phase and a decreased percentage of cells in G1 phase, suggesting that upon FXR1 downregulation cells accumulate in S phase.

Together, these data indicate that the absence of FXR1 leads to protein export defects in G1 and perturbation in cell cycle progression.

Absence of RanBP2 rescues FXR1 depletion induced aberrant cytoplasmic Nup condensation

Recent publications suggest that the Nup RanBP2 is a key Nup in NPC biogenesis through the pathway of ALs. We investigated if FXR1 could specifically regulate RanBP2 levels and/or localization and therefore induce an incorrect Nup condensation. We found that FXR1 and RanBP2 regulate each other's protein levels and subcellular localization. Interestingly, RanBP2 depletion abolished the aberrant Nup condensation induced by FXR1 or dynein downregulation and microtubule depolymerization.

Discussion

Our data suggest a model where FXR proteins and dynein regulate the localization of a cytoplasmic pool of Nups to the NE during early G1. Absence of FXR proteins or dynein-mediated transport leads to the formation of previously uncharacterized ectopic Nup granules. We speculate that the FXR-dynein pathway regulates the pool of soluble Nups either remaining in the cytoplasm after postmitotic NPC assembly or being translated in early interphase, which is important for functions in nuclear export and shape and in cell cycle progression.

Previous findings from other teams are in line with our model of FXR-dynein mediated Nup dispersal. FMRP was demonstrated to form a complex with the dynein motor and with the dynein adaptor protein BICD2 in neuronal cells. Our data are consistent with these findings

and show the interaction of dynein and BICD2 with the FMRP paralog protein FXR1 in cultured human cancer cells. Molecular interactions of Nups and dynein-BICD2 complexes were also reported during mitotic entry. We speculate that formation of FXR1-dynein-Nup complexes and their transport would disperse cytoplasmic Nups, thereby inhibiting formation of Nup-containing cytoplasmic condensates. It will be interesting to study if these cytoplasmic Nup granules can sequester any other cohesive proteins.

We did not observe an increase in co-localization of the endogenous FXR1 and Nups in the absence of dynein/BICD2. We predict that either all three components are needed to form the transport complexes in the cytoplasm or that the formation of the FXR-Nup complex is very transient and is needed for the transport of soluble Nups which are harder to visualize in the cytoplasm. The cytoplasmic Nup granules that we observe would be the result of the absence of this transport mechanism and the consequent local increase of Nups levels leading to aberrant formation of bigger (easy to visualize) Nup granules that do not necessarily contain FXR1.

We were unable to detect any changes in protein levels of several analyzed Nups or levels and stability of the Nups mRNAs. However, given that translational regulation represents one of the best-studied roles of the FXR protein family, it cannot be formally excluded that expression of other, yet to be identified Nups or Nup-associated factors, is regulated by FXR proteins.

Our data suggest that the FXR-dynein pathway is important for the maintenance of nuclear shape during early G1. We believe that a moderate delay in the export during G1 could (through an unknown mechanism) lead to nuclear morphology defects. Alternatively, the nuclear size and shape could be related to the established structural roles of Nups independent of their functions in protein and RNA transport. Indeed, changes in nuclear shape in cells deficient for individual Nups have been documented in various organisms. Interestingly, Nups were previously implicated in G1/S progression by regulating export of specific mRNAs of key cell cycle genes. Furthermore, in yeast, modulation of NPCs has been reported to delay their cell cycle entry in the daughter cells. Previous study in myoblasts proposed the role of FXR1 in cell cycle progression, whereby deletion of this protein led to longer G1 phase, shorter S phase and premature mitotic exit. Our results demonstrate shorter G1, longer S phases and no defects in mitotic progression in the absence of FXR1, suggesting another unrelated function of FXR1 in cancer cells.

Excitingly, transient defects in protein export were observed in FXR1-deficient cells specifically during early G1 cell cycle stage. It is plausible to predict that under stress conditions or in the fast dividing cells of a developing embryo, this small decrease in protein

export rate would significantly affect cellular homeostasis and asymmetric division. An alternative explanation is that CNGs exert cytotoxic effects by sequestering yet unknown factors important for nuclear shape and cell cycle progression.

Our preliminary results indicate that RanBP2 is required for Nup condensation in cytoplasmic granules. We speculate that RanBP2 acts as a Nup granule fusing agent necessary to mix Nups in small granules that will be transported to the NE. Excessive Nup granule fusion (due to increased cytoplasmic Nup levels or increased RanBP2 levels) would lead to aberrant big cytoplasmic Nup granules difficult to transport and their accumulation in the cytoplasm.

While future studies are needed to understand the precise mechanism underlying FXR-dynein-Nup axis and RanBP2's role in Nup condensation, defects in these pathways are predicted to significantly perturb cellular homeostasis and may contribute to the pathology of FXS. Collectively, our data demonstrate an unexpected role of FXR proteins and dynein in the spatial regulation of soluble Nups, and provide an example of a mechanism that regulates localized protein condensate formation.

List of abbreviations

AA	Amino acid
AD	Alzheimer's disease
AL	Annulate lamellae
ALPC	Annulate lamellar pore complex
ALS	Amyotrophic lateral sclerosis
BAF	Barrier to autointegration factor
BICD2	Bicaudal D homologue 2
Bp	Base pair
BSA	Bovine serum albumin
CDK	Cyclin-dependent kinase
CHD	Cyclophilin homology domain
CHX	Cycloheximide
CLEM	Correlative Light Electron Microscopy
CNG	Cytoplasmic nucleoporin granules
CRM1	Chromosomal region maintenance 1 protein
CyPN	Cytoplasmic accumulations of PML and nucleoporins
DAPI	4′,6-Diamidino-2-phenylindole dihydrochloride
DMEM	Dulbecco's modified Eagle Medium
DMSO	Dimethyl sulfoxide
DNA	Deoxyribonucleic acid
EDTA	Ethylenediaminetetraacetic acid
EM	Electron microscopy
ER	Endoplasmic reticulum
FACS	Fluorescence-activated cell sorting
FG	Phenylalanine-glycine
FISH	Fluorescent In Situ Hybridization
FMRP	Fragile X Mental Retardation Protein
FRAP	Fluorescence recovery after photobleaching
FTD	Frontotemporal dementia
FXPOI	Fragile X-associated Fragile X-associated primary ovarian insufficiency
FXR	Fragile X Related

FXR1	Fragile X Related Protein 1
FXR2	Fragile X Related Protein 2
FXTAS	Fragile X-associated tremor/ataxia syndrome
FUS	Fused in sarcoma
FXS	Fragile X Syndrome
GDP	Guanosine-5'-diphosphate
GFP	Green fluorescent protein
GTP	Guanosine-5'-triphosphate
HC	Heavy chain
HD	Huntington's disease
HeLa K	Human cervix carcinoma cells, K stands for Kyoto
HP1	Heterochromatin protein 1
IC	Intermediate chain
IDR	Intrinsically disordered region
IF	Immunofluorescence
IgG	Immunoglobulin G
INM	Inner Nuclear Membrane
IP	Immunoprecipitation
iPSC	Induced pluripotent stem cell
IR	Internal repeats
KH	K homology domain
LAP2	Lamina associated protein 2
LBR	Lamin B Receptor
LC	Light chain
LE	Long exposure
LINC	Linker of nucleoskeleton and cytoskeleton
Live SR	Super resolution module
LTD	Long-term depression
MEF	Mouse embryonic fibroblast
MG132	Proteasome inhibitor
mGluR	Metabotropic glutamate receptor
mRNA	messenger Ribonucleic acid
MTOC	Microtubule-organizing center
MW	Molecular weight

NE	Nuclear envelope
NEBD	Nuclear envelope breakdown
NES	Nuclear export sequence
NLS	Nuclear localization sequence
NoS	Nucleolar targeting signal
NPC	Nuclear pore complex
NTR	Nuclear transport receptor
Nup	Nucleoporin
ONM	Outer Nuclear Membrane
PBS	Phosphate buffered saline
PFA	Paraformaldehyde
PLK1	Polo-like kinase 1
PML	Promyelocytic leukemia protein
PNS	Perinuclear space
p-Rb	phospho-Retinoblastoma protein
PSD-95	Postsynaptic density protein 95
PTM	Post-translational modification
qPCR	Quantitative real-time polymerase chain reaction
RAN	Repeat-associated non-ATG
RanBP2	Ran-Binding Protein 2
RanGAP1	Ran GTPase-activating protein 1
RanGEF	Ran guanine nucleotide exchange factor
Rb	Retinoblastoma protein
RBP	RNA-binding protein
RCC1	Regulator of chromosome condensation 1
RGG	Arginine-glycine-glycine
RNA	Ribonucleic acid
RT	Room temperature
SD	Standard deviation
SE	Short exposure
SEM	Standard Error of the Mean
SG	Stress granule
siRNA	Small interfering RNA
SSC	Saline Sodium Citrate

SUMO	Small Ubiquitin-Like Modifier
TBS	Tris-buffered saline
U2OS	U-2 Osteosarcoma
WB	Western blotting
WT	Wild type

1. General introduction

1.1. Organization of the nuclear envelope

Cellular compartmentalization has allowed eukaryotic cells to increase the efficiency and regulation of biochemical processes by concentrating the specific players to limited spaces termed organelles. The genomic material within the nucleus is separated from the rest of the cell by the nuclear envelope (NE) which has a intrincate organization (Figure 1) (Güttinger *et al*, 2009). The NE is a double lipid bilayer composed by the outer nuclear membrane (ONM) facing the cytoplasm and continuous with the endoplasmic reticulum (ER), and the inner nuclear membrane (INM) in the nuclear side separated by the 40-50 nm perinuclear space (PNS). The ONM has a very similar protein composition to the ER membrane and has associated ribosomes while the INM has its own set of around 60 different transmembrane proteins. These INM proteins (Lamina associated protein 2 (LAP2), Emerin, MAN1, and Lamin B Receptor (LBR) among others) vary between different cell types and link the NE with the nuclear lamina and chromatin. For example, LBR interacts with lamin B and binds chromatin through the heterochromatin protein 1 (HP1) while LAP2, Emerin, and MAN1 interact with barrier to autointegration factor (BAF) which also binds chromatin (Holmer & Worman, 2001).

The nuclear lamina is a fibrillar network present in metazoans (15-20 nm thick in mammals) and composed of A-type and B-type lamins which are type V intermediate filament proteins. In mammalian somatic cells, lamin A and lamin C are the most abundant A-type lamins while Lamin B1 and LaminB2 are the main B-type lamins. The nuclear lamina provides structural support to the NE and also interacts with chromatin (Burke & Stewart, 2013). Indeed, changes in lamin levels or mutations in their sequence result in aberrant nuclear shape, a hallmark of laminopathies such as, the Hutchinson-Gilford progeria syndrome and the Emery-Dreifuss muscular dystrophy (Polychronidou & Großhans, 2011; Capell & Collins, 2006).

The NE is also stabilized by the linker of nucleoskeleton and cytoskeleton (LINC) complexes than span both membranes and interact with the cytoskeleton in the cytoplasmic side and with the nuclear lamina in the nucleoplasmic side. LINC complexes consist of two sets of transmembrane proteins (nesprins are embedded in the ONM and SUN domain proteins in the INM) which interact in the PNS via specific domains and link both membranes of the NE. The LINC complex is implicated in signal mechanotransduction and nucleus positioning (Bouzid *et al*, 2019; Lee & Burke, 2018) (Figure 1).

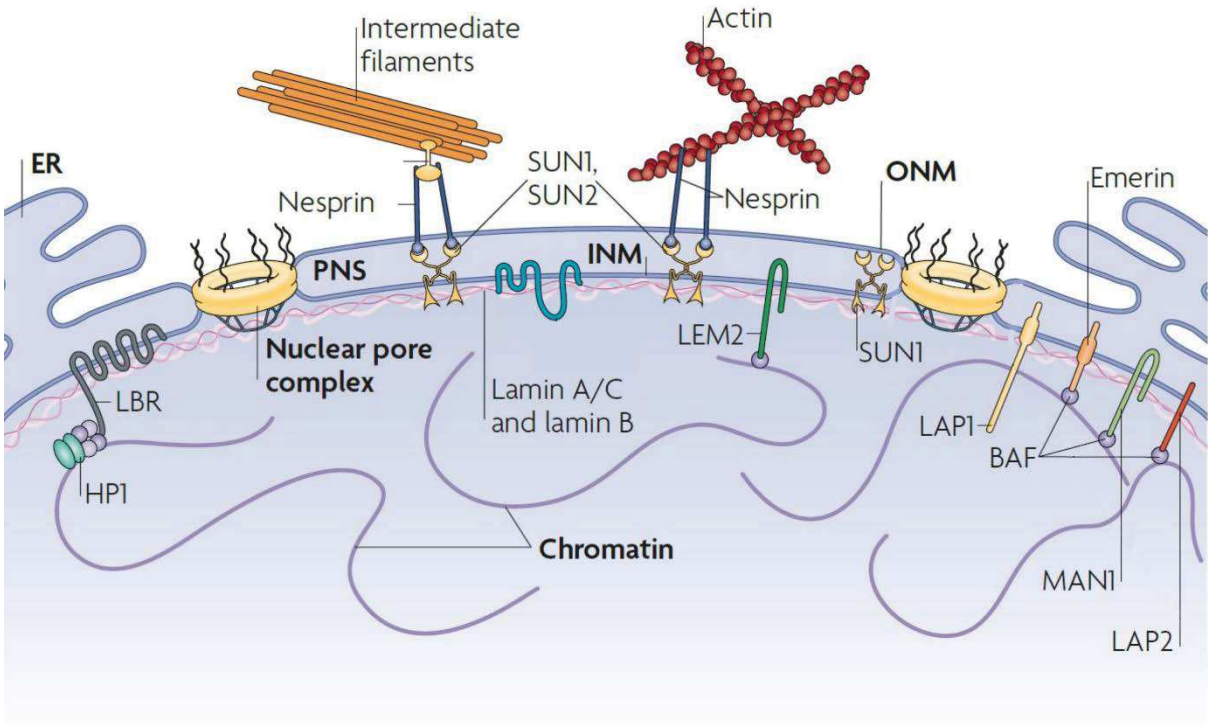

Figure 1 - Organization of the NE. The PNS separates the INM and the ONM. Lamin A/C and Lamin B polymers are located at the nucleoplasmic side of the INM forming the nuclear lamina. ONM proteins connect the NE with the cytoskeleton while the INM proteins link the NE to the lamina and chromatin. LBR interacts both with lamins and chromatin through the chromatin-associated HP1. LAP2, emerin and MAN1 bind to lamins and interact with chromatin through BAF. SUN proteins present in the INM interact with nesprins located in the ONM, thereby forming the so-called LINC complexes that connect with the cytoskeleton (actin and intermediate filaments). The nuclear pore complexes form the channels through which the nucleocytoplasmic transport of proteins and RNAs occurs. Figure adapted from (Güttinger, Laurell, and Kutay 2009).

1.2. The nucleocytoplasmic transport system

The exchange of proteins and mRNAs between the nucleus and the cytoplasm is driven by the Nuclear Pore Complexes (NPCs) which are located in the pores of the NE (Figure 1). Small molecules can passively diffuse through the NPCs while cargos bigger than ~30-50 kDa or ~5 nm in diameter need to be actively transported by Nuclear Transport Receptors (NTRs) (also called karyopherins, or importins and exportins), establishing the so-called permeability barrier (Wente & Rout, 2010). The mechanism of active nuclear transport of cargos requires that they contain specific amino acid sequences, termed nuclear localization sequence (NLS) and nuclear export sequence (NESs) which are recognized by NTRs. The directionality of this transport is ensured by the nucleocytoplasmic gradient of the small GTPase Ran bound to GTP or GDP.

Briefly, the importin-cargo dimer formed after NLS recognition traverses the central channel of the NPC and, once in the nucleoplasm, Ran-GTP (which is found in high concentration in the nucleoplasm compared to the cytoplasm) binds the importin causing the release of the cargo. Exportins together with Ran-GTP recognize the NES of cargo proteins in the nucleus and cross the NPC towards the cytoplasm where they are disassembled by Ran-GTP hydrolysis mediated by RanGAP1 (Ran GTPase-activating protein 1) which localizes to the cytoplasmic side of NPCs. Ran-GDP is then recycled to the nucleoplasm by its own importin. Back in the nucleoplasm, the chromosome bound Ran guanine nucleotide exchange factor (RanGEF also called Regulator of Chromosome Condensation 1 (RCC1)) catalyzes the RanGTP conversion. This way, the two enzymes RCC1 and RanGAP1 maintain the nucleocytoplasmic Ran-GTP/GDP gradient: RanGAP1 makes sure that low Ran-GTP and high Ran-GDP levels are maintained in the cytoplasm while RCC1 ensures the opposite levels in the nucleoplasm (Figure 2) (Wente & Rout, 2010).

In addition to protein transport, dedicated NTRs exist for RNA export (Natalizio & Wente, 2013).

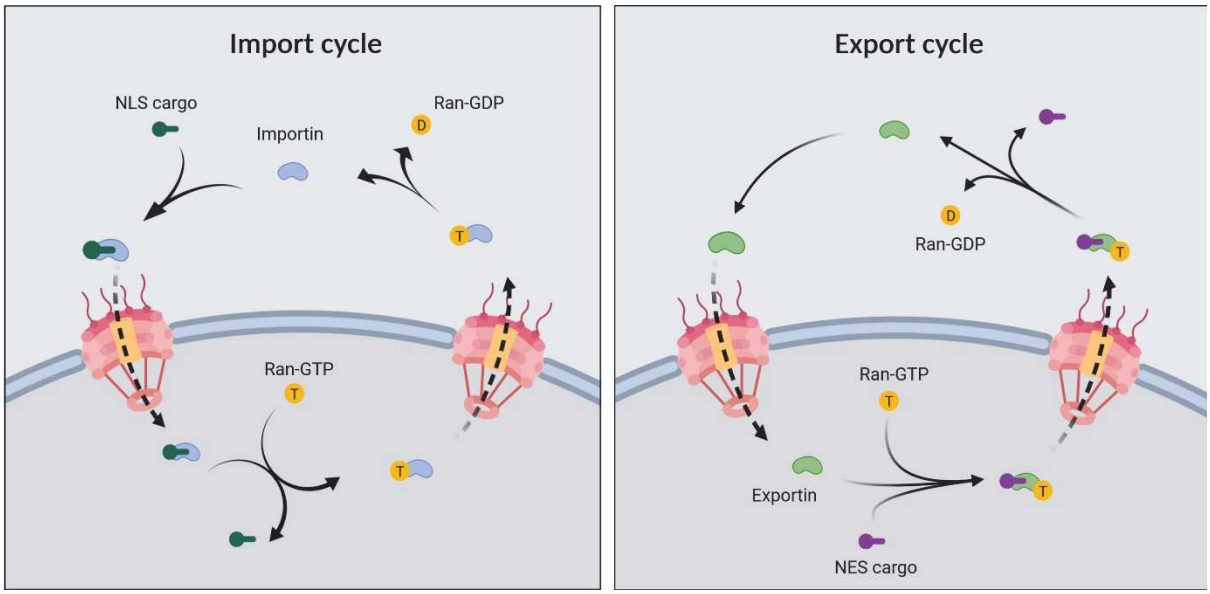

Figure 2 - The nuclear transport cycles for NTRs and their cargos. The import cycle (left panel) begins when an importin (light blue) recognizes the NLS of the cargo protein (dark green) and a dimer is formed. This dimer can cross the NPC central channel and, in the nuclear side, Ran-GTP (yellow) binds the importin and dissociates the import dimer. The export cycle (right panel) starts when an exportin (light green) interacting with Ran-GTP recognizes a NES of a cargo protein (purple) in the nucleoplasm. The triple complex can traverse the NPC central channel and dissociates when RanGAP1 (attached to the cytoplasmic NPC filaments and non-depicted in the figure) hydrolyzes Ran-GTP. Figure adapted from (Wente & Rout, 2010) and created with BioRender.com.

The transport capacity of NPCs is impressive, every second a single NPC can sustain a transport load of 100 MDa and rates of around 1000 translocations (Ribbeck & Görlich, 2001). On average, an active transport event of a small cargo lasts a few milliseconds (Yang *et al*, 2004), although this time depends on each cargo. Bigger cargos need progressively more time and more NTRs (even if they increase the complex's size) to cross the NPC, as it is the case of the 60S ribosomal subunit which requires several NTRs to be exported to the cytoplasm (Wild *et al*, 2010). Even when the cargo is not big, the translocation speed has been shown to depend on the NTR:cargo ratio; small cargos are transported significantly faster when bound to more NTRs (Ribbeck & Görlich, 2002).

Despite the efforts to study the biophysical mechanism of nuclear transport, it is still not completely understood. However, the properties of the central channel of the NPCs seem to have a key role in establishing the permeability barrier (Lemke, 2016).

1.3. Nucleoporins and NPCs

NPCs were first observed in 1949 by H. G. Callan as pores in the nuclear membrane in oocytes from *Triturus cristatus* and *Xenopus laevis* (Callan *et al*, 1949). After decades of study, we now know that NPCs are the biggest nonpolymeric protein complexes (60 MDa in yeast and 120 MDa in vertebrates) that span the NE and are located where the INM and the ONM highly curve and fuse. They show a cylindrical shape broadly conserved throughout eukaryotes measuring 100-150 nm in diameter and 50-70 nm in thickness depending on the organism (Hampoelz *et al*, 2019a; Beck & Hurt, 2017). These massive structures open up ~50 nm-wide transport ducts which are the only communication channels between the nucleus and the cytoplasm and facilitate the dynamic bidirectional transport of components with a wide range of molecular weights.

NPCs are built from roughly 30 different nucleoporins (Nups) that are arranged in several subcomplexes. Multiple copies of these subcomplexes assemble to sum up 500-1000 Nups per NPC following a highly organized eight-fold symmetry (Knockenhauer & Schwartz, 2016). Regarding their function, Nups can be classified into three categories. First, transmembrane Nups anchor the NPC to the highly curved NE of the pore. In metazoan there are three known transmembrane Nups: POM121, ND1 and Nup210. Second, scaffold Nups which organize into stacked ring structures forming the channel that communicates the nucleoplasm and the cytoplasm. Third, disordered Nups containing several copies of phenylalanine-glycine (FG) repeats (the so-called FG-Nups) which localize to the central region of the scaffold channel

and are essential for the permeability barrier (Figure 3). It has been observed that the turnover and residence time at the NPC vary among different Nups; scaffold components show almost no turnover and are stably associated, while peripheral Nups only transiently interact with the NPC (Rabut *et al*, 2004).

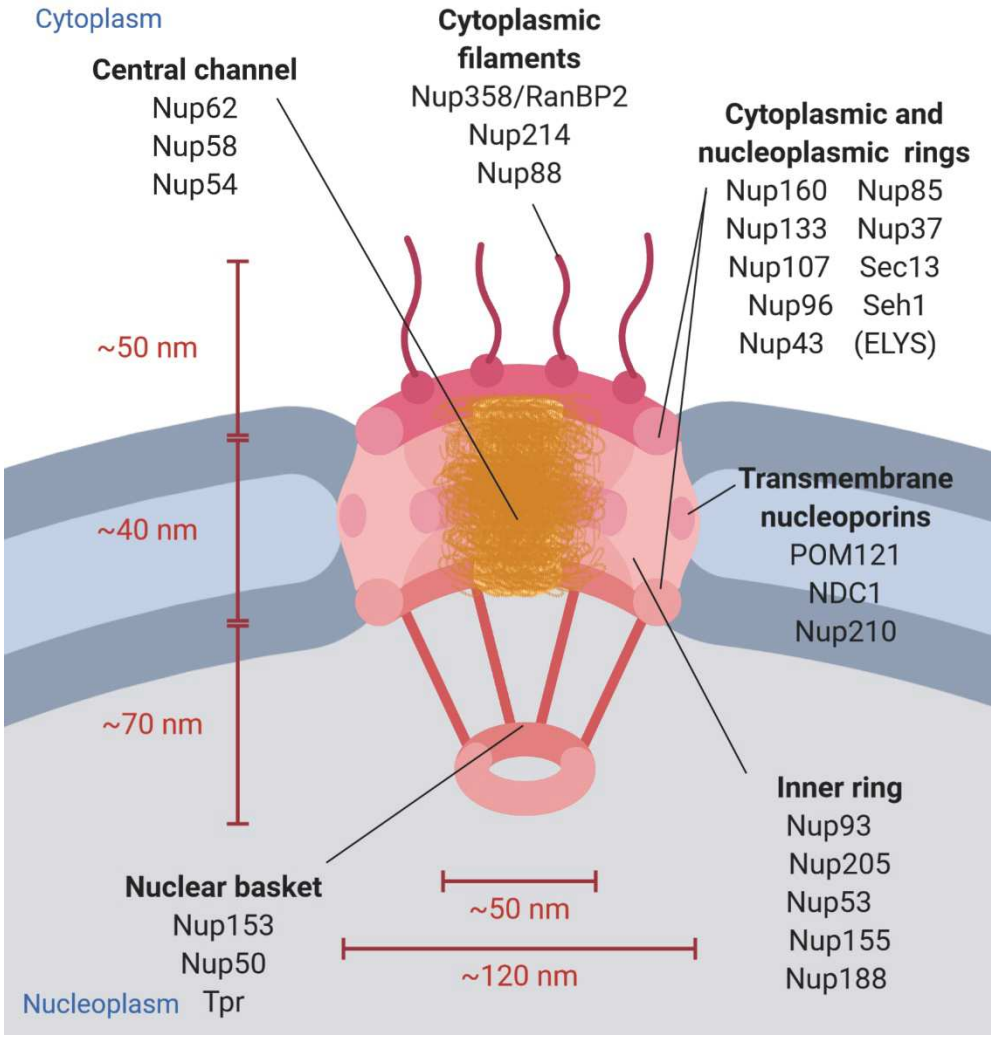

Figure 3 - Organization of the human NPC. Scheme of the human NPC showing the structural elements and their conforming Nups. The cytoplasmic and nucleoplasmic rings are each composed of 16 copies of the Nup107-160 complex organized in two rings of 8 complexes. The Nup ELYS is part of this complex only in the nucleocytoplasmic rings. Attached to cytoplasmic and nucleoplasmic rings, on each side of the NPC there are the cytoplasmic filaments and the nuclear basket, respectively. The inner ring is composed of 32 copies of the Nup93 complex organized in 4 stacked rings of 8 complexes each. Transmembrane Nups are attached to the inner ring and anchor the NPC to the pore membrane. Attached to the inner ring, the Nup62 complexes fill in the central channel and form the permeability barrier of the NPC. Figure created with BioRender.com.

From a structural point of view, the NPC scaffold consists of three stacked rings known as the nucleoplasmic, the cytoplasmic and the inner rings (Grossman *et al*, 2012) which mediate the

association to the NE membrane. The first two rings (in the nuclear and the cytoplasmic side respectively) are formed by several copies of the Nup107-Nup160 complex (or Y-complex, which contains Nup107, Nup160, Nup133, Nup96, Nup43, Nup85, Nup37, Sec13 and Seh1, with the exception of ELYS which is only present in the nucleoplasmic ring). Each ring is actually formed by 16 copies of the complex organized in two concentric rings of 8 complexes (Bui *et al*, 2013) and they are believed to play a role in maintaining the curvature of the NE at the pore. The inner ring consists of 32 copies of the Nup93 complex (which contain Nup93, Nup205, Nup188, Nup53 and Nup155) organized in four stacked rings (Kosinski *et al*, 2016). Interacting with the inner ring, the transmembrane Nups anchor the scaffold of the NPC to the pore membrane.

In addition to the symmetric scaffold, the NPCs also consist of the nuclear basket and the cytoplasmic filaments which work as interaction platforms for transport complexes. Cytoplasmic filaments are long and unstructured polypeptides of Nup214 and Nup358 that facilitate the cargo-NPC interactions. The nuclear basket on the other hand, consists of eight extensions of Nup153, Nup50 and Tpr that emerge from the nucleoplasmic ring and converge into a distal ring. These extensions have roles in mRNA export (Frosst *et al*, 2002; Coyle *et al*, 2011) and in anchoring the NPC to the nuclear lamina (Smythe *et al*, 2000; Xie *et al*, 2016b).

Finally, multiple copies of the Nup62 complex (composed of Nup62, Nup58 and Nup54) form the permeability barrier while interacting with the inner ring through Nup93 and occupying the central channel of the NPC (Sachdev *et al*, 2012; Chug *et al*; Finlay *et al*, 1991). These Nups belong to the FG-Nup family as they contain regions characterized by the presence of FG repeats (Figure 4). One third of all NPC proteins are FG-Nups and they are present in the central channel but also extend into the nuclear and cytoplasmic compartments. Different types of FG repeats exist and they consist of up to 50 copies of small hydrophobic segments (FG, GLFG, FxFG, PxFG, or SxFG where L is leucine, P is proline, S is serine, and x is any residue) that intersperse long stretches of hydrophilic amino acids (between 20 and 70 residues) (Figure 4). This combination of repeats results in flexible and intrinsically disordered regions without a fixed secondary structure (Frey *et al*, 2006; Denning *et al*, 2003), which extend towards the center of the NPC channel and form a meshwork of FG-repeats that offers multiple low-affinity and high-affinity interaction sites to NTRs. These multiple interactions provide the permeability barrier to the NPC; they allow the passive transit of small molecules while excluding macromolecules unless they are bound to NTRs that interact with FG-Nups and diffuse through the pore.

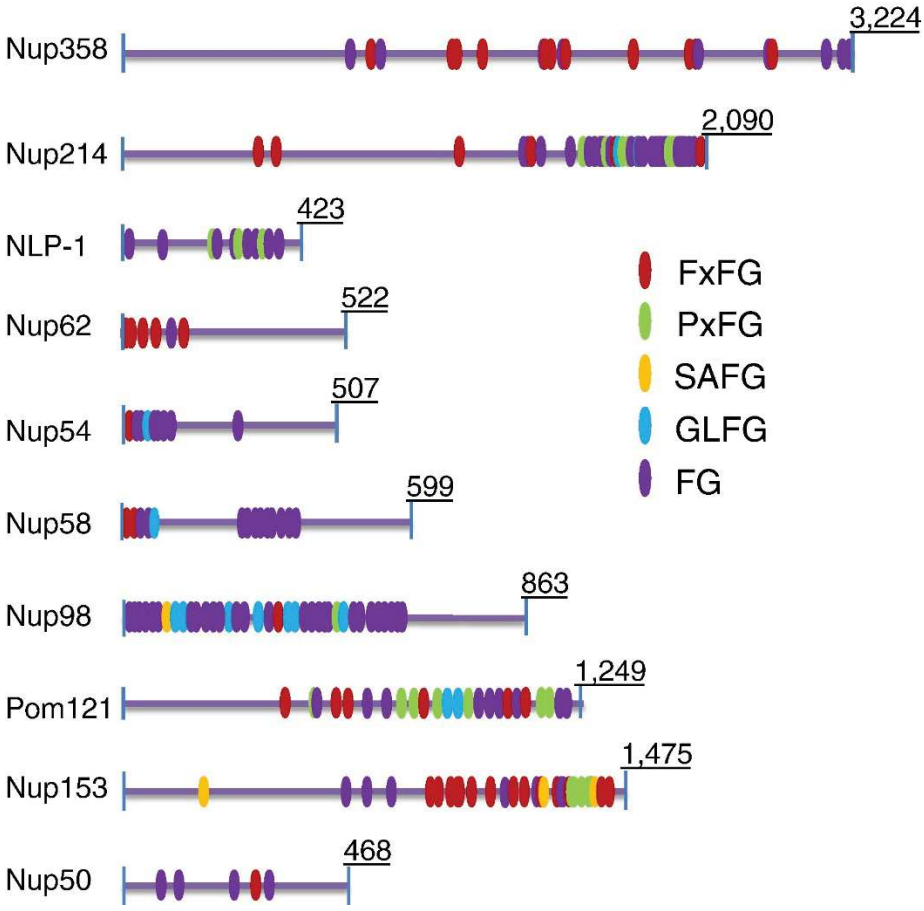

Figure 4 - Distribution FG repeats in human FG-Nups. The following types of FG repeats are depicted in an assortment of disordered human FG-Nups: FxFG (red), PxFG (green), SAFG (yellow), GLFG (blue) or FG (purple) where L is leucine, P is proline, S is serine, and x is any residue. Figure from (Lemke, 2016).

Despite many research efforts, our understanding of the molecular mechanism that determines the NPC permeability barrier remains limited and currently several hypothetical models exist that try to explain it (reviewed in Li, Goryaynov, and Yang 2016). The "Brownian/virtual gate/polymer brushes" model proposes that the FG-Nups sterically hinder the inert molecules brushing them away. Cargo-bound NTRs interact with FG-Nups filaments making them collapse and lowering the energy level of the barrier. The "selective phase/hydrogel" model suggests that phenylalanines of FG-domains are crosslinked with one another and form a cohesive meshwork or hydrogel that constitutes a selective and permeable barrier which only allows the passage of NTRs that can dissolve the crosslinks (Frey *et al*, 2006). Actually, this ability of the FG-Nups to form permeable hydrogels that bind to NTRs can also be reconstituted *in vitro* and is highly conserved through the evolution (Frey & Görlich, 2007). Furthermore, the "reduction of dimensionality" model suggests that FG-Nups collapse when interacting with NTRs allowing for a 2-dimensional movement rather than in a 3D Brownian movement of the NTR-cargo. Alternatively, the "forest/gate" model takes into account the different properties

of FG-Nups and proposes that peripheral FG-domains function as a repulsive gate and that cohesive FG-domains in the central channel act as the selective gate. It is important to mention that all these models are not mutually exclusive, meaning that probably hybrid solutions are employed in the cells depending on specific transport pathways and/or physiological context.

1.4.NPC assembly pathways

How is this gigantic NPC assembled? In higher eukaryotes which undergo open mitosis there are two main NPC assembly pathways operating in different stages of the cell cycle (Figure 5). At the end of mitosis, when the NE is reassembled around the two daughter chromosome masses, NPCs rapidly reform following the so-called postmitotic NPC assembly pathway. During interphase, as the cells grow, new NPCs need to be embedded in the NE to assist the transport needs of the expanding nuclei following the so-called interphasic NPC assembly pathway. These two pathways show fundamentally distinct mechanisms to assemble the same complex which is probably due to the different conditions when they function (the presence or absence of pre-existing building blocks and enclosed NE) (reviewed in (Otsuka & Ellenberg, 2018; Weberruss & Antonin, 2016)). A third way to efficiently increase the NPC number has been described in cells with rapid cell cycles like germ, early embryonic and cancer cells. This pathway is based on the existence of cytoplasmic stacks of double membranes, termed Annulate lamellae (AL), which accommodate a high number of NPCs that can be inserted *en bloc* into the expanding NE (reviewed in Kessel 1992).

In the following sections, these three NPC assembly pathways will be described in more detail.

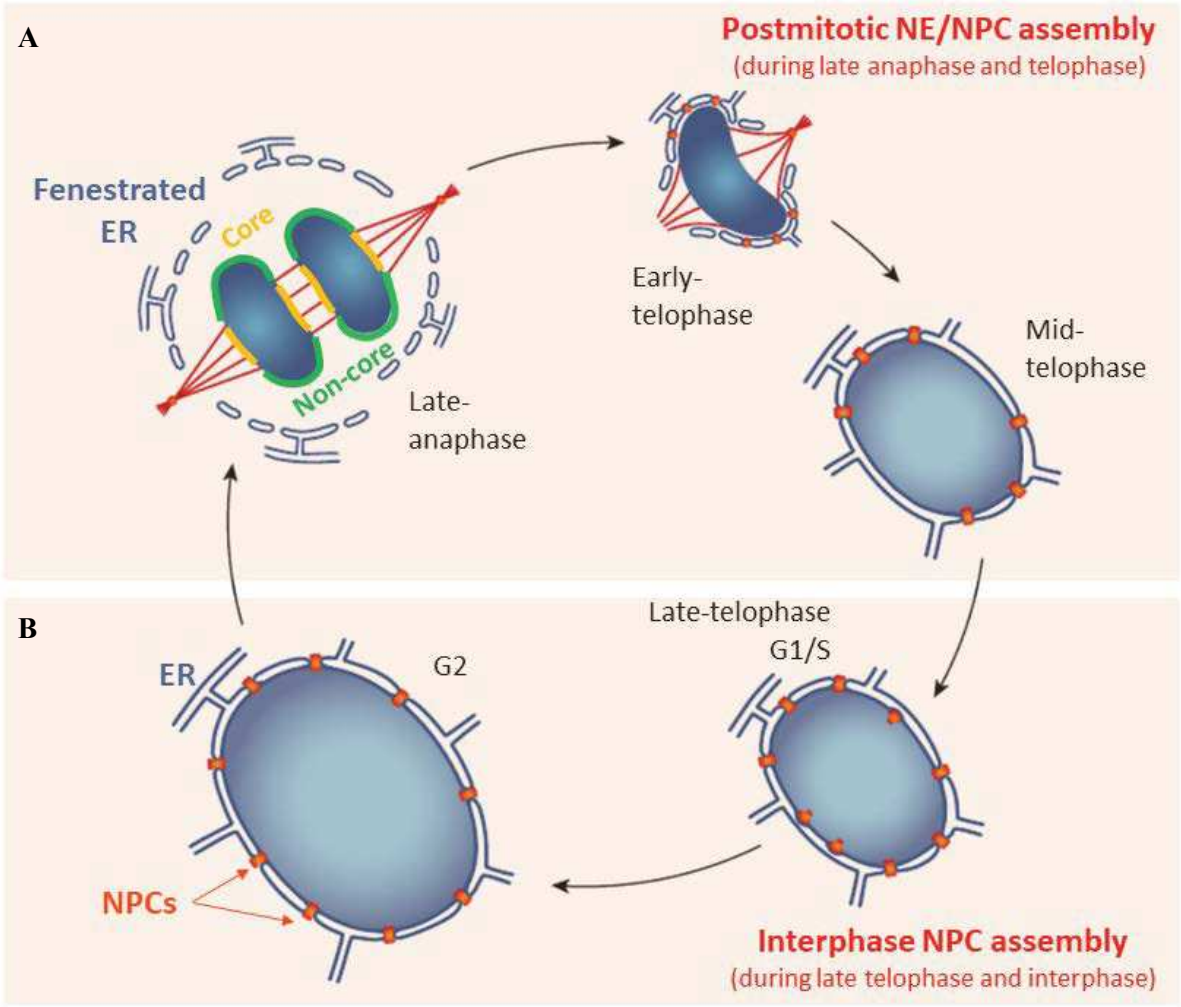

Figure 5 - NPC assembly during cell cycle. Two main NPC assembly pathways operate depending on the cell cycle stage; the postmitotic NPC assembly pathway during late anaphase and telophase and the interphase NPC assembly pathway during late telophase and along interphase.
A Postmitotic NPC assembly pathway (upper panel): at the beginning of mitosis, the NE breaks down and it is absorbed in a highly fenestrated ER (blue lines). Concomitantly, NPCs (orange) are disassembled and Nup subcomplexes are dispersed in the mitotic cytoplasm. During late-anaphase and early-telophase, the NE and NPCs reassemble on the surface of chromatin (blue gradient). The NE assembly is delayed in the chromosome regions facing the mitotic spindle (called 'core' region, yellow) because of the high density of spindle microtubules (red lines). For the same reasons, NPC reassembly is restricted to the 'non-core' regions (green).
B Interphasic NPC assembly pathway (bottom panel): in late-telophase and during the subsequent interphase, the nucleus expands and NPCs assemble *de novo* into the NE.
Figure adapted from (Otsuka & Ellenberg, 2018).

1.4.1. Postmitotic NPC assembly pathway

At the beginning of mitosis the spindle microtubules require the NE breakdown (NEBD) in order to access the condensed chromosomes which will be segregated. This process begins with the removal of the NE membranes from chromosomes and the disassembly of NPCs and

the nuclear lamina in prophase. NEBD is triggered by phosphorylation of several targets by mitotic kinases including cyclin-dependent kinase 1 (CDK1) and polo-like kinase 1 (PLK1) (reviewed in (Güttinger *et al*, 2009; Ungricht & Kutay, 2017). Concomitantly with NE disassembly, the bipolar mitotic spindle is formed. The minus end directed motor protein dynein is attached to NPCs and it contributes to centrosome separation by pulling on astral microtubules, while the kinesin-5 (EG5) pushes the chromosomes apart. Dynein recruitment to NPCs relies on two different pathways which involve the dynein cofactors bicaudal D homologue 2 (BICD2) in late G2 and NUDE/NUDEL-mitosin in prophase (Splinter *et al*, 2010; Bolhy *et al*, 2011). During prophase, dynein-dependent forces generate NE invaginations around the centrosomes promoting fenestrations (Salina *et al*, 2002; Beaudouin *et al*, 2002).

Phosphorylation of nuclear lamins and INM proteins leads to lamina disassembly and retraction of NE membranes into the ER which organizes in highly fenestrated sheets excluded from the spindle area (Figure 5). Nup98 phosphorylation by multiple kinases has been shown to be the first event of the dispersion of NPCs into stable Nup subcomplexes (Dultz *et al*, 2008) which are prevented from re-assembling the NPCs by interacting with importins (Harel *et al*, 2003). After chromosome segregation, postmitotic dephosphorylation events allow the contacts between INM proteins, DNA and lamins which make the fenestrated ER to cover the periphery of the decondensing chromosome masses (called 'non-core' region). The NE reassembly is slower in the chromosome areas facing the spindle pole and the central spindle ('core' region) due to the high density of microtubules (Haraguchi *et al*, 2008; Liu *et al*, 2018). However, overall the NE reassembly is incredibly fast; it requires 2-4 min to reform around the daughter chromosomes and it occurs concomitantly with NPC reassembly.

Postmitotic NPC reassembly is a well-documented stepwise process (Figure 6) (reviewed in (Otsuka & Ellenberg, 2018). It begins with the binding of the nuclear ring specific Nup ELYS to chromatin in mid-anaphase which then recruits the Nup107-160 complex. The latter complex allows for the incorporation of transmembrane Nups (NDC1 and POM121) and Nup53. Subsequently, the inner ring components are recruited in the following order: Nup155, Nup205, Nup188 and Nup93. These components set the ground for the subsequent addition of the Nup62 complex, the cytoplasmic filaments and the nuclear basket. The reassembly of NPCs is limited to the NE surface because of the attachment of ELYS to chromosomes and the localized release of Nups from the inhibitory importins (Franz *et al*, 2007; Harel *et al*, 2003; Rotem *et al*, 2009) promoted by high RanGTP concentrations restricted by DNA bound RCC1 (Walther *et al*, 2003b).

From a structural point of view, correlating live imaging with high-resolution electron tomography has allowed to observe that, first, small pre-pores of about half the size of mature NPCs are formed in small membrane fenestrations which then dilate (Otsuka *et al*, 2018). This suggests that reassembling NPCs take place on the pre-existing NE openings.
Postmitotic NPC assembly is a remarkably fast process which allows daughter nuclei to reestablish active nuclear import within 10 min after anaphase onset, although total reformation of the permeability barrier needs 2 hours to complete (Dultz *et al*, 2009).

1.4.2. Interphasic NPC assembly pathway

The interphasic NPC assembly pathway starts already in late telophase and it doubles the number of NPCs during interphase to support the nucleocytoplasmic transport needs of the growing nuclei and the next cell division (Maul *et al*, 1971; Doucet *et al*, 2010). As opposed to the postmitotic pathway, the interphasic NPC assembly pathway takes places on an already closed NE, therefore the INM and ONM need to fuse to create the pore that will host the NPC. This membrane fusion step together with the fact that the Nup subcomplexes need to be produced are probably the reasons why this assembly is a much slower and sporadic process. High-resolution imaging techniques have shed light on the assembly process (Figure 6). The interphasic assembly begins with a dome shaped evagination of the INM which seems to be pushed by a visible mushroom-shaped density in locations where an 8-fold rotationally symmetric nuclear ring is already located. The evagination dilates and grows until it merges with the ONM (Otsuka *et al*, 2016). It has been suggested that Nups play a role in promoting and stabilizing the membrane curvature required in this fusion since Nup133, Nup53 and Nup153 have been shown to contain amphipathic helices that can bind and/or bend membranes (Drin *et al*, 2007; Doucet *et al*, 2010; Vollmer *et al*, 2012, 2015). Moreover, the fact that Y-complex shows similarity to protein complexes coating endocytic vesicles is in line with this reasoning (Devos *et al*, 2004; Brohawn *et al*, 2008).
Regarding the fusion between ONM and INM, the specific mediating factors are still unknown, although torsins have been proposed to play a role, because in their absence interphasic NPC assembly intermediates have been shown to accumulate (Rampello *et al*, 2020).
The underlying molecular mechanisms of the interphasic NPC assembly pathway are still poorly characterized although it is known that Nups are recruited in a different order as compared to the postmitotic pathway (Figure 6) (D'Angelo et al, 2006a; Dultz & Ellenberg, 2010). Nup53, Nup153, POM121 as well as INM protein SUN1 seem to be recruited to the assembly site early and their membrane association has been shown to be required for the

assembly (Doucet *et al*, 2010; Vollmer *et al*, 2012, 2015; Talamas & Hetzer, 2011). Nup153 can further recruit the Nup107-Nup160 complex, while Nup53 interacts with the Nup93 and the Nup62 complexes attracting them to the assembling NPC. Only after these events, the cytoplasmic filament component Nup358 is recruited (Otsuka *et al*, 2016). Noteworthy, ELYS has been shown to be dispensable for the interphasic assembly while it is essential in the postmitotic pathway (Doucet *et al*, 2010; Vollmer *et al*, 2015).

Interestingly, the NPC spacing is kept homogeneous in the growing NE which points to a NPC distribution regulatory mechanism which must act concomitantly to their assembly (Maul *et al*, 1971; Otsuka *et al*, 2016).

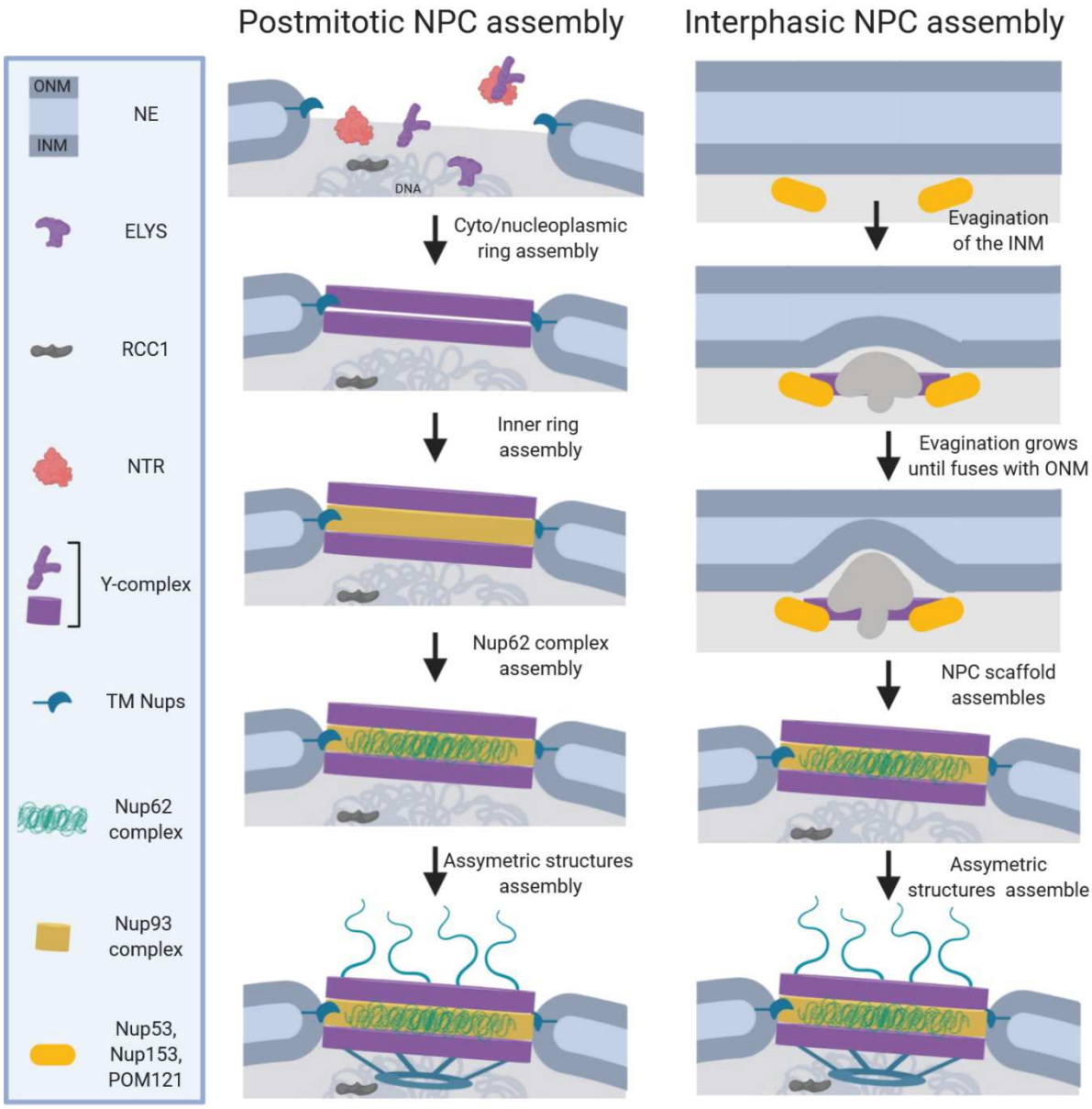

Figure 6 – Postmitotic and interphasic NPC assembly pathways. NPC assembly takes place in two different stages of the cell cycle, at the end of mitosis (left) and during interphase (right). Postmitotic NPC assembly is initiated when ELYS binds the chromatin in early anaphase and recruits the Nup107-

Nup160 complex of the nucleocytoplasmic rings. Soluble Nups sequestered by NTRs are released in the proximity of the DNA due to the RCC1 driven high Ran-GTP concentration, allowing them to be incorporated into the NPC. The resulting nucleocytoplasmic rings recruit transmembrane Nups (NDC1, POM121) which will drag the fenestrated ER membranes and will start to shrink and establish contacts with the chromatin. Then, Nup93, Nup98 and Nup62 are sequentially incorporated and the inner ring and the central channel are assembled. Finally, Nups that constitute the asymmetric structures, the cytoplasmic filaments and the nuclear basket, are recruited to form the mature NPC. During interphase, the NE is intact so the NPCs need to assemble *de novo*. At the beginning, an inside-out evagination of the INM takes place. The first Nups recruited to the region and probably needed for the membrane curvature are believed to be Nup153, Nup53 and POM21. This region already contains the nuclear ring structure underneath and the dome-shaped evagination grows and dilates until it fuses with the ONM. Additional Nups or subcomplexes are further recruited, although the sequence of the events is still unclear. Figure adapted from (Grossman et al, 2012; Otsuka & Ellenberg, 2018) and created with BioRender.com.

1.4.3. AL assembly pathway

In quickly dividing cells interphase is too short for the slow interphasic pathway to double the NPC number. These cells make use of a third pathway relying on structures called AL to keep their NPC density constant while the cell grows. ALs are cytoplasmic stacks of membranes continuous with the ER embedded with pore complexes termed Annulate lamellae pore complexes (ALPCs). These complexes are morphologically comparable to NE NPCs although their context differs since they face the cytoplasm on both sides of the membrane and they do not establish contacts with lamins, chromatin nor INM proteins. Regarding protein composition, ALPCs appear alike NPCs although some specific Nups are not present (ELYS, POM121, Tpr) (Raghunayakula *et al*, 2015). ALs have been found in nearly all cell types but they are highly abundant in germ cells and early embryonic cells, and they have been suggested to function as a maternally given storage of NPCs for their rapid cell cycles. Certainly, this pathway does not depend on *de novo* NPC assembly what makes it optimal to support quick cell divisions in early embryogenesis. A recent study has proposed that in Drosophila blastoderm embryos, where interphase takes roughly 10 minutes, ALs are inserted *en bloc* into the NE thus feeding the expanding nuclei with membranes and pore complexes at the same time (Figure 7) (Hampoelz *et al*, 2016).

Indeed, Hampoelz and colleagues showed that ALPCs in this context consist of the symmetric scaffold and they suggest that it matures and acquires the cytoplasmic filaments, the nuclear basket and the Nup62 complex only after their incorporation into the NE. Surprisingly, the permeability barrier remains unperturbed while these pore complexes are introduced into the NE (Hampoelz *et al*, 2016).

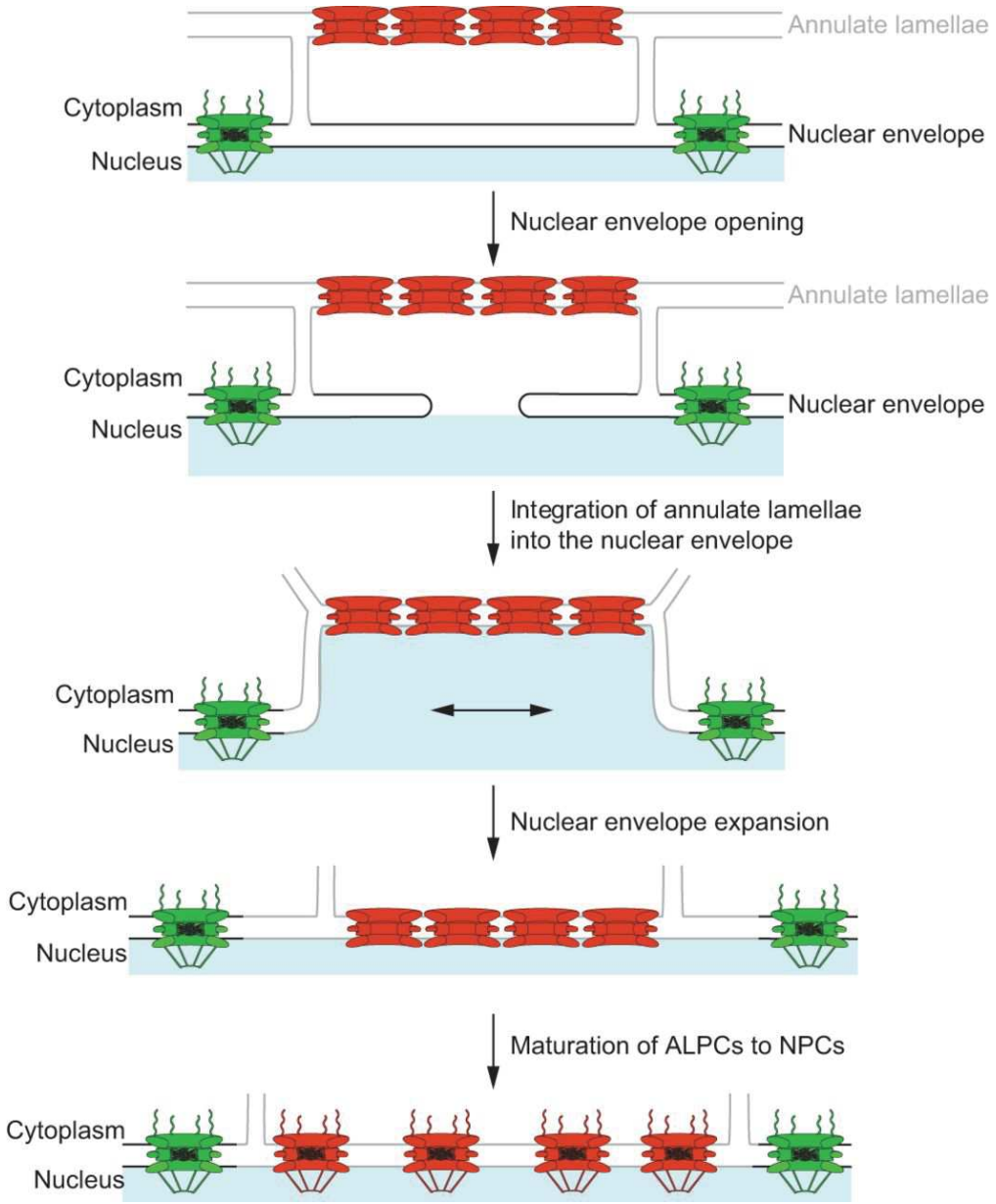

Figure 7 - Model of ALPC insertion. Hampoelz *et al.* propose that ER membrane stacks harboring immature pore complexes termed AL exist in the cytoplasm during early embryogenesis. ALs will get to the proximity of the NE and the region of the NE underlying the AL will open and retract. This way, the AL double membrane will become the new local NE and the ALPCs will mature into NPCs in the expanding nucleus. Figure from (Weberruss & Antonin, 2016).

Given that ALPC biogenesis occurs in a very different context away from the interface between the nucleoplasm and the cytoplasm, their assembly probably follows a different mechanism as compared to the two canonical assembly pathways. Indeed, the same group has also studied the origin of ALPCs during Drosophila oogenesis and found that it relies on the formation of various granules containing condensed Nups (Hampoelz *et al*, 2019b). In the maternal nurse cells of the Drosophila egg chamber Nup358 (also known as RanBP2) condenses and forms larger granules which are surrounded by nup358 mRNA (suggesting a localized translation

process that could promote condensation). At the same time, scaffold and FG-Nups condense into distinct granules in the oocyte. Nup358 granules travel towards the oocyte and interact with oocyte-specific granules in a microtubule dependent manner and near ER membranes. It has been suggested that AL biogenesis is inhibited in nurse cells by the high Ran-GDP cytoplasmic levels, which promotes formation of the importin-Nup complexes to keep the Nups in a soluble state and inhibit their condensation. On the contrary, the oocyte cytoplasm shows high levels of Ran-GTP, which is likely to promote condensation of FG-Nups and scaffold Nups into the oocyte-specific granules by inhibiting importins' chaperoning role. Once the Nup358 granules travel to the cytoplasm of the oocyte, microtubule dynamics promote contacts, mixture and material transfer between the different types of Nup granules. This model (Figure 8) proposes that after these granules interact, Nups are transferred to a neighboring ER membrane where AL-PCs assemble. Eventually, larger stacks with multiple membrane sheets form and can be used as a NPC storage in rapidly dividing cells during early embryogenesis.

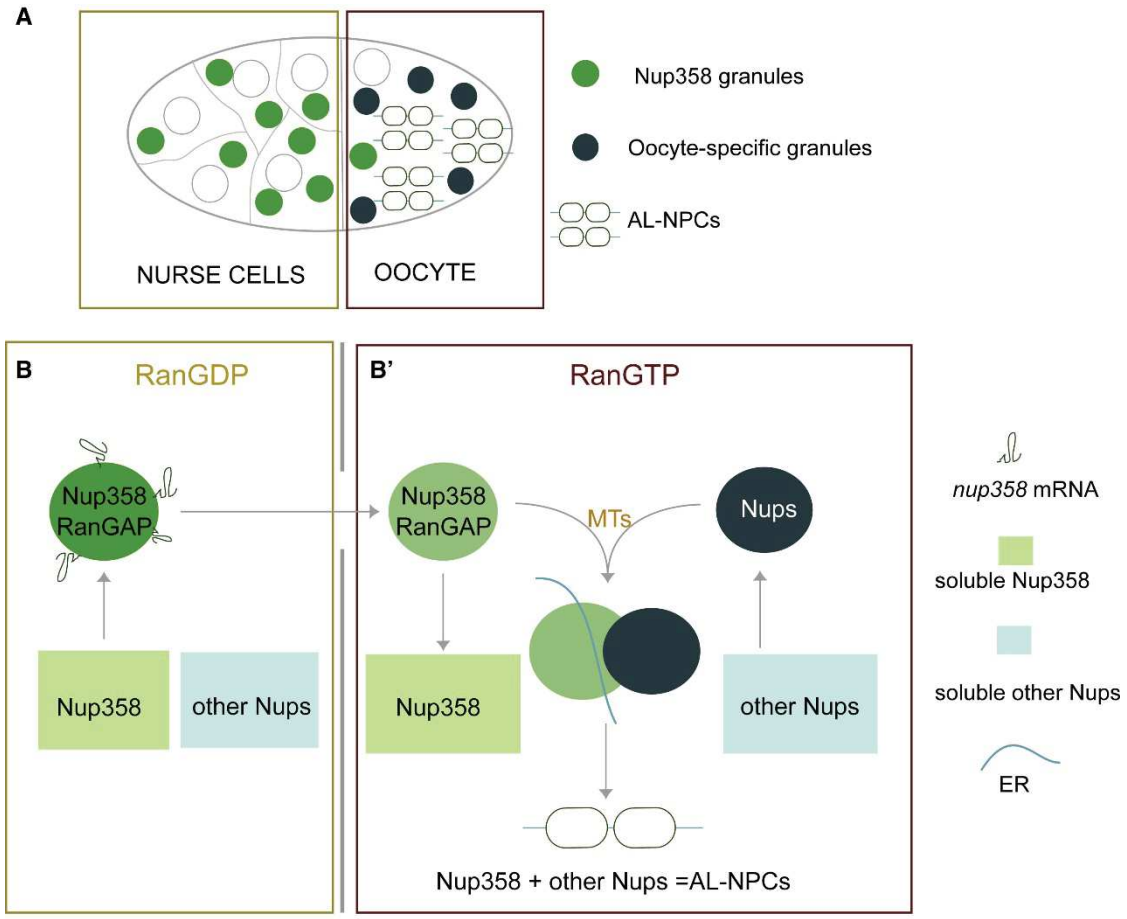

Figure 8 - ALPC biogenesis model in *Drosophila melanogaster* oocytes.
A A scheme of the Drosophila egg chamber: nurse cells (left chamber) and the oocyte (right chamber) form the germline and both are surrounded by follicle cells (not shown). In mid oogenesis, nurse cells show high concentration of cytoplasmic condensed Nup358 granules while the oocyte cytoplasm is rich

in oocyte-specific granules (containing condensed scaffold Nups and other FG-Nups), ALs, and, to a lesser extent, also Nup358 granules.
B Nurse cells contain condensed Nup358 granules decorated with Nup358 mRNA, which suggests localized translation and condensation events. The condensation of other types of Nups would be inhibited by the high Ran-GDP concentration of the cytoplasm in nurse cells where importins would keep them in a soluble state. On the contrary, the oocyte cytoplasm shows high levels of Ran-GTP, which is likely to promote FG-Nup and scaffold Nup condensation in oocyte-specific granules by avoiding importins' chaperoning role. Nup358 granules travel to the oocyte where they interact with oocyte-specific granules in a microtubule dependent fashion and transfer their contents to ER sheets allowing ALPC assembly. During early embryogenesis, these ALPCs are inherited to the embryo where they feed the rapidly dividing nuclei with membranes and future NPCs.
Figure from (Hampoelz *et al*, 2019b).

1.5. Phase separation

As mentioned before, FG-Nups contain intrinsically disordered regions (IDRs) meaning that they do not have a stable secondary nor tertiary structure. This feature makes them prone to phase separation and aggregation (Lemke, 2016; Schmidt & Görlich, 2016). Indeed, Nups have been found in several phases as amyloid fibers (Halfmann *et al*, 2012; Milles & Lemke, 2011), hydrogels (Frey *et al*, 2006; Frey & Görlich, 2007) and liquid droplets (Hampoelz *et al*, 2019b).

1.5.1. Phase separation in cells

Phase separation is understood as a physical process by which a supersaturated solution of components (as the cytoplasm can be) spontaneously separates into a concentrated phase and a diluted phase for a specific component or a selection of components. These two phases can coexist in a stable manner. Although this phenomenon has been long known and used in chemistry, its implication in cell biology and in the formation of membrane-less organelles (cellular compartments with specific components and functions that are not enclosed by lipid bilayers) has only started to be studied in the last two decades (reviewed in (Boeynaems *et al*, 2018). The role of phase separation in membrane-less organelle formation was first proposed in 2009 when Brangwynne and colleagues showed that P granules (a class of perinuclear granules in *Caenorhabditis elegans* germline containing specific RNAs and proteins) behave like liquid and their localization and enrichment is regulated by dissolution and condensation (Brangwynne *et al*, 2009). They described these liquid droplets as bodies with round appearance, deformable (they underwent fission and fusion) and constantly exchanging components with the surrounding milieu. After this seminal discovery, many other granules have been described as supramolecular assemblies and membrane-less organelles governed by

the phase separation phenomenon; such as the nucleolus, Cajal bodies, nuclear speckles, stress granules (SG), P-bodies, germ granules and PML bodies which all play specific roles in cellular homeostasis (Boeynaems *et al*, 2018; Courchaine *et al*, 2016). From this point of view, macromolecules in the cell can be seen as components that transition between different material states, ranging from soluble to liquid, to hydrogel and to amyloid fibers depending on their behavior (further explained in Figure 9).

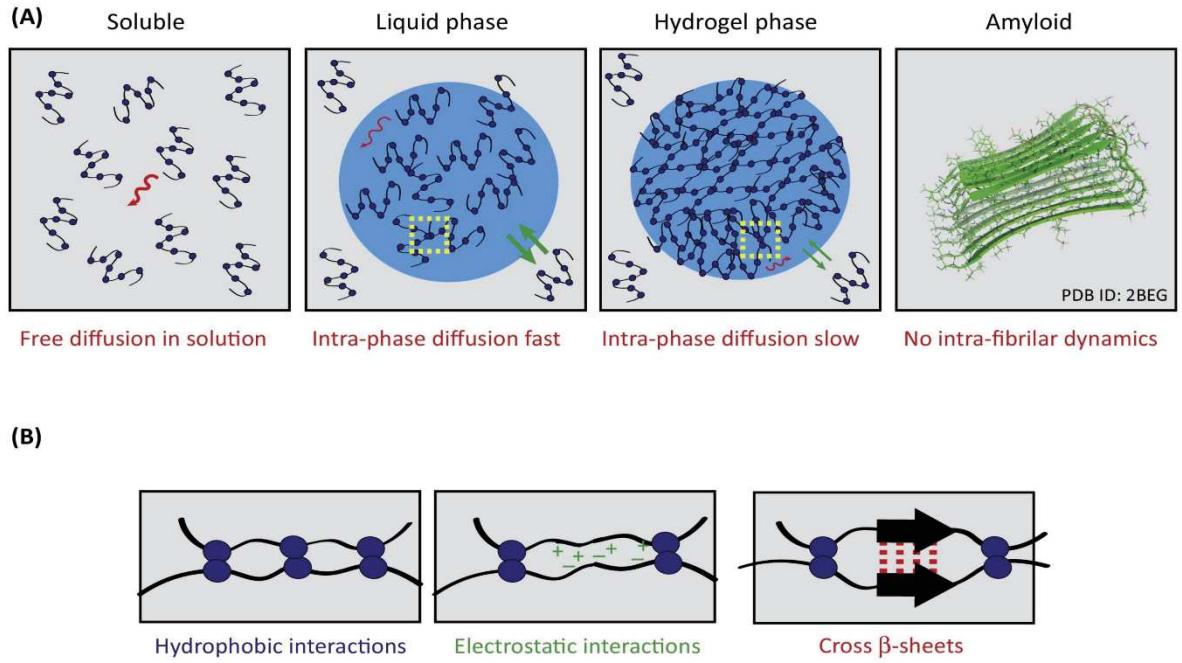

Figure 9 - Intracellular protein phases and the interactions that maintain them.
A Soluble proteins move freely in the cells (red arrow). Proteins with certain characteristics and under specific conditions undergo liquid-liquid phase separation and form liquid droplets. These droplets still show rapid protein diffusion (red arrow) and also exchange with soluble monomers outside the droplet (green arrows). In hydrogels, the diffusion rate of proteins within the droplet (small red arrows) and the exchange speed with the environment (small green arrows) are much slower. When proteins form amyloid fibrils, they show a static behavior and they do not go back to the surrounding milieu as soluble monomers.
B Proteins that phase separate are usually rich in hydrophobic and charged residues. Hydrophobic interactions are thought to be responsible for bringing proteins together, and electrostatic interactions additionally stabilize phase separation. Liquid droplet and hydrogels rely on these mentioned interactions. When the constituent proteins organize in cross beta-sheet structures they form amyloid fibrils.
Figure adapted from (H. Broder Schmidt and Görlich 2016).

These states can be distinguished by studying their constituents' dynamic behavior. Liquid droplets for example can fuse and deform in response to flows (Brangwynne *et al*, 2009), and the quick rearrangement of their constituents and exchange with the environment can be observed by fluorescence recovery after photobleaching (FRAP) experiments (Hampoelz *et al*,

2019b). By contrast, the fluorescence recovery speed is much lower in hydrogels which have a solid-like behavior (Schmidt & Görlich, 2015; Frey *et al*, 2006). Amyloids are structurally formed by cross-beta spines and can be detected *in vitro* or in histological sections using thioflavin-T which increases its fluorescence when bound to amyloid fibrils (Biancalana & Koide, 2010).

1.5.2. Factors regulating phase transition

The factors controlling phase transitions include the intracellular concentration and distribution of the components, interaction multivalence among proteins and RNAs, molecular chaperones and post-translational modifications (PTMs), which will be discussed further in this chapter.

The ability of the components to form multivalent protein-protein, and protein-RNA interactions is crucial for phase separation (Feng *et al*, 2019). A protein is considered to be multivalent when it can establish simultaneous inter- or intra-molecular interactions with several partners or target sites. As a result of these interactions, proteins tend to form oligomers or polymers which are less soluble and more likely to undergo phase separation (demix). In this context, IDRs are ideal scaffolds to contain multiple short linear interacting motifs due to their unfolded and exposed nature. Proteins which are prone to phase separate very often contain IDRs, and indeed, concentrated solutions of different IDRs have been shown to spontaneously form hydrogels (Kato *et al*, 2012). IDRs are often enriched in uncharged polar amino acids, charged polar amino acids or aromatic amino acids, and they are often found in short motifs alternating charged sequences.

Another factor regulating phase separation is the nucleic acid content. RNA has been shown to have a nucleating role in membrane-less organelles and to promote phase separation of its RNA-binding proteins (RBPs) (Boeynaems *et al*, 2017; Kedersha *et al*, 2013; Van Treeck *et al*, 2018). For example, NEAT-1 non-coding RNA is required for para-speckle formation (Fox & Lamond, 2010) while free mRNA released from polysomes upon stress induction nucleates SGs (Kedersha *et al*, 2000). Moreover, the structure of RBPs themselves also contributes to phase separation because they are multivalent modular domain proteins (Lunde *et al*, 2007). Indeed, many RBPs that demix into liquid states can be subsequently transformed into pathological amyloids (Harrison & Shorter, 2017; Lin *et al*, 2015; Shorter, 2019), which have been linked to many neurological disorders (Shin & Brangwynne, 2017).

PTMs play an important role in phase separation and several events of phosphorylation, methylation, acetylation, citrullination, N-acetylglucosaminylation, ribosylation, SUMOylation and ubiquitylation have been shown to regulate the formation and disassembly

of condensates and to modulate their characteristics (Hofweber & Dormann, 2019; Snead & Gladfelter, 2019; Owen & Shewmaker, 2019). PTMs can regulate the interactions between components to promote or reverse phase separation depending on the physiological context in order to adapt to cellular needs. The speed and reversibility of protein phosphorylation makes it ideal to influence phase transition in response to different conditions (Aumiller & Keating, 2016). For example, the phase separation of the RBPs Fused in Sarcoma (FUS), TDP-43 and Tau (all known to be implicated in neurological diseases) is regulated by phosphorylation (Monahan *et al*, 2017; Wang *et al*, 2018). In the case of Tau protein (which misfolds and accumulates into neurofibrillary tangles in Alzheimer's disease), phosphorylation promotes its phase separation (Ambadipudi *et al*, 2017) and N-acetylglucosaminylation, inhibits its aggregation (Yuzwa *et al*, 2012). Another example of N-acetylglucosaminylation was reported by Labokha and colleagues, who showed that this PTM drastically changed the permeability properties of a Nup98 hydrogel (Labokha *et al*, 2012). Additionally, the phase separation of the RBP Fragile X Mental Retardation Protein is promoted by phosphorylation and opposed by methylation (Tsang *et al*, 2019).

The cellular condensates are also regulated by molecular chaperones. Chaperones are proteins that consume energy to help in protein folding and to modulate protein-protein interactions. Recently, the chaperone concept has been adopted by the phase separation field to refer to proteins that regulate the material features and biomolecular condensates. For example, SG chaperones have been reported to be part of these condensates and regulate their dynamics and dissolution after stress release (Cherkasov *et al*, 2013). Another study described that amyotrophic lateral sclerosis (ALS) misfolded SOD1 variants aggregate in SGs in human cells altering their behavior. Chaperone recruitment to these compartments inhibited the formation of these abnormal SGs and stimulated their disassembly when the stress ceased (Mateju *et al*, 2017). It has also been observed that NTRs such as Karyopherin β2 and Importin α/β can inhibit phase transition of target RBPs and also solubilize fibrils of already phase separated target proteins (for example FUS in the case of Karyopherin β2 and TDP-43 in the case of Importin α/β) (Springhower *et al*, 2020). Overall, chaperones function as guardians of proper phase transitions.

1.5.3. Nups and phase separation

One example of a large protein assembly consisting of IDR-containing proteins (the FG-Nups) is the NPC (Knockenhauer & Schwartz, 2016; Sakuma & D'Angelo, 2017). In vertebrates the NPC contains 11 different FG-Nups (Figure 4), 13 MDa of FG-domain mass and 5000 FG

motifs (Ori *et al*, 2013). Interestingly, FG-domains do not follow the rules of traditional IDRs which usually have low hydrophobicity and high net charge that allow them to keep their unfolded state in solution (Uversky *et al*). Instead, FG-Nups are highly hydrophobic and contain very few charged amino acids (Schmidt & Görlich, 2016). For this reason, aliphatic alcohols like hexanediols are good solvents for FG-Nup condensates because they probably compete with the hydrophobic interactions between FG-repeats (Patel *et al*, 2007).

The cohesive interactions between different and the same types of FG-domains and also NTR-cargo complexes are multivalent, and they are essential for the integrity of the permeability barrier (Frey & Görlich, 2007; Patel *et al*, 2007; Frey *et al*, 2006; Ader *et al*, 2010; Milles & Lemke, 2011). Indeed, it was shown that FG domains can form elastic and reversible hydrogels that mimic the permeability properties of NPCs (Labokha *et al*, 2012; Schmidt & Görlich, 2015), and that this is due to the cross-linking of the FG-domains by interactions between phenylalanines (Frey & Görlich, 2007). Importantly, it has been shown that this hydrogel formation is essential for survival in yeast (Frey *et al*, 2006). Of note, the cohesive abilities of FG-Nups allow not only for the formation of the permeability barrier but also for building the links with the structural scaffold elements of the NPC (Onischenko *et al*, 2017).

Nuclear magnetic resonance spectroscopy studies have allowed to identify another type of interactions within an Nsp1 yeast Nup hydrogel which involve the asparagine-rich linker sequences of different FG-Nups. These sequences form amyloid-like beta-sheets and they have been proposed to confer kinetic stability to the permeability barrier and to suppress the passive transport through NPCs (Ader *et al*, 2010). The observed amyloid-like beta-sheets are not likely to be similar to traditionally known amyloid fibrils that accumulate in several pathologies like Alzheimer's disease, since amyloid-like Nup166 hydrogels are hexanediol-sensitive while amyloids are not (Schmidt & Görlich, 2015).

Nups can also form liquid-like condensates; they have been observed to form AL precursor liquid droplets (Hampoelz *et al*, 2019b) and also to be sequestered into SGs (Zhang *et al*, 2018) and in various pathological aggregates in the nucleus and in the cytoplasm (Hutten & Dormann, 2020; Li & Lagier-Tourenne, 2018). A fraction of cytoplasmic Nups was also identified in the promyelocytic leukemia protein (PML)-positive structures, the so-called CyPNs (cytoplasmic accumulations of PML and Nups), which could move along the microtubules to dock at the NE (Jul-Larsen *et al*, 2009), although the cellular roles of the CyPNs remain to be understood.

Altogether, the cited studies indicate that Nups have an intrinsic capacity to phase separate, suggesting that regulatory mechanisms that control transitions may exist in the cell. Indeed, Nups are synthesized as soluble proteins in the cytoplasm (Davis & Blobel, 1987) and in

Drosophila embryos a large excess of soluble Nups has been reported (Onischenko *et al*, 2004). How the balance of soluble Nups is controlled, and which factors regulate the localized assembly of Nups is currently unknown.

1.5.4. Nup mislocalization in neurological diseases

Several neurodegenerative disorders have been associated with pathological aggregation of specific proteins, such as Amyotrophic lateral sclerosis (ALS), Frontotemporal dementia (FTD), Alzheimer's disease (AD) and Huntington's disease (HD) amongst others (Figure 10). In the case of ALS and FTD patients, the RBP TDP-43 or FUS proteins accumulate and aggregate in the cytoplasm of neurons (Mackenzie *et al*, 2010). These two pathologies are considered the same disease spectrum and can rely on the same molecular causes such as, for example, the hexanucleotide (G4C2) expansion in the C9ORF72 gene (DeJesus-Hernandez *et al*, 2011). Some FTD patients exhibit another type of cytoplasmic aggregates containing the microtubule-binding protein Tau in neurofibrillary tangles, a phenotype shared with AD patients (Bodea *et al*, 2016). HD is caused by a CAG trinucleotide expansion in the huntingtin gene which is expressed as a huntingtin protein with glutamine repeats (polyGln) that tends to aggregate in the cell (Jimenez-Sanchez *et al*, 2017).

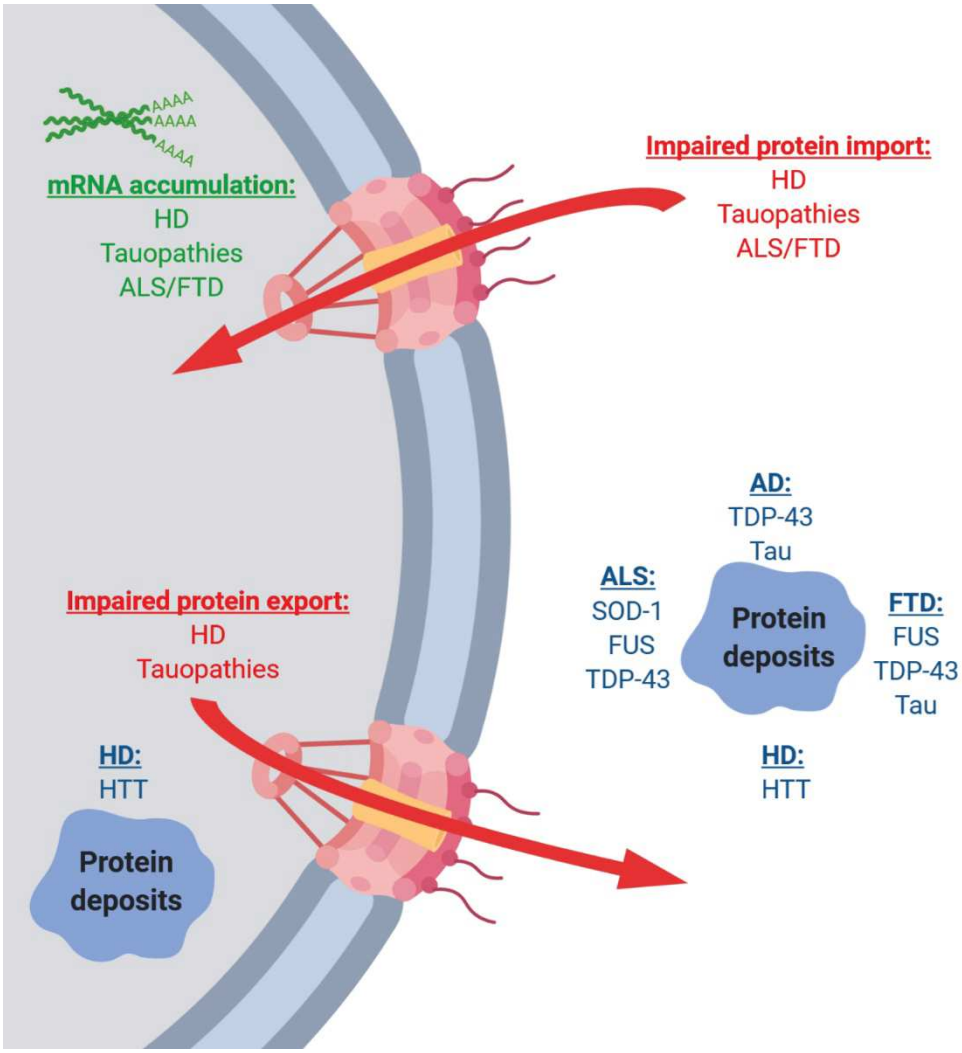

Figure 10 - Intracellular protein aggregates and nucleocytoplasmic transport defects in neurodegenerative diseases. Proteins that aggregate in their respective neurodegenerative diseases and subcellular locations are indicated in blue. Nucleocytoplasmic transport defects (impaired protein import or export) and related disorders are indicated in red. Neurodegenerative diseases in which nuclear mRNA accumulation has been observed are shown in green. Figure adapted from (Hutten & Dormann, 2020) and created with BioRender.com.

Studies during the last years have identified NPC alterations and disruption of nucleocytoplasmic transport as a new hallmark of these pathologies (Figure 10) (reviewed in N. Li and Lagier-Tourenne 2018; Hutten and Dormann 2020). The team of Jeffrey D. Rothstein reported these defects in several diseases. In the case of ALS, protein import assays displayed a decreased import rate in iPSC derived from patient neurons and the presence of RanGAP1 in the pathological cytoplasmic protein aggregates (Zhang *et al*, 2015). They also observed import and export defects, a leaky permeability barrier and aberrant Nup62 and RanGAP1 nuclear aggregation using induced pluripotent stem cell derived neurons from HD patients and a Drosophila model of HD (Grima *et al*, 2017). Similar observations were reported for AD;

pathological Tau cytoplasmic aggregates and fibrils were shown to directly interact with Nups and affect NPC functioning causing nuclear leakiness and Ran mislocalization in AD brain tissue and in Tau-overexpressing transgenic mice (Eftekharzadeh *et al*, 2018). Another way of indirectly investigating the export defects is the analysis of the nucleocytoplasmic ratio of polyA-mRNA, although these experiments must be interpreted with caution since nuclear mRNA accumulation could be also caused by other defects. In this regard, several groups have observed an accumulation of nuclear polyA-mRNA in different neurodegenerative models, such as a transgenic ALS and FTD fly models (Freibaum *et al*, 2015), a Drosphila model of tauopathy overexpressing a Tau mutant (Cornelison *et al*, 2019), human cells transfected with fragments of mutant huntingtin and TDP-43 (Woerner *et al*, 2016) and HD patients and mouse models (Gasset-Rosa *et al*, 2017). It is important to keep in mind that, mechanistically, it is still unknown if the nucleocytoplasmic transport defects observed in these different neurodegenerative diseases are a cause or a consequence of the pathological protein aggregates/fibrils.

As mentioned above, import and export defects have often been observed simultaneously with mislocalization of NPC components and/or factors of the nucleocytoplasmic transport machinery (Table 1). Almost all different parts of the NPC and Nups belonging to different types (FG-Nups and non-FG-Nups) have been shown to be affected or mislocalized in different neurodegenerative disorders (Hutten & Dormann, 2020). It is still not known when these mislocalization events occur in the course of the diseases and if they are indeed responsible for the import and export defects. It is also unclear what the origin of these mislocalized Nups is; if they are extracted from pre-inserted NPCs at the NE or if they are newly made soluble Nups utilized for the NPC turnover. Moreover, almost all NPC assembly studies have been carried out in actively proliferating cells, which constitute a very different context as compared to quiescent populations like neurons, making the applicability of this knowledge very limited.

	ALS / FTD			Tauopathies	HD
	TDP43-opathy	C9-ALS/FTD	FUS-opathy	SOD1-opathy	AD/Tau-FTD	
Cytoplasmic mislocalization	Nup358 Nup98 Nup214 Nup93 Nup160 Nup88 Nup153 Nup62 Nup155 Nup58 Nup205 Nup35 Nup107 GC1 Aladin Gle1 POM121 Importin-α3	POM121 Nup205 Nup107 Importin-α3 RanGAP1 RCC1 Ran	TNPO1	Nup205 Nup107 Nup88 Nup50 Nup62 RanGAP1 Importin-α/β	Nup98 Nup62 Importin-α NTF2 Ran	Gle1 RanGAP1 Ran
Nuclear mislocalization	Nup205 Nup107 POM121 RanGAP1					Nup88 Nup62 RanGAP1

Table 1 - Mislocalization of nucleocytoplasmic transport components in neurodegenerative diseases. The table shows Nups (in black) and other nucleocytoplasmic transport factors that are not part of the NPC (red) reported to be mislocalized in the cytoplasm (upper part) or the nucleus (lower part) relative to each neurodegenerative disease mentioned in the text (ALS/FTD, Tauopathies and HD). Table adapted from (Hutten and Dormann 2020).

Concomitant with the non-functional nucleocytoplasmic transport and mislocalized Nups, aberrant nuclear shape has also been reported in several of the above-mentioned neurodegenerative diseases, such as HD (Liu *et al*, 2015; Gasset-Rosa *et al*, 2017), AD (Eftekharzadeh *et al*, 2018; Sheffield *et al*, 2006; Frost *et al*, 2016) or ALS/FTD (Paonessa *et al*, 2019; Gautam *et al*, 2019; Kinoshita *et al*, 2009; Chou *et al*, 2018). In many disease models and in patient samples the NE looks irregular and displays "wrinkles", invaginations or herniations. However, the implication of these defects in the diseases are not known; it is again unclear whether they are a cause or a consequence of the nuclear import and export deficiencies.

Interestingly, the aforementioned defects in nucleocytoplasmic transport, Nup localization and NE shape are also features shared by ageing cells (D'Angelo *et al*, 2009). D'Angelo and colleagues observed in ageing *C. elegans* that scaffold Nups do not turnover in differentiated cells and they are part of NPCs during the whole life of the cell. Moreover, they suggest that these long-lived Nups accumulate damage during aging and contribute to NE permeability defects making them leaky.

1.6.Fragile X Syndrome and Fragile X related proteins

1.6.1. Fragile X syndrome

The Fragile X syndrome (FXS) is the most common form of inherited intellectual human disability worldwide, for which no efficient therapy exists to date (Santoro *et al*, 2012; De Vries *et al*, 1997; Mullard, 2015). It is caused by the inactivation of the fragile X mental retardation protein (FMRP) protein which is encoded by the *FMR1* gene located at the X chromosome in the position Xq27.3. The 5'UTR of the gene contains CGG trinucleotide repeats which vary from 5 to 50 repeats in the normal population (Oberlé *et al*, 1991). When the CGG expansion exceeds 200 CGG units (known as "full mutation" or FXS) the repeat region and the promoter are hypermethylated and the *FMR1* gene is transcriptionally silenced (Pieretti *et al*, 1991) leading to an absence of the encoded FMRP protein and the development of FXS (Verheij *et al*, 1993) (Figure 11). While carrying out metaphase spreads to observe the chromosomes, this hypermethylated region in the X chromosome appears as a constriction, which was traditionally used as a marker for diagnosis of this disease accordingly termed "Fragile X syndrome". In the majority of cases, the syndrome is caused by the described hypermethylation and the silencing of the *FMR1* gene, however missense mutations and deletions of the gene have also been reported to cause this syndrome (De Boulle *et al*, 1993; Myrick *et al*, 2014; Coffee *et al*, 2008).

When the CGG repeats amplify in the gene to a lesser extent (from 55 to 200 CGG repeats), they are known as 'premutation' and are associated with a risk for the fragile X-associated tremor/ataxia syndrome (FXTAS, a neurodegenerative disorder with intention tremor that occurs mainly in old men with the premutation) and the fragile X-associated primary ovarian insufficiency (FXPOI, in which one out of five women have fertility problems early in life) (Patzlaff *et al*, 2018). The FMR1 gene with the premutation is transcribed to a higher extent than the wild type (WT) gene, although the FMRP protein levels are lower (Figure 11). Recently, it was suggested that the repeat-associated non-ATG (RAN) translation of the gene results in a FMRpolyGlycine protein which is pathogenic and affects the NE architecture in neurons (Sellier *et al*, 2017).

Since this gene is located on the X chromosome, men are more affected by this disease than women (penetrance is almost 100% in males and 50% in females) because of the compensation of the second X chromosome and its random inactivation, having an estimated frequency of 1/4000 and 1/7000 respectively (Santoro *et al*, 2012). Moreover, the CGG premutation repeats

of the 5'UTR of *FMR1* gene have the tendency to expand through meiosis meaning that full mutations are observed in later generations.

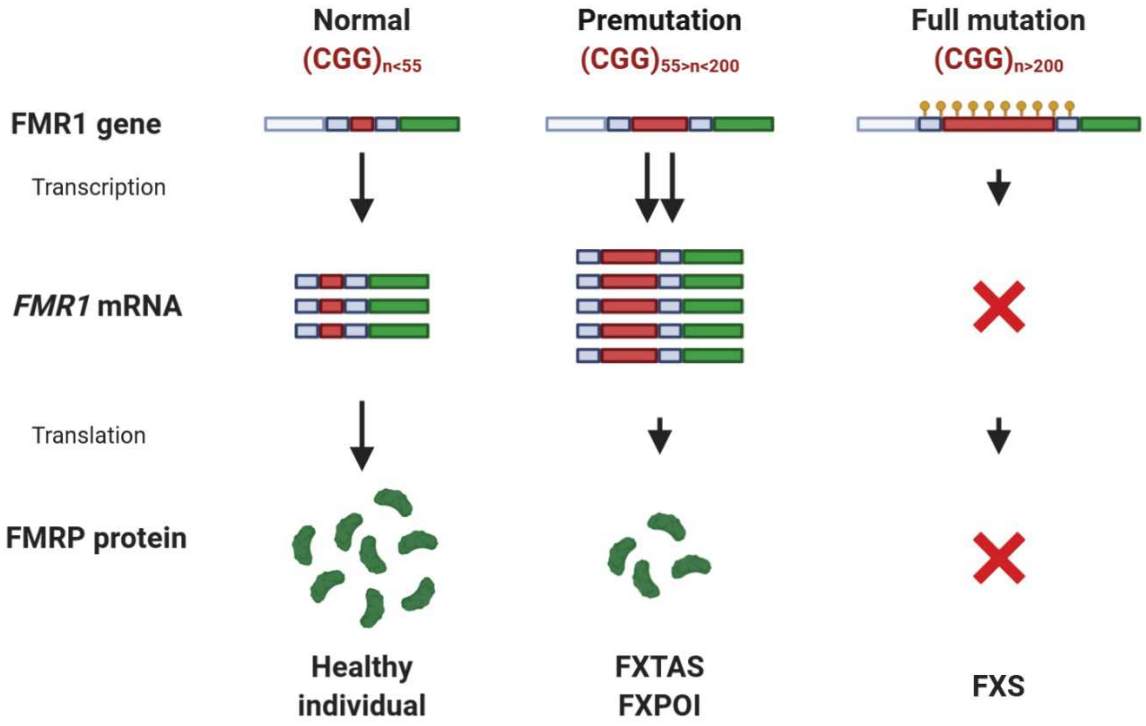

Figure 11 - *FMR1* gene expression patterns in normal, premutation and full-mutation individuals. The 3'UTR region is indicated in blue, the CGG repeats are indicated in red and the coding region and proteins are indicated in green. Healthy individuals have less than 55 CGG repeats in the 5'UTR region of *FMR1* gene, which leads to normal transcription of the gene and appropriate FMRP levels. In the premutation (55-200 CGG repeats), FRM1 mRNA levels are increased although FMRP protein levels are decreased. Individuals with the premutation are at risk to develop FXTAS and fragile X–related FXPOI. In the full mutation (more than 200 CGG repeats), the 5'UTR region is hypermethylated (yellow) and the gene is transcriptionally silenced. These individuals lack FMRP and develop FXS. Figure adapted from (Hagerman & Hagerman, 2002) and created with BioRender.com.

FXS patients display various symptoms including a delay in cognitive development (such as language delay), a wide range of mental retardation from mild to severe, autism, anxiety, aggressiveness, spontaneous epileptic seizures, attention deficits, poor eye contact, hypotonia and coordination problems, macroorchidism in males, prominent ears, macrocephaly, long face with prominent jaw and forehead, hyperextensible joints and flat feet among others (Hagerman *et al*, 2009). Patients with mosaicism (related to the number of repeats or to the methylation) are more mildly affected because disease severity is related to the extent of the methylation and FMRP levels. At the cellular level, immature dendritic spines in neurons of FXS patients and

Fmr1 knockout mouse models have been reported (Comery *et al*, 1997; Kaufmann & Moser), which have been postulated to cause the mental retardation phenotypes.

1.6.2. FXR protein genes and expression pattern

FMRP belongs to the Fragile X related (FXR) protein family together with Fragile X related protein 1 and 2 (FXR1P and FXR2P) and they are RBPs displaying a high degree of structural and sequence similarity (sequence similarity of 60%) (Li & Zhao, 2014). *FXR1* gene is located at chromosome 3q27 and *FXR2* at chromosome 17p13.

As already mentioned, in humans, the *FMR1* gene contains 5-50 CGG repeats in the 5' UTR, however, this is not a conserved feature across species since they are not found in *X. laevis* (Siomi *et al*, 1995, 1) and in *Drosophila melanogaster* only 8 repeats are found (Ashley *et al*, 1993). Besides, CGG repeats are not present in 5'UTRs of *FXR1* nor *FXR2* genes.

Regarding the expression pattern, the three genes are expressed ubiquitously in fetal and adult tissues and are particularly high in brain and testis (De Diego Otero *et al*, 2002; Tamanini, 1997; Agulhon *et al*, 1999; Devys *et al*, 1993). In the brain, FMRP, FXR1P, and FXR2P are co-expressed in the cytoplasm of neurons. *FXR1* is especially highly expressed in skeletal and cardiac muscle tissue where FMRP levels are particularly low (De Diego Otero *et al*, 2002; Kirkpatrick *et al*, 1999; Tamanini, 2000; Khandjian, 1998; Bakker *et al*, 2000). During embryonic development, the three genes are differently expressed, *FXR1*'s expression being higher and earlier than its paralogues'. Moreover, the expression pattern of the FXR1P also changes over time; is cytoplasmic and nuclear in fetal brain while only cytoplasmic in adult neurons. These observations suggest that FXR1P has a specific function not shared by its paralogues (De Diego Otero *et al*, 2002) and it probably explains why *Fxr1* knockout mice die shortly after birth in contrast to *Fmr1* or *Fxr2* knockout mice (Hoogeveen *et al*, 2002). Contrary to FXR1P, FXR2P levels in fetal brain are much lower than in adults.

The fact that FXR1P and FXR2P are co-expressed with FMRP in neurons and they are still expressed in FXS patients indicates that they cannot completely compensate the absence of FMRP.

FMR1 and *FXR1* transcripts are known to undergo alternative splicing generating isoforms with molecular weights in the range of 70-80 kDa (Ashley *et al*, 1993; Verheij *et al*, 1993; Siomi *et al*, 1995; Kirkpatrick *et al*, 1999) (Figure 12). Contrary to *FMR1, FXR1* gene's alternative splicing is tissue-specific suggesting that different FXR1P isoforms could have different functions depending on the tissue (Kirkpatrick *et al*, 1999). Regarding subcellular localization, the three FXR proteins shuttle between nucleoplasm and cytoplasm. FXR2P and

some FXR1P isoforms also localize to the nucleolus because of their nucleolar targeting signal (NoS) which is absent in FMRP (Tamanini *et al*, 1999a; Tamanini, 2000). Altogether, this suggests that the three members of the FXR protein family play some specific functions.

1.6.3. Animal models

In order to understand the role of FXR proteins at the molecular, cellular and the behavioral level in a more physiological context, several animal models have been developed. Special efforts have been made to develop FXS animal models and study FMRP's functions in several species due to its implication in disease, such as mouse, fruit fly and zebrafish (Tucker *et al*, 2004; Kooy *et al*, 1996; Drozd *et al*, 2018).

The *Fmr1* KO mouse was created in 1994 by disrupting the *Fmr1* exon 5 and initially characterized by the Dutch-Belgian Fragile X Consortium (Bakker & Reyniers, 1994). Since then, it has become the most used FXS mouse model and many laboratories continue to use it to study FMRP and FXS. Despite not being a genetically faithful model of the FXS, the *Fmr1* knockout mouse also leads to the absence of FMRP. This mouse model does not reproduce the majority FXS physical characteristics but it displays macroorchidism, abnormal dendritic spine morphology and behavioral and cognitive defects (Kooy *et al*, 1996). Importantly, different studies over time have shown distinct and even contradictory behavioral, anxiety and cognition phenotypes in the knockout mouse model (Kazdoba *et al*, 2014). This could be due to genotypic differences between the KO mice and the FXS patients (deletion versus CGG expansion and hypermethylation), although it could also reflect the phenotypic heterogeneity of FXS patients. Indeed, FXS affected individuals show a wide range of cognitive defect symptoms. *Fmr1* KO mice are being used in pharmacological studies and proving to be a valid model since they mimic findings in FXS patient trials.

In the case of *Fxr2* KO mouse model, it did not show defects in the tissue level in brain or testis, where it is more highly expressed as compared to *Fmr1*. However, behavioral and cognitive tests showed that these mice had a similar phenotype to *Fmr1* KO mice including the hyperactivity (Bontekoe, 2002).

Homozygous *Fxr1* knockout mice have also been created and observed to die shortly after birth presumably because of cardiac muscle and lung failures (histochemical analysis showed altered muscle cellular architecture) (Mientjes, 2004). These results suggest that, unlike FXR2P and FMRP, FXR1P is an essential protein for development.

In *Drosophila melanogaster* only one homologue has been identified, known as *dFMR1*, which facilitates *FMR1* genetic studies. It shares high level of sequence homology with human *FMR1*,

FXR1 and *FXR2* genes (Drozd *et al*, 2018). Null d*FMR1* fly mutants show defects in neuron morphology and synaptic function along with deficient long-term memory and abnormal behavior (decreased interest in courtship) (Dockendorff *et al*, 2002; Morales *et al*, 2002; Bolduc *et al*, 2008).

1.6.4. FXR proteins' domain organization

The three members of the FXR protein family share high homology in their amino acid sequence and in domain organization (Figure 12), especially in the N-terminal (86% identity between FMRP and FXR1P, and 70% identity between FMRP and FXR2P).

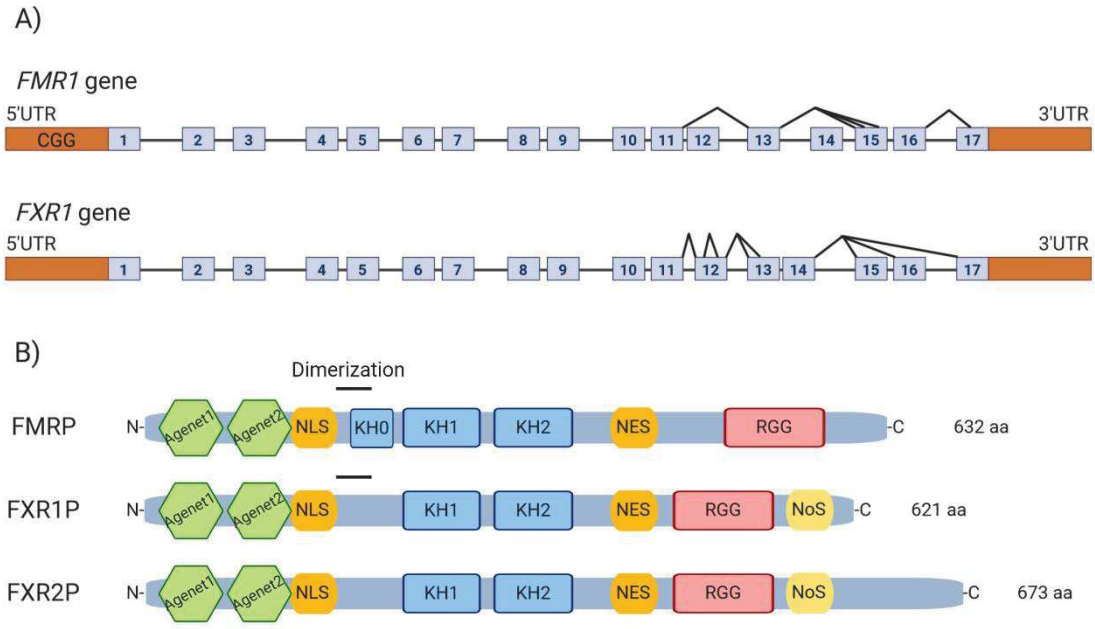

Figure 12 - *FMR1* and *FXR1* genes and FXR protein family.
A *FMR1* and *FXR1* genes. Exons are depicted in blue and untranslated regions in brown. Black lines indicate introns and alternative splicing leading to 12 FMRP isoforms and 7 FXR1P isoforms. The CGG trinucleotide repeats which get expanded in FXS are indicated in the 5'UTR of *FMR1* gene.
B FXR proteins. FMRP, FXR1P and FXR2P constitute the FXR protein family. They share high homology in the protein sequence of domains. They contain two Agenet domains (green) which can interact with methylated histones, a NLS and a NES (yellow) that allow the proteins to shuttle between nucleus and cytoplasm, three RNA binding domains (K homology domains in blue, KH, and arginine-glycine rich domain in pink, RGG) and a nucleolar-targeting signal (NoS, in light brown). FXR proteins have been show to form homo and heterodimers through a dimerization region (black line). Figure adapted from (Santoro, Bray, and Warren 2012; Kirkpatrick, McIlwain, and Nelson 1999; Y. Li and Zhao 2014) and created with BioRender.com.

FXR proteins possess a tandem Agenet domain in their N-terminal region which mediates the interaction with methylated histones (Adams-Cioaba *et al*, 2010; Alpatov *et al*, 2014; Maurer-Stroh *et al*, 2003). FMRP binding to chromatin through this domain has been shown to be

required for the role of FMRP in DNA damage response (Alpatov *et al*, 2014). Moreover, it has been reported that the tandem Agenet domain of FMRP interacts with the aggregation-prone protein FUS, and interestingly, FMRP downregulation inhibits cytoplasmic FUS aggregation (He & Ge, 2017).

FXR proteins contain several conserved RNA-binding domains: two centrally located K homology domains (KH1 and KH2) and the arginine-glycine-glycine (RGG) box in the C-terminal region. These domains have been extensively studied in FMRP and are known for a long time to allow for the binding and negative regulation of synaptic mRNAs (Brown *et al*, 2001; Darnell *et al*, 2011). Arginine methylation in the RGG box has been shown to regulate the affinity of FMRP to specific RNAs (Blackwell *et al*, 2010). A third KH domain (K0) has been identified in FMRP although its contribution remains to be studied (Myrick *et al*, 2015).

The three proteins of the family also contain NLS and NES that allow them to shuttle between the nucleus and the cytoplasm (Feng *et al*, 1997), the latter being their main localization at a steady state where they associate with ribosomes. The nuclear export of FXR proteins is dependent on CRM1 (Tamanini *et al*, 1999a). They also present a dimerization domain through which FXR protein hetero- and preferentially homo-dimers or multimers are formed (Siomi *et al*, 1996) (Tamanini *et al*, 1999b), however, the functional implications of these interactions are not yet understood.

As already mentioned, FXR2P and some FXR1P isoforms contain a NoS sequence which mediates their nucleolar localization and its function remains to be investigated.

It has also been seen that the C-terminal region of mouse FMRP interacts with kinesins and has a role in dendritic transport (Dictenberg *et al*, 2008).

1.6.5. Functions of FXR proteins

Because of its implication in FXS and related diseases, research on FXR proteins has mainly focused on FMRP, particularly on its role in neurons where it inhibits translation of transcripts related to synaptic function (Santoro *et al*, 2012).

FMRP is an RNA binding protein that interacts with 4% of mRNAs in the mammalian brain. In neurons, FMRP travels in ribonucleoprotein granules along dendrites in a kinesin- and dynein-dependent manner (Ling *et al*, 2004). Along this journey and in the postsynaptic spaces of dendrites, FMRP inhibits the translation of its bound mRNAs until proper synaptic signals are received. The lack of this spatial and temporal translational control exerted by FMRP and the subsequent excessive protein synthesis in the spines is thought to cause neuronal abnormalities and constitute the molecular basis of FXS (Chen & Joseph, 2015). Indeed,

FMRP's implication in synaptic plasticity is well understood and this aspect is believed to explain the neurological symptoms developed by FXS patients. Synaptic plasticity is the capacity of neurons to change the strength of their pre-existing synaptic connections as a result of neural activity, and it is believed to be a key mechanism in memory and learning. Synaptic plasticity is in part mediated by group 1 metabotropic glutamate receptor (mGluR)-mediated long-term depression (LTD) which results in the weakening of the connection between two neurons. This LTD requires the local translation of postsynaptic dendritic mRNAs. According to the mGluR-based theory of FXS (Bear *et al*, 2004), FMRP is proposed to inhibit translation of proteins necessary for LTD until mGluR is activated and represses FMRP. This way, LTD is linked to mGluR activation and local protein translation. *Fmr1* KO mice show exaggerated LTD uncoupled to mGluR stimulation and FXS patient neurons are insensitive to mGluR stimulation while healthy individuals respond with an increase in FMRP target protein synthesis. This constitutively active LTD and the incapability to specifically respond to synaptic stimuli are believed to explain mental retardation in FXS patients. In accordance with this theory, mGluR antagonists can rescue behavioral and dendritic defects in the several animal FXS models (de Vrij *et al*, 2008; Nakamoto *et al*, 2007), and mGluR pathway has been targeted by several drugs in undergoing clinical trials (Erickson *et al*, 2017).

In order to better understand the function of FMRP, several studies have aimed at identifying the critical mRNA targets. *In vitro* studies showed that the FMRP RGG domain binds to the G-quadrupex (GQ) aptamer sequences while KH2 domain binds to the pseudoknot aptamers (Darnell, 2005; Darnell *et al*, 2001; Brown *et al*, 2001). However, cross-linking immunoprecipitation studies in mouse brain samples identified around 800 mRNAs encoding pre- and post-synaptic proteins and transcripts implicated in autism spectrum disorders as FMRP targets, but none of them contained an evident GQ or pseudoknot sequences (Darnell *et al*, 2011). Another study in HEK293T cells found around 6000 putative mRNA targets but their potential sequences recognized by FMRP are still under debate (Ascano *et al*, 2012). All in all, only a few target mRNAs have been validated by direct biochemical interaction experiments and the specific RNA sequences or secondary structures recognized by FMRP are not completely clear.

Regarding the molecular function of FMRP on its target mRNAs, several studies have shown that FMRP plays a role as a translational repressor and several of its target mRNAs are overexpressed in *Fmr1* KO mouse cells (Mazroui, 2002). Several different mechanisms of action of FMRP have been proposed in this context (reviewed in Chen and Joseph 2015). One of these mechanisms proposes that FMRP interacts with factors of the microRNA pathway

such as Dicer, Argonaute2 and microRNAs to inhibit translation of its target mRNAs. Indeed, FMRP has been reported to inhibit translation of its target mRNA postsynaptic density protein 95 (PSD-95) in postsynaptic regions of neurons in a phosphorylation dependent manner and making use of the microRNA pathway. Upon FMRP dephosphorylation induced by mGluR signaling, this inhibition is no longer maintained and PSD-95 is translated (Muddashetty *et al*, 2011). Another study describes FMRP as an inhibitor of translation initiation because of its capacity to recruit CYFP1 protein to mRNA which is known to bind the translation initiation factor eIF4E. This CYFP1-eIF4E interaction impedes the further assembly of the translation initiation complex eIF4F for which eIF4E is necessary (Napoli *et al*, 2008). A third mechanism by which FMRP has been proposed to repress translation is by directly blocking the action of the translating ribosome. This is based on studies showing that FMRP interacts with active polyribosomes (Stefani, 2004) and a study from Darnell and colleagues showing that FMRP stalls ribosomes in the elongation phase of translation (Darnell *et al*, 2011). In line with these ideas, cryoEM data reported that FMRP can locate in the space between the large and the small subunits of the ribosome in a way that could potentially inhibit the binding of tRNAs during the elongation process therefore stalling the ribosome (Chen *et al*, 2014). Furthermore, FMRP has also been shown to be part of SGs known for their role in suppressing translation and to assist their formation (Didiot *et al*, 2009).

However, FMRP has also been reported to act as a positive translational regulator of diacylglycerol kinase kappa, overexpression of which can rescue dendritic spine defects of *Fmr1* KO neurons (Tabet *et al*, 2016).

Few years ago, a new function of FMRP in the nuclear compartment was discovered which makes use of the two Agenet tandem domains to interact with chromatin and regulate DNA damage repair (Alpatov *et al*, 2014).

It is important to highlight that the different aforementioned mechanisms are not mutually exclusive. It is likely that depending on different variables, such as the target transcript or the subcellular localization, FMRP's translational regulation relies on different mechanisms.

Regarding the other two members of the FXR protein family, much less research has been carried out. FXR1P has also been shown to bind hundreds of mRNA transcripts and regulate translation (Ascano *et al*, 2012). Furthermore, it was suggested to regulate muscle development affecting cell cycle progression (Davidovic *et al*, 2013) and inflammatory processes (Garnon *et al*, 2005; Le Tonqueze *et al*, 2016). FXR1P has also been observed to have oncogenic activity in lung squamous cell carcinoma and colorectal cancer although the underlying molecular mechanism is still not understood (Comtesse *et al*, 2007; Qian *et al*, 2015; Jin *et al*, 2016). In

addition to its role in regulating mRNA translation, FXR1P has also been reported to promote cell proliferation in certain cancers by recruiting transcription factors to gene promoters (Fan *et al*, 2017). FXR2P is the least studied member of the FXR protein family. It is thought to have similar functions to FMRP due to their sequence homology, their similar expression pattern in brain and comparable behavioral phenotype of the knockout mice models (hyperactivity, memory defects, repetitive actions and reduced sleep). Indeed, *Fmr1/Fxr2* double knockout mice displayed exaggerated behavioral and circadian phenotypes suggesting that these two proteins could cooperate in regulating cognitive processes (Spencer *et al*, 2006; Zhang *et al*, 2008).

2. PART 1: Spatial control of nucleoporin condensation by Fragile X-related proteins

The work related to the first part of the results section is entitled "Spatial control of nucleoporin condensation by Fragile X-related proteins" and it has been published in *The EMBO Journal* (Agote-Aran *et al*, 2020). I include the final manuscript which is the result of one round of major revision and a second round of minor revision. Main figures and legends have been properly positioned with the intention of facilitating readers' comprehension. Expanded view and appendix figures and legends mentioned are located following the main text. 'Material and methods' part of the manuscript has been omitted in this chapter and its content has been included in the general 'Materials and methodology' section of the thesis (page 145).

2.1. Aims of the study

Background: NPCs are multisubunit protein complexes that drive the nucleocytoplasmic transport of proteins and RNAs. They are formed by multiple copies of 30 different Nups. One third of these Nups contain IDRs and are prone to phase separate, a phenomenon that can be observed in both healthy and pathological contexts. Given that Nups have an intrinsic capacity to aberrantly assemble, protective mechanisms to prevent the phase separation of newly synthesized Nups may exist in the cell.

Previous results: This project was based on previous immunoprecipitation coupled to Mass Spectrometry data from the laboratory showing that FXR1 interacts with several Nups, and that Nups tend to form cytoplasmic granules in the absence of FXR1. Thus, the main aim of this project was to understand the functional link between FXR proteins and Nup.

Aim 1: To confirm the interaction between FXR1 and Nups.

Aim 2: To characterize the nature of the cytoplasmic Nups granules that formed upon the downregulation of FXR1.

Aim 3: To study the mechanism by which FXR1 regulates Nups localization and to understand how cytoplasmic Nup granules are formed.

Aim 4: To investigate if all members of FXR protein family regulate Nups localization, and if FXS cellular models display cytoplasmic Nups granules.

Aim 5: To investigate the functional consequences of Nups mislocalization upon FXR1 downregulation regarding protein import/export and cell cycle progression.

2.2. Author's contribution to the manuscript "Spatial control of nucleoporin condensation by Fragile X-related proteins"

In the EMBO Journal manuscript (Agote-Aran *et al*, 2020), each author contributed in the following manner:

Stephane Schmucker established and validated the GFP, GFP-FXR1 and 3xGFP-Nup85 cell lines which were used throughout the manuscript. Using these GFP and GFP-FXR1 cell lines, he carried out the immunoprecipitation coupled with mass spectrometry studies where the first interaction between FXR1 and Nups was observed. He showed that FXR1 does not regulate protein or mRNA levels of several Nups nor mitotic progression. Additionally, he identified and quantified the cytoplasmic Nup granules and irregular nuclei phenotypes upon FXR1 downregulation and he performed the live video experiments showing that both events were first detected at the beginning of G1 phase. He also performed the rescue experiments showing that cytoplasmic Nup granule formation and nuclear atypia are specific to FXR1 absence. Stephane showed that the ectopic Nup granule formation occurs in the absence of all FXR protein family members. He also helped writing the manuscript.

Katerina Jerabkova performed the experiments with FXS patient primary fibroblasts where the cytoplasmic Nup granule formation was also observed.

Inès Jmel Boyer performed the GFP-FXR1 immunoprecipitation experiments where the binding factor BICD2 was identified. She also characterized the cytoplasmic Nup granule and irregular nuclei phenotypes upon BICD2 downregulation.

Alessandro Berto performed immunofluorescence (IF) experiments to observe the NE localization of the Fragile X protein family members.

Paolo Ronchi performed the electron microscopy sample preparation and image acquisition and processing.

Charlotte Kleiss helped with experiments throughout my whole PhD.

Laurent Guerard and **Alexia Loyton** performed the super resolution image acquisition and processing.

Hervé Moine, Jean-Louis Mandel and **Yannick Schwab** helped designing the experiments.
Laura Pacini, Sebastien Jacquemont and **Claudia Bagni** prepared and provided human patient samples.
Izabela Sumara quantified the experiments from FXS patient primary fibroblasts. She also designed experiments, figures and wrote the manuscript, and she conceptually guided, supervised and coordinated the whole project.
I demonstrated the interaction between FXR1 and Nups and that FXR1 localized to the ONM. I also showed that Nup signal at the NE decreases upon FXR1 downregulation.
I characterized cytoplasmic Nup granule formation in early G1 phase by live video microscopy and I showed that these granules have condensate-like behavior (the fuse and split, and dissolve upon 1,6-Hexanediol treatment). I also showed the interaction between FXR1 and dynein complex, and observed that both, dynein downregulation and microtubule depolymerization, induce a significant increase in cytoplasmic Nup granules. I studied the dynamics Nup granules formed by microtubule depolymerization upon Dynein and FXR1 downregulation, and observed that granule fusion and fission events were more frequent in these two conditions than in the control situation.
I confirmed the cytoplasmic Nup granule presence in different FXS models (FXS patient derived iPSC and FMRP KO MEFs). I also observed that cytoplasmic Nup granules have functional consequences in protein export and cell cycle progression.
I observed that FXR1 downregulation does not affect the recruitment of nuclear lamina or INM proteins, and I showed that cytoplasmic Nup granules are distinct from ALs and SGs. I also showed that cytoplasmic Nup granules do not contain RNA, and that RNA is dispensable for their maintenance. I also helped writing the manuscript.

2.3. Manuscript title

Spatial control of nucleoporin condensation by Fragile X-related proteins

Arantxa Agote-Arán[1,2,3,4,*], Stephane Schmucker[1,2,3,4,*], Katerina Jerabkova[1,2,3,4], Inès Jmel Boyer[1,2,3,4], Alessandro Berto[5,6,14], Laura Pacini[7,15], Paolo Ronchi[8], Charlotte Kleiss[1,2,3,4], Laurent Guerard[9], Yannick Schwab[8,10], Hervé Moine[1,2,3,4], Jean-Louis Mandel[1,2,3,4], Sebastien Jacquemont[11,12], Claudia Bagni[7,13] and Izabela Sumara[1,2,3,4].

[*] These authors contributed equally to this work

[1] Institut de Génétique et de Biologie Moléculaire et Cellulaire (IGBMC), Illkirch, France.
[2] Centre National de la Recherche Scientifique UMR 7104, Strasbourg, France.
[3] Institut National de la Santé et de la Recherche Médicale U964, Strasbourg, France.
[4] Université de Strasbourg, Strasbourg, France.
[5] Institut Jacques Monod, CNRS UMR7592-Université Paris Diderot, Sorbonne Paris Cité, Paris, France.
[6] Ecole Doctorale SDSV, Université Paris Sud, Orsay, France.
[7] Department of Biomedicine and Prevention, University of Rome Tor Vergata, Rome, Italy.
[8] European Molecular Biology Laboratory, Electron Microscopy Core Facility, Heidelberg, Germany.
[9] Imaging Core Facility, Biozentrum, University of Basel, Klingelbergstrasse 50/70, 4056 Basel, Switzerland.
[10] European Molecular Biology Laboratory, European Molecular Biology Laboratory, Cell Biology and Biophysics Unit, Heidelberg, Germany.
[11] Service de Génétique Médicale, Centre Hospitalier Universitaire Vaudois, Rue du Bugnon 46, 1011 Lausanne, University of Lausanne, Switzerland.
[12] CHU Sainte-Justine Research Centre, University of Montreal, 3175 Chemin de la Côte-Sainte-Catherine, Montreal, Quebec H3T 1C5, Canada.
[13] Department of Fundamental Neuroscience, University of Lausanne, Lausanne, Switzerland.
[14] Current address: Swiss Institute for Experimental Cancer Research (ISREC), School of Life Sciences, Swiss Federal Institute of Technology Lausanne (EPFL), Lausanne, Switzerland.
[15] Current address: UniCamillus - Saint Camillus International University of Health and Medical Sciences, Rome, Italy.

2.4. General summary and bullet points

Fragile X-related proteins and dynein inhibit ectopic phase separation of Nups in the cytoplasm and facilitate their localization to the NE during G1 phase of the cell cycle.

Bullet points:

- Fragile X-related (FXR) proteins and dynein regulate localization of cytoplasmic Nups
- FXR-Dynein pathway downregulation induces aberrant cytoplasmic condensation of Nups
- Cellular models of FXS accumulate aberrant cytoplasmic Nup condensates

- FXR-Dynein pathway regulates nuclear morphology and cell cycle progression

2.5. Abstract

Nucleoporins (Nups) build highly organized Nuclear Pore Complexes (NPCs) at the nuclear envelope (NE). Several Nups assemble into a sieve-like hydrogel within the central channel of the NPCs. In the cytoplasm, the soluble Nups exist, but how their assembly is restricted to the NE is currently unknown. Here we show that fragile X-related protein 1 (FXR1) can interact with several Nups and facilitate their localization to the NE during interphase through a microtubule-dependent mechanism. Downregulation of FXR1 or closely related orthologs FXR2 and fragile X mental retardation protein (FMRP) leads to the accumulation of cytoplasmic Nup condensates. Likewise, models of fragile X syndrome (FXS), characterized by a loss of FMRP, accumulate Nup granules. The Nup granules-containing cells show defects in protein export, nuclear morphology and cell cycle progression. Our results reveal an unexpected role for the FXR protein family in the spatial regulation of Nup condensation.

2.6. Introduction

Formation of supramolecular assemblies and membrane-less organelles such as the nucleolus, Cajal bodies, nuclear speckles, stress granules (SG), P-bodies, germ granules and PML bodies are important for cellular homeostasis (Boeynaems *et al*, 2018). Among the factors controlling their formation and turnover is the presence of intrinsically disordered regions (IDRs) in protein components, their ability to form multivalent protein-protein, and protein-RNA interactions (Feng *et al*, 2019) and proteins' local concentration. Indeed, many RBPs have the ability to demix into liquid states (liquid droplets), which can be subsequently transformed into pathological amyloids both (Harrison & Shorter, 2017; Lin *et al*, 2015; Shorter, 2019) that have been linked to many neurological disorders (Shin & Brangwynne, 2017). One example of a large protein assembly consisting of IDR-containing proteins is the Nuclear Pore Complex (NPC), which plays an essential role in cellular homeostasis (Knockenhauer & Schwartz, 2016; Sakuma & D'Angelo, 2017).

NPCs are large, multisubunit protein complexes (Beck & Hurt, 2017; Hampoelz *et al*, 2019a) spanning the nuclear envelope (NE) that constitute the transport channels controlling the exchange of proteins and mRNAs between the nucleus and the cytoplasm. They are built from roughly 30 different nucleoporins (Nups) each present in multiple copies in the NPCs. The ring-like NPC scaffold is embedded in the NE and shows highly organized eight-fold symmetry (Knockenhauer & Schwartz, 2016). In contrast, the central channel of the NPC is formed from Nups containing disordered elements characterized by the presence of phenylalanine-glycine (FG) repeats, the so-called FG-Nups. The FG-Nups have the ability to phase separate into sieve-like hydrogels that constitute a selective and permeable barrier for diffusing molecules and transported cargos through the NPCs (Schmidt & Görlich, 2016). This ability of the FG-Nups to form permeable hydrogels can also be reconstituted *in vitro* and is highly conserved through the evolution (Frey & Görlich, 2007; Frey *et al*, 2006; Schmidt & Görlich, 2015). The cohesive abilities of FG-Nups allow not only for the formation of the permeability barrier but also for building the links with the structural scaffold elements of the NPC (Onischenko *et al*, 2017). The non-FG-Nups can also form condensates in cells as they are sequestered in the SGs (Zhang *et al*, 2018) and in various pathological aggregates in the nucleus and in the cytoplasm (Hutten & Dormann, 2020; Li & Lagier-Tourenne, 2018). A fraction of cytoplasmic Nups was also identified in the promyelocytic leukemia protein (PML)-positive structures, the so-called CyPNs (cytoplasmic accumulations of PML and Nups), which could move on microtubules to dock at the NE (Jul-Larsen *et al*, 2009), although the cellular roles of the CyPNs remain to be

understood. This indicates that Nups have an intrinsic capacity to aberrantly assemble, suggesting protective mechanisms may exist to prevent it in the cell. Indeed, in Drosophila embryos a large excess of soluble Nups has been reported (Onischenko *et al*, 2004) and in cells Nups are synthesized as soluble proteins in the cytoplasm (Davis & Blobel, 1987). How the balance of soluble Nups is controlled, and what factors regulate the localized assembly of Nups is currently unknown.

The Fragile X related (FXR) proteins (FXR1, FXR2 and Fragile X mental retardation protein (FMRP)) are a family of RBPs displaying a high degree of sequence and structural similarity and playing important roles in protein translation (Li & Zhao, 2014). Silencing of the *FMR1* gene that encodes the FMRP protein (Santoro *et al*, 2012) leads to Fragile X syndrome (FXS), the most common form of inherited intellectual human disability worldwide, for which no efficient therapy exists to date (Mullard, 2015). For this reason, the role of FXR proteins has been mostly investigated in brain, in the context of neurodevelopmental disorders (Bagni & Zukin, 2019) and genome-wide association studies suggest the involvement of this family in a wide spectrum of mental illnesses (Guo *et al*, 2015; Khlghatyan *et al*, 2018).

More recent studies have linked FXR proteins to cancer progression, in particular FMRP and FXR1 were found overexpressed in different types of cancer (Lucá *et al*, 2013; Zalfa *et al*, 2017; Jin *et al*, 2016; Cao *et al*, 2019). Although many overlapping functions have been proposed for this protein family, different tissue, cellular and intracellular distributions of the FXR proteins, suggest that they might have, in addition to their canonical role as RNA binding proteins, independent functions (Darnell *et al*, 2009). Interestingly, the protein region containing the RGG box (arginine- and glycine-rich region) of FMRP has a low-complexity sequence composition and is unfolded and flexible (Ramos, 2003), implicating its role in the membrane-less assemblies. Here we identify an unexpected role for the FXR protein family and dynein in the spatial regulation of Nup condensation.

2.7.Results

2.7.1. FXR1 protein localizes to the NE and interacts with Nups

FXR1 co-localizes with various cytoplasmic protein-RNA assemblies, but it is also present in the nuclear compartment in human cells (Oldenburg *et al*, 2014; Tamanini *et al*, 1999a). In search for possible cellular functions of FXR1 independent of its role in RNA binding, we performed immunoprecipitations (IPs) of stably expressed GFP-FXR1 protein and analyzed the interacting partners by mass spectrometry. Of the interacting proteins, including the known FXR1 partners, FXR2 and FMRP, four Nups, Nup210, Nup188, Nup133 and Nup85, were detected specifically in GFP-FXR1 IPs (Dataset EV1). We confirmed the GFP-FXR1 interaction with endogenous Nup133 and Nup85, which are components of the evolutionary conserved Nup107-160 NPC sub-complex also called the Y-complex (Fig 1A) (Beck & Hurt, 2017; Knockenhauer & Schwartz, 2016). IP of stably expressed GFP-Nup85 also demonstrated an interaction with two endogenous FXR1 isoforms in HeLa cells (Fig 1B), and both Nup85 and Nup133 co-immunoprecipitated with endogenous FXR1 in HEK293T cells (Fig 1C).
Both endogenous FXR1 and GFP-FXR1 localized to the NE (Fig 1D, E) and also occasionally to small cytoplasmic foci labelled by the monoclonal antibody mAb414, which recognizes a panel of FG-Nups (Fig 1E). FXR1 localization to the NE and the cytoplasmic foci was abolished by treatment with FXR1 siRNA (Fig 1D), demonstrating antibody specificity. Treatment with Digitonin, which in contrast to permabilization protocol with the Triton and SDS can selectively permeabilize the plasma membrane while leaving the NE intact, revealed that FXR1 localized to the ONM (Fig 1F). We conclude that FXR1 interacts with Nups, and can localize to both the ONM and to cytoplasmic foci containing Nups.

Figure 1

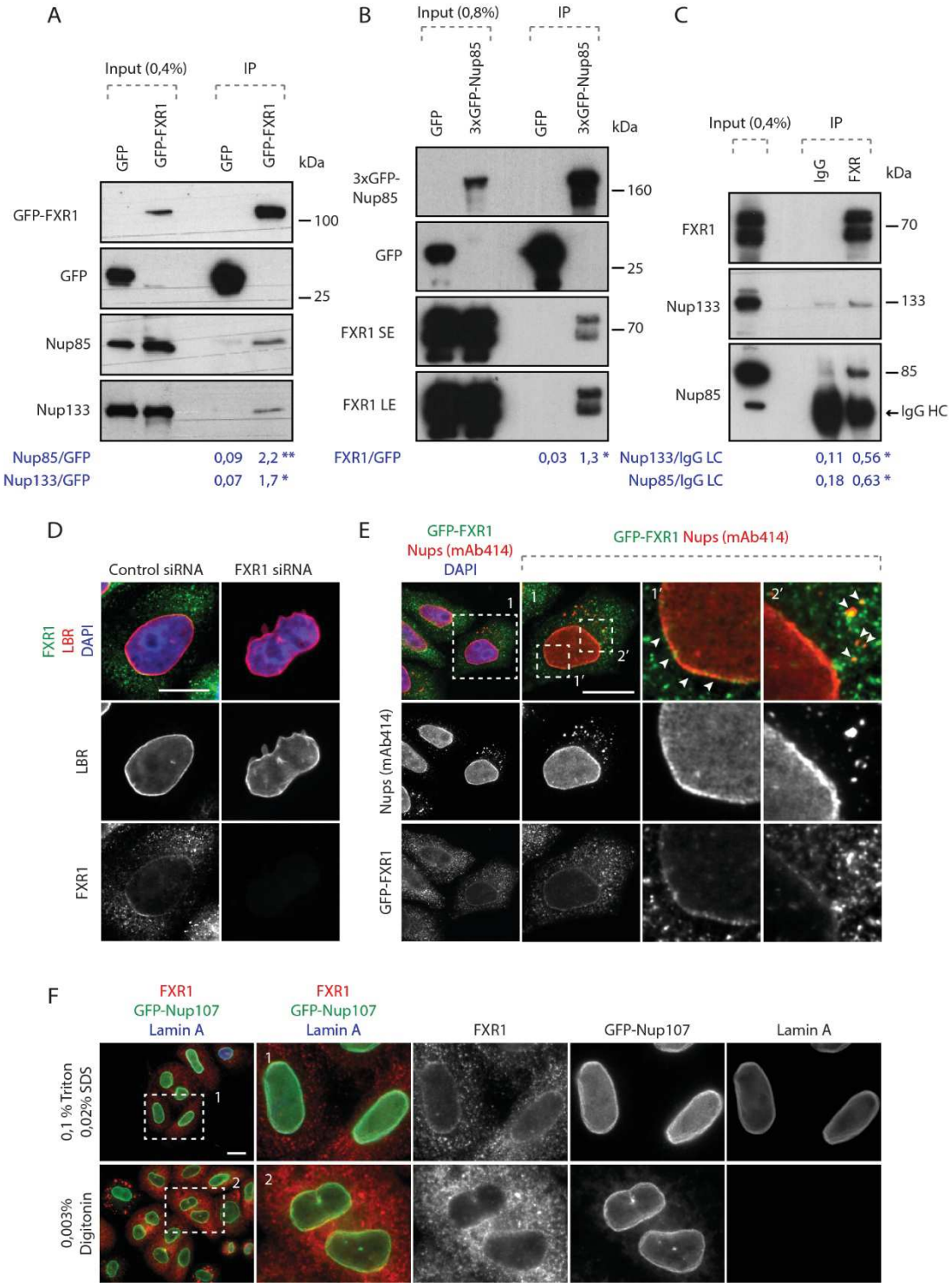

Figure 1 - FXR1 protein localizes to the NE and interacts with NUPs.

A Lysates of HeLa cells stably expressing GFP alone or GFP-FXR1 were subjected to IP using GFP-Trap beads (GFP-IP), analyzed by Western blot and quantified (shown a mean value, *P < 0.05, **P < 0.01; N = 3).

B Lysates of HeLa cells stably expressing GFP alone or 3xGFP-Nup85 were immunoprecipitated using GFP-Trap beads (GFP-IP), analyzed by Western blot and quantified (SE, short exposure, LE, long exposure) (shown a mean value, *P < 0.05; N = 3).

C IP from HEK293T cell lysates using FXR1 antibody or IgG analyzed by Western blot. The arrow points to the heavy chain of IgG (IgG HC) (shown a mean value, *P < 0.05; N = 3).

D HeLa cells were treated with indicated siRNAs, synchronized by double thymidine block, and released for 12 hours and analyzed by IF microscopy for the LBR to label the NE, and FXR1.

E HeLa cells stably expressing GFP-FXR1 were analyzed by IF microscopy for GFP and mAb414, which labels FG-Nups. The magnified framed regions are shown in the corresponding numbered panels. The arrowheads indicate NE and cytoplasmic localization of GFP-FXR1.

F HeLa cells stably expressing GFP-Nup107 were synchronized by double thymidine block and released for 12 hours, permeabilized with Triton/SDS or digitonin for antibodies to access the nuclear and cytoplasmic or cytoplamsic side of the nucleus, respectively, and analyzed by IF microscopy.

Data information: Scale bars are 5 μm. Statistical significance was assessed by unpaired two-tailed Student's T-test.

2.7.2. FXR1 inhibits aberrant assembly of cytoplasmic Nups

To assess the biological function of the FXR1-Nup interactions, we treated cultured human cells with FXR1-specific siRNA oligonucleotides. Downregulation of FXR1 in HeLa cells led to an accumulation of FG-Nups in the cytoplasm in the form of irregular aggregate-like assemblies of various sizes (Fig. 2A, B; Fig EV1, Appendix Figure S1A, B, E, F, H) and in U2OS cells (Fig 2G, Appendix Figure S1J). These Nup assemblies were observed using two different siRNAs targeting FXR1 and could be rescued by stable ectopic expression of a form of GFP-FXR1 that is resistant to one of the siRNAs used (Fig 2B; Fig EV1).

Downregulation of FXR1 led to the cytoplasmic retention and co-localization in granules of at least 10 Nups spanning several functional and structural NPC groups, including FG-Nups (Nup98, Nup214; and RanBP2); transmembrane Nups (Nup210 and POM121); Y-complex Nups (Nup133 and Nup85, stably expressed GFP-Nup133, stably expressed GFP-Nup85 and stably expressed GFP-Nup107) as well as Nup88 and NPC-associated the RanGTPase activating protein (RanGAP1) (Fig 2C; Appendix Figure S1A-H, Appendix Figure S2C, D). Absent from the Nup granules were the nuclear ring Nup ELYS and the inner nuclear basket component Nup153, although their levels at the NE were both slightly reduced (Fig 2C; Fig Appendix Figure S1I, Appendix Figure S2B, C). FXR1 downregulation also moderately reduced the NE localization of FG-Nups, RanBP2 and stably expressed GFP-Nup107 in HeLa

cells (Fig 2D-F) and of FG-Nups in U2OS cells (Fig 2H, Appendix Figure S1J). Collectively, these data show that loss of FXR1 induces inappropriate assembly of Nups in the cytoplasm.

Figure 2

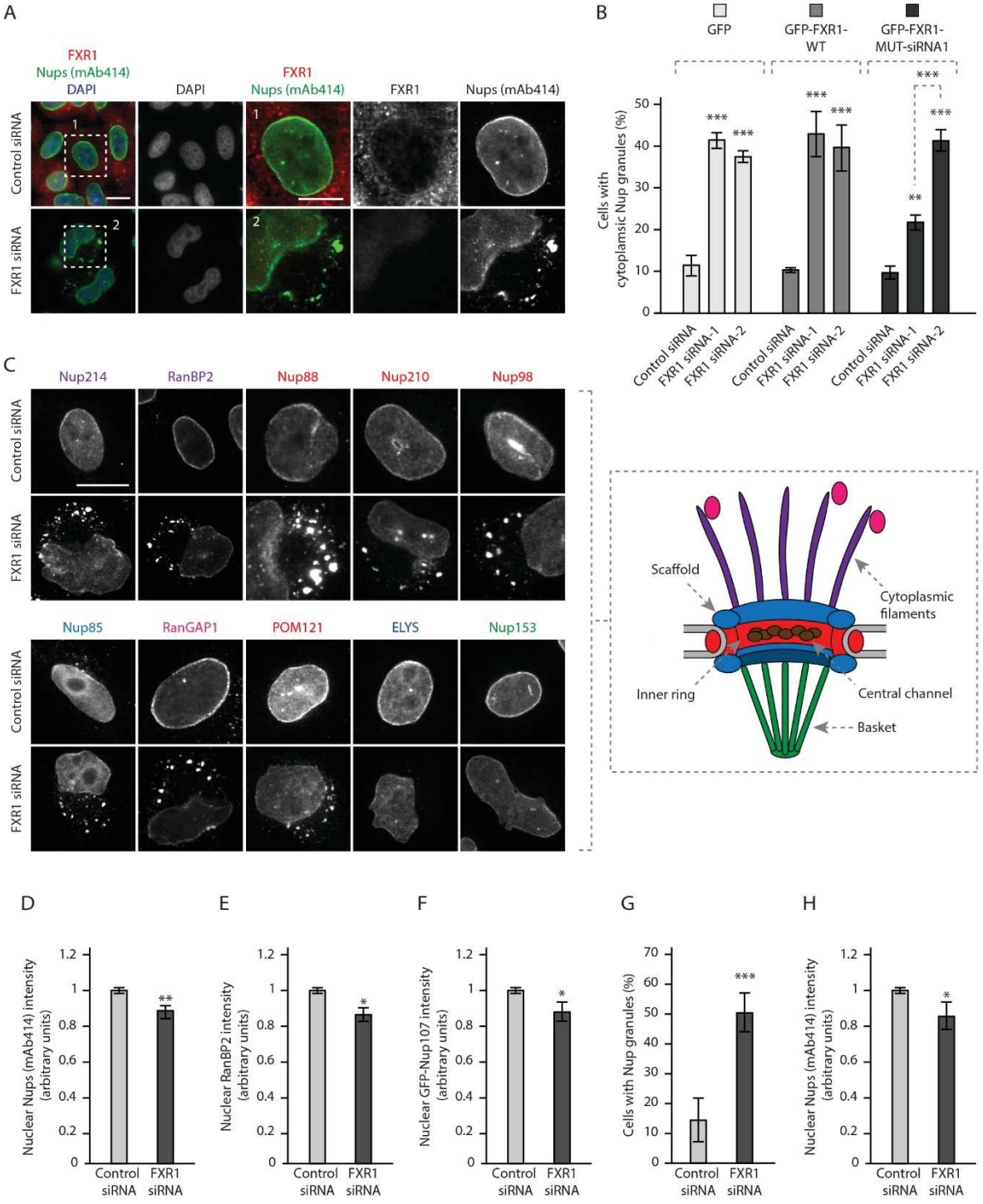

Figure 2 - FXR1 inhibits aberrant assembly of cytoplasmic Nups.

A HeLa cells were treated with the indicated siRNAs, synchronized by double thymidine block and release for 12 hours and analyzed by IF microscopy. The magnified framed regions are shown in the corresponding numbered panels.

B HeLa cells stably expressing GFP, GFP-FXR1 WT and GFP-FXR1 mutated in the sequence recognized by FXR1 siRNA-1 (GFP-FXR1-MUT-siRNA1) were treated with the indicated siRNAs, synchronized by double thymidine block, released for 24 hours and then analyzed by IF microscopy. The percentage of cells with cytoplasmic Nup granules was quantified, 1000 cells were analyzed for each graph (mean ±SD, **P < 0.01; ***P < 0.001, N = 3). The corresponding representative pictures are shown in Figure EV1 and the corresponding Western blot analysis is shown in Figure 3B.

C-F HeLa cells were treated with the indicated siRNAs, synchronized by double thymidine block, released for 12 hours and analyzed by IF microscopy. Nups present in different NPC subcomplexes are depicted in the color code corresponding to the NPC scheme shown on the right. Additional or complementary representative images and channels of cells depicted in (**C**) are shown in Appendix Figures S1 and S2B-D. Nuclear intensity of FG-Nups labelled by mAb414 (**D**), RanBP2 (**E**) and GFP-Nup107 (**F**) was quantified. 1800 cells were analyzed for each graph (mean ±SD, *P < 0.05; **P < 0.01; N = 3).

G, H Asynchronously proliferating U2OS cells were treated with the indicated siRNAs and analyzed by IF microscopy. The percentage of cells with cytoplasmic Nup granules (**G**) was quantified and nuclear intensity of FG-Nups labelled by mAb414 (**H**) was quantified. 1600 cells were analyzed in (**G**) and 2100 cells were analyzed in (**H**) (mean ±SD, *P < 0.05; *** P<0.001; N = 3).

Data information: Scale bars are 5 μm. Statistical significance was assessed by unpaired two-tailed Student's T-test.

2.7.3. The FXR1 regulates nuclear morphology during G1 cell cycle phase

We noticed that the Nup granules-containing cells often displayed strong nuclear atypia (Fig 1D, 2A, C; Fig EV1, 2; Appendix Figure S1, S2). Interestingly, downregulation of FXR1 did not affect the recruitment of the nuclear lamina components LBR (Fig 1D), lamin A (Fig EV2A, B), lamin B1 (Fig EV2C, D) or emerin (Fig EV2E, F) to the NE in interphase or telophase cells, while Lap2β recuitment was moderately increased upon FXR1 downregulation (Fig EV2E, G). However, these lamina and INM components displayed irregular distribution along with the misshaped nuclear rim and intranuclear foci (Fig EV2A, C, E). Morever, the size of nucleus was moderately increased upon downregulation of FXR1 (Fig EV2H). Defects in nuclear architecture including irregular and blebbed nuclei (Fig 3A) could be largely rescued by stable ectopic expression of the siRNA-resistant form of GFP-FXR1 (Fig 3B, C; Fig EV1).

Live video microscopy of HeLa cells stably expressing histone H2B labelled with mCherry revealed that progression and timing through different mitotic stages or fidelity of chromosome segregation was not affected in the FXR1-deficient cells (Fig 3D-H). The nuclear morphology

defects in FXR1-deficient cells (Fig 3H, I) could first be detected approximately 30 min after the onset of chromosome segregation (Fig 3H, J), which strongly correlated with the onset of nuclear growth. Our data suggest that downregulation of FXR1 specifically affects cytoplasmic Nups and nuclear architecture during early G1.

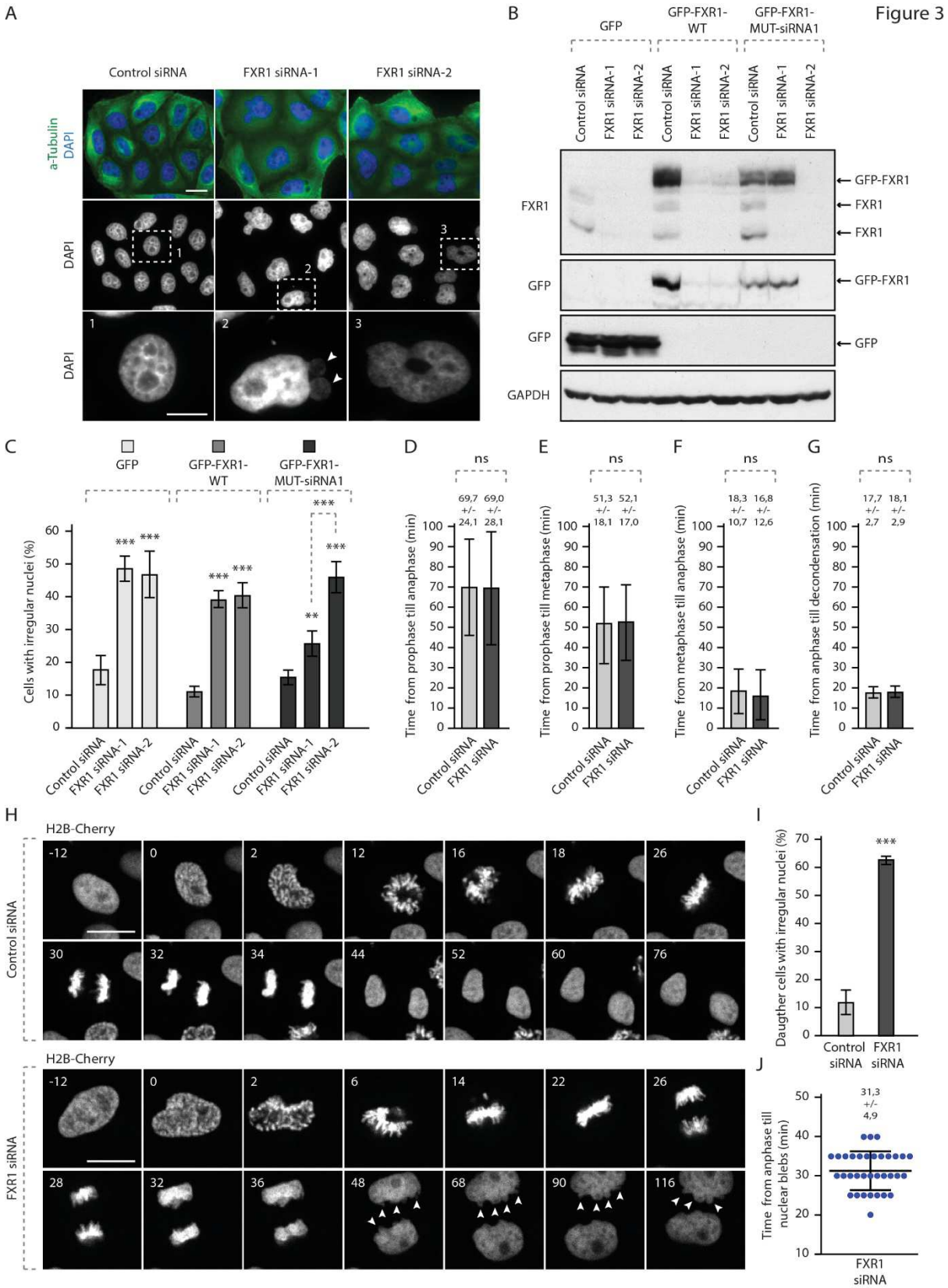

Figure 3 - The FXR1 regulates nuclear morphology during G1 cell cycle phase.

A HeLa cells were treated with the indicated siRNAs, synchronized by double thymidine block, released for 24 hours and analyzed by IF microscopy. The magnified framed regions are shown in the corresponding numbered panels. Arrowheads point to nuclear blebs observed in FXR1-deficient cells.

B, C HeLa cells stably expressing GFP, GFP-FXR1 WT and GFP-FXR1 mutated in the sequence recognized by FXR1 siRNA-1 (GFP-FXR1-MUT-siRNA1) were treated with the indicated siRNAs, synchronized by double thymidine block, released for 24 hours and analyzed by Western blot (**B**) and IF microscopy (**C**). The percentage of cells with irregular nuclei was quantified, 1000 cells were analyzed (mean ±SD, **P < 0.01, ***P < 0.001; N = 3). The corresponding representative pictures are shown in Figure EV1.

D-J HeLa cells stably expressing the chromatin marker histone H2B labelled with mCherry were treated with indicated siRNAs, synchronized by double thymidine block, released for 12 hours and analyzed by IF microscopy. Time from prophase till anaphase (**D**), from prophase till metaphase (**E**), from metaphase till anaphase (**F**) and from anaphase till chromatin decondensation (**G**) was quantified. The selected frames of the movies are depicted and time is shown in minutes (**H**). Arrowheads point to nuclear blebs appearing during nuclear expansion of FXR1-deficient cells. Percentage of daughter cells with irregular nuclei was quantified in (**I**) and time from anaphase till nuclear blebs was quantified in (**J**). 66 cells were analyzed (mean ±SD, ***P < 0.001; N = 3).

Data information: Scale bars are 5 μm. Statistical significance was assessed by unpaired two-tailed Student's T-test.

2.7.4. FXR1 regulates cytoplasmic Nups during early interphase

Our data so far suggest that FXR1 regulates cytoplasmic Nups and may facilitate localization of a very small pool of soluble Nups to the NE (Fig 2D-F, H). To date, two temporally and mechanistically distinct pathways of NPC assembly at the NE have been described during the cell cycle in higher eukaryotic cells (Weberruss & Antonin, 2016). In the postmitotic pathway, ELYS initiates NPC assembly on segregated chromosomes, while during interphase, both Nup153 and POM121 drive *de novo* assembly of NPCs into an enclosed NE (D'Angelo *et al*, 2006b; Doucet *et al*, 2010; Vollmer *et al*, 2015). ELYS assembled normally on segregating chromosomes in anaphase and on decondensing chromatin in telophase in FXR1-deficient cells (Appendix Figure S2A). In addition, we found that ELYS and Nup153 were not recruited to the cytoplasmic Nup granules whereas POM121 was (Fig 2C; Appendix Figure S2B-D). This suggests that FXR1 affects localization of most but not all cytoplasmic Nups.

To understand the precise timing of the FXR1-Nup pathway, we used live video microscopy of a reporter cell line stably expressing GFP-Nup107 (Fig 4A-D, Movie EV1-5). As expected, downregulation of FXR1 led to the accumulation of GFP-Nup107 in cytoplasmic granules (Fig 4A-C; Movie EV2, 4, 5) with similar appearance and distribution to that observed in the fixed specimens and that had a tendency to fuse into bigger assemblies with time (Fig 4A, B; Movie

EV4, 5). In the control cells, smaller GFP-Nup107 granules were occasionally observed, which had a tendency to fuse with the NE (Fig 4A, B; Movie EV1, 3).

GFP-Nup107-positive granules in control and FXR1-deficient cells became detectable in the cytoplasm on average 44 and 35 min after chromosome segregation, respectively (Fig 4D, Movie EV1-5), which strongly correlated with the timing of the nuclear morphology defects in early G1 (Fig 3H, J) described earlier.

We considered that this effect may be mediated by a modulation of Nups levels. The protein levels of Nup85, Nup93, Nup133 and Nup155 (Fig EV3A-C), and the mRNA levels of Nup85 and Nup133 (Fig EV3D, E), as well as the known cell cycle-linked degradation of Nup85 (Fig EV3A, B) and Nup133 dephosphorylation, which occurs during mitotic exit (Fig EV3B), were unchanged upon depletion of FXR1. Consistent with the live video experiments, degradation of several mitotic factors in synchronized cells (Fig EV3A, B) was not affected by FXR1 downregulation, suggesting that Nup localization defects are likely also not due to changes in mitotic progression and exit or misregulation of the levels of the analyzed Nups. However, it cannot be formally excluded that expression of other yet to be identified Nups or Nup-associated factors is regulated by FXR1. Together, our results suggest that loss of FXR1 regulates cytoplasmic Nups during early interphase but it remains to be understood if this Nup regulation occurs in the context of any specific NPC assembly pathway.

Figure 4

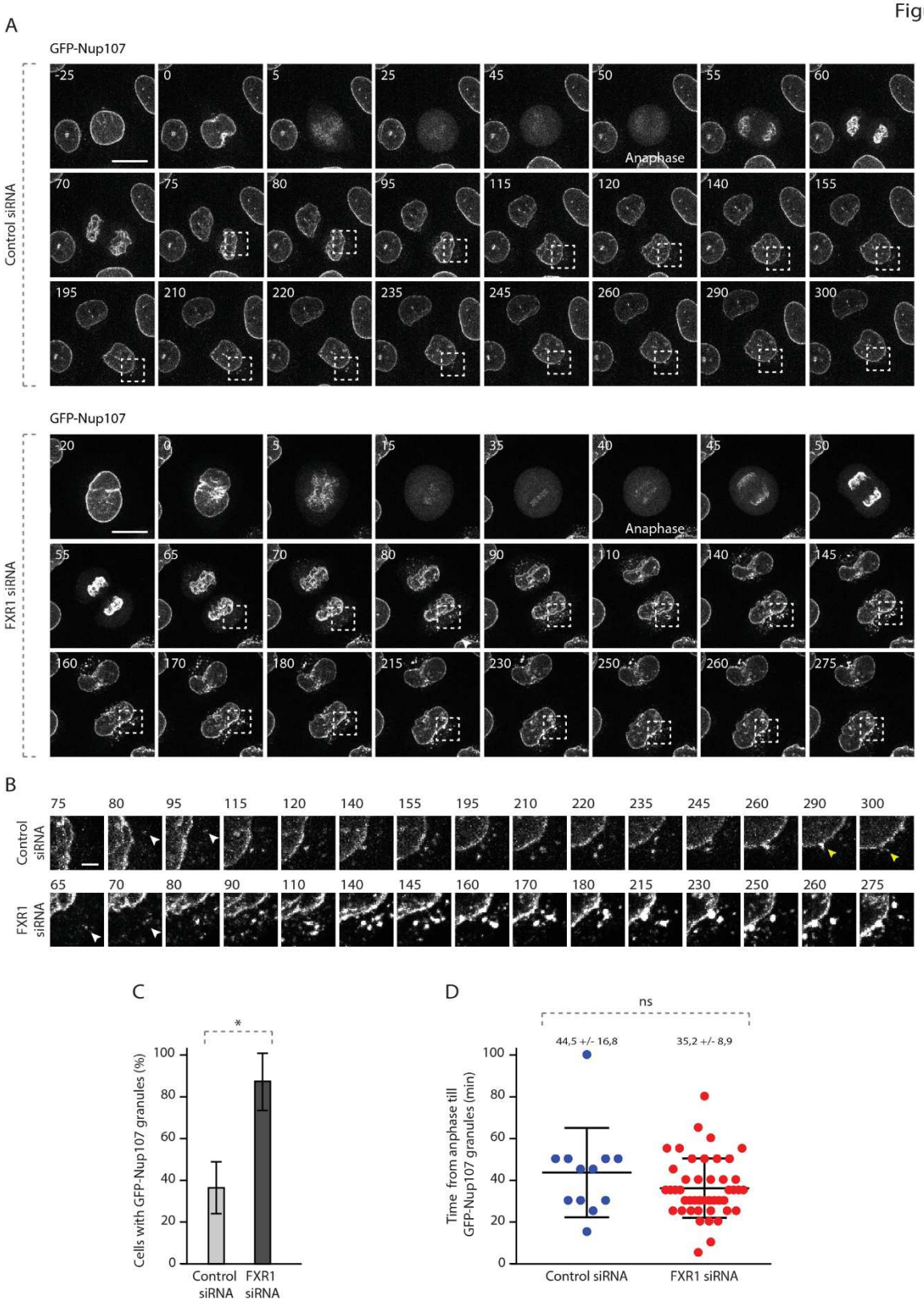

Figure 4 - FXR1 regulates cytoplasmic Nups during early interphase.

A-D HeLa cells stably expressing GFP-Nup107 were treated with indicated siRNAs, synchronized by double thymidine block, released and analyzed by live video spinning disk confocal microscopy (**A**). The selected frames of the movies are depicted and time is shown in minutes. The onset of anaphase is

indicated. The magnified framed regions with time indicated in minutes are shown in (**B**). White arrowheads point to the cytoplasmic GFP-NUP107 granules appearing during nuclear expansion of control and FXR1-deficient cells, yellow arrowheads point to the fussion events of GFP-NUP107 granules with NE in control cells. The percentage of cells with cytoplasmic GFP-Nup107 granules was quantified in (**C**). Time from anaphase till GFP-Nup107 cytoplasmic granule formation was quantified in (**D**). 57 cells were analyzed (mean ±SD, *P < 0.05; ns = non-significant; N = 3).

Data information: Scale bars are 5 μm (**A**) and 1 μm (**B**). Statistical significance was assessed by unpaired two-tailed Student's T-test.

2.7.5. Nup granules are resistant to RNA degradation but sensitive to 1,6-Hexanediol

The cytoplasmic Nup granules in FXR1-deficient cells could correspond to ALs, which are preassembled NPCs embedded in the ER membrane (Merisko, 1989), as suggested by co-localization of various Nups in these assemblies. Indeed, cytoplasmic AL-NPCs can be inserted "*en bloc*" into an intact NE during embryogenesis in Drosophila (Hampoelz *et al*, 2016). A closer analysis by superresolution microscopy revealed an amorphous organization of the Nup assemblies in the perinuclear area of FXR1-deficient cells relative to the more regular, round shape of the small cytoplasmic Nup foci observed in the control cells (Appendix Figure S3A). Moreover, we were unable to detect any AL-typical structures (characterized by parallel stacks of ER-membranes with embedded regularly spaced NPCs), in the FXR1-deficient cells by electron microscopy (EM) (Appendix Figure S3B), and no co-localization with the ER membranes could be observed (Appendix Figure S3C). Cytoplasmic Nups were also found to be recruited to assembling SGs upon induction of cellular stress (Zhang *et al*, 2018). Consistently, our results demonstrated co-localization of the Nup RanBP2 with the markers of SGs, TIA-1 and G3BP1, in the control stress-induced cells (Appendix Figure S4A). However, TIA-1 and G3BP1 did not co-localize with the Nup granules in the FXR1-deficient cells exposed to stress, and both the SGs and Nup granules present in these cells localized to different cytoplasmic compartments. We conclude that the Nup granules in FXR1-deficient cells are distinct from ALs and SGs.

Given the established role of the FXR protein family in RNA-binding and the frequent role of RBPs in the formation and dynamics of membrane-less protein assemblies, we next analyzed whether Nup granules contain any RNAs or could be linked to RNA-based processes. Hybridization with an RNA Fluorescent In Situ Hybridization (FISH) probe against Poly-A revealed no difference in the percentage of nuclear mRNAs in the FXR1-deficient cells relative to control cells (Appendix Figure S4B, C), suggesting that the FXR1-Nup pathway is not

implicated in mRNA export to the cytoplasm. Additionally, no cytoplasmic enrichment of mRNAs could be observed in GFP-Nup107 granules in the FXR1-downregulated cells (Appendix Figure S4B, D). To test whether RNAs play a role in the maintenance or dynamics of the Nup granules in the cytoplasm, we treated permeabilized, FXR-downregulated cells with RNAse. This treatment failed to disrupt the Nup granules or change their shape and distribution relative to control cells (Appendix Figure S5A, B), suggesting that RNAs are dispensable for their maintenance and dynamics.

Many components of protein assemblies formed by phase separation, including FG-Nups, are highly hydrophobic and contain very few charged amino acids (Schmidt & Görlich, 2016). For this reason, aliphatic alcohols like hexanediols are good solvents for FG-Nups because they probably compete with the hydrophobic interactions between FG-repeats (Patel *et al*, 2007). Indeed, hexanediols are known to disrupt FG-hydrogels and the NPC permeability barrier, while FG-derived amyloid fibers are hexanediol resistant (Kroschwald *et al*, 2015; Ribbeck & Görlich, 2002). Thus, hexanediols can be used to distinguish between these two types of Nup condensates. Moreover, 1,6-Hexanediol treatment can also disperse the phase separated condensates formed of Nup358 and the Y-complex component Nup107 in Drosophila embryos (Hampoelz *et al*, 2019b) and SGs formed in HeLa cells exposed to stress (Fig 5A).

To understand if the cytoplasmic Nup granules have properties of phase separated condensates, we treated control and FXR1-deficient cells with 1,6-Hexanediol using the protocol established for SGs (Fig 5A). 1,6-Hexanediol treatment led to the dispersion of the small Nup foci present in control cells as well as the Nup granules observed upon FXR1 downregulation relative to the non-treated cells (Fig 5B, C). Collectively, we propose that the Nup granules represent previously unknown assemblies with the properties of protein condensates that accumulate in the absence of FXR1 in human cells.

Figure 5

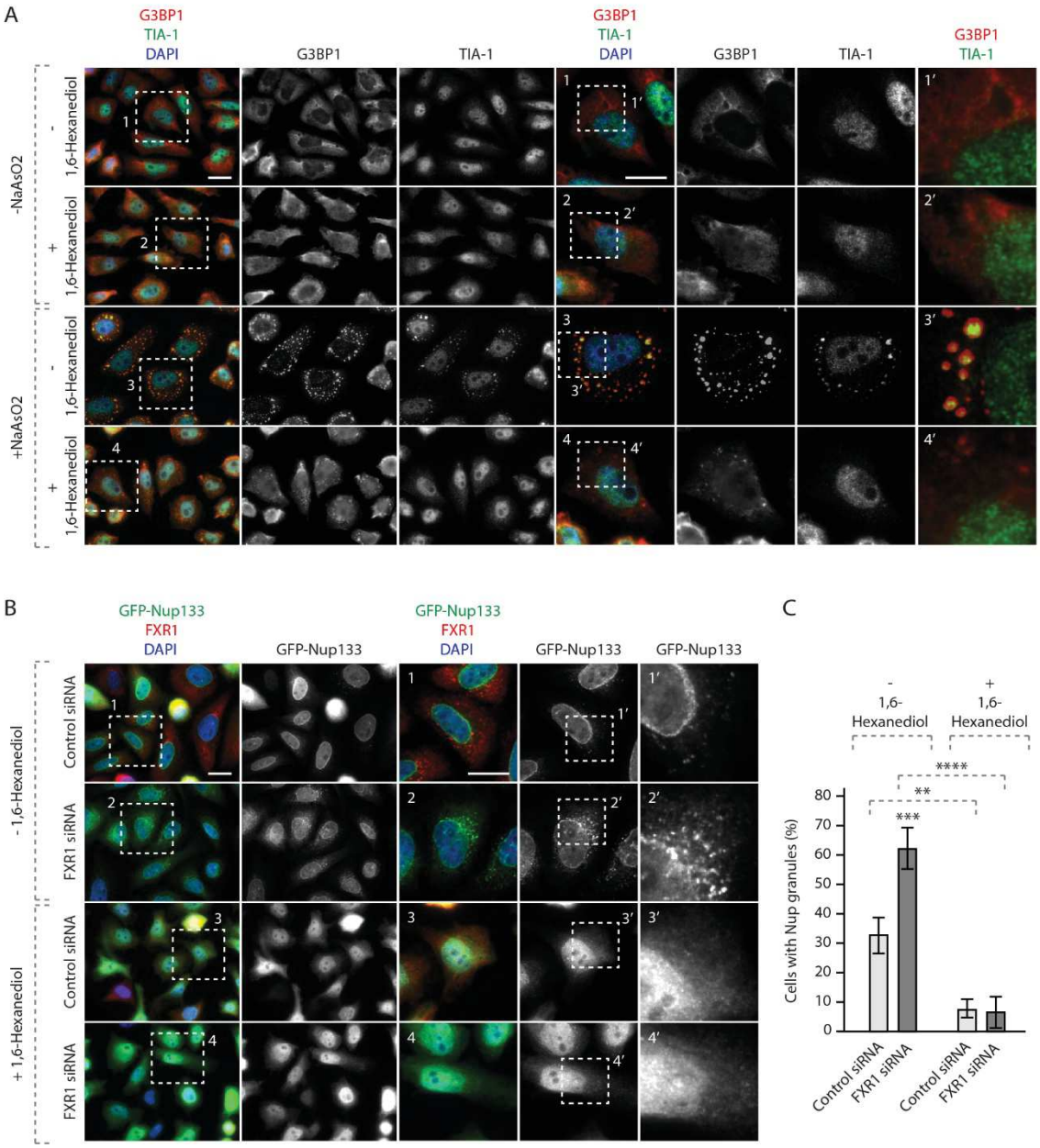

Figure 5 - Cytoplasmic Nup granules are sensitive to 1,6-Hexanediol.

A HeLa cells stably expressing GFP-Nup133 were synchronized by double thymidine block, released for 12 hours, treated or not with $NaAsO_2$ to induce SG formation and with 1,6 Hexanediol, and analyzed by IF microscopy. The magnified framed regions are shown in the corresponding numbered panels.

B, C HeLa cells stably expressing GFP-Nup133 were treated with the indicated siRNAs, synchronized by double thymidine block, released for 12 hours, treated with or without 1,6-Hexanediol and analyzed by IF microscopy. The magnified framed regions are shown in the corresponding numbered panels. The percentage of cells with cytoplasmic GFP-Nup133 granules was quantified in (**C**), 3100 cells were analyzed (mean ±SD, **P < 0.01; ***P < 0.001; ****P < 0.0001; N = 3).

Data information: Scale bars are 5 μm. Statistical significance was assessed by one-way ANOVA test with Sidak's correction.

2.7.6. FXR1 inhibits Nup condensate formation by dynein-based microtubule-dependent transport

We next investigated the mechanism by which loss of FXR1 promotes the formation of Nup condensates. We noticed that the Nup granules were not scattered randomly in the cytoplasm but often formed a crescent-like shape around the microtubule-organizing centre (MTOC) suggesting a role for microtubules (Appendix Figure S6A). Indeed, we found that nocodazole-mediated microtubule depolymerization also induced Nup granules (Appendix Figure S6B, C). Notably, our earlier mass spectrometry analysis identified the cytoplasmic minus-end directed motor protein dynein heavy chain (HC) co-immunoprecipitating specifically with GFP-FXR1, along with the Nups (Dataset EV1). We demonstrated an interaction of GFP-FXR1 with other components of the dynein complex, specifically dynein intermediate chain (IC) (which was visualized as a slower migrating band relative to the input lysate) and dynactin $p150^{Glued}$ (Fig 6A). Downregulation of dynein HC by two independent siRNAs, which also depleted dynein IC as reported (Splinter *et al*, 2010) (Appendix Figure S6D), led to the accumulation of the cytoplasmic Nup granules (Fig 6B, C; Appendix Figure S6E), and to the irregular nuclei (Appendix Figure S6F) highly reminiscent of FXR1 depletion.

Analysis of several known dynein adaptor proteins in a co-IP assay with GFP-FXR1 revealed an interaction with BICD2, but not Mitosin or HOOK3 (Fig 6D). Downregulation of BICD2 by two independent siRNAs likewise led to accumulation of the cytoplasmic Nup granules (Fig 6E, F). Our results suggest that FXR1, working together with the microtubule motor dynein-BICD2 complex, inhibits formation of cytoplasmic Nup granules.

Figure 6

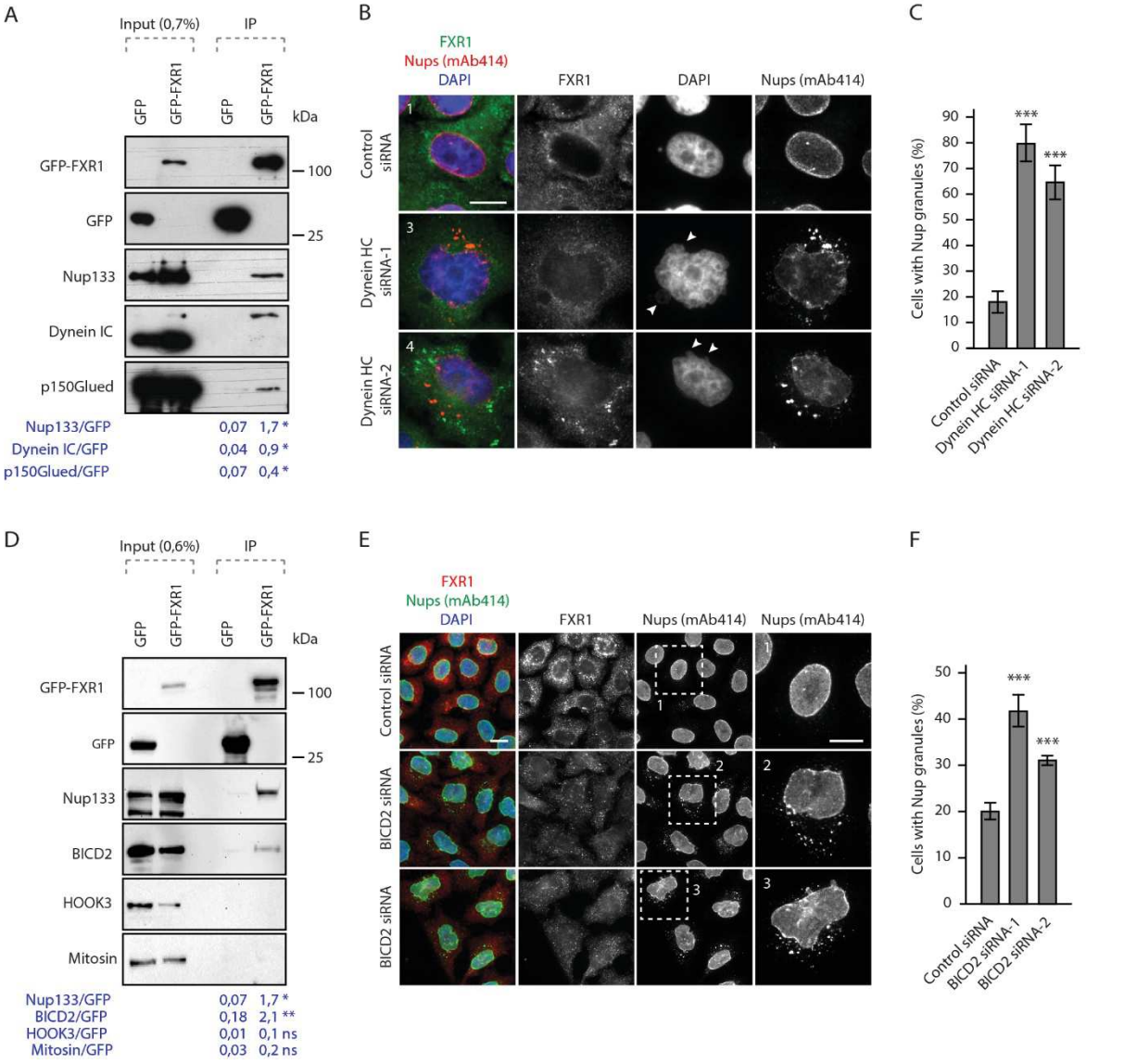

Figure 6 - FXR1 works together with the dynein-BICD2 complex to inhibit cytoplasmic Nup granules formation.

A HeLa cells stably expressing GFP alone or GFP-FXR1 were immunoprecipitated using GFP-Trap beads (GFP-IP), analyzed by Western blot and quantified (mean, *P < 0.05; N = 3).

B, C HeLa cells were treated with the indicated siRNAs, synchronized by double thymidine block, released for 12 hours and analyzed by IF microscopy. Images in (**B**) correspond to the numbered magnified framed regions indicated in the pictures shown in

Appendix Figure S6E. Arrowheads indicate blebbed regions of nuclei. The percentage of interphasic cells with Nup granules was quantified (**C**), 900 cells were analyzed (mean ±SD, ***P < 0.001; N = 3). The corresponding Western blot analysis is shown in Appendix Figure S6D.

D Lysates of HeLa cells stably expressing GFP alone or GFP-FXR1 were subjected to IP using GFP-Trap beads (GFP-IP), analyzed by Western blot and quantified (mean, *P < 0.05; **P < 0.01; N = 3).

E, F HeLa cells were treated with the indicated siRNAs, synchronized by double thymidine block and released for 12 hours and analyzed by IF microscopy for FXR1 and mAb414. The magnified framed

regions are shown in the corresponding numbered panels in (**E**). The percentage of cells with cytoplasmic Nup granules was quantified in (**F**), 2700 cells were analyzed (mean ±SD, ***P < 0.001; N = 3).
Data information: Scale bars are 5 μm. Statistical significance was assessed by unpaired two-tailed Student's T-test (**A, D**) and one-way ANOVA test with Dunnett's correction (**C, F**).

Our earlier results in living GFP-Nup107 cells showed cytoplasmic Nup granule formation in early interphase, which occasionally fused with the NE in control cells but became bigger in FXR1-deficient cells (Fig 4A, B; Movie EV3, 4, 5). We also observed moderate decrease in Nup localization at the NE in FXR1-deficient cells (Fig 2D-F, H). These results suggest that at least a very small pool of the Nups is no longer incorporated into the NE during interphase. Interestingly, in Drosophila oocytes, precursor Nup granules were observed being incorporated into membranes forming the AL-specific NPCs (Hampoelz *et al*, 2019b). Thus, we considered that FXR1 together with the microtubule motor dynein-BICD2 complex may mediate the transport of small pool of cytoplasmic Nups to the NE during interphase of human cells. To test this, we first treated the cells stably expressing GFP-Nup133 with nocodazole to induce Nup granule formation in a reversible way (Fig 7A). Downregulation of FXR1 or dynein potentiated the effect of nocodazole and led to the increase in a number of cells with Nup granules relative to control (Fig 7A, B). Interestingly, following nocodazole wash-out, we observed a strong reduction of Nup granules in control cells while FXR1 and dynein downregulation did not reduce cytoplasmic Nup granules to the same extent under these conditions (Fig 7A, B). To corroborate these findings, we performed live video spinning disk microscopy of cell lines stably expressing GFP-Nup107. Following nocodazole wash-out, we observed the dynamics of the Nup aggregates in control, FXR1- and dynein-downregulated cells (Fig 7C-E). GFP-Nup107-positive aggregates showed dynamic behavior and both fusion and splitting of the granules were observed under all conditions (Fig 7C-E) supporting the condensate properties of these Nup cytoplasmic granules. As expected from the results in fixed specimens (Fig 7A, B), the percentage of cells with fusion and fission events of GFP-Nup107 granules was increased in FXR1- and dynein-downregulated cells (Fig 7D) but the frequency of these events per cell (2 to 3), observed in all cells positive for GFP-Nup107 granules did not differ significantly (Fig 7E).

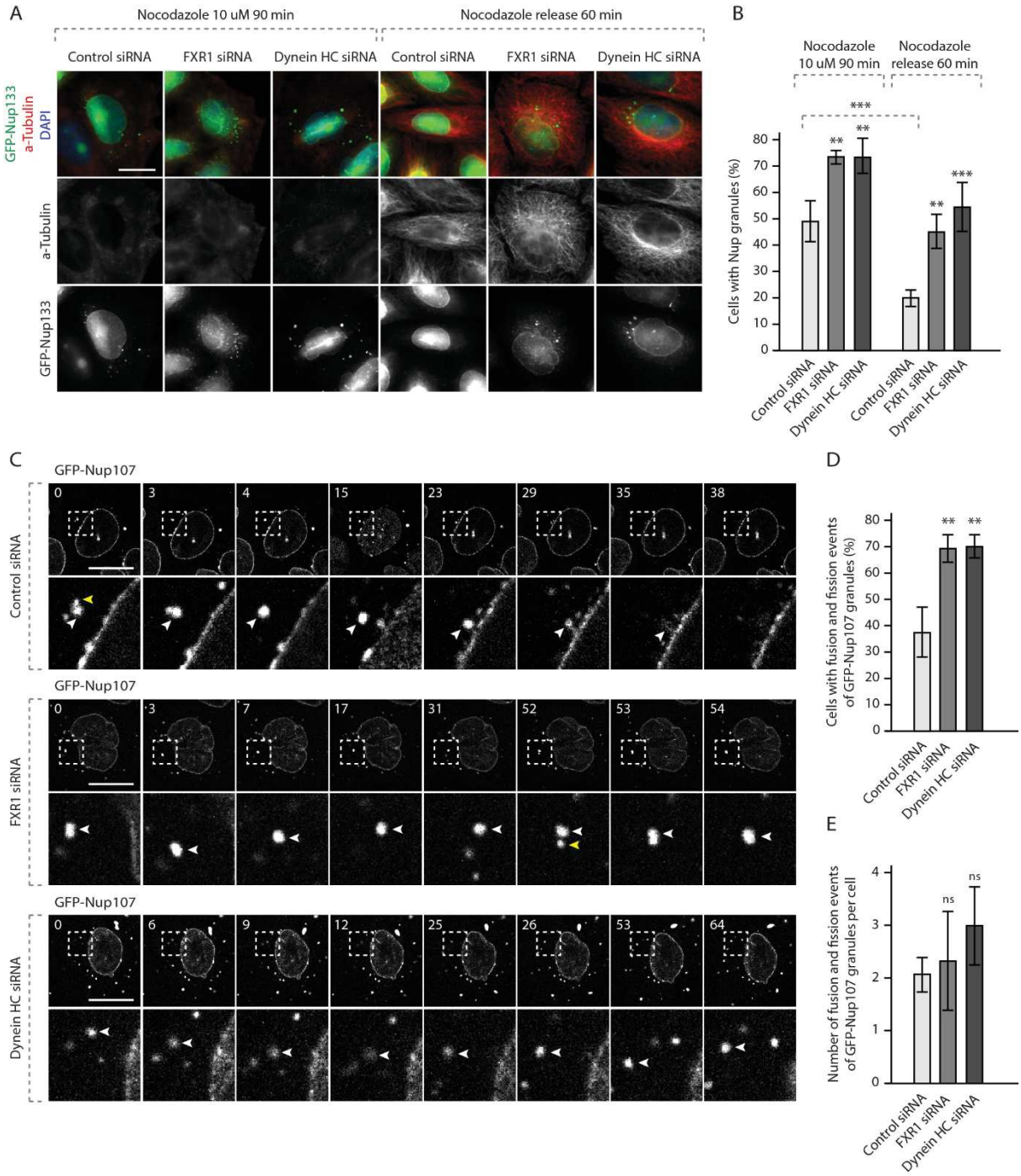

Figure 7 - FXR1 regulates cytoplasmic Nups by dynein-based microtubule-dependent transport.

A, B HeLa cells stably expressing GFP-Nup133 were treated with the indicated siRNAs, synchronized by double thymidine block, released for 12 hours, treated with nocodazole to induce granule formation and washed-out as indicated and analyzed by IF microscopy. The percentage of cells with cytoplasmic GFP-Nup133 granules was quantified in (**B**), 5200 cells were analyzed (mean ±SD, **P < 0.01; ***P < 0.001; N = 3).

C-E HeLa cells stably expressing GFP-Nup107 were treated with the indicated siRNAs, synchronized by double thymidine block, released for 12 hours, treated with nocodazole to induce granule formation

and washed-out as in (**A**) and analyzed by live video spinning disk confocal microscopy. The selected frames of the movies are depicted and time is shown in minutes. The magnified framed regions are depicted in the lower rows. White arrowheads point to individual GFP-Nup107-positive granules. Yellow arrowheads point to the granules undergoing fusion events. The percentage of cells with fusion/fission events of GFP-Nup107 granules was quantified in (**D**), 815 cells were analyzed (mean ±SD, **P < 0.01; N = 3). The number of fusion/fission events per cell was quantified in (**E**), 815 cells were analyzed (mean ±SD; N = 3).
Data information: Scale bars are 5 μm. Statistical significance was assessed by unpaired one-way ANOVA test with Sidak's (**B**) or Dunnet's (**D, E**) correction.

Interestingly in control cells, nocodazole wash-out led to NE-directed transport and fusion of GFP-Nup107-granules with the NE. In contrast, downregulation of FXR1 or dynein in nocodazole washed-out cells led to retention of the GFP-Nup107-granules in the cytoplasm. Under these conditions, the GFP-NUP107-granules were still mobile but little NE-directed movement was observed, and they continued to fuse and often increased in size (Fig 7C) consistent with the previous results in cells not treated with nocodazole (Fig 4A, B; Movies EV1-5). These observations suggest that microtubule-based transport by the FXR1-dynein complex can decrease local concentrations of cytoplasmic Nups thereby preventing their assembly into condensates.

2.7.7. Nup localization defects can be linked to FXS

Next, we analyzed whether all members of the FXR protein family share analogous roles in the spatial control of Nup self-assembly. Our data show that in addition to FXR1, FXR2 and FMRP can localize at the NE in HeLa cells (Fig EV4A) and in mouse myoblasts (Fig EV4B). Interestingly, depletion of each of the three members of this protein family led to the condensation of cytoplasmic Nups relative to control cells (Fig EV4C, D). Downregulation of all three FXR proteins also led to nuclear morphology defects (Fig EV4E). Simultaneous downregulation of all three FXR proteins did not further increase the penetrance of these phenotypes (Fig EV4D, E), suggesting that FXR proteins together form a protein complex in human cells consistent with our mass spectrometry results (Dataset EV1). Interestingly, downregulation of FMRP and FXR1 led to more severe defects as compared to FXR2 (Fig EV4D, E). We speculate that higher protein sequence identity between FMRP and FXR1 (86%) (Hoogeveen *et al*, 2002) as compared to FMRP and FXR2 (70%), leads to sharing more common functions by these two family members.

Since FMRP is silenced in FXS (Santoro *et al*, 2012), we asked if the Nup localization defects are observed in cellular models of this disease. We stimulated FXS patient-derived fibroblasts which lack the FMRP protein (Fig 8A) to undergo synchronous mitotic exit and nuclear reformation. FXS fibroblasts displayed accumulation of cytoplasmic Nup granules relative to control fibroblasts (Fig 8B, C) and similar to those observed in HeLa cells, and structurally abnormal nuclei (Fig 8D). To corroborate these findings, we used human induced pluripotent stem cells (iPSCs) derived from an FXS patient (FXS-iPSCs) and the isogenic rescue cells (C1_2-iPSCs), where reactivation of the *FMR1* locus is achieved by CRISPR-mediated excision of the expanded CGG-repeat from the 5'UTR of the *FMR1* gene (Xie *et al*, 2016a). In the FXS-iPSCs, accumulation of large Nup133-positive cytoplasmic condensates was observed (Fig 8E), which were reduced in the FMRP re-expressing cells, although they were still present (Fig 8E, F). Re-expressed FMRP in the reactivated cell line localized to both the NE and to the cytoplasmic perinuclear region, which often also contained Nup133 (Fig 8G). We speculate that these perinuclear FMRP-Nup133 signals could represent assembly intermediates before Nup133 is properly transferred and inserted into the NE due to lower levels of FMRP protein re-expression in the rescue system (Xie *et al*, 2016a) which could result in a slowdown of the process and similar to the GFP-FXR1-Nups signals occasionally observed in HeLa cells (Fig 1E).

Figure 8

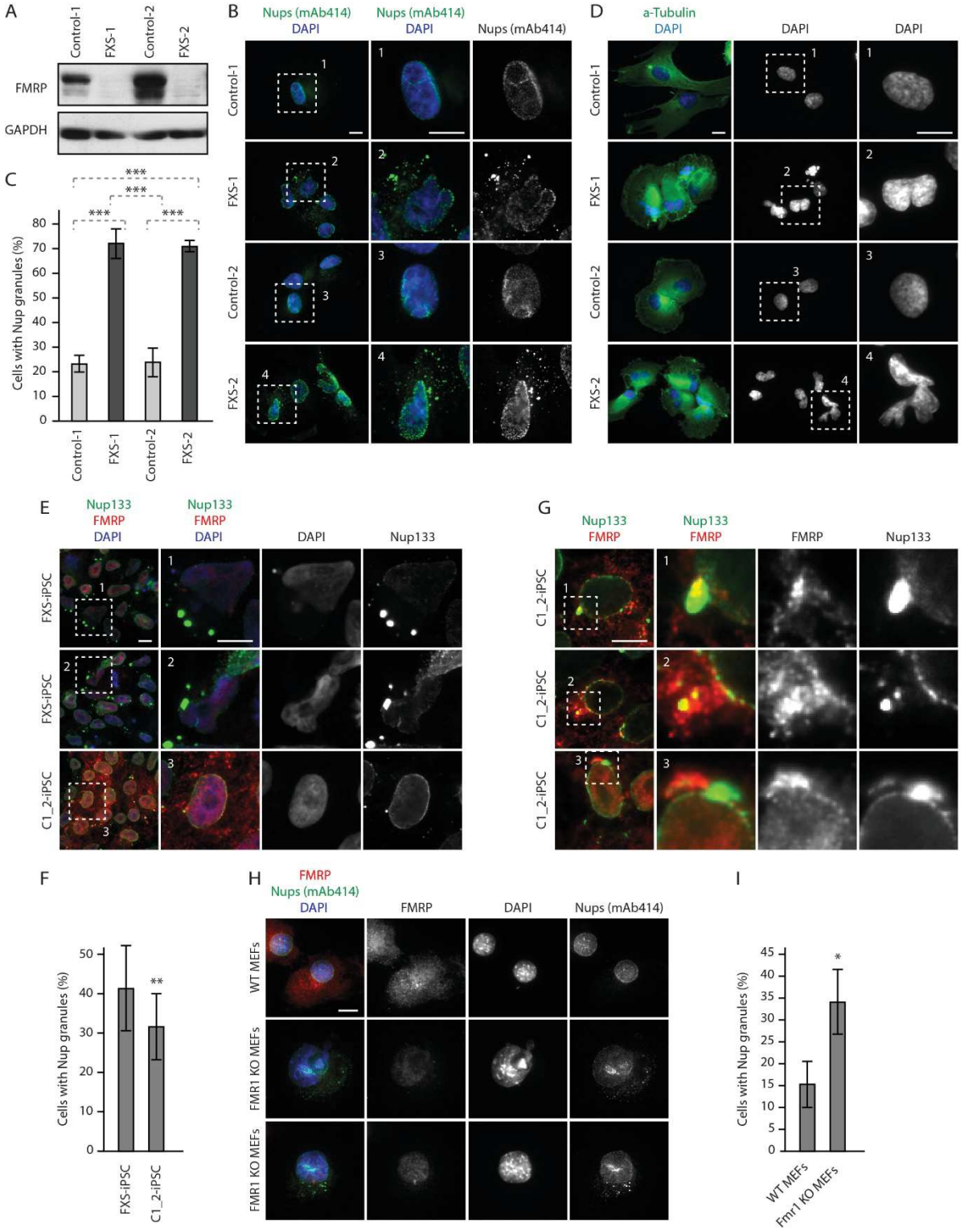

Figure 8 - Nup localization defects can be linked to FXS.

A-D Human FXS-patient derived fibroblasts (FXS-1, FXS-2) and control human fibroblasts were synchronized in early G1 by Monastrol release and analyzed by Western blot (**A**) and IF microscopy (**B, D**). The percentage of cells with cytoplasmic Nup granules was quantified in (**C**), 283 cells were

analyzed (mean ±SD, ***P < 0.001; N = 3). Examples of Nup localization defects are shown in (**B**) and examples of nuclear architecture defects are shown in (**D**).

E-G Human iPSCs derived from a FXS patient (FXS-iPSC) and the isogenic rescue cells (C1_2-iPSC) were analyzed by IF microscopy **(E, G)**. The percentage of cells with cytoplasmic Nup133 granules was quantified in (**F**), 5500 cells were analyzed (mean ±SD, **P < 0.01; N = 3). Examples of co-localization events of re-expressed FMRP and Nup133 are shown in (**G**).

H, I Mouse Embryonic Fibroblasts (MEFs) derived from the *Fmr1* knock-out (KO) mice and WT controls were synchronized in early G1 by Monastrol release and analyzed by IF microscopy (**H**). The percentage of cells with cytoplasmic Nup granules was quantified in (**I**), 2400 cells were analyzed (mean ±SD, *P < 0.05; N = 3).

Data information: Scale bars are 5 µm. Statistical significance was assessed by one-way ANOVA test with Sidak's correction (**C**), paired two-tailed Student's T-test (**F**) and unpaired two-tailed Student's T-test (**I**).

Thus, the absence of human FMRP in primary cell lines and in iPSs cells leads to the accumulation of Nup granules as also seen in the cancer cell lines.

To confirm these findings in an animal model of FXS, we used mouse embryonic fibroblasts (MEFs) derived from the *Fmr1* knock-out (KO) mice. *Fmr1* KO MEFs also displayed accumulation of perinuclear Nup granules relative to WT MEFs (Fig 8H, I). Taken together, our results demonstrate the presence of ectopic Nup assemblies in several cellular models of FXS. These defects may perturb cellular homeostasis and contribute to FXS pathology.

2.7.8. The FXR1 regulates protein export and cell cycle progression

What could be the biological consequences of misregulation of the FXR proteins-dynein pathway and how could Nup assembly defects perturb cellular homeostasis? To understand if ectopic Nup condensation during early G1 in FXR-deficient cells affects the function of the nuclear pores, we measured the rates of nucleocytoplasmic transport of an ectopic import/export reporter plasmid XRGG-GFP that shuttles to the nucleus when induced with dexamethasone. FXR1 downregulation did not change the rates of nuclear import (Fig EV5A, B) relative to control cells, whereas downregulation of the Nup ELYS clearly demonstrated import defects in the same experiments, as expected (Fig EV5A, B). This indicates that, at least in the steady-state, nucleocytoplasmic import is largely unaffected by formation of Nup granules in FXR1-deficient cells. Interestingly, while the overall rate of protein export remained unchanged in FXR1-deficient cells relative to controls (Fig EV5C, D), FXR1

downregulation reduced the export rate solely in early G1 cells (time points 20 and 30 minutes) similar to ELYS (Fig EV5D; Fig 9A), suggesting that FXR1-downregulation mediated Nup defects may affect the function of nuclear pores specifically during this cell cycle stage. Consistent with the observed export defects in FXR1-deficient G1 cells, the nuclear export factor chromosomal region maintenance 1 (CRM1) protein was sequestered to Nup granules labeled with the mAb414 antibody and with GFP-Nup133 (Fig 9B).

These observations prompted us to test whether the FXR1-Nup pathway could also be important for cell cycle progression of cells in interphase. For this, we analyzed retinoblastoma (Rb) protein which is phosphorylated during G1/S phase transition (p-Rb) and is kept in this state until mitotic exit. Downregulation of FXR1 led to accumulation of cells with strong nuclear p-Rb signal (Fig 9C, D), suggesting perturbations in cell cycle progression. To elucidate if this accumulation was specific to any cell cycle phases, we analyzed p-Rb together with EdU incorporation (S phase marker) or Cyclin B (G2 marker) in interphasic cells. Downregulation of FXR1 led to an increased percentage of cells positive for both p-Rb and EdU signal (Fig 9E) but not for p-Rb and Cyclin B signal, (Fig 9F), suggesting that upon FXR1 downregulation cells accumulate in S phase. Accordingly, the percentage of p-Rb negative cells (corresponding to G1 phase) was decreased in all cases. Together, these data indicate that the absence of FXR1 leads to protein export defects in G1 and perturbation in cell cycle progression.

Figure 9

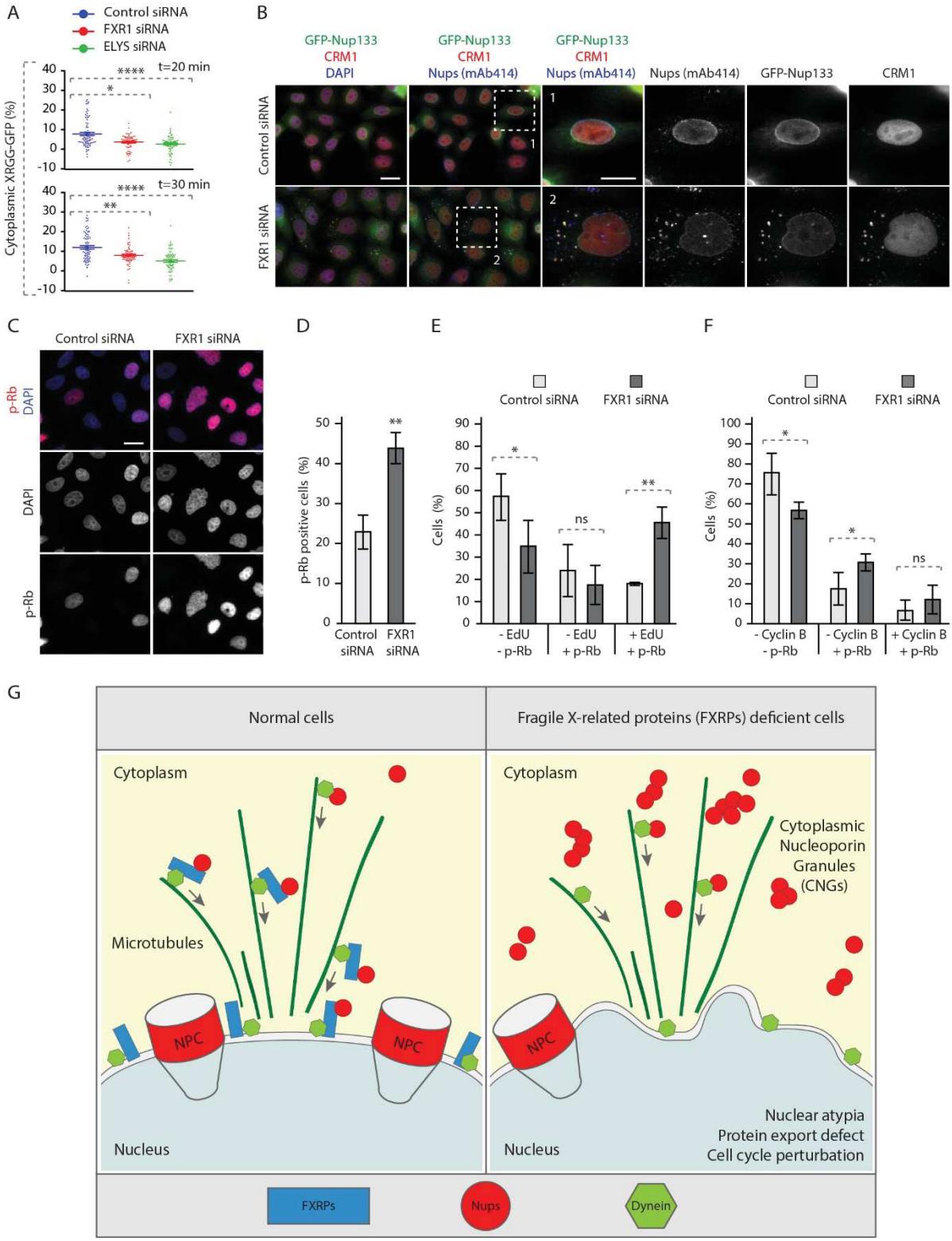

Figure 9 - FXR1 regulates G1 cell cycle progression.

A HeLa cells were transfected with the import/export reporter plasmid XRGG-GFP, treated with the indicated siRNAs and synchronized in early G1 phase by Monastrol release. Dexamethasone was added for 3 hours to induce XRGG-GFP nuclear import. Following wash-out the nuclear export of XRGG-GFP was analyzed by live video spinning disk confocal microscopy. The selected frames of the movies

are depicted in Figure EV5C. The percentage of cytoplasmic XRGG-GFP over time was quantified in Figure EV5D and quantifications of individual cells from the 20 and 30 minutes time points are depicted in (**A**), 199 cells were analyzed (mean ±SD, *P < 0.05; **P < 0.01; N = 3).

B HeLa cells stably expressing GFP-Nup133 were treated with the indicated siRNAs, synchronized by double thymidine block, released for 12 hours and analyzed by IF microscopy. The magnified framed regions are shown in the corresponding numbered panels.

C, D Asynchronously proliferating HeLa cells were treated with indicated siRNAs and analyzed by IF microscopy (**C**). The percentage of p-Rb positive cells was quantified in (**D**), 2800 cells were analyzed (mean ±SD, **P < 0.01; N = 3).

E, F Asynchronously proliferating HeLa cells were treated with indicated siRNAs, incubated with EdU during 30min and analyzed by IF microscopy. The percentage of p-Rb and/or EdU positive cells was quantified in (**E**), 2100 cells were analyzed (mean ±SD, *P < 0.05; **P < 0.01; N = 3), and the percentage of p-Rb and/or cyclin B positive cells was quantified in (**F**), 3300 cells were analyzed (mean ±SD, *P < 0.05; N = 3).

G A hypothetical model how Fragile X-related proteins spatially regulate Nup condensation. FXR proteins (blue) interact with cytoplasmic soluble Nups (red circles) and dynein (green) and facilitate their localization to the NE during early G1. This function of FXR proteins inhibits formation of aberrant cytoplasmic Nup assemblies, the Cytoplasmic Nup Granules (CNGs), contributing to the equilibrium of NE-NPCs and driving the G1-specific protein export and maintenance of nuclear shape and cell cycle progression. Silencing of FXR proteins, for instance in FXS patients, leads to the accumulation of CNGs, nuclear atypia, protein export defects, and defects in cell cycle progression, which may contribute to the pathology of FXS.

Data information: Scale bars are 5 μm. Statistical significance was assessed by Kruskal-Wallis test with Dunn's correction (**A**), unpaired two-tailed Student's T-test (**D**) and One-way ANOVA test with Sidak's correction (**E, F**).

2.7.9. Expanded View Figures

Figure EV1

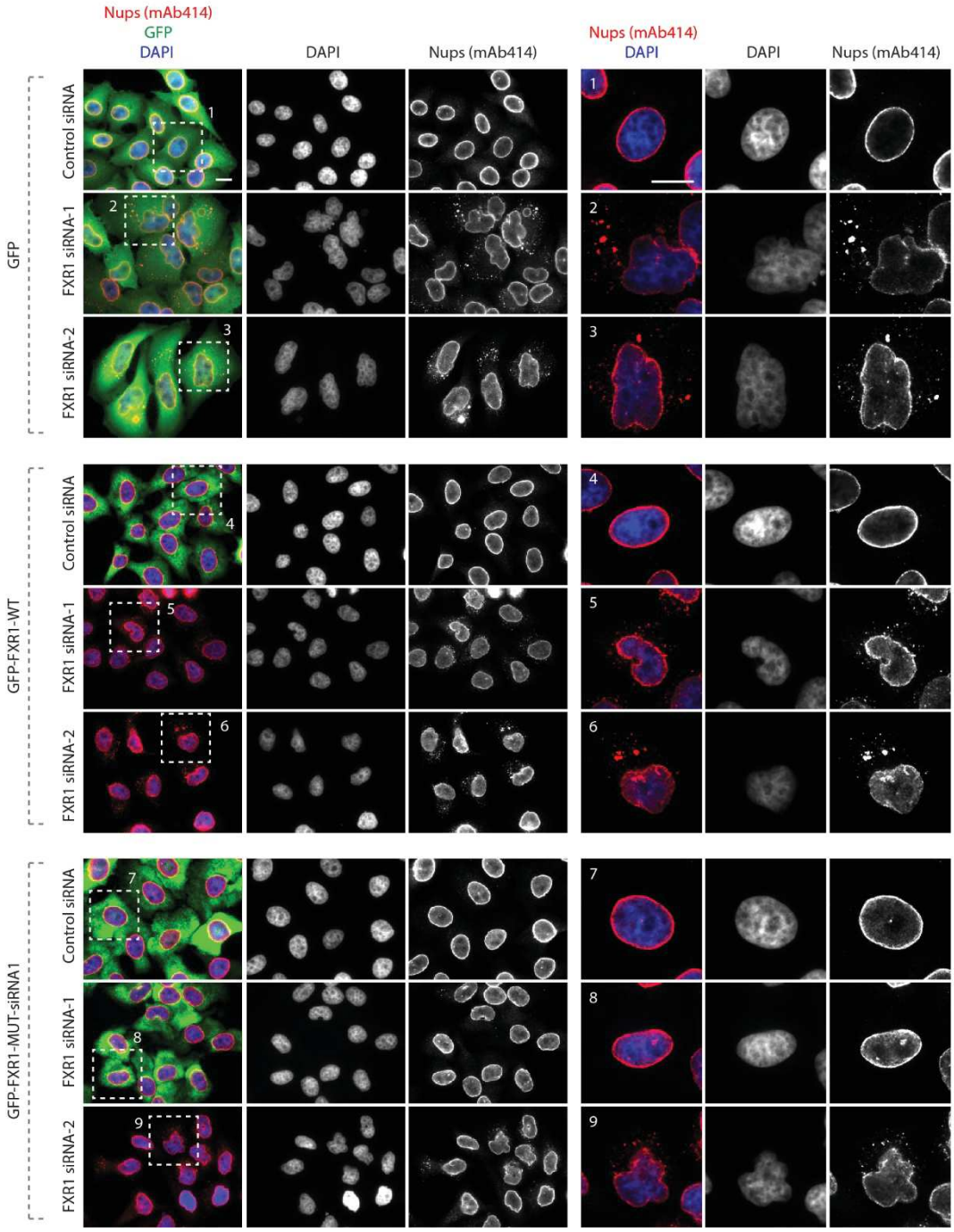

Figure EV1 - FXR1 specifically controls cytoplasmic Nups and nuclear shape.
HeLa cells stably expressing GFP, GFP-FXR1 WT and GFP-FXR1 mutated in the sequence recognized by FXR1 siRNA-1 (GFP-FXR1-MUT-siRNA1) were treated with the indicated siRNAs, synchronized by double thymidine block and released for 24 hours and analyzed by IF microscopy for mAb414 (**related to Figures 2B, 3B, C**). Scale bars are 5 μm.

Figure EV2

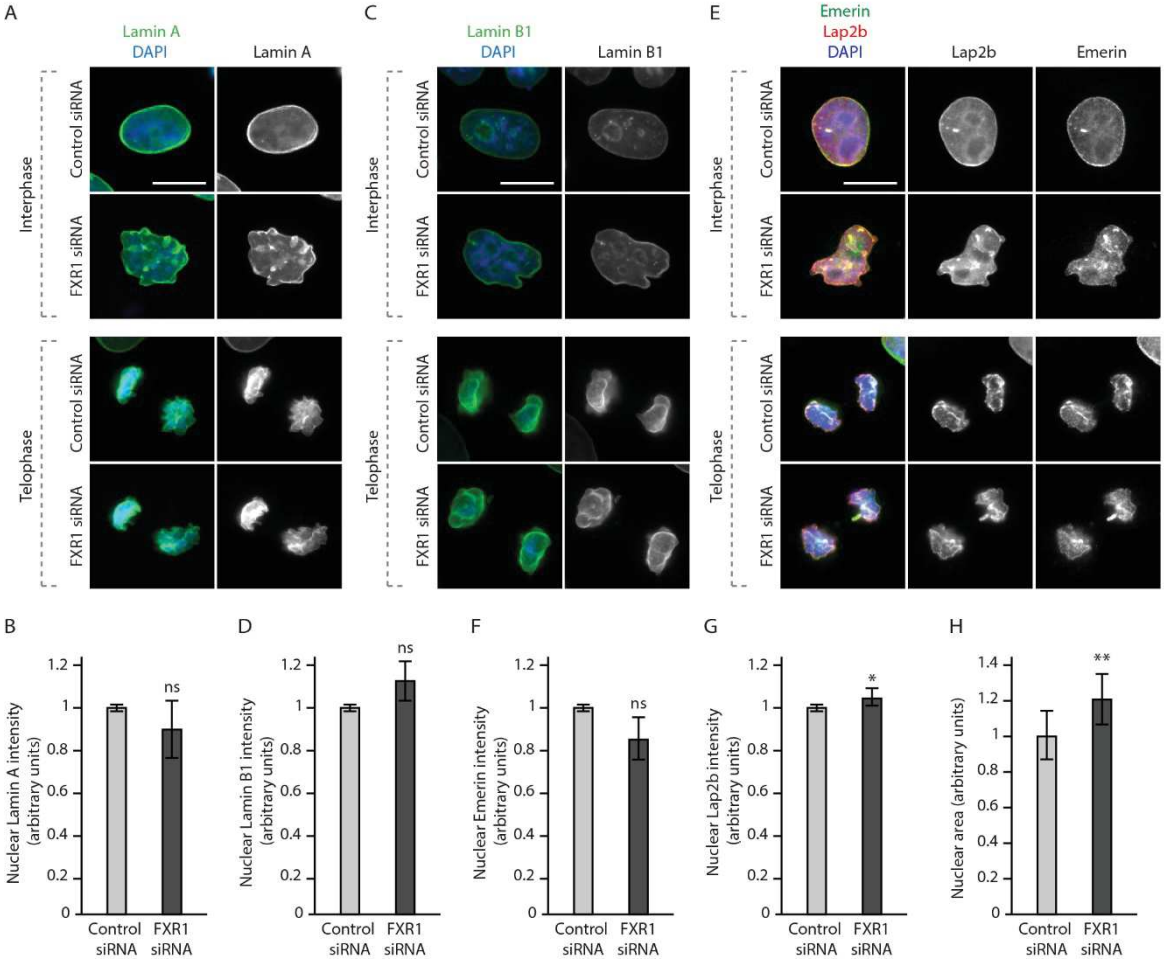

Figure EV2 - FXR1 does not drive recruitment of lamina-associated proteins.

A-H HeLa cells were treated with the indicated siRNAs, synchronized by double thymidine block and released for 9 (telophase) and 12 (interphase) hours and analyzed by IF microscopy. The nuclear intensity of Lamin A (**B**), Lamin B1 (**D**), Emerin (**F**) and Lap2β (**G**) was quantified. 2000 cells were analyzed (mean ±SD, *P < 0.05; ns = non-significant; N = 3). The nuclear area was quantified (**H**), 3300 cells were analyzed (mean ±SD, **P < 0.01; N = 5).

Data information: Scale bars are 5 μm. Statistical significance was assessed by one-sample two-tailed Student's T-test.

Figure EV3

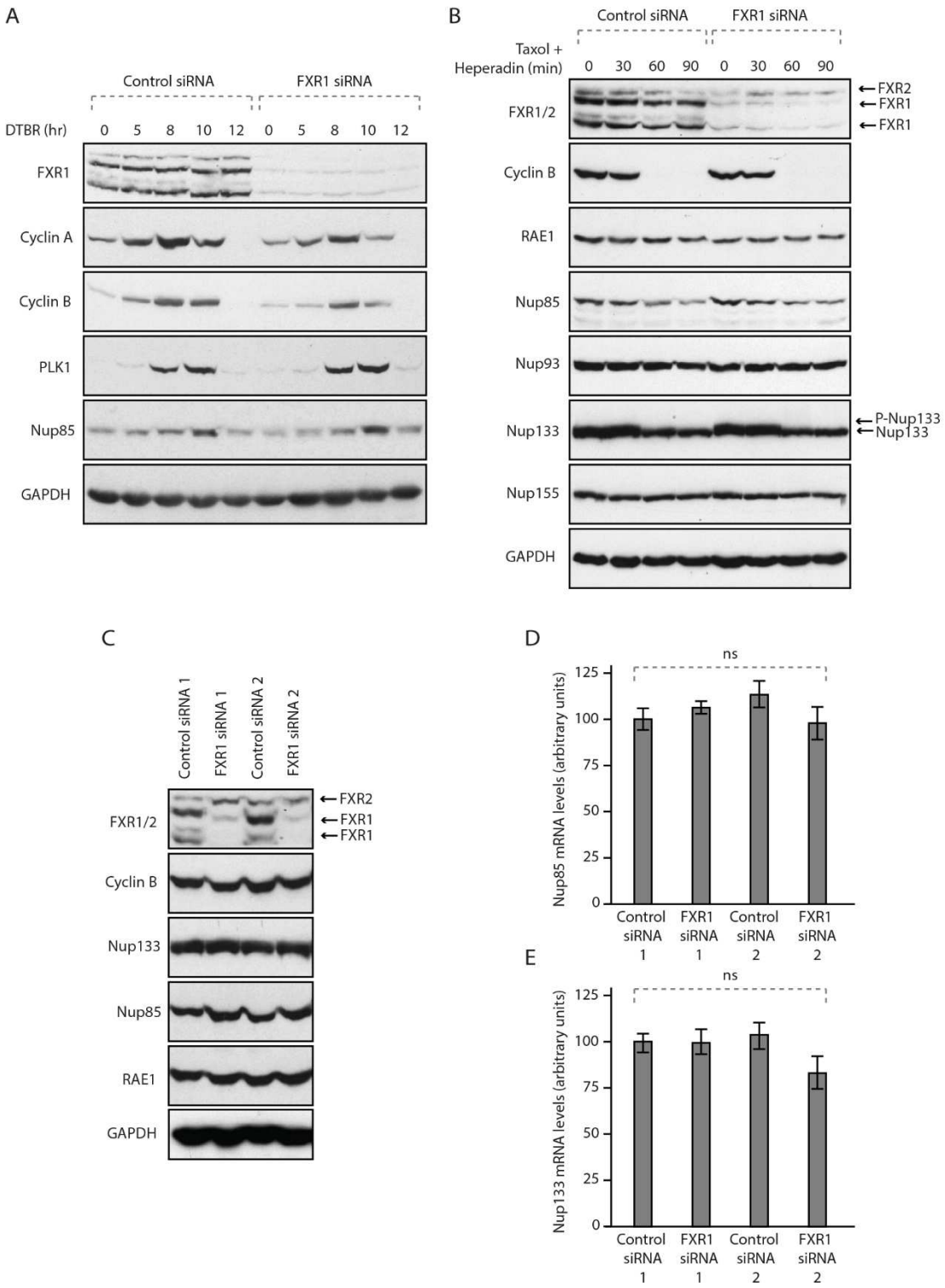

Figure EV3 - FXR1 does not regulate mitotic exit and protein levels of several Nups.
A HeLa cells were treated with the indicated siRNAs, synchronized by double thymidine block and released for the indicated times (hours) and analyzed by Western blot.

B HeLa cells were treated with the indicated siRNAs, synchronized by Hesperadin release from mitotic arrest induced by Taxol and analyzed by Western blot. Arrows point to FXR1 isoforms, FXR2 and phosphorylated (P-Nup133) and unmodified form of Nup133, respectively.
C HeLa cells were treated with the indicated siRNAs, synchronized by double thymidine block, released in interphase and analyzed by Western blot. Arrows point to FXR1 isoforms and FXR2 protein.
D, E HeLa cells were treated with the indicated siRNAs and mRNA levels of Nup85 (**D**) and Nup133 (**E**) were analyzed by Quantitative Real-Time PCR (mean ±SD, ns = non-significant; N = 3).
Data information: Statistical significance was assessed by two-tailed Student's T-test.

Figure EV4

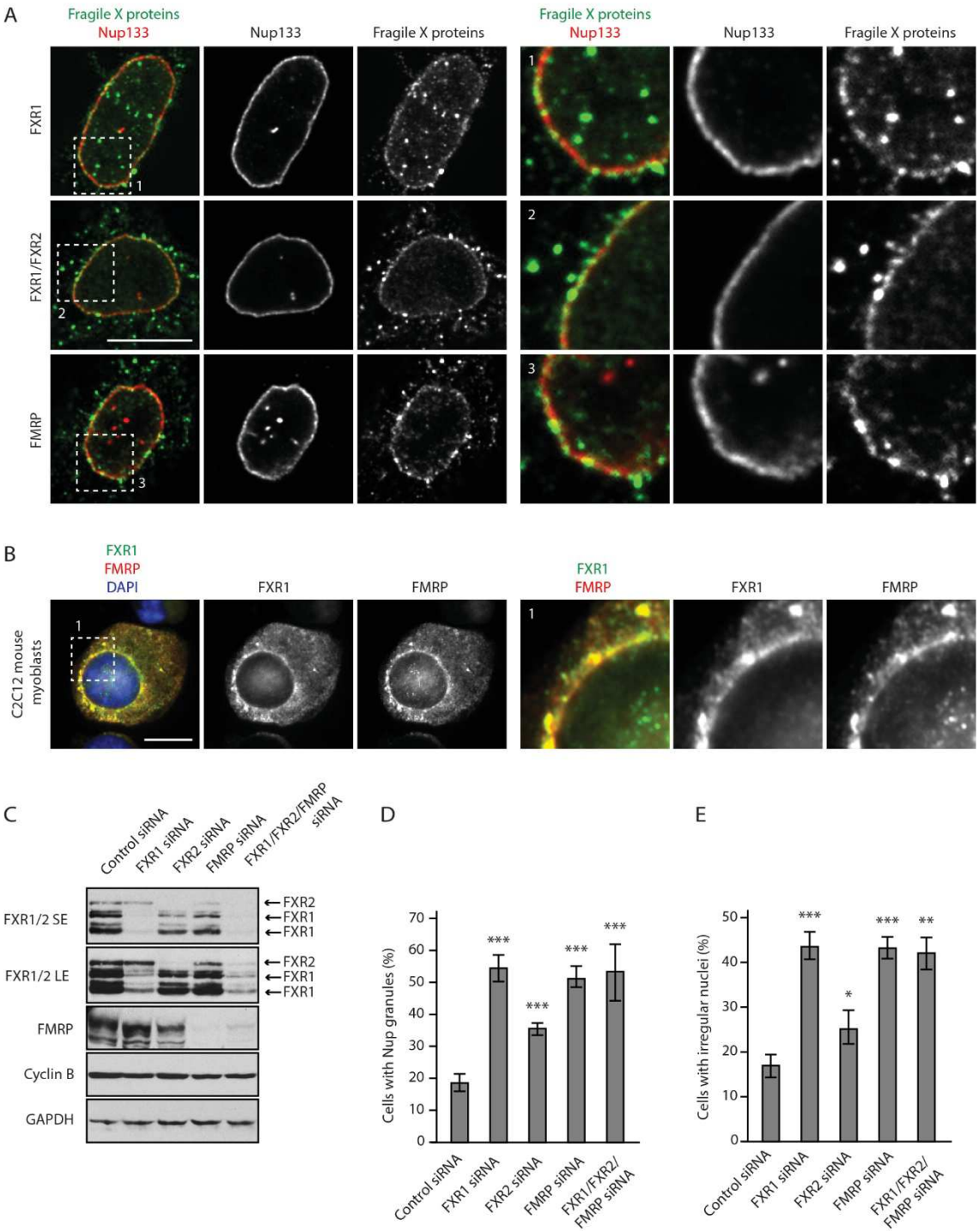

Figure EV4 - FXR protein family members localize to NE and regulate cytoplasmic Nups.
A, B HeLa cells (**A**) and mouse C2C12 myoblasts (**B**) were analyzed by IF microscopy for FXR1, FXR1+2 and FMRP. The magnified framed regions are shown in the corresponding numbered panels. **C-E** HeLa cells were treated with the indicated siRNAs, synchronized by double thymidine block and released for 12 hours and analyzed by Western blot (SE – short exposure, LE – long exposure) (**C**) and IF microscopy (**D, E**). The percentage of cells with cytoplasmic Nup granules (**D**) and irregular nuclei (**E**) was quantified, 900 cells were analyzed (mean ±SD, *P < 0.05; **P < 0.01; ***P < 0.001; N = 3).

Data information: Scale bars are 5 µm. Statistical significance was assessed by one-way ANOVA test with Dunnett's correction (**D, E**).

Figure EV5

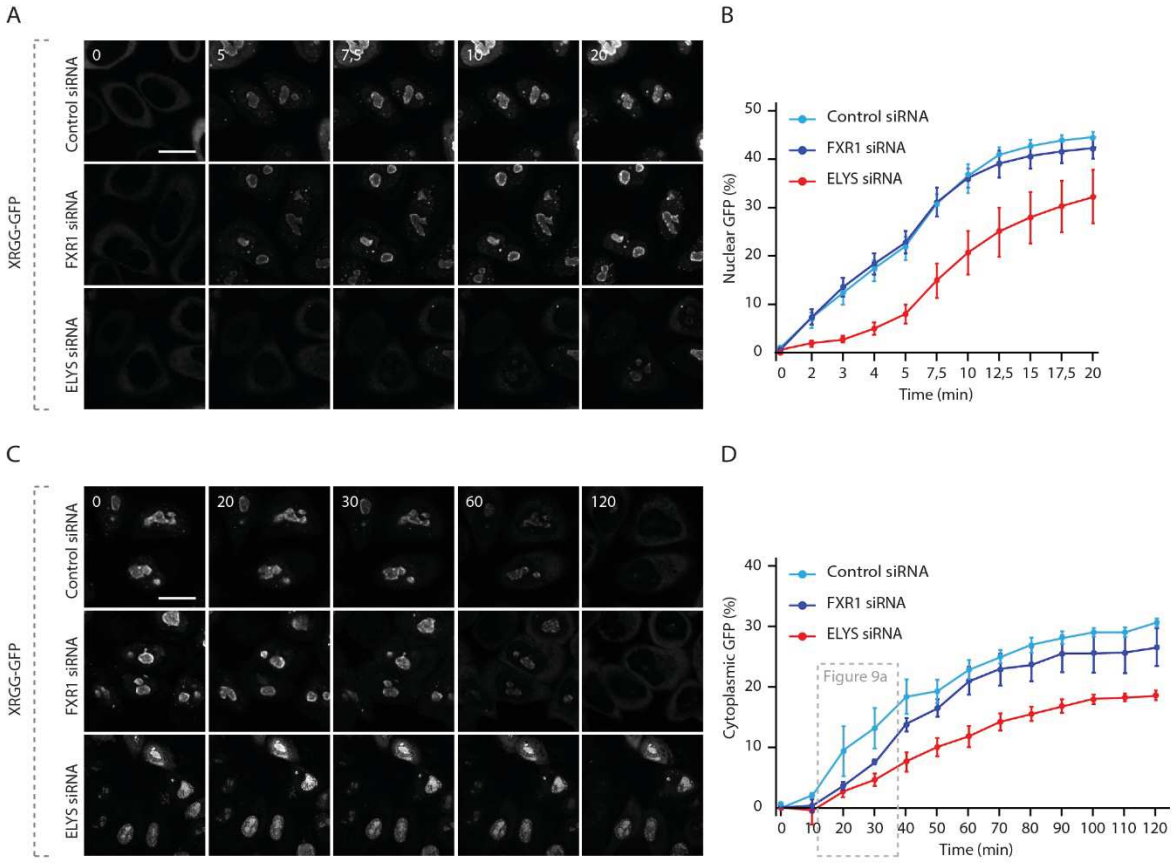

Figure EV5 - FXR1 protein does not regulate steady-state nucleocytoplasmic transport.
A, B HeLa cells were transfected with the import reporter plasmid XRGG-GFP, treated with the indicated siRNAs and synchronized in early G1 phase by Monastrol release. Dexamethasone-induced nuclear import of XRGG-GFP was analyzed by live video spinning disk confocal microscopy (**A**). The selected frames of the movies are depicted and time is shown in min. The increase in the percentage of nuclear XRGG-GFP over time was quantified in (**B**), 247 cells were analyzed (mean ±SEM, N = 3).
C, D HeLa cells were treated as in (**A, B**) and Dexamethasone was added for 3 hours to induce XRGG-GFP nuclear import. Following wash-out the nuclear export of XRGG-GFP was analyzed by live video spinning disk confocal microscopy (**C**). The selected frames of the movies are depicted and time is shown in min. The increase in the percentage of cytoplasmic XRGG-GFP over time was quantified in (**D**), 199 cells were analyzed (mean ±SEM; N = 3).
The distribution of cells with cytoplasmic XRGG-GFP from the time points corresponding to early G1 cell cycle stage (20 and 30 min) are depicted in **Figure 9A**.
Data information: Scale bars are 5 µm.

2.7.10. Expanded View Dataset

Dataset EV1							GFP				GFP-FXR1						
Accession	Description	Σ Coverage	Σ# Proteins	Σ# Unique	Σ# Peptides	Σ# PSMs	Score A2	Coverage A2	# Peptides	# PSM A2	Score B2	Coverage B2	# Peptides	# PSM B2	# AAs	MW [kDa]	calc. pI
P51114-2	Isoform 2 of Fragile X mental retardation syndrome-related protein 1 OS=Homo sapiens GN=FXR1 - [FXR1_HUMAN]	70.50	1	5	42	195					689.34	68.46	41	163	539	60.8	6.39
P51114	Fragile X mental retardation syndrome-related protein 1 OS=Homo sapiens GN=FXR1 PE=1 SV=3 - [FXR1_HUMAN]	64.41	1	4	41	192					648.56	62.64	40	157	621	69.7	6.15
Q14204	Cytoplasmic dynein 1 heavy chain 1 OS=Homo sapiens GN=DYNC1H1 PE=1 SV=5 - [DYHC1_HUMAN]	26.39	1	82	82	185	#####	14.06	43	53	328.06	20.49	62	82	4646	532.1	6.40
P51116	Fragile X mental retardation syndrome-related protein 2 OS=Homo sapiens GN=FXR2 PE=1 SV=2 - [FXR2_HUMAN]	39.38	1	17	19	49		0.00			138.08	39.38	19	32	673	74.2	6.23
Q06787-6	Isoform 5 of Fragile X mental retardation protein 1 OS=Homo sapiens GN=FMR1 - [FMR1_HUMAN]	45.76	4	17	18	39		0.00			115.08	45.76	18	27	590	66.4	8.38
Q8TEM1	Nuclear pore membrane glycoprotein 210 OS=Homo sapiens GN=NUP210 PE=1 SV=3 - [PO210_HUMAN]	8.85	1	11	11	17	11.67	1.22	2	3	25.09	4.98	6	6	1887	205.0	6.81
Q5SRE5-2	Isoform 2 of Nucleoporin NUP188 homolog OS=Homo sapiens GN=NUP188 - [NU188_HUMAN]	3.72	2	4	4	5		0.00			17.28	3.72	4	5	1638	182.2	6.83
Q8WUM0	Nuclear pore complex protein Nup133 OS=Homo sapiens GN=NUP133 PE=1 SV=2 - [NU133_HUMAN]	14.10	1	11	11	22	20.67	6.92	6	6	35.22	11.94	9	9	1156	128.9	5.10
Q9BW27-2	Isoform 2 of Nuclear pore complex protein Nup85 OS=Homo sapiens GN=NUP85 - [NUP85_HUMAN]	12.99	3	4	4	6		0.00			16.59	10.17	3	4	462	52.6	6.52

Dataset EV1 – Selection of GFP-FXR1-interacting partners from mass spectrometry analysis. HeLa cells expressing GFP alone or GFP-FXR1 were immunoprecipitated using agarose GFP-Trap A beads (GFP-IP) and analyzed by mass spectrometry. Sample loading and bead saturation was verified by Western blot. For each hit, the following parameters are depicted: accession (uniprot accession number), Σcoverage (total coverage of the indicated protein in all the experiment), Σ#proteins (the

number of proteins that could correspond to the identified peptides), Σ#Unique peptide (the number of peptides that are found exclusively in the hit protein), Σ#peptides (the number of peptides found corresponding to the hit protein), Σ#PSM (the number of peptides detected for a hit protein), the score (representing an arbitrary quantification calculated by integration of the coverage, the size of the protein and the PSM), #AAs (number of amino acids in the protein sequence), MW (predicted molecular weight in kDa) and PI (isoelectric point). The score was used to discriminate the hits in addition to the number of unique peptides, and hits were considered significant if three or more peptides were unique for the GFP-FXR1 IPs.

Note: the original dataset of the manuscript contains all raw data. Here, only relevant hits for this study are represented.

2.7.11. Appendix Figures

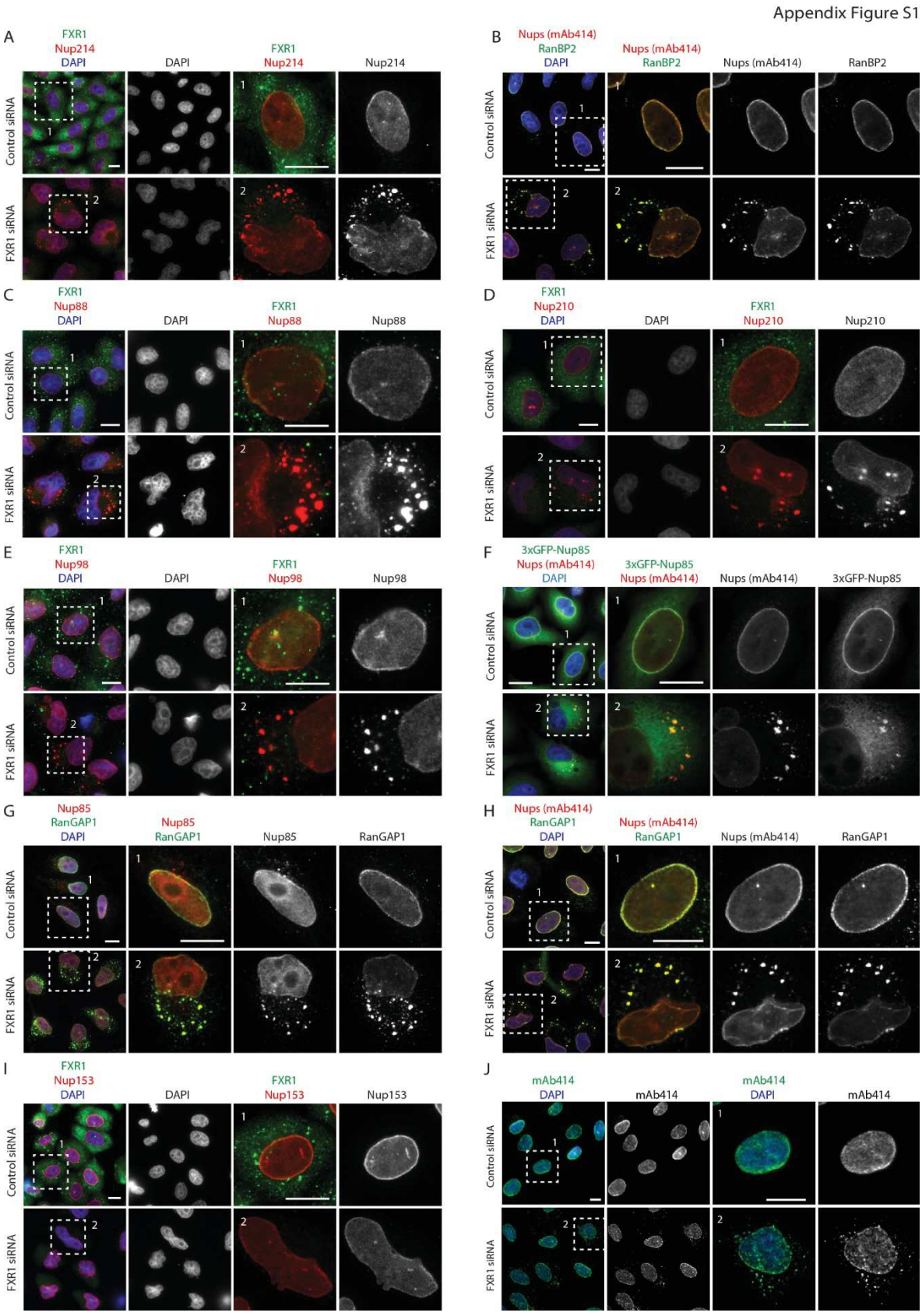

Appendix Figure S1 - FXR1 inhibits aberrant assembly of cytoplasmic Nups.

A-I HeLa cells were treated with the indicated siRNAs, synchronized by double thymidine block and released for 12 hours and analyzed by IF microscopy. The magnified framed regions are shown in the corresponding numbered panels (**related to Figure 2C**). Scale bars are 5 µm.
J U2OS cells were treated with the indicated siRNAs and analyzed by IF microscopy for FG-Nups using mAb414 antibody. The magnified framed regions are shown in the corresponding numbered panels (**related to Figure 2G, H**). Scale bars are 5 µm.

Appendix Figure S2

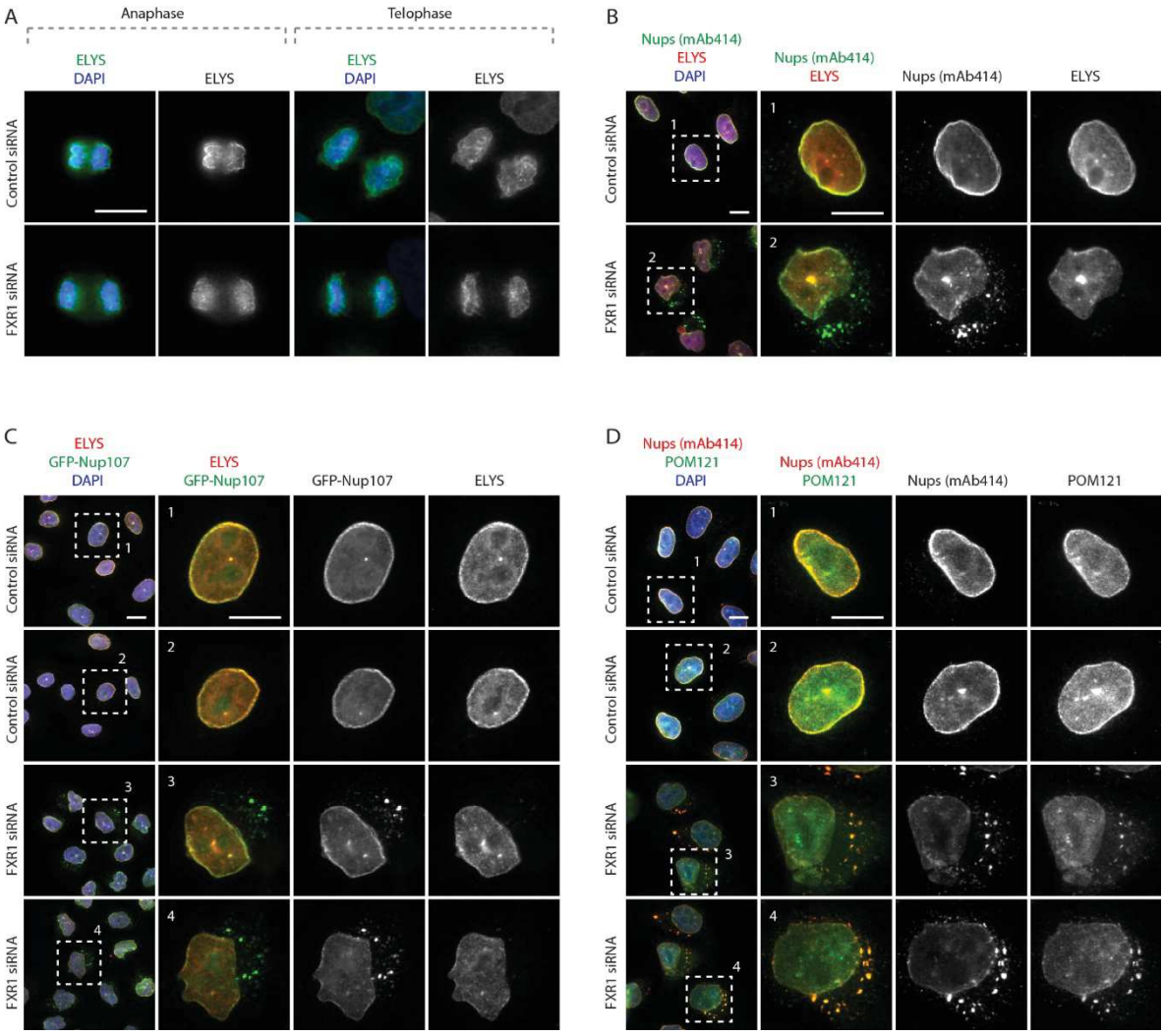

Appendix Figure S2 - FXR1 inhibits aberrant assembly of cytoplasmic POM121 but not ELYS.
A-D HeLa cells (**A, B, D**) or HeLa cells stably expressing GFP-Nup107 (**C**) were treated with the indicated siRNAs, synchronized by double thymidine block and released for 9 (telophase) (**A**) and 12 (early G1 phase) (**B-D**) hours and analyzed by IF microscopy. The magnified framed regions are shown in the corresponding numbered panels (**related to Figure 2C**). Scale bars are 5 µm.

Appendix Figure S3

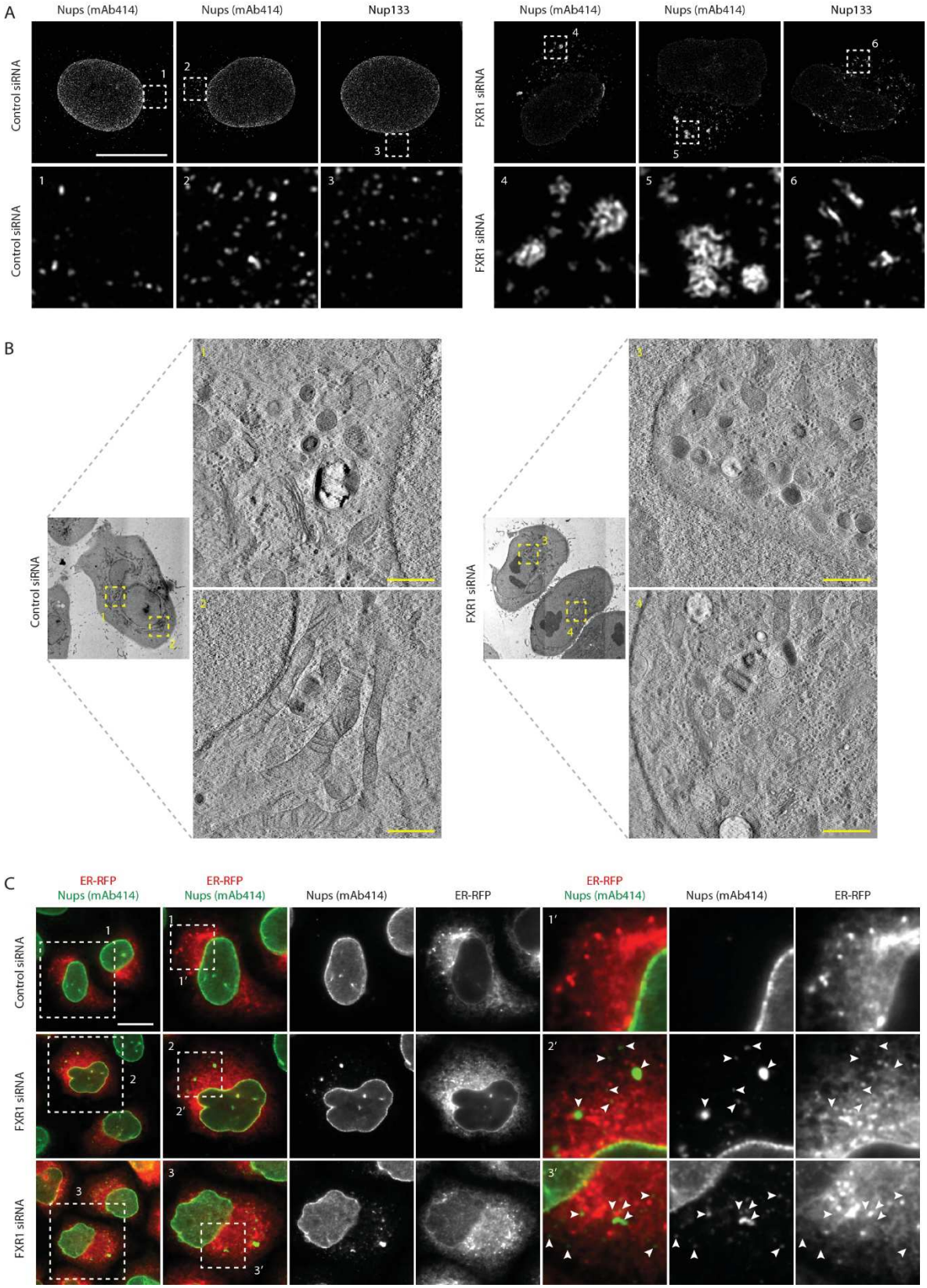

Appendix Figure S3 - The cytoplasmic Nup granules are distinct from ALs.

A HeLa cells were treated with the indicated siRNAs, synchronized by double thymidine block and released for 12 hours and analyzed by super-resolution confocal microscopy. Scale bar is 5 µm.

B HeLa cells were treated with the indicated siRNAs, synchronized by double thymidine block and released for 12 hours and analyzed by EM. The magnified framed regions are shown in the corresponding numbered panels. Scale bar is 1 μm.
C HeLa cells were treated with indicated siRNAs, transfected with ER-RFP reporter for 24h, synchronized by double thymidine block and released for 12 hours and analyzed by IF microscopy. The magnified framed regions are shown in the corresponding numbered panels. Arrowheads point to the FG-Nup-positive cytoplasmic granules. Scale bar is 5 μm.

Appendix Figure S4

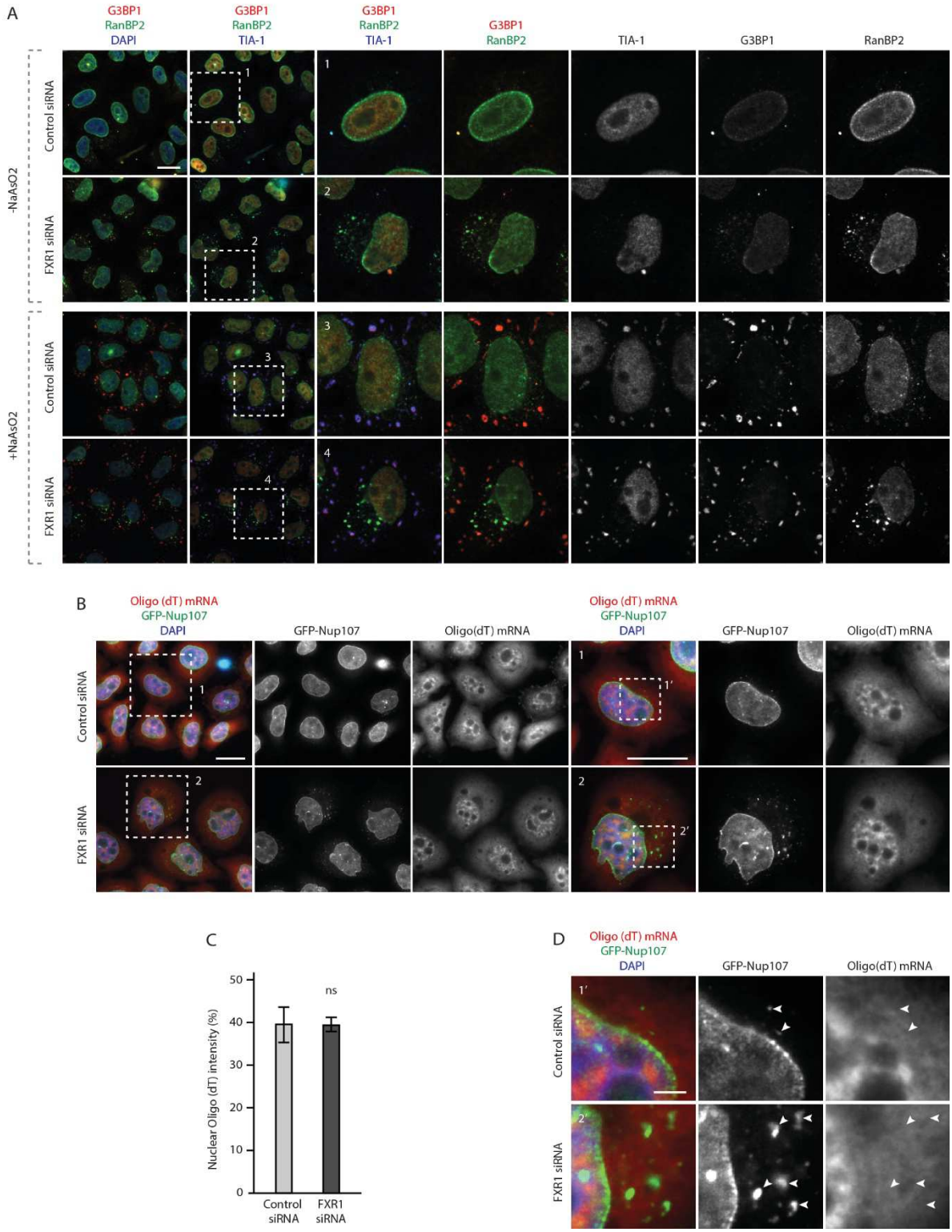

Appendix Figure S4 - The cytoplasmic Nup granules are distinct from SGs and do not contain mRNAs.

A HeLa cells were treated with the indicated siRNAs, synchronized by double thymidine block and released for 12 hours, treated with or without the stress inducing factor NaAsO2 0.5 mM for 1 hour and

analyzed by IF microscopy for the SG markers G3BP1 and TIA-1 and the Nup RanBP2. The magnified framed regions are shown in the corresponding numbered panels.
B-D HeLa cells stably expressing GFP-Nup107 were treated with the indicated siRNAs, synchronized by double thymidine block and released for 12 hours, hybridized with the oligo d(T) mRNA FISH probe and analyzed by IF microscopy. The magnified framed regions are shown in the corresponding numbered panels in (**B**) and higher magnifications are shown in (**D**). Arrowheads point to GFP-Nup107-positive cytoplasmic granules. The percentage of nuclear mRNA intensity was quantified in (**C**), 600 cells were analyzed (mean ±SD, ns = non-significant; N = 3).
Data information: Scale bars are 5 μm (**A, B**) and 1 μm (**D**). Statistical significance was assessed by two-tailed unpaired Student's T-test.

Appendix Figure S5

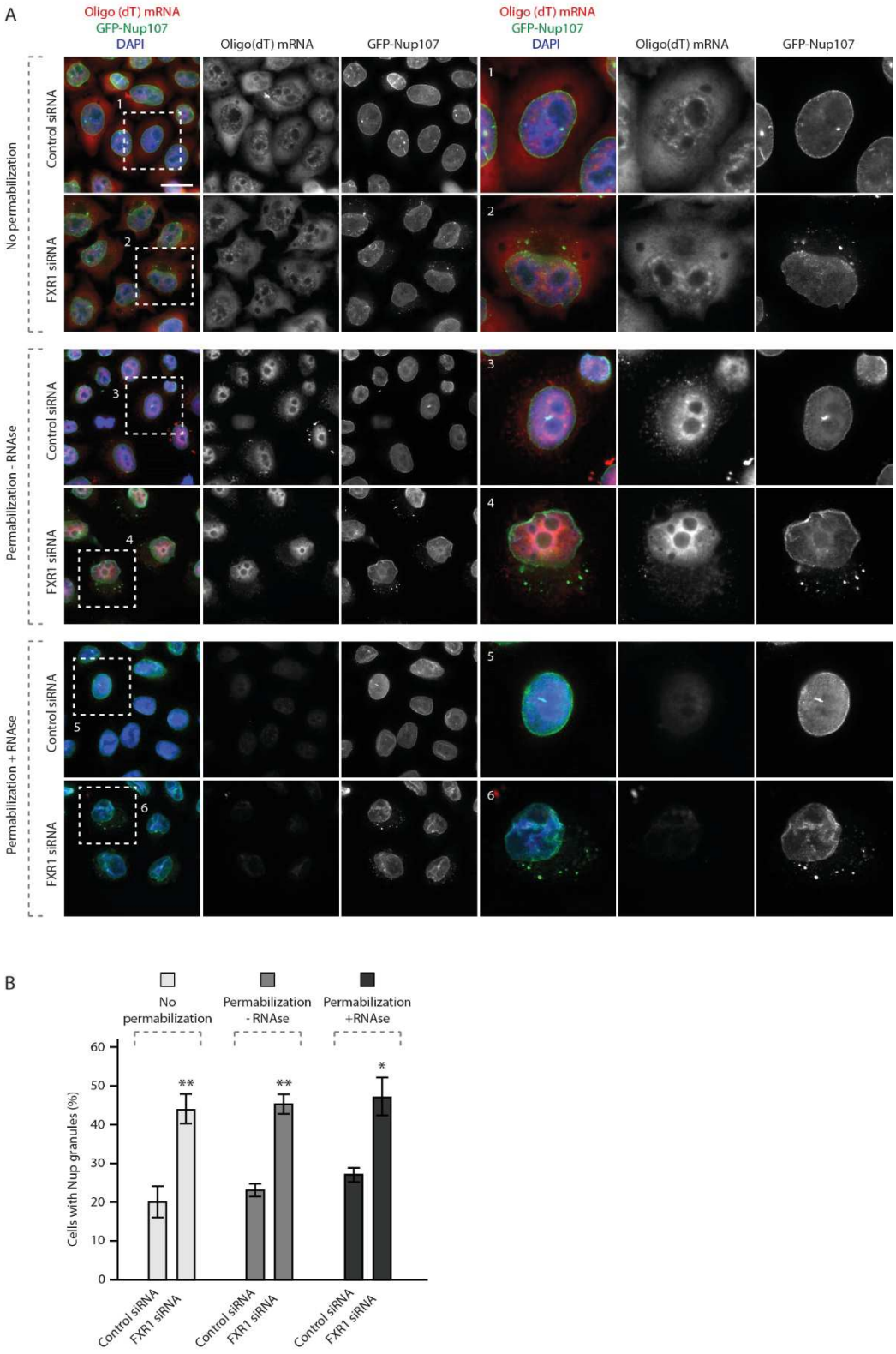

Appendix Figure S5 - RNAs are dispensable for maintenance and dynamics of the cytoplasmic Nup granules.

A, B HeLa cells stably expressing GFP-Nup107 were treated with the indicated siRNAs, synchronized by double thymidine block and released for 12 hours, hybridized with the oligo d(T) mRNA FISH

probe, treated with or without RNaseA/T1 and/or digitonin permabilization for 5 min and analyzed by fluorescence microscopy. The magnified framed regions are shown in the corresponding numbered panels. The percentage of cells with GFP-Nup107-positive cytoplasmic granules was quantified in (**B**), 8900 cells were analyzed (mean ±SD, *P < 0.05; **P < 0.01; N = 4). Scale bar is 5 μm.
Data information: Statistical significance was assessed by one-way ANOVA test with Sidak's correction.

Appendix Figure S6

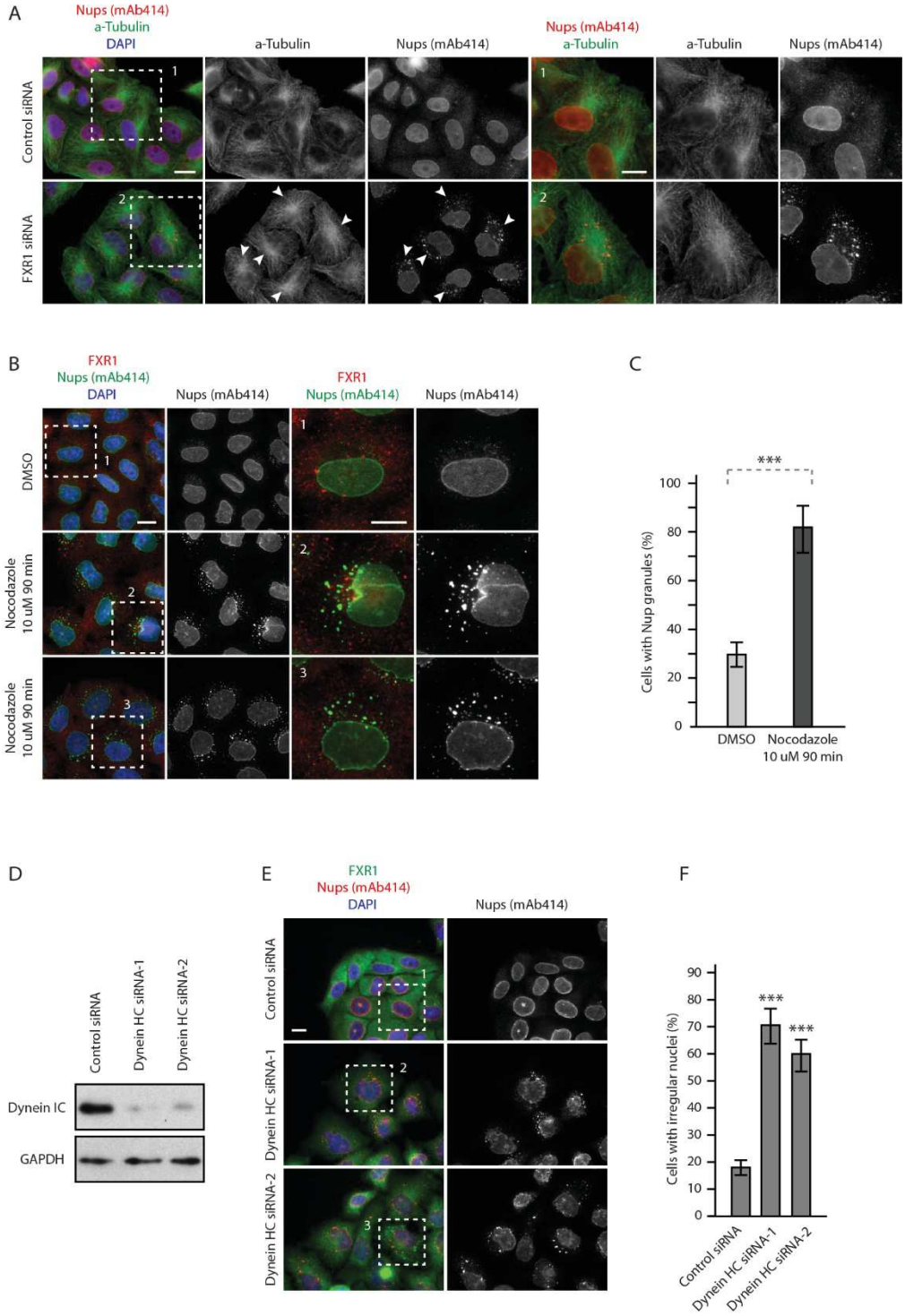

Appendix Figure S6 - FXR1 inhibits formation of the cytoplasmic Nup granules by dynein microtubule-dependent transport.

A HeLa cells were treated with the indicated siRNAs, synchronized by double thymidine block and released for 12 hours and analyzed by IF microscopy. Arrowheads point to the positions of the cytoplasmic Nup granules relative to MTOC.
B, C HeLa cells were synchronized by double thymidine block and released for 12 hours, treated with nocodazole 10 uM or solvent (DMSO) for 90 min and analyzed by IF microscopy. The magnified framed regions are shown in the corresponding numbered panels in (**B**). The percentage of cells with cytoplasmic Nup granules was quantified in (**C**), 2500 cells were analyzed (mean ±SD, ***P < 0.001; N = 3).
D-F HeLa cells were treated with the indicated siRNAs, synchronized by double thymidine block and released for 12 hours and analyzed by Western blot (**D**) and IF microscopy (**E**). The percentage of cells with irregular nuclei was quantified in (**F**), 900 cells were analyzed (mean ±SD, ***P < 0.001; N = 3).
Data information: Scale bars are 5 μm. Statistical significance was assessed by two-tailed unpaired Student's T-test (**C**) and one-way ANOVA test with Dunnett's correction (**F**).

2.8. Discussion

Collectively, our data suggest a model where FXR proteins and dynein regulate the localization of a cytoplasmic pool of Nups during early G1 (Fig 9G). Absence of FXR proteins or dynein-mediated transport leads to the formation of previously uncharacterized ectopic Nup assemblies. We speculate that the FXR-dynein pathway regulates the pool of soluble Nups either remaining in the cytoplasm after postmitotic NPC assembly or being translated in early interphase, which is important for functions in nuclear export and shape and in cell cycle progression. Defects in this pathway, as seen in cellular models of FXS, may therefore compromise cellular fitness and contribute to the pathology of this human disease.

Our analysis demonstrates that FXR proteins can facilitate dispersal of Nups and reversal of cytoplasmic Nup assemblies, which we propose to name Cytoplasmic Nup Granules (CNGs) (Fig 9G). Consistent with this hypothesis, re-expressed FMRP in iPS cells (Fig 8G) and occasionally GFP-FXR1 in cancer cells (Fig 1E) could co-localize in foci with a pool of cytoplasmic Nups often found in the proximity of the NE. FXR1 could also interact with Nups and rescue experiments with the siRNA resistant form of FXR1 could reverse the formation of CNGs in cancer cells (Fig 2B; Fig EV1). Finally, the CNGs fusion events observed in the live video experiments, resulted in increase of the CNGs' size in the absence of FXR1 or dynein relative to control cells (Fig 7C). However, we did not observe an increase in co-localization of the endogenous FXR1 and Nups in the absence of dynein/BICD2 (Fig 6B, E). We predict that either all three components are needed to form the transport complexes in the cytoplasm or that the formation of the FXR-Nup complex is very transient and is needed for the transport of soluble Nups which are harder to visualize in the cytoplasm. The CNGs that we observe would be the result of the absence of this transport mechanism and the consequent local increase of Nups levels leading to aberrant formation of bigger (easy to visualize) Nup granules that do not necessarily contain FXR1.

The CNGs formed in the absence of FXR proteins likely represent distinct structures from ALs based on our EM analysis (Appendix Figure S3B) and lack of direct contacts with the ER membranes (Appendix Figure S3C). However, it cannot be excluded that some membranes or lipid species are part of the CNGs due to the presence of the integral membrane proteins POM121 and Nup210, both components of the NPC at the NE, and the scaffold NPC components Nup133, Nup85 and Nyp107 in these structures. The CNGs formed in the absence of FXR proteins are also distinct from SGs (Appendix Figure S4A) previously shown to recruit Nups (Zhang *et al*, 2018) and cannot be directly linked to RNA-based processes (Appendix

Figure S4B-D, S5) at this point. We were unable to detect any changes in protein levels of several analyzed Nups (Fig EV3A-C) or levels and stability of the Nups mRNAs (Fig EV3D, E). However, given that translational regulation represents one of the best-studied roles of the FXR protein family (Darnell *et al*, 2009; Ascano *et al*, 2012), it cannot be formally excluded that expression of other, yet to be identified Nups or Nup-associated factors, is regulated by FXR proteins.

Our data suggest a model where FXR proteins interact with the cytoplasmic pool of the scaffold NPC components Nup85 and Nup133 and act to decrease their local concentration either by their microtubule-based, non-NE directed transport and/or by transferring their small pool towards the NE. Due to the cohesive ability of many Nups and the fact that the scaffold components can directly bind to the FG-Nups (Onischenko *et al*, 2017), it is therefore reasonable to predict that in the absence of the FXR proteins, the local cytoplasmic pools of Nup85 and Nup133 increase, and could result in the formation of cytoplasmic condensates containing many different NPC sub-complexes, which is consistent with our observations (Fig 2; Appendix Figure S1, S2). It remains to be investigated why some Nups including ELYS and Nup153 could not be detected in CNGs and if this observation could be linked to their well-established roles in the postmitotic (ELYS) (Doucet *et al*, 2010) and interphase (Nup153) (Vollmer *et al*, 2015) NPC assembly pathways. The condensate properties of the CNGs are supported by our results with the 1,6-Hexanediol treatment, which led to the dispersion of the Nup granules (Fig 5B, C) as well as the dynamic fusion and splitting events of CNGs observed in live video experiments with the GFP-Nup107 cell line (Fig 4A, B, 7C-E, Movie EV1-5).

What is the molecular engine for the FXR-mediated Nup dispersal? Interestingly, FMRP was demonstrated to form a complex with the dynein motor (Bianco *et al*, 2010; Ling *et al*, 2004) and with the dynein adaptor protein BICD2 (Bianco *et al*, 2010) in neuronal cells. Our data are consistent with these findings and show the interaction of dynein and BICD2 with the FMRP paralog protein FXR1 (Fig 6A, D) in cultured human cancer cells. Molecular interactions of Nups and dynein-BICD2 complexes were also reported during mitotic entry (Bolhy *et al*, 2011; Splinter *et al*, 2010). Our model proposes that FXR proteins provide the molecular links between cytoplasmic Nups and the dynein-BICD2 complex during the G1 phase of the cell cycle, allowing for the Nups dispersal and the transfer of at least a small pool of scaffold Nups towards the NE. It is interesting that FXR proteins localize to the NE (Fig 1D-F; Fig EV4A, B), the predicted final destination of the cytoplasmic Nups. Our live video experiments are in line with the transport hypothesis and suggest that nocodazole-induced CNGs can indeed be transferred towards intact NE (Fig 7C) in an FXR1- and dynein-dependent manner. However,

the observed movement rate is slower than an expected motor dependent transport. We believe that the CNGs induced by microtubule depolymerization are not the natural substrate of dynein but the result of the aberrant fusion of small cytoplasmic Nup granules observed in untreated cells and which would be the physiological transport cargo. Alternatively, FMRP could interact with dynein and kinesins, as has been reported in literature (Ling *et al*, 2004), leading to a slow net movement of Nups towards the NE. We speculate that formation of FXR1-dynein-Nup complexes and their transport would disperse cytoplasmic Nups, thereby inhibiting formation of Nup-containing big cytoplasmic condensates. A similar function has been ascribed to the nuclear import receptors, which transfer proteins and RNAs to the nucleus across the NPCs. They were able to prevent aberrant phase separation of cytoplasmic membrane-less organelles present in several neurological diseases (Guo *et al*, 2019). Thus, nuclear import receptors can also play important chaperone-like functions by inhibiting aggregation of cargo proteins. For instance, protein FUS is mutated in amyotrophic lateral sclerosis (ALS) within its nuclear localization signal (NLS), which subsequently reduces its binding to the nuclear import receptor Transportin leading to cytoplasmic FUS accumulation favoring phase separation (Dormann *et al*, 2010). Our work also demonstrates the importance of the regulation of localized protein demixing by preventing Nup accumulation in the wrong cellular compartment (cytoplasm). In the future, it would be interesting to study if the NLS signals present in the FXR proteins are important for their functions on Nups. It also remains to be investigated if, in contrast to SGs components (Appendix Figure S4A) (Zhang *et al*, 2018), CNGs can sequester any other cohesive proteins known to form membrane-less assemblies. For example Nups can be sequestered in various pathological fibrillary amyloids, which were implicated in neurodegenerative diseases (Hutten & Dormann, 2020; Li & Lagier-Tourenne, 2018) and in the CyPNs (Jul-Larsen *et al*, 2009), for which the cellular role remains unknown.

Our data suggest that the FXR-dynein pathway is important for the maintenance of nuclear shape during early G1. Downregulation of all members of the FXR family (Fig EV4E) and dynein (Appendix Figure S6F) led to strong defects in nuclear shape in human cancer cells and nuclear atypia has been also observed in human primary fibroblasts derived from FXS patients (Fig 8D). We believe that a moderate delay in the export during G1 could (through an unknown mechanism) lead to a small yet significant difference in the nuclear area and in nuclear morphology defects. Alternatively, the nuclear size and shape could be related to the established structural roles of Nups independent of their functions in protein and RNA transport (Grossman *et al*, 2012). Indeed, changes in nuclear shape in cells deficient for individual Nups have been documented in various organisms (Hetzer & Wente, 2009; Mitchell *et al*, 2010;

Onischenko *et al*, 2017; Ungricht *et al*, 2015). The first changes in nuclear morphology are observed during early G1, which correlate with the appearance of CNGs in the FXR1-deficient cells and may perturb the progression of the cell cycle through G1 and S phases. Interestingly, the components of the Y-complex were previously implicated in G1/S progression by regulating export of specific mRNAs of key cell cycle genes (Chakraborty *et al*, 2008). Furthermore, in yeast, modulation of NPCs has been reported to delay their cell cycle entry in the daughter cells (Kumar *et al*, 2018). Previous study in myoblasts proposed the role of FXR1 in cell cycle progression, whereby deletion of this protein led to longer G1 phase, shorter S phase and premature mitotic exit (Davidovic *et al*, 2013). Our results demonstrate shorter G1, longer S phases (Fig 9E, F) and no defects in mitotic progression (Fig 3D-H) in the absence of FXR1, suggesting another unrelated function of FXR1 in cancer cells.

Our data do not show global changes in the rates of export and import (Fig EV5) under normal conditions, which is expected given the small reduction of NE-associated Nups observed in FXR1-downregulated cells (Fig 2D-F, H). Excitingly, transient defects in protein export were observed in FXR1-deficient cells specifically during early G1 cell cycle stage (Fig EV5D; Fig 9A) and export factor CRM1 was sequestered to CNGs (Fig 9B). It is plausible to predict that under stress conditions or in the fast dividing cells of a developing embryo, this small decrease in protein export rate would significantly affect cellular homeostasis and asymmetric divisions. It is also possible that the export of CRM1-dependent G1-specific or more demanding cargos through NPCs is regulated by the FXR-dynein pathway. An alternative and equally plausible explanation is that CNGs exert cytotoxic effects by sequestering yet unknown factors important for nuclear shape and cell cycle progression.

While future studies are needed to understand the precise mechanism underlying cell cycle control by the FXR-dynein axis, and if and how it is linked to the regulation of cytoplasmic Nups, defects in this pathway are predicted to significantly perturb cellular homeostasis and may contribute to the pathology of FXS, consistent with our observations in the cellular models of FXS (Fig 8). Collectively, our data demonstrate an unexpected role of FXR proteins and dynein in the spatial regulation of soluble Nups, and provide an example of a mechanism that regulates localized protein condensate formation.

2.9. Acknowledgements

We thank patients and their families for their contribution. Y. Barral, S. Oliferenko, G. Sumara, O. Sumara, M. Mendoza, N. Djouder, K. Krupina, O. Bielska, Z. Zhang, Life Science Editors and the members of the Sumara group for helpful discussions on the manuscript. We are grateful to Valérie Doye for generous help with reagents. We thank Ulrike Kutay, Frauke Melchior, Hélène Puccio, Jin Peng, Stephen Warren, Romeo Ricci, Jan M. van Deursen, Matej Durik, Ioanna Mitrentsi and Nicolas Charlet-Berguerand for help with reagents. We are grateful to Jean-Marc Egly and Michel Labouesse for their mentorship and support. We thank the Imaging Center of the IGBMC (ICI) for help on confocal microscopy and to the IGBMC core facilities for their support on this research. Alexia Loynton-Ferrand from the Biozentrum, University of Basel for support on superresolution imaging. A.A.A. was supported by a Labex international PhD fellowship from IGBMC and a fellowship from the “Ligue Nationale Contre le Cancer”. S.S. was supported by a postdoctoral fellowship from the University of Strasbourg Institute of Advanced Studies (USIAS). K.J. was supported by a fellowship from Gouvernement français et L’Institut français de Prague, a LabEx international PhD fellowship from IGBMC and a fellowship from the “Ligue Nationale Contre le Cancer”. A.B. received PhD fellowships from the “Ministère de l’Enseignement Supérieur et de la Recherche” and the “Ligue Nationale contre le Cancer”. Research of L.P. and C. B. was supported by Associazione Italiana Sindrome X Fragile, Telethon GGP15257, PRIN 201789LFKB and Swiss National Science Foundation (SNSF) 310030-182651. This study was supported by the grant ANR-10-LABX-0030-INRT, a French State fund managed by the Agence Nationale de la Recherche under the frame program Investissements d’Avenir ANR-10-IDEX-0002-02. Research in I.S. laboratory was supported by IGBMC, CNRS, Fondation ARC pour la recherche sur le cancer, Institut National du Cancer (INCa), Agence Nationale de la Recherche (ANR), Ligue Nationale contre le Cancer, USIAS and Sanofi iAward Europe.

The authors declare no competing financial interests.

3. PART 2: Role of RanBP2 regulating nucleoporin condensation

The second part contains recent results on the role of the Nup called RanBP2 in the regulation of Nups condensation, which are not part of the EMBO Journal manuscript. They create a basis for a new future project and they already comprise key findings.

NOTE: The number of datapoints in some of the following experiments does not allow to perform statistical tests. All the data in this section should be considered as preliminary.

3.1. Introduction

Ran-Binding Protein 2 (RanBP2), also called Nup358, is a 358 kDa protein located in the cytoplasmic filaments of the NPC (Wu *et al*, 1995). It contains different domains implicated in binding to components of nucleocytoplasmic transport pathways and Small Ubiquitin-Like Modifier (SUMO) conjugation machinery (Figure 13). These components include: 1) an N-terminal region including a leucine-rich domain which anchors RanBP2 to the NPC and has been implicated in microtubule binding (Joseph & Dasso, 2008), 2) a central region containing a zinc finger motif which interacts with the export receptor CRM1 (Singh *et al*, 1999), 3) four RanGTP binding domains distributed throughout the protein, 4) a kinesin and motor adaptor BICD2 binding domain between R2 and R3 (Cai *et al*, 2001; Splinter *et al*, 2010), 5) an IR domain (internal repeats) which accommodates the platform for complex formation with SUMOylated RanGAP1 and Ubc9 and the SUMO E3 ligase core and 6) a cyclophilin homology domain (CHD). RanBP2 contains several FG and FxFG motifs which serve as low-affinity binding sites for importins and exportins. It has a preference for the exportin CRM1 which can lead to the disassembly of CRM1-dependent export complexes (Ritterhoff *et al*, 2016).

RanBP2 is rarely observed free in the cell and it is mainly associated with SUMOylated RanGAP1 and the SUMO-conjugating enzyme Ubc9, forming a stable multi-subunit complex (the RanBP2/RanGAP1*SUMO/Ubc9 complex) at the cytoplasmic filaments of the NPC (Figure 13B) (Flotho & Werner, 2012). RanBP2-RanGAP1 interaction depends on SUMOylation of the C-terminal region of RanGAP1 (Matunis *et al*, 1996) and this modification requires the SUMO E2 conjugating enzyme Ubc9 which acts as a linker (Saitoh *et al*, 1997) (Figure 13B). In vertebrates, the RanBP2/RanGAP1*SUMO/Ubc9 complex contributes to the continuity of nucleocytoplasmic transport cycles because it acts as an export

receptor and Ran-GTP disassembly machinery. The Ran-GTP binding domains together with RanGAP1 promote the hydrolysis of Ran-GTP to dissociate export receptors from cargos and Ran-GTP, what allows the recycling of Ran-GDP and the release of the cargo in the cytoplasm (Ritterhoff *et al*, 2016).

Conserved in all eukaryotes, another basic disassembly machinery exists which is not attached to the NPC but resides in the cytoplasm. This machinery is made up of soluble RanGAP1 and RanBP1, and they are also required for the disassembly of both trimeric export complexes and recycling import/Ran-GTP complexes (Bischoff *et al*, 1995; Floer & Blobel, 1999). The RanBP1 yeast homologue (*Yrb1*) is an essential gene in *Saccharomyces cerevisiae* although it is not in vertebrates (Nagai *et al*, 2011) due to compensation by RanBP2. In contrast, RanBP2 is vital to vertebrates (Dawlaty *et al*, 2008) although not evolutionarily conserved.

During mitosis the RanBP2/RanGAP1∗SUMO/Ubc9 complex performs different functions: it is recruited to kinetochores only after microtubules have attached to these structures and it is required for the stability of kinetochore–microtubule attachments, spindle assembly and chromosome segregation (Salina *et al*, 2003; Joseph *et al*, 2004; Arnaoutov *et al*, 2005; Mossaid & Fahrenkrog, 2015). The recruitment of the RanBP2/RanGAP1∗SUMO/Ubc9 complex at kinetochores depends on CRM1, RanGTP, Importin-β and the presence of the Nup107-160 complex on site (Zuccolo *et al*, 2007; Joseph *et al*, 2002; Roscioli *et al*, 2012).

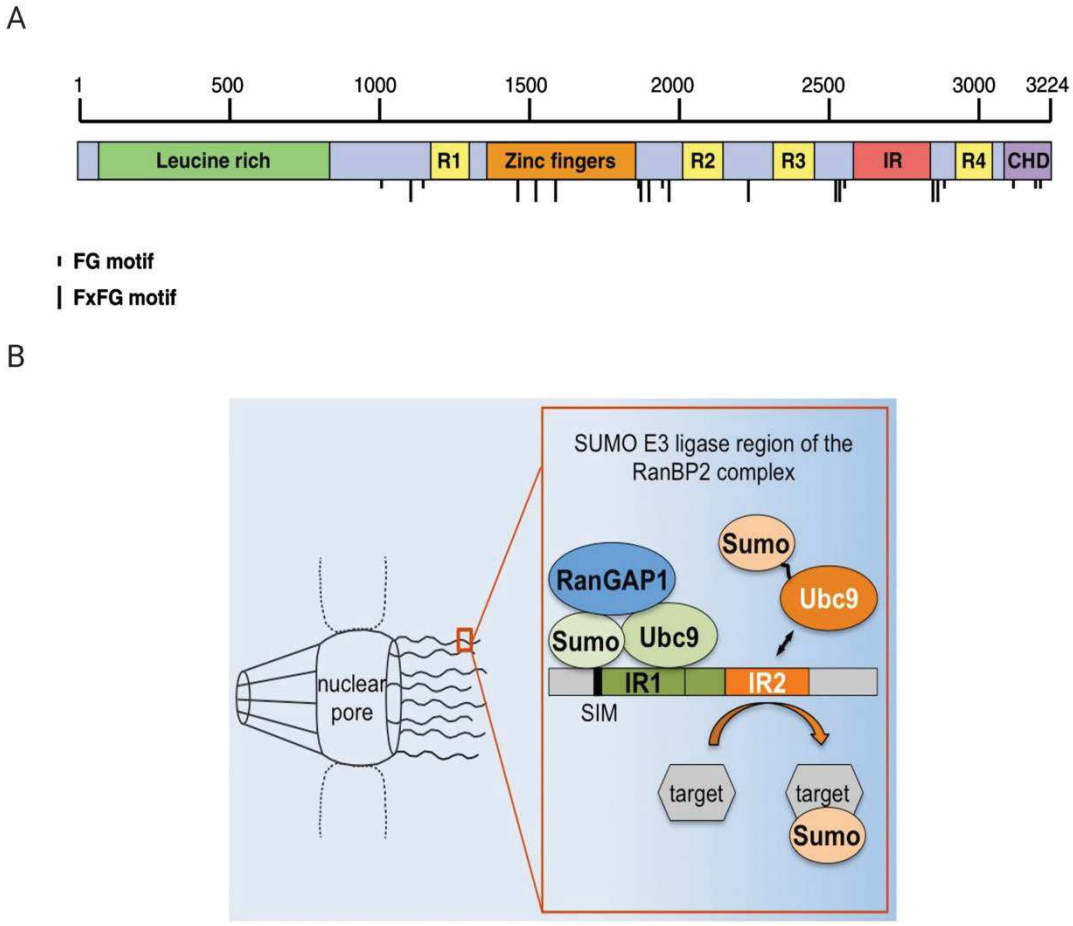

Figure 13 - RanBP2 protein and complex.
A Domain organization of RanBP2 protein. RanBP2 is a huge protein of 3224 amino acids and it contains several interacting domains: leucine-rich domain (green), four Ran binding domains (yellow, R1-4), a zinc finger domain (orange), an IR domain (red, internal repeats; characterized by two 50 amino acid internal repeats IR1 and IR2), a cyclophilin homology domain (purple, CHD). RanBP2's E3 ligase region resides between R3 and R4, contains IR1 and IR2, and is natively unfolded. Vertical dashes denote FG and FxFG motifs. Upper numbers indicate amino acids.
B RanBP2 localizes to the cytoplasmic filaments of the NPC. It interacts with SUMOylated RanGAP1 (blue) and the SUMO E2 conjugating enzyme Ubc9 (light green) through its IR domain (which contains IR1, green and IR2, orange). RanBP2/RanGAP1*SUMO/Ubc9 complex is a multisubunit SUMO E3 ligase. Two Ubc9 molecules (light green and light orange) are required for SUMOylation by the RanBP2 complex.
Figure adapted from (Azuma & Dasso, 2002) (**A**) and (Ritterhoff *et al*, 2016) (**B**).

As mentioned in the general introduction, a recent publication from Hampoelz *et al*. proposed a model for ALPC biogenesis in Drosophila oocytes (Figure 8) (Hampoelz *et al*, 2019b). Briefly, they found that ALPC assembly relies on different granules containing condensed Nups which interact with each other. In the nurse cells of the Drosophila egg chamber, RanBP2 condenses and forms large granules decorated with RanBP2 mRNA on the surface (suggesting a localized translation and condensation events), while scaffold- and FG-Nups condense into

granules in the oocyte. RanBP2 granules travel to the oocyte where they encounter the oocyte-specific granules. Microtubule dynamics promote the fusion of these two types of condensed Nup granules. They propose that these fused granules' Nups are transferred to a neighboring ER membrane where ALPCs assemble. Eventually, larger stacks with multiple membrane sheets form ALs and can be used as a NPC storage in rapidly dividing cells during early embryogenesis.

These findings propose a controlled Nup condensation and microtubule-based transport as a mechanism to facilitate contacts between different Nups and their transfer to membranes to build pore complexes in Drosophila oocytes. In line with these results, a subpopulation of RanBP2 has been observed to localize to the cytoplasm away from the NPC and to interact with interphase microtubules contributing to their stability (Joseph & Dasso, 2008).

In the context of AL formation in Drosophila oocytes, the Nup RanBP2 seems to be a key player in driving the assembly of Nups in pore complexes, since the oocyte-specific granules alone do not lead to NPC assembly and the fusion of RanBP2 granules is required for this event. Although ALs seem to be restricted to cells with fast cell divisions that require a rapid nuclear growth, it is plausible to think that differentiated cells use a similar Nup condensation and transport mechanism to bring Nups directly to the NE (instead of the ER) as a part of the interphasic NPC assembly pathway.

3.2. Aims of the study

In our manuscript (Agote-Aran *et al*, 2020), we proposed that FXR proteins act as molecular chaperones that regulate Nup condensation by promoting their dynein-based transport towards the NE, thereby inhibiting their accumulation and condensation into big granules in the cytoplasm. However, given that translational regulation is the main studied role of the FXR protein family (Ascano *et al*, 2012; Darnell *et al*, 2009), it cannot be formally excluded that these proteins regulate the expression of other yet to be identified Nups. As RanBP2 is a key Nup in ALPC biogenensis, we investigated if FXR1 could specifically regulate RanBP2 levels and/or localization and therefore induce an incorrect Nup condensation/localization.

Aim 1: To analyze if FXR1 interacts with RanBP2 and if regulates RanBP2 protein and/or mRNA levels.

Aim 2: To study if RanBP2 is required for cytoplasmic Nup condensation induced by FXR1 depletion.

Aim 3: To study if RanBP2 is required for cytoplasmic Nup condensation induced dynein depletion and/or microtubule depolymerization.

Aim 4: To investigate if the formation of cytoplasmic Nup granules in early G1 depends on active protein translation.

3.3. Results

3.3.1. FXR1 interacts with RanBP2 and may regulate its proteins levels

Given that RanBP2 is a key Nup in ALPC biogenensis, we investigated if FXR1 could specifically regulate RanBP2 levels and/or localization. To this end, we treated cultured HeLa cells with FXR1-specific siRNA oligonucleotide and analyzed RanBP2 protein levels by Western blot. RanBP2 protein levels were moderately increased upon FXR1 depletion in three different experiments (Figure 14A, B, C) while other Nup protein levels (Nup85 and Nup133) were unchanged (Figure 14A', B', C). RanBP2 signal was significantly decreased by treatment with two different RanBP2 siRNAs demonstrating antibody specificity (Figure 14A, B, C). Interestingly, FXR1 levels appeared slightly decreased upon RanBP2 downregulation (Figure 14A, B, C). We considered that FXR1 effect on RanBP2 protein levels may be mediated by a modulation of RanBP2 mRNA levels, but qPCR analysis did not reveal changes upon FXR1 downregulation (Figure 14D), while they were significantly decreased by two RanBP2 siRNAs as predicted.

We also analyzed if FXR1 interacts with RanBP2 protein as it does with other Nups (Nup85 and Nup133) (Agote-Aran *et al*, 2020). IP of stably expressed GFP-FXR1 demonstrated an interaction with endogenous RanBP2 in HeLa cells (Figure 14E). In future, reverse GFP-IP experiments using a GFP-RanBP2 stable cell line and endogenous IPs against FXR and RanBP2 will be used to further verify this interaction.

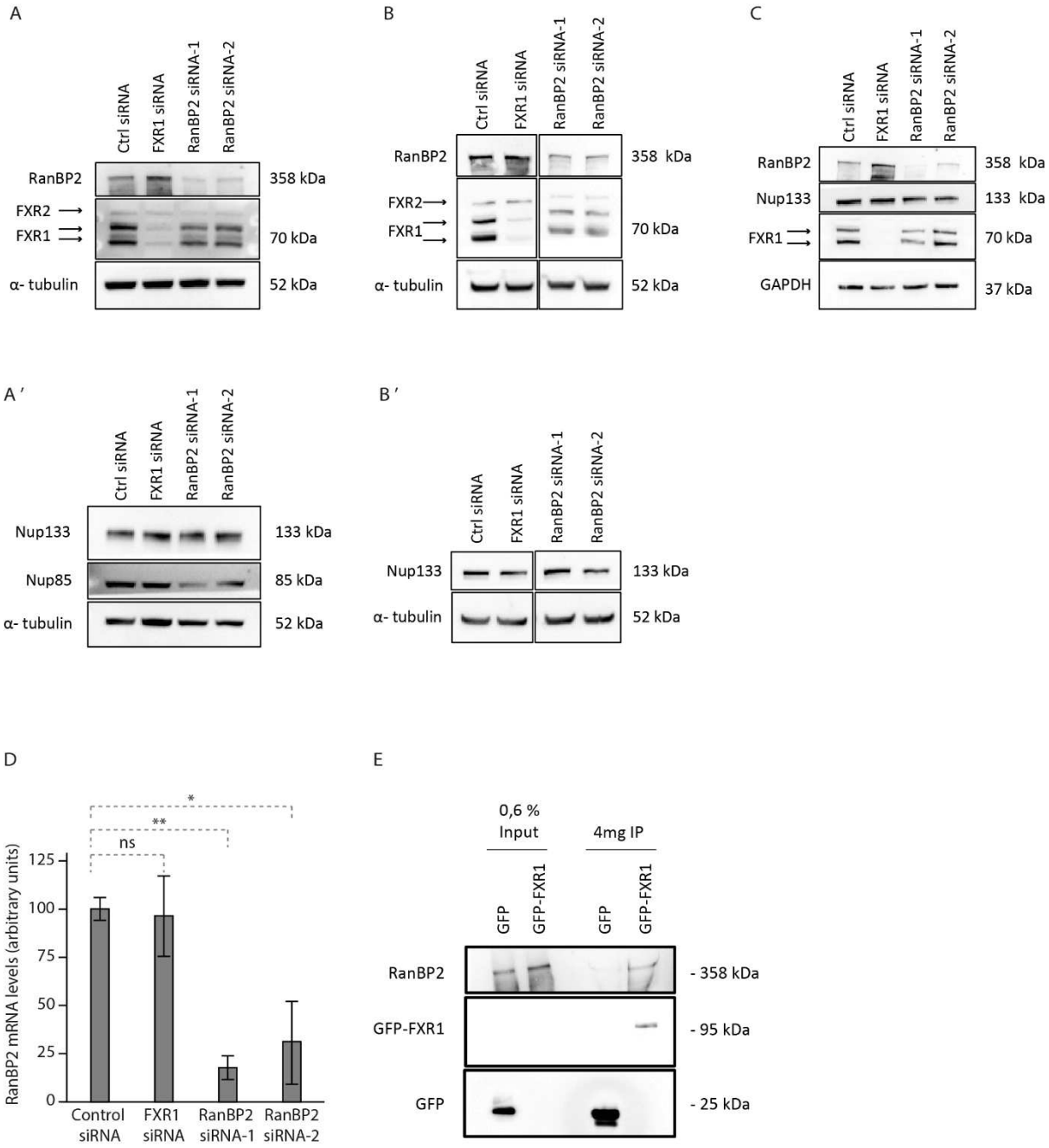

Figure 14 - FXR1 interacts with RanBP2 and regulates its proteins levels but not mRNA levels.
A, B, C HeLa cells were treated with the indicated siRNAs, synchronized by double thymidine block and released for 12 hours. Whole cell extracts of three independent experiments (**A**, **B** and **C**) were analyzed by Western blot.
D HeLa cells were treated with the indicated siRNAs, synchronized by double thymidine block and released for 12 hours. mRNA levels of RanBP2 were analyzed by qPCR (mean ±SD, *P < 0.05; **P < 0.01, N = 3).
E Lysates of HeLa cells stably expressing GFP alone or GFP-FXR1 were subjected to IP using GFP-Trap beads (GFP-IP), analyzed by Western blot.
Data information: Statistical significance was assessed by two-tailed one sample Student's T-test (**D**).

To analyze the subcellular localization of RanBP2 upon FXR1 depletion we performed IF experiments in HeLa cells. Downregulation of FXR1 led to an accumulation of RanBP2

granules in the cytoplasm (Figure 15A, B) following the same pattern previously described for other Nups (Agote-Aran *et al*, 2020). Interestingly, FXR1 localization was also changed when RanBP2 was depleted using two different siRNAs and relative to control siRNA (Figure 15A, B). In the absence of RanBP2, FXR1 localized to discrete foci and was no longer enriched at the NE. Collectively, these data show that FXR1 interacts with RanBP2 and loss of FXR1 or RanBP2 affect each other's localization and levels. FXR1 depletion induces a moderate increase in RanBP2 levels and inappropriate assembly in the cytoplasm, while RanBP2 depletion induces a mild FXR1 protein level decrease and its localization in discrete cytoplasmic foci. These results raise the possibility that a slight imbalance in RanBP2 protein levels caused by FXR1 depletion could induce an uncontrolled Nup condensation and/or Nup granule fusion in the cytoplasm. Whether the aberrant Nup condensation upon FXR1 depletion is mediated by this modest increase in RanBP2 concentration, by an impaired Nup transport towards the cytoplasm or by a combination of both events remains to be further characterized.

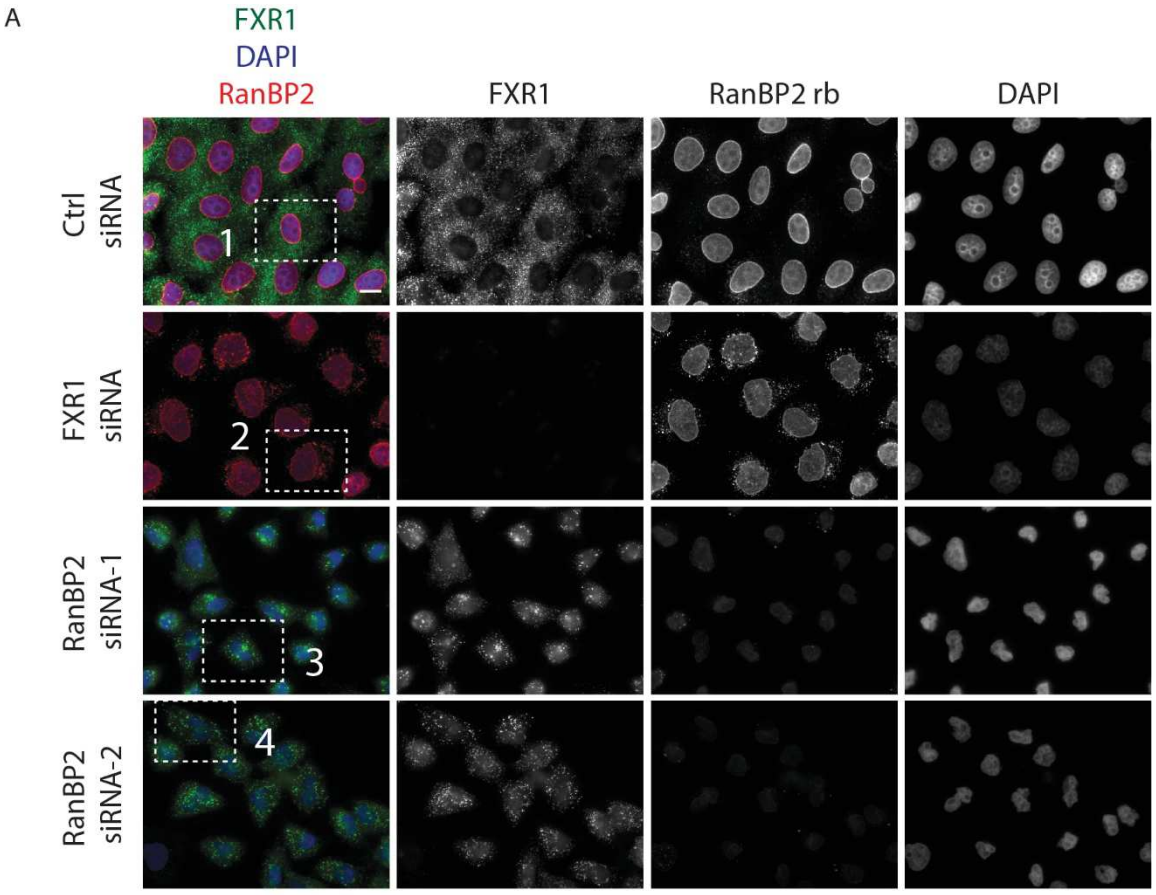
A
FXR1
DAPI
RanBP2
FXR1
RanBP2 rb
DAPI
Ctrl siRNA
FXR1 siRNA
RanBP2 siRNA-1
RanBP2 siRNA-2
1
2
3
4

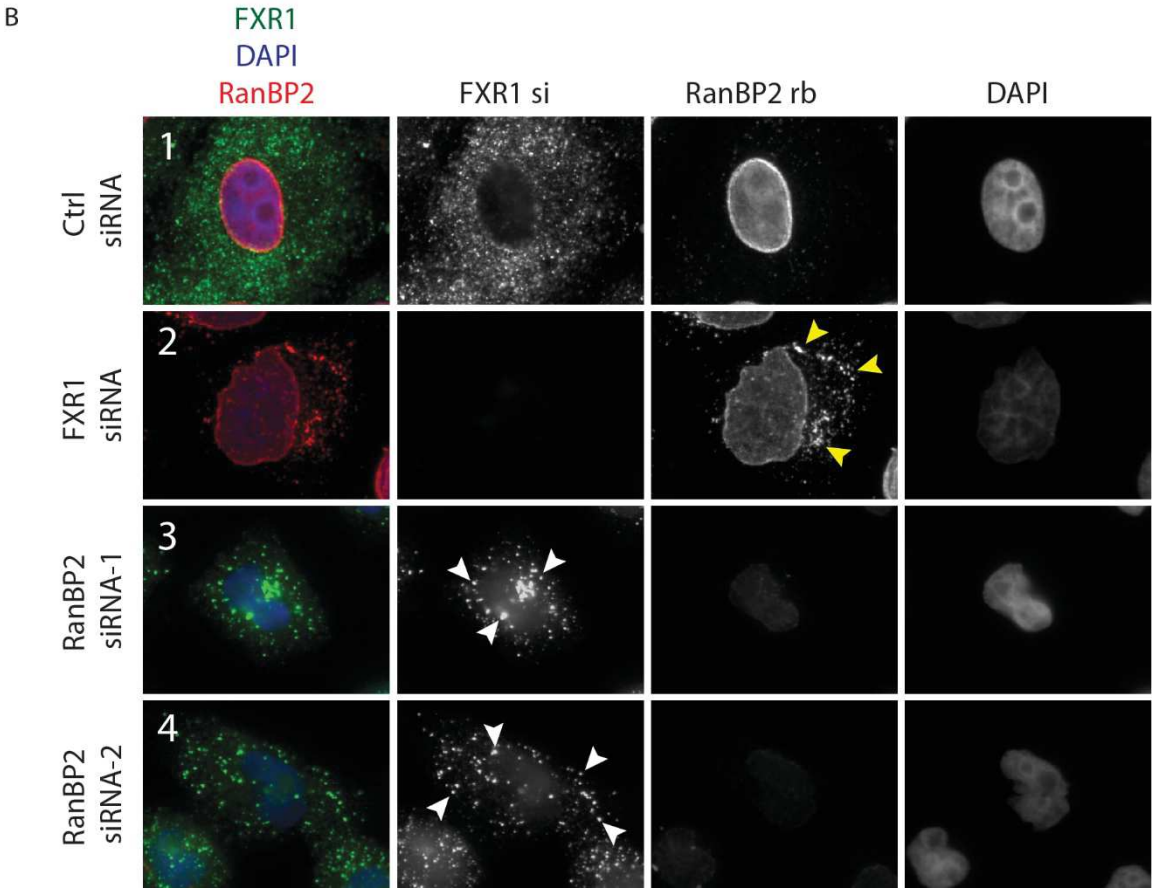
B
FXR1
DAPI
RanBP2
FXR1 si
RanBP2 rb
DAPI
Ctrl siRNA
FXR1 siRNA
RanBP2 siRNA-1
RanBP2 siRNA-2
1
2
3
4

Figure 15 - FXR1 and RanBP2 affect each other's localization upon depletion.
A HeLa cells were treated with the indicated siRNAs, synchronized by double thymidine block and released for 12 hours and analyzed by IF microscopy. The magnified framed regions are shown in the corresponding numbered panels in (**B**).
B Magnified regions corresponding to numbered panels in (**A**). Yellow arrowheads indicate cytoplasmic RanBP2 granules observed upon FXR1 depletion. White arrowheads indicate FXR1 discrete foci formed upon RanBP2 depletion.
Data information: Scale bars are 5 μm. N = 3.

3.3.2. RanBP2 is required for cytoplasmic Nup condensation into big granules induced by FXR1 depletion

As previously shown, RanBP2 mislocalizes to cytoplasmic Nup granules in the absence of FXR1, and RanBP2 condensation has been proposed to be an initial step necessary for different Nup granule fusion during ALPC assembly (Hampoelz *et al*, 2019b). Do FXR1 depletion-induced cytoplasmic Nup granules require RanBP2 for their formation? To answer this question, we downregulated FXR1 and/or RanBP2 in HeLa cells using specific oligonucleotides and analyzed Nup localization by IF. Consistent with our previous results, FXR1 siRNA led to accumulation of big Nup granules in the cytoplasm relative to the control siRNA cells which displayed a dotty Nup staining in the same compartment (Figure 16A, B). These granules also contained SUMO1 protein, which can localize to the NE and shows a similar localization pattern to Nup staining. The SUMO signal likely corresponds to SUMOylated RanGAP1 as part of the RanBP2/RanGAP1/SUMO/Ubc9 complex, which appears to be present in both compartments, NE and cytoplasmic Nup granules. As expected, the dotty signal of SUMO1 at the NE is abolished by RanBP2 depletion. Strikingly, RanBP2 downregulation combined with FXR1 siRNA treatment dramatically reduced the percentage of cells with big cytoplasmic Nup granules (Figure 16A, B). RanBP2 downregulation also reduced the number of cells with big cytoplasmic Nup granules in the control cells (Figure 16A, B). These results suggest that RanBP2 protein and/or RanBP2 mRNA is required for cytoplasmic Nup condensation into big granules in normal conditions as well as in the absence of FXR1. Given that Nup granules have the tendency to fuse upon FXR1 or dynein depletion and that the small Nup granules are also dissolved by 1,6-Hexanediol (page 74), the big granules present in FXR1-deficient cells are likely to result from fusion events among small Nup granules which RanBP2 would be necessary for. In this scenario, RanBP2 could act as a Nup granule fusing or nucleating agent.

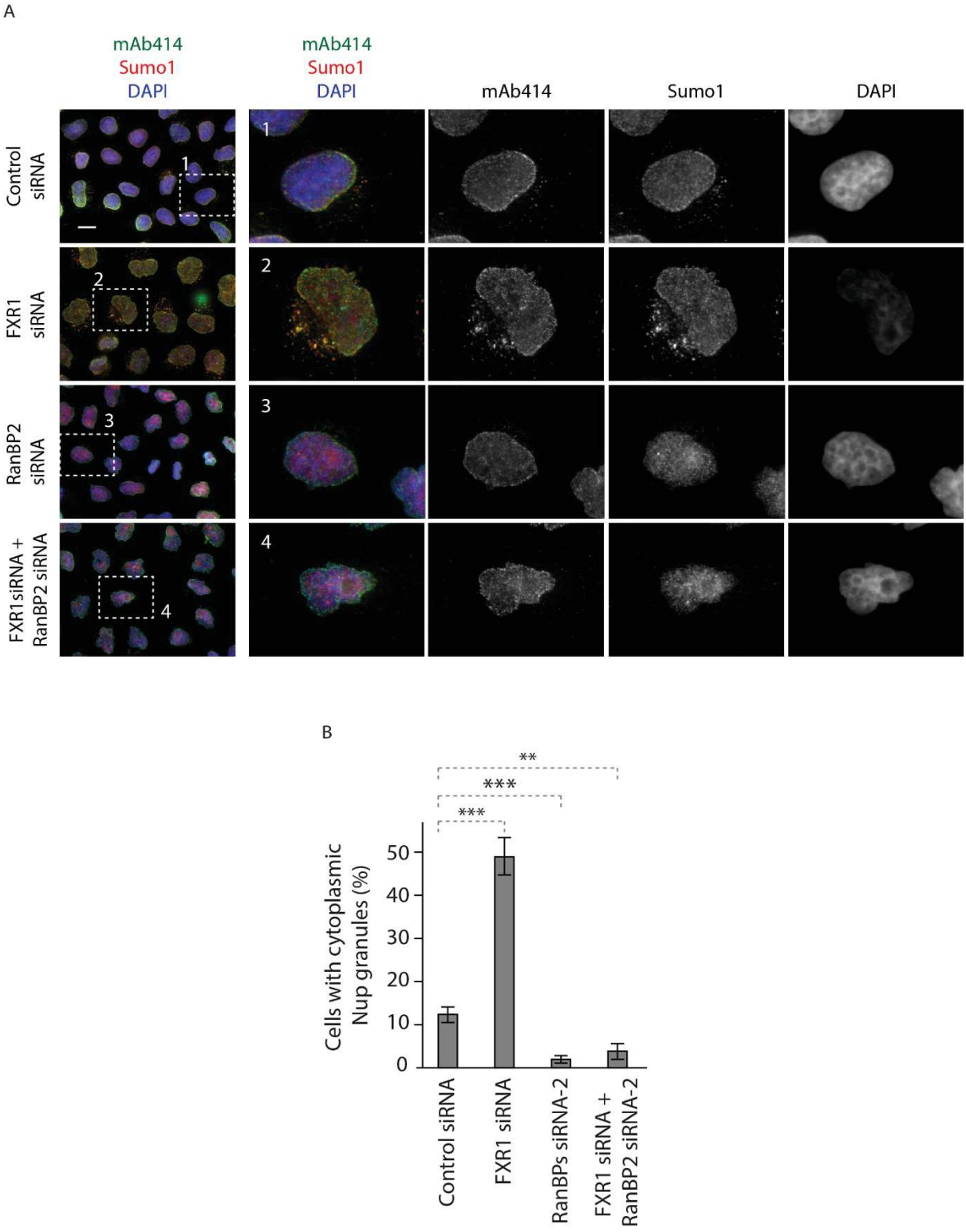

Figure 16 - RanBP2 is required for the formation of big cytoplasmic Nup granules.
A, B HeLa cells were treated with the indicated siRNAs, synchronized by double thymidine block, released for 12 hours and analyzed by IF. The magnified framed regions are shown in the corresponding numbered panels. The percentage of cells with big cytoplasmic Nup granules was quantified in (**B**), 3350 cells were analyzed (mean ±SD, **P < 0.01; ***P < 0.001; N = 3).
Data information: Scale bar is 5 μm. Statistical significance was assessed by two-tailed one sample Student's T-test (**B**).

3.3.3. Diversity of cytoplasmic Nup granules in human cancer cells

Hampoelz *et al* postulated that ALPC biogenesis relies on the fusion of different types of Nup granules (Hampoelz *et al*, 2019b). They observed granules containing solely either FG-Nups, scaffold Nups or RanBP2, as well as these Nup subtypes together as a result of granule fusion events. We hypothesized that Nup granules present in human cells could also be an intermediate step in the interphasic NPC assembly pathway in human cells, and we wondered if Nup granules containing solely either Nup133 (scaffold Nup), Nup62 (FG-Nup) or RanBP2 could be observed in HeLa cells. To this end, we treated HeLa cells with control, FXR1 and RanBP2 siRNAs and synchronized them in early G1 phase. Subsequently, we performed IF microscopy against either Nup62 or Nup133 together with RanBP2 using a spinning disk confocal microscope at 100x magnification with live super resolution module (Live SR). Control siRNA treated cells showed the typical cytoplasmic Nup pattern in small dots. The vast majority of these small cytoplasmic granules contained both markers (Nup62 and RanBP2 or Nup133 and RanBP2), and very rarely we could observe granules that contained only Nup62, Nup133 or RanBP2 (Figure 17A, B). FXR1 siRNA treated cells also showed a similar cytoplasmic small dot Nup pattern in addition to prevalent big granules which exclusively contained both markers (Figure 17A, B). In this analysis, we were unable to identify any big Nup granules that contained only one Nup type. In the case of RanBP2 siRNA treated cells, the small cytoplasmic Nup granules were still observed and were negative for RanBP2 as expected (Figure 17A, B), although some double positive granules could be found, probably due to incomplete RanBP2 downregulation. As demonstrated above, these cells very rarely contained big cytoplasmic Nup granules.

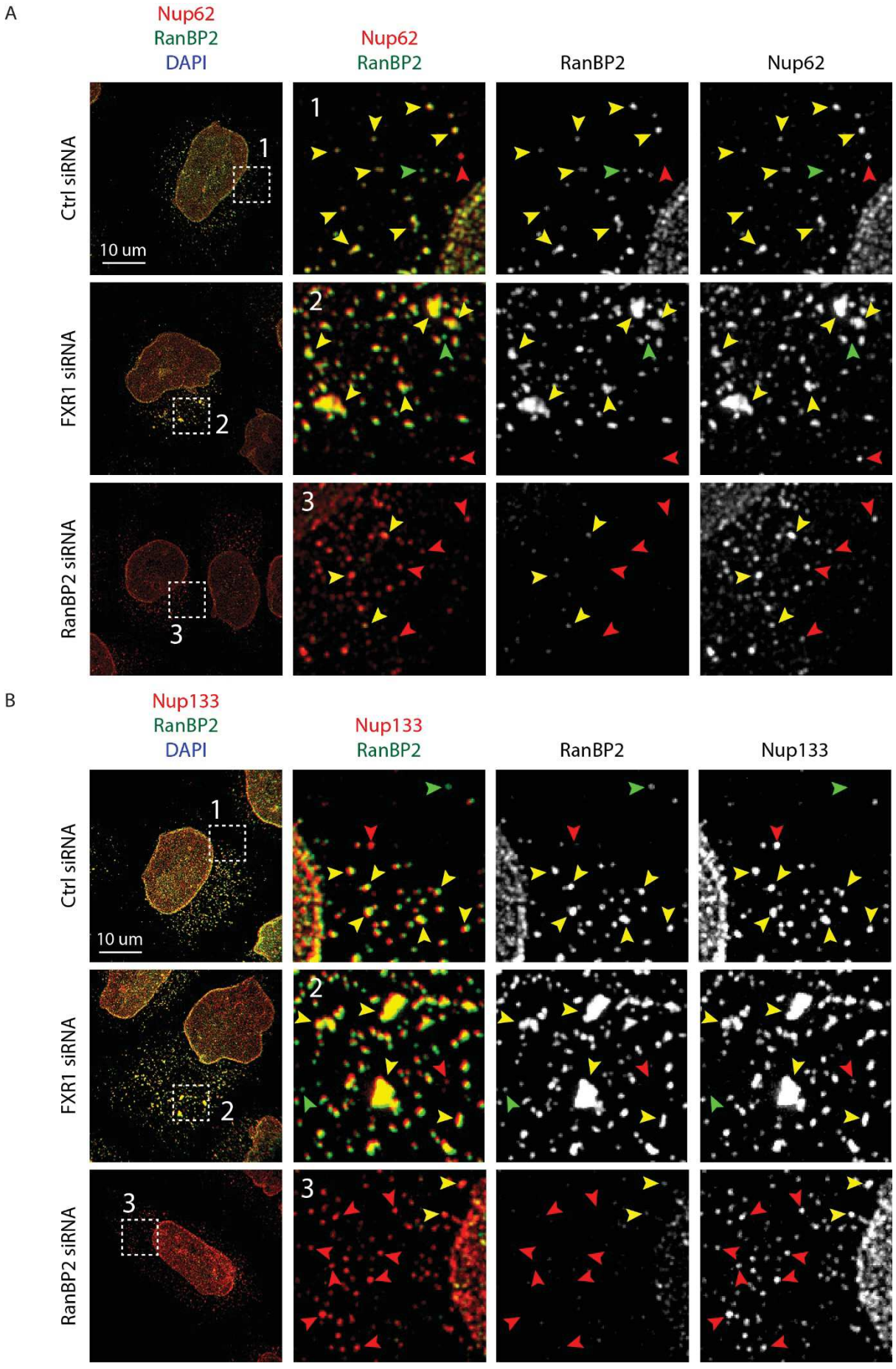
A
Nup62
RanBP2
DAPI
Nup62
RanBP2
RanBP2
Nup62
Ctrl siRNA
FXR1 siRNA
RanBP2 siRNA
10 um
1
2
3
B
Nup133
RanBP2
DAPI
Nup133
RanBP2
RanBP2
Nup133
Ctrl siRNA
FXR1 siRNA
RanBP2 siRNA
10 um
1
2
3

Figure 17 - FXR1 depletion induced big cytoplasmic Nup granules contain different Nups and require RanBP2 to be formed.
A, B HeLa cells were treated with the indicated siRNAs, synchronized by double thymidine block, released for 12 hours and analyzed by IF using a spinning disk confocal microscope at 100x magnification with live super resolution module. Cells were simultaneously stained for Nup62 (FG-Nup) and RanBP2 (cytoplasmic filament Nup) (**A**), and Nup133 (scaffold Nup) and RanBP2 (**B**). The magnified framed regions are shown in the corresponding numbered panels.
Data information: Scale bar is 10 μm.

Similar results were obtained when treating HeLa cells in early G1 with the microtubule depolymerizing agent nocodazole, which induces big cytoplasmic Nup granule formation. Control DMSO-treated cells showed the cytoplasmic Nup pattern in small dots from which the majority contained both markers (Nup62 and RanBP2 or Nup133 and RanBP2). Only few granules contained only Nup62, Nup133 or RanBP2 (Figure 18A, B). Nocodazole treated cells showed prevalently big Nup granules, which always contained both markers (Figure 18A, B). Some smaller granules present in nocodazole-treated cells were very rarely positive for a single marker. Also in this analysis, we were unable to find big Nup granules that contained only one Nup type.

These results are in line with the hypothesis that RanBP2 is a Nup granule fusing agent since very few Nup62- or Nup133-positive granules were devoid of it, and big Nup granules always contained RanBP2. Furthermore, big cytoplasmic Nup granules could not be observed upon RanBP2 depletion. To corroborate this idea, live video experiments of the stable GFP-Nup107 cell line treated with Ctrl siRNA or RanBP2 siRNA could be used to study the behavior of the cytoplasmic small Nup granules upon nocodazole addition. It would also be interesting to analyze if the ratio of small Nup granules containing only Nup133 or Nup62 is increased upon RanBP2 depletion.

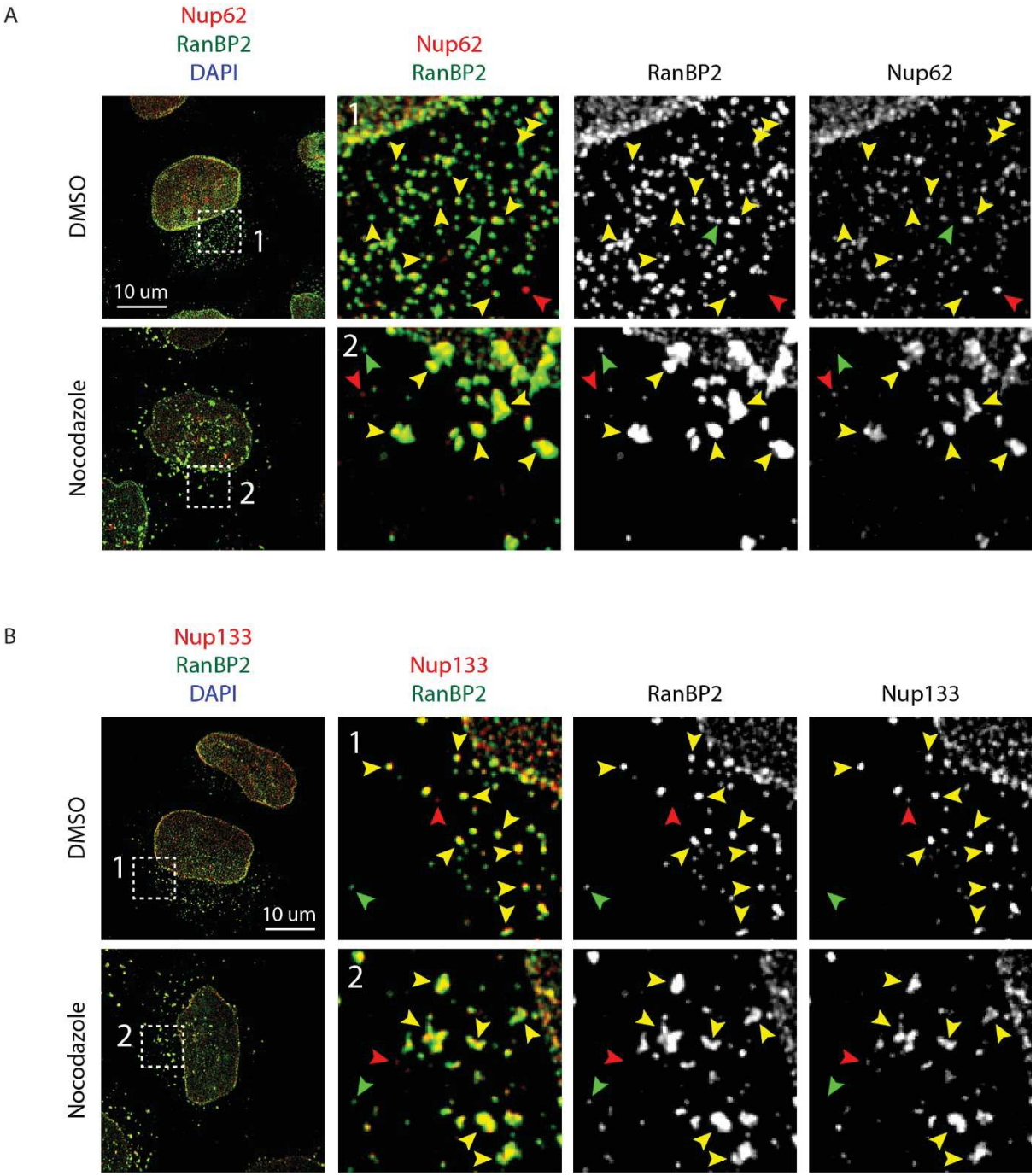

Figure 18 - Microtubule depolymerization induced big cytoplasmic Nup granules contain different Nups.

A, B HeLa cells were synchronized by double thymidine block, released for 12 hours, treated with nocodazole 10 µM or vehicle (DMSO) for 1h 30 and analyzed by IF using a spinning disk confocal microscope at 100x magnification with live super resolution module. Cells were simultaneously stained for Nup62 (FG-Nup) and RanBP2 (cytoplasmic filament Nup) (**A**), and Nup133 (scaffold Nup) and RanBP2 (**B**). The magnified framed regions are shown in the corresponding numbered panels.
Data information: Scale bar is 10 µm.

3.3.4. RanBP2 but not Nup133 or ELYS is required for the formation and/or maintenance of the FXR1-induced cytoplasmic Nup granules

Is Nup granule fusion role restricted only to RanBP2 or can other Nup proteins also share this function? To address this question, we downregulated RanBP2, Nup133 or ELYS together with FXR1 to see if depletion of different Nups could also abolish big Nup granules in the absence of FXR1. As previously reported, individual Nup133 or ELYS depletion in HeLa cells induced a strong cytoplasmic Nup accumulation (Figure 19A, B), which has been suggested to correspond to ALs (Franz *et al*, 2007; Walther *et al*, 2003a; Doucet *et al*, 2010). Unlike RanBP2, co-depletion of these Nups together with FXR1 did not reduce the percentage of cells with big cytoplasmic Nup granules, instead, this percentage was similar to the individual Nup133 or ELYS depletion condition (Figure 19A, B). Nevertheless, at this stage of analysis it cannot be ruled out that other yet to be identified Nups also share this Nup granule fusion function. Since RanBP2 belongs to the cytoplasmic filaments of the NPCs, it would be of special interest to analyze if depletion of Nups building the asymmetric NPC structures (for example Nup214 from the filaments and Nup153 from the nuclear basket) also abolished Nup fusion into big cytoplasmic granules in the absence of FXR1.

Interestingly, Nup133 or ELYS downregulation also affected FXR1 localization in a manner highly reminiscent of RanBP2 depletion (Figure 19A, B; Figure 15A, B). Upon Nup133 or ELYS downregulation, FXR1 no longer localized ubiquitously at the cytoplasm nor was enriched at the NE. Instead, it formed discrete cytoplasmic foci compared to control siRNA treated cells. This suggests that FXR1 localization somehow links to levels of different Nups.

In conclusion, RanBP2 protein and/or its mRNA is required for the formation and/or maintenance of big cytoplasmic Nup granules induced by FXR1 depletion, a function which is not shared by other Nups like Nup133 and ELYS.

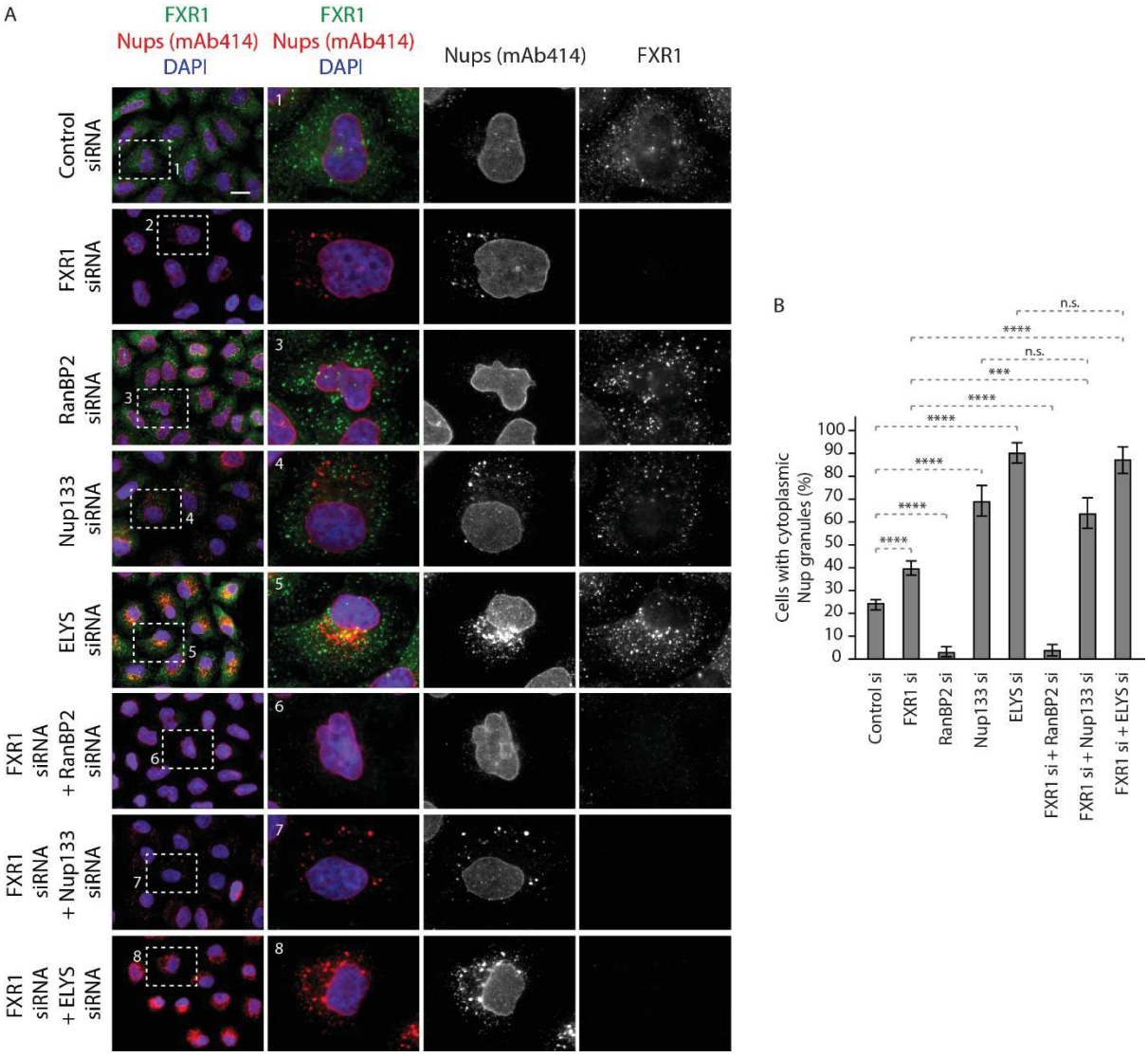

Figure 19 - RanBP2 but not Nup133 or ELYS is required for FXR1 induced big cytoplasmic Nup granule formation and/or maintenance.

A, B HeLa cells were treated with the indicated siRNAs, synchronized by double thymidine block and released for 12 hours and analyzed by IF microscopy. The magnified framed regions are shown in the corresponding numbered panels. The percentage of cells with big cytoplasmic Nup granules was quantified in (**B**), 11500 cells were analyzed (mean ±SD, **P < 0.01; ***P < 0.001; N = 5).

Data information: Scale bars are 5 µm. Statistical significance was assessed by two-tailed two sample Student's T-test (**B**).

3.3.5. RanBP2 is required for big cytoplasmic Nup granule accumulation induced by microtubule depolymerization or dynein downregulation

Our earlier results showed that the presence of RanBP2 protein is required for Nup condensation into big cytoplasmic granules in the absence of FXR1. We asked if RanBP2 is specifically required for Nup granule fusion induced by absence of FXR1 or if it has a broader function in promoting any kind of cytoplasmic Nup granule fusion events. To answer this

question, we first induced the formation of big cytoplasmic Nup granules by depolymerizing microtubules with nocodazole in early G1 phase HeLa cells. As expected, nocodazole treatment induced a strong accumulation of big cytoplasmic Nup granules compared to cells treated with the vehicle (DMSO) (Figure 18A, B; Figure 20A, B). In nocodazole treated cells, accumulation of big cytoplasmic Nup granules in control and FXR1 siRNA treated cells was similar, while it was slightly enhanced in Nup133 or ELYS depleted cells. In contrast, the nocodazole-induced formation of big cytoplasmic Nup granules was dramatically reduced in RanBP2 downregulated cells almost to the levels observed in the DMSO-treated cells (Figure 20A, B).

Our published data demonstrated that downregulation of dynein can induce big cytoplasmic Nup granules, probably due to inhibition of the transport of cytoplasmic Nups to the NE. For this reason, we depleted FXR1 or dynein HC together with RanBP2 in early G1 HeLa cells (Figure 20C, D). As expected, only dynein siRNA as well as FXR1 siRNA treated cells accumulated big cytoplasmic Nup granules compared to control siRNA treated cells, while RanBP2 siRNA alone reduced this phenotype. Dynein and FXR1 co-depletion also showed accumulation of big cytoplasmic Nup granules in contrast to control or RanBP2 depletion (Figure 20C, D). Strikingly, co-depletion of dynein and RanBP2 abolished accumulation of Nup granules (Figure 20C, D).

These data suggest that formation or maintenance of big cytoplasmic Nup granules upon disruption of microtubule-based transport (either by microtubule depolymerization or dynein depletion) require the presence of RanBP2 protein and/or mRNA.

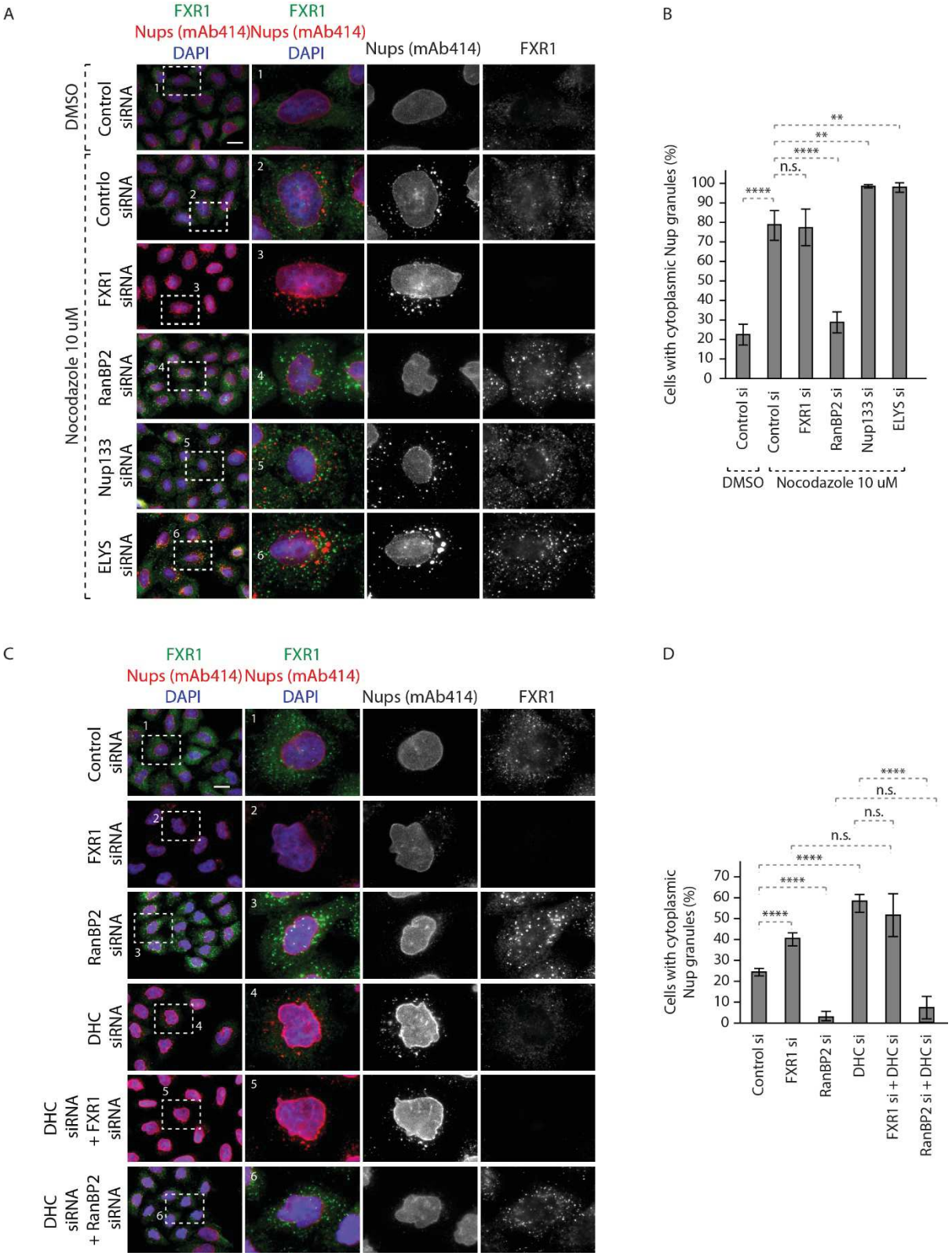

Figure 20 - RanBP2 depletion can reduce cytoplasmic Nup localization induced by microtubule depolymerization or dynein downregulation

A, B HeLa cells were treated with the indicated siRNAs, synchronized by double thymidine block, released for 12 hours, treated with DMSO or nocodazole 10 uM for 90 min and analyzed by IF (**A**). The magnified framed regions are shown in the corresponding numbered panels. The percentage of cells

with big cytoplasmic Nup granules was quantified in (**B**), 6100 cells were analyzed (mean ±SD, **P<0.01; ****P < 0.0001; n.s. = non-significant; N = 4).
C, D HeLa cells were treated with the indicated siRNAs, synchronized by double thymidine block, released for 12 hours and analyzed by IF (**C**). The magnified framed regions are shown in the corresponding numbered panels. The percentage of cells with big cytoplasmic Nup granules was quantified in (**D**), 8100 cells were analyzed (mean ±SD, ****P < 0.0001; n.s. = non-significant; N = 5).
Data information: Scale bars are 5 µm. Statistical significance was assessed by two-tailed two sample Student's T-test (**B, D**).

3.3.6. RanBP2 is required for the formation and/or maintenance of big cytoplasmic Nup granules induced by depletion of Nup133 or ELYS

As shown by Hampoelz *et al*, AL formation in Drosophila oocytes relies on RanBP2 condensation in a co-translational manner and its subsequent fusion with other condensed Nup granules. The resulting fused granules are transferred to neighboring ER membranes to constitute the ALs (Hampoelz *et al*, 2019b). Since we have previously observed that RanBP2 depletion can abolish the formation and/or accumulation of big cytoplasmic Nup granules in cancer cells, we wondered if its absence could also affect AL biogenesis in these cells. To answer this question, we decided to induce AL formation by downregulating Nup133 or ELYS together with RanBP2 in HeLa cells. Indeed, as previously reported, individual depletions of Nup133 or ELYS in HeLa cells induced a strong cytoplasmic Nup accumulation (Figure 19A, B). Co-depletion of RanBP2 together with these Nups significantly reduced the percentage of cells with big cytoplasmic Nup granules. In contrast, the extent of cytoplasmic Nup granule formation was similar to the individual Nup133 or ELYS depletion when co-depleting these two proteins together (Figure 21A, B). These results indicate that RanBP2 is required for Nup133- or ELYS-depletion induced big cytoplasmic Nup granules in cancer cells, which likely correspond to Nup condensates formed prior to AL biogenensis or to mature ALs. Correlative Light Electron Microscopy (CLEM) studies will be necessary to characterize these granules in detail and to distinguish between these two possibilities whereabout ribosome exclusion zones would be expected in the case of Nup condensates and stacked ER membranes with inserted pores should be detected in the case of mature ALs.

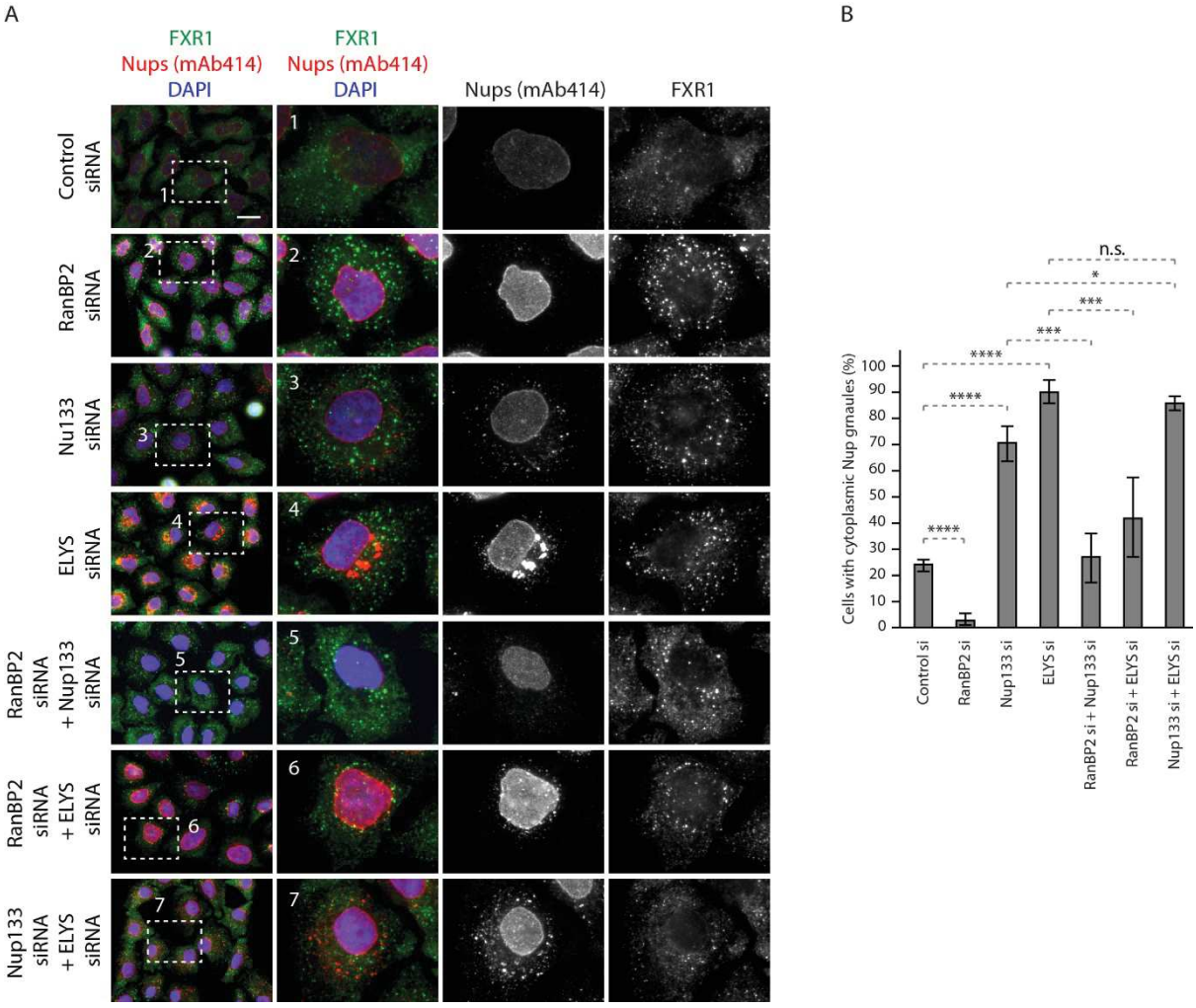

Figure 21 - RanBP2 depletion can reduce cytoplasmic Nup localization induced by Nup133 or ELYS downregulation.

A, B HeLa cells were treated with the indicated siRNAs, synchronized by double thymidine block, released for 12 hours and analyzed by IF (**A**). The magnified framed regions are shown in the corresponding numbered panels. The percentage of cells with big cytoplasmic Nup granules was quantified in (**B**), 9700 cells were analyzed (mean ±SD, *P<0.05; ***P<0.001; ****P < 0.0001; n.s. = non-significant; N = 5).

Data information: Scale bars are 5 µm. Statistical significance was assessed by two-tailed two sample Student's T-test (**B**).

3.3.7. Formation of big cytoplasmic Nup granules in early G1 does not depend on active protein translation

Several Nup and importin mRNAs enriched on the surface of ALs were observed in Drosophila oocytes by Hampoelz and colleagues. The mRNA localization was lost upon translation inhibition, suggesting an ongoing translation of Nups in these compartments. Further to that, the authors suggested that simultaneous Nup translation may contribute to effective condensation into granules prior to AL assembly (Hampoelz *et al*, 2019b). We reasoned that a

similar Nup translation and condensation processes could take place in early G1 in order to produce a newly translated pool of Nups necessary to "feed" the expanding nuclei with NPCs through the interphasic assembly pathway. This pool of newly made Nups could be transported in a dynein/FXR1/microtubule-mediated manner to the NE, and would tend to accumulate and fuse in the cytoplasm when these factors are missing. In order to test if the formation of big cytoplasmic granules in HeLa cells requires active protein translation, we designed the following experiment setup (Figure 22A). We synchronized HeLa cells by double thymidine block and release and we added translation inhibitors cycloheximide (CHX) and puromycin (or the vehicles DMSO and H_2O respectively) 9h after the second thymidine release i.e. at the time when the synchronized population of cells reached anaphase and no more cyclin B needed to be produced for mitosis to proceed. 5h 30 after anaphase and while maintaining translation inhibitors in the media, nocodazole (or the vehicle DMSO) was added for 1h 30 to induce formation of big cytoplasmic Nup granules. Subsequently, cells were analyzed by IF and Western blot. As expected, low percentage of cells that were not treated with nocodazole showed cytoplasmic accumulation of big Nup granules (Figure 22B, C conditions 1-4). CHX and H_2O (conditions 2 and 3) seemed to moderately increase the accumulation of big Nup granules, although this results need to be confirmed by additional experimental replicates. As expected, microtubule depolymerization with nocodazole in cells where translation was not inhibited dramatically increased the percentage of cells that showed big cytoplasmic Nup granules up to 80% (Figure 22B, C conditions 5 and 7). Interestingly, translation inhibition with CHX and puromycin did not abolish the formation of big cytoplasmic Nup granules upon microtubule depolymerization (Figure 22B, C conditions 6 and 8). The inhibitory effect of CHX and puromycin on active translation was confirmed by Western blotting against FXR1 and Cyclin D1 (Figure 22D conditions 2, 4, 6, 8), where both markers were decreased relative to the levels in cells treated with the respective vehicles DMSO and H_2O (Figure 22D conditions 1, 3, 5, 7). Based on the strong reduction in the protein levels of the G1 marker Cyclin D1, we presume that in the cells in which translation has been inhibited for 7h after anaphase, no new Nups have been produced and yet, big cytoplasmic granules could be induced upon microtubule depolymerization. These results suggest that ongoing translation is not required for the formation of big cytoplasmic Nup granules induced by nocodazole. Furthermore, these data also indicate that a pool of Nups produced in the previous cell cycle have not been incorporated into the NE of the daughter nuclei through the postmitotic NPC assembly pathway. These Nups reside in the cytoplasm during early G1 phase and are presumably prone to granule formation. This pool of Nups in the cytoplasm may allow a

smooth transition from the postmitotic NPC assembly pathway to the interphasic pathway without relying on the translation of new Nups. In fact, this idea is in line with RanBP2 and Nup133 protein levels not being affected by translation inhibition during late mitosis and early G1 phase (Figure 22D conditions 2, 4, 6, 8 compared to conditions 1, 3, 5, 7).

Taken together our results suggest that RanBP2 is specifically required for Nup condensation into big granules in the cytoplasm of cultured cancer cells, an event which may not be dependent on active protein translation.

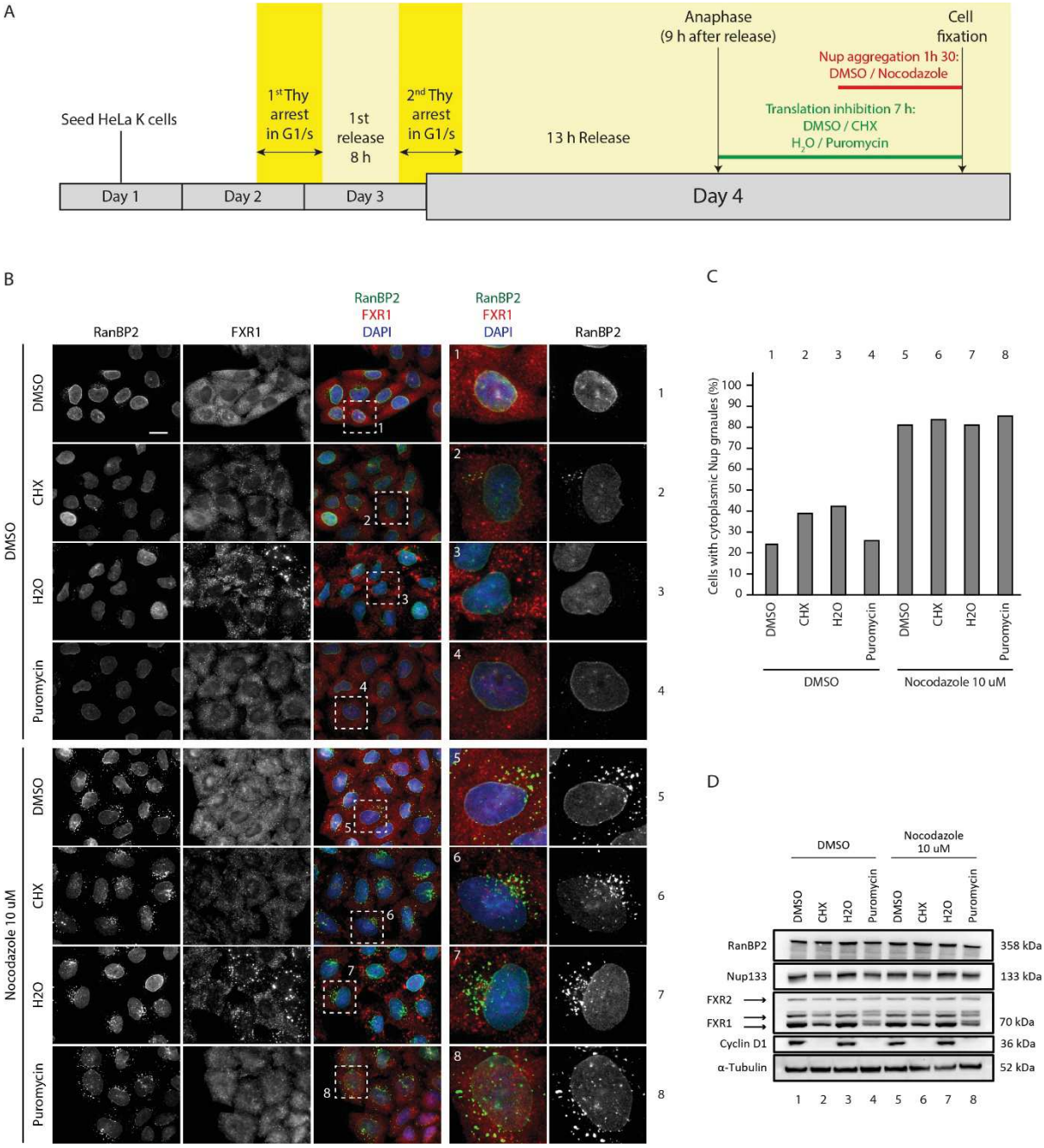

Figure 22 – Big cytoplasmic Nup granule formation in early G1 does not rely on protein translation.

A Scheme of the experimental setup. HeLa cells were seeded on glass coverslips, synchronized by double thymidine block and released for 9 hours. At this moment (when synchronized cells where in anaphase) translational inhibitors CHX and puromycin (and respective vehicles DMSO and H_2O) where added to the media and cells where incubated for 5h 30. Subsequently, big cytoplasmic Nup granule formation was induced by adding nocodazole 10 uM to the media (or the vehicle DMSO) for 1h 30, while keeping the translational inhibitors in the media. At the end of the experiment cells were analyzed by IF and Western blot.
B, C Cells were treated as in (**A**) and analyzed by IF (**B**). The magnified framed regions are shown in the corresponding numbered panels. The percentage of cells with big cytoplasmic Nup granules was quantified in (**C**), 2400 cells were analyzed (N = 1).
D Cells were treated as in (**A**) and analyzed by Western blot.
Data information: Scale bars are 5 μm (**B**). Numbers 1- 8 were assigned to different conditions for easier understanding of the text (**B**, **C**, **D**).

3.4. Discussion

The current model

As it has already been described in the Part 1, small cytoplasmic Nup granules (observed as a dotty pattern) are a feature of human cancer cells in normal conditions and only around 20% of them show accumulation of bigger granules. Both, small and big granules display characteristics of liquid droplets since they split and fuse and they are dissolved upon 1,6-Hexanediol treatment, suggesting that they are phase separated Nup entities. The percentage of cells with big cytoplasmic Nup granules is increased when challenging them with FXR1 depletion or microtubule transport hindrance (by dynein depletion or microtubule depolymerization). These results, together with the fact that FXR1 interacts with dynein and Nups, prompted us to propose a hypothetical model in which Fragile X-related proteins interact with cytoplasmic Nups and dynein facilitating their localization to the NE during early G1. This function of FXR proteins inhibits the accumulation of Nups in the cytoplasm and inhibits formation of aberrant cytoplasmic Nup granules (the big cytoplasmic Nup granules), contributing to the equilibrium of NE-NPCs (model described in Part 1 and depicted in the Section 2.7.8, page 84, recently published in The EMBO Journal).

In the second part of the thesis we have identified RanBP2 as a new key player in the regulation of Nup condensation. Our results suggest a model where, in addition to FXR proteins and microtubule dependent transport, RanBP2 regulates the localization and condensation of a cytoplasmic pool of Nups during early G1 phase (Figure 23). Under normal conditions, a pool of Nups synthesized in the previous cell cycle remains in the cytoplasm of early G1 cells, which appears as intrinsically phase-separated small Nup granules. These small cytoplasmic Nup granules can be transported through microtubules towards the NE where they assemble into NPCs. FXR protein depletion or compromised transport leads to a deficient Nup granule transport and their subsequent accumulation in the cytoplasm tending to fuse and form aberrant big cytoplasmic Nup granules. Fusion among cytoplasmic Nups is promoted by RanBP2 which may act as a Nup ‘glue’. Upon RanBP2 depletion, fusion between cytoplasmic Nups is abolished and the formation of bigger granules is drastically reduced, even in the absence of FXR proteins or microtubule-based transport (Figure 23).

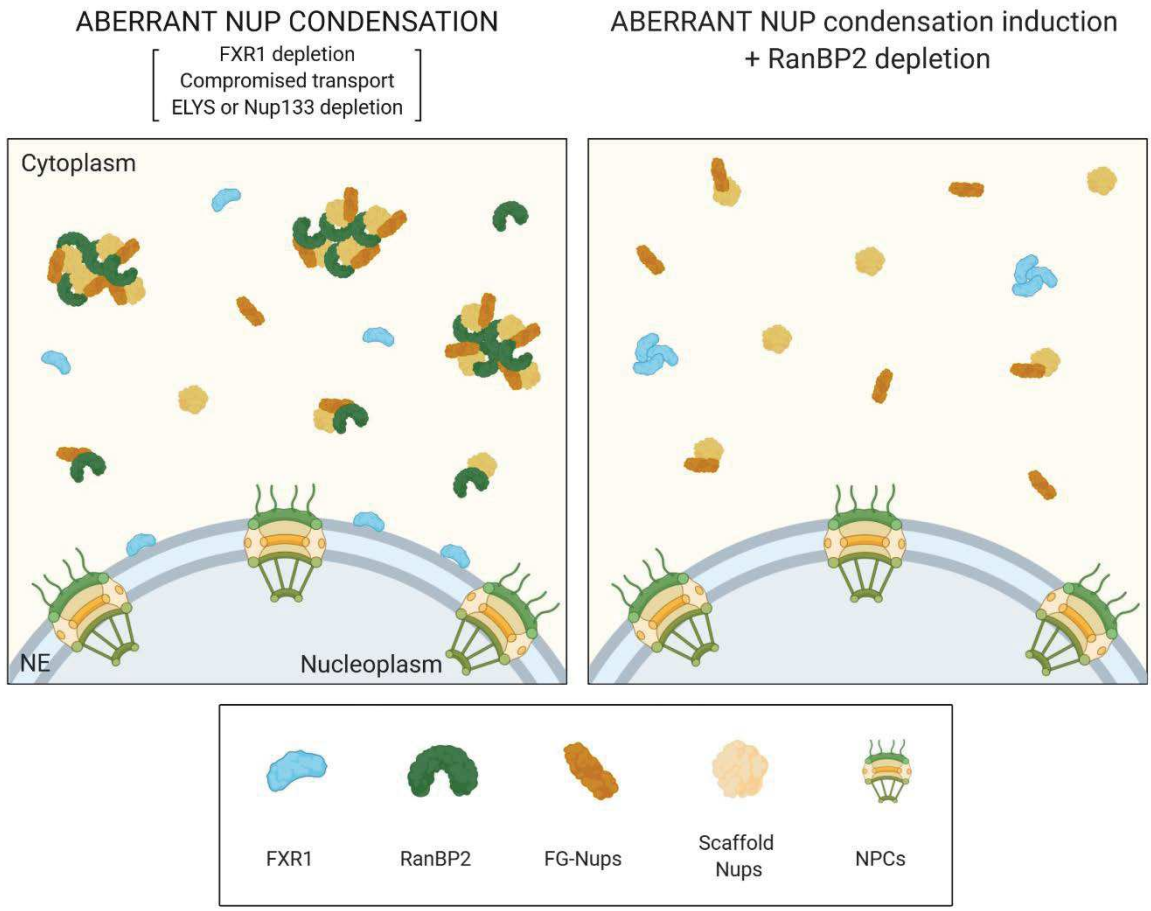

Figure 23 - Model on how RanBP2 regulates the condensation state of a cytoplasmic pool of Nups during early G1 phase.
A hypothetical model on how RanBP2 regulates Nup condensation in early G1 phase of the cell cycle. A cytoplasmic pool of Nups exists during early G1 phase. Aberrant condensation of these Nups into big granules is induced by different stimuli that increase Nup local concentration, such as FXR depletion, inhibition of microtubule based transport (microtubule depolymerization or dynein downregulation) or depletion of some Nup (ELYS or Nup133). RanBP2 protein acts as a Nup fusion agent necessary for aberrant Nup granule formation. Thus, in the absence of RanBP2 big cytoplasmic Nup granules are not formed. Figure created with BioRender.com.

It is important to mention that in the Part 1 we have focused solely on the big granules and proposed to call them 'cytoplasmic Nup granules, CNGs'. In view of the recent results which suggest that RanBP2 is necessary for the formation of the big granules but not the small ones, we find important to highlight this size difference. Therefore, we will hereinafter refer to small and big cytoplasmic Nup granules.

The second part of the thesis is focused on investigating the role of RanBP2 in the regulation of Nup condensation in cancer cells based on the recently published functions of RanBP2 in AL biogenesis during Drosophila oogenesis. A study by Hampoelz *et al* proposed that RanBP2

is a key player that condenses into granules which are transported in a microtubule dependent manner to fuse with other Nup granules and form AL assembly platforms (Hampoelz *et al*, 2019b). Although this function of RanBP2 was described in a very specific context (oogenesis in Drosophila) and ALs seem to be restricted to cells with fast cell divisions that require a rapid nuclear growth, it could very well be that the interphasic NPC assembly pathway also makes use of a Nup condensation and transport mechanism to direct NPC assembly at the NE instead of the ER. Driven by these idea, we obtained some preliminary results which set the ground for a follow up project.

Could FXR1 regulate RanBP2 translation?

Hampoelz and colleagues observed that RanBP2 mRNA decorated RanBP2 granules in nurse cells in an active translation-dependent manner (Hampoelz *et al*, 2019b), which suggested a co-translational mechanism for formation of these granules. Given that translational regulation is the main described function of FXR proteins, it was tempting to speculate that FXR1 could modulate RanBP2 translation for correct RanBP2 granule formation. In fact, a recent study from Van Driesche and colleagues identified RanBP2 mRNA as an interactor of the FXR1 paralogue FMRP *in vivo* by RNA:protein crosslinking and immunoprecipitation technique (Van Driesche *et al*, 2019), suggesting that FMRP could regulate RanBP2 translation. Following this reasoning, we first assessed if FXR1 regulates RanBP2 protein and/or mRNA levels. We observed that FXR1 downregulation does not affect RanBP2 mRNA levels although it can occasionally induce a mild increase in RanBP2 protein levels in HeLa cells (Figure 14). Furthermore, our Western blot results suggest that there may be a crosstalk between FXR1 and RanBP2 in terms of protein levels and subcellular localization in HeLa cells. FXR1 downregulation induces a moderate increase in RanBP2 protein levels which localizes to big cytoplasmic granules; in turn, RanBP2 depletion induces a mild decrease in FXR1 protein levels and its localization in cytoplasmic foci away from the NE (Figure 14).

An increase in RanBP2 protein levels upon FXR1 depletion suggests that this Nup accumulates in the cytoplasm upon FXR1 siRNA and attracts other Nups to this compartment. It would be interesting to overexpress RanBP2 in HeLa cells and to analyze whether its high protein levels are sufficient to induce formation of similar big cytoplasmic granules and if they also contain other Nups. Furthermore, to understand whether putative regulation of RanBP2 protein levels is a feature shared by all FXR proteins, it would be interesting to analyze if FXR2 and FMRP depletion also leads to higher RanBP2 levels. Similarly, RanBP2 protein levels could be analyzed in FXS patient-derived cells compared to healthy individuals.

However, in our experiments in cancer cells the formation of big cytoplasmic Nup granules does not depend on active translation since their formation can still be induced by acute microtubule depolymerization in the presence of translational inhibitors during early G1 phase (Figure 22). Therefore, occasional and rather moderate increase in RanBP2 protein levels upon FXR1 depletion and dispensability of the active translation argue against translational regulation by FXR1 as the driving mechanism for big Nup granule formation in early G1 phase. Interestingly, the fact that these experiments were carried out in synchronized populations where translation was inhibited for 7 hours after anaphase onset implies that there was no ongoing protein translation in these daughter cells and yet big cytoplasmic granules were formed (Figure 22). Thus, our data suggest that the cytoplasmic Nup granules may not be made of newly synthesized Nups and instead they might contain Nups produced in the previous cell cycle. These "older" Nups may remain in the cytoplasm without being inserted into the reforming NE during the postmitotic NPC assembly pathway acting in anaphase and telophase. This suggests that at this stage of the cell cycle the interphasic NPC assembly pathway would not entirely rely on the production of newly translated Nups and it would make use of the remaining pool of the cytoplasmic Nups. This pool of Nups could allow for a rapid initiation of the interphasic NPC assembly pathway and buffer the transition from the postmitotic assembly mode without requirement of energetically-demanding protein translation process.

RanBP2 could act as a Nup fusing agent

We have investigated if RanBP2 is required for formation of big cytoplasmic Nup granules upon different stimuli such as FXR1 or dynein depletion, microtubule depolymerization and absence of specific Nups (Figure 16; Figure 20; Figure 21). RanBP2 depletion dramatically reduces the percentage of cells with these granules in all conditions as well as control situations, which suggests that RanBP2 is required for the formation or for maintenance of these granules. From experiments presented in the Part 1, we know that Nup granules have the tendency to fuse and that the small Nup granules are also dissolved by 1,6-Hexanediol (section 2.7.5, page 74), which prompt us to think that the big granules present in FXR1-deficient cells are likely to result from fusion events among small Nup granules. In this scenario, RanBP2 could act as a small granule fusion-promoting agent or as a solubilizing inhibitor. Our data in fixed cells do not allow to conclude if RanBP2 depletion abolishes big Nup granule formation or if it induces their fast disassembly. To distinguish between these two posibilities, live video experiments need to be performed to observe the behavior of stably expressed GFP-tagged Nups in living cells upon Nup granule induction by nocodazole in the presence and absence of RanBP2.

We have performed some preliminary analysis in cancer cells to understand if they also contain distinct types of cytoplasmic granules where different populations of Nups are present (Figure 17; Figure 18). This could indicate that cancer cells may also rely on a similar mechanism as Drosophila oocytes to form NPC assembly platforms. In our experiments, we combined RanBP2 staining with scaffold Nups or FG-Nups co-labeling, and we occasionally found small cytoplasmic granules with only one type of Nup although the big majority of small granules contained both markers. The big granules always contained both markers (Figure 17; Figure 18). It will be interesting to test the remaining combination: to co-stain scaffold and FG-granules other than RanBP2 (Nup133 and Nup62 for example) to analyze if majority of granules are double positive or if different subpopulations exist. This would clarify if RanBP2 is the only ubiquitous Nup or if all Nups colocalize in the majority of big and small granules. Additionally, to study whether RanBP2 is indeed a Nup granule-fusing agent, it would be interesting to carry out the same stainings in RanBP2 depleted cells and to analyze the changes in the distribution of small granules; whether we see an accumulation of single Nup type granules or if they still contain different types of Nups.

Is RanBP2 a specific Nup regulating Nup granule fusion?

The role of RanBP2 in the Nup granule fusion or maintenance seems to be specific since depletion of other Nups including Nup133 and ELYS did not reduce formation of big cytoplasmic Nup granules but even increase it (Figure 19). However, ELYS and Nup133 are probably not the most relevant Nups in this context since they have been shown to play important roles in NPC assembly pathways (Franz *et al*, 2007; Doucet *et al*, 2010; Walther *et al*, 2003a) and their depletion has been proposed to induce ALs. Therefore, more Nups should be tested for this Nup-fusion function and especially Nups belonging to the asymmetric NPC structures (such as Nup153 and Nup214 which belong to the nuclear basket and cytoplasmic filaments, respectively) as RanBP2 itself is the main component of the cytoplasmic filaments. In this regard, several studies in which single Nups were depleted such as Nup133 (Walther *et al*, 2003a), ELYS (Doucet *et al*, 2010), Nup107 (Doucet *et al*, 2010; Boehmer *et al*, 2002) and Nup88 (Hutten & Kehlenbach, 2006) have reported the formation of big cytoplasmic granules in a qualitative manner. However, a precise quantitative analysis should be performed to study the role of all Nups in the regulation of Nup condensation.

Furthermore, to confirm the direct and specific role of RanBP2 in this process and to dissect which domains are implicated in Nup granule fusion, rescue experiments with overexpression of different RanPB2 constructs should be performed in RanBP2 depleted cells.

How could RanBP2 promote the fusion of Nup granules?

How could RanBP2 promote the fusion of Nup granules? RanBP2 has been proposed to function as a platform to recruit import receptors and increase their local concentrations (Wälde *et al*, 2012; Hutten *et al*, 2008, 2009). Moreover, RanBP2 is the biggest Nup and contains several FG repeats scattered all along its protein sequence (Figure 4; Figure 13A) which confer the ability to establish cohesive interactions with other Nups. In fact, FG-Nups have been shown to stabilize each other and also scaffold Nups during yeast NPC assembly (Onischenko *et al*, 2017) and RanBP2 condensates have been proposed to act as a NPC assembly platforms in Drosophila oogenesis (Hampoelz *et al*, 2019b). Furthermore, RanBP2 contains several domains which interact with importins (Importin β for example) and exportins (such as CRM1) (Figure 13), and both types of NTRs have been shown to be implicated in regulating Nup condensation. Importin β is a well-known Nup chaperone which interacts with them keeping them in a soluble state (Walther *et al*, 2003b), while CRM1 seems to have opposite functions since depletion of the Drosophila CRM1 homologue 'embargoed' abolished RanBP2 condensation (Hampoelz *et al*, 2019b). Therefore, due to its large size, high content of FG-repeats, presence of the chaperone-like interacting domains, RanBP2 could concentrate several Nup-regulating factors in space and drive their condensation/fusion.

Another possibility is that RanBP2 regulates Nup condensation/fusion through its SUMO E3 ligase activity (Pichler *et al*, 2002). In fact, several studies have shown that SUMOylation is implicated in phase separation; SUMO has been shown to modulate the composition of *in vitro* and *in cellulo* condensates (Banani *et al*, 2016), eIF4A2 SUMOylation in response to arsenite correlates with its localization to SGs (Jongjitwimol *et al*, 2016) and PML SUMOylation contributes to the formation of PML nuclear bodies (Li *et al*, 2017; Shen *et al*, 2006). Importantly, several components of the SUMO pathway localize to the NPC: the E3 ligase RanBP2 and SUMO conjugating enzyme Ubc9 localize to the cytoplasmic filaments (Pichler *et al*, 2002) and the SUMO proteases SENP1 and SENP2 localize to the nuclear basket (Chow *et al*, 2012). The localization of SUMO E3 ligases and proteases at the NPC links these complexes to several biological functions (Palancade & Doye, 2008), suggesting there could also be a functional link between SUMOylation and Nups' condensation and/or NPC assembly. Indeed, several Nups are known to be SUMOylated (Folz *et al*, 2019) and SENP1 and SENP2 depletion has been shown to promote Nup mislocalization in cytoplasmic foci (Chow *et al*, 2014) highly reminiscent of the big cytoplasmic granules observed upon FXR1 downregulation. Furthermore, an NPC quality control mechanism involving SUMO has been

proposed in budding yeast, which relies on Ulp1 SUMO protease (SENP1 and SENP1 homologue) as a sensor of NPC integrity and the SUMO target Hek2 as a repressor of NPC biogenesis (Rouvière *et al*, 2018). Moreover, SUMOylation of FMRP has been shown to be essential to allow for its dissociation from dendritic mRNA granules and to promote spine elimination and maturation in neurons (Khayachi *et al*, 2018). Altogether, RanBP2 could link SUMO-regulated processes and Nup fusion regulation. To explore this hypothesis, it would be interesting to test whether interference with different SUMOylation steps could affect Nup condensation. For this purpose, nocodazole-induced Nup condensation could be analyzed in HeLa cells upon the following treatments: SUMO conjugating enzyme Ubc9 depletion with siRNA, SUMOylation inhibition with SUMO activating enzyme 1 specific inhibitor ML-792 (He *et al*, 2017) and RanBP2 depletion with siRNA together with overexpression of the wild-type and SUMO-ligase deficient versions of RanBP2.

It is important to mention that the aforementioned mechanisms through which RanBP2 could promote Nup granule fusion are not mutually exclusive; RanBP2 could act as a platform to recruit several proteins due to its big size and multiple FG repeats, such as Nups, chaperones and SUMO related proteins, and modulate them through SUMOylation of different relevant targets.

What could be the implications of RanBP2's function as a Nup nucleating agent?

As we have observed, RanBP2 depletion abolished formation of big Nup granules, even under conditions such as FXR1 or dynein downregulation or microtubule depolymerization. As described in the Part 1, we had observed that upon FXR1 downregulation, big cytoplasmic Nup granule formation correlates with irregular nuclear shape (section 2.7.3, page 68), transient protein export defects and altered cell cycle progression (section 2.7.8, page 84). To study if these defects are related to FXR1 functions in regulating Nup condensation and not to other unrelated roles, it would be interesting to analyze if FXR1 and RanBP2 co-depletion could rescue these phenotypes. However, it needs to be taken into account that RanBP2 has been reported to have roles in proper mitotic progression (Dawlaty *et al*, 2008; Salina *et al*, 2003; Arnaoutov *et al*, 2005) and in nuclear import of specific targets (Wälde *et al*, 2012; Hutten *et al*, 2009, 2008) but not in general import (Salina *et al*, 2003) or export of proteins (Ritterhoff *et al*, 2016), complicating the design and interpretation of these experiments. Regarding the nuclear architecture, in our experiments in human cancer cells we already observed that RanBP2 depletion alone induces irregular nuclei probably due to its mitotic functions, and accordingly FXR1 and RanBP2 co-depleted cells also show irregular nuclei.

Regarding NPC assembly, it would be interesting to study if the role of RanBP2 as a Nup granule fusing agent is required for proper NPC formation. Salina and colleagues performed indirect IF and EM studies in RanBP2-depleted HeLa cells revealing that there was little or no change in the levels or localization of multiple Nups to the NE (Salina *et al*, 2003). However, these experiments were not quantitative and have not been performed in synchronized cells, suggesting that these conclusions should be interpreted cautiously. Dedicated quantitative experiments in cell populations synchronized in late mitosis, early G1 and G2 will be needed in order to understand the specific role of RanBP2 in the different NPC assembly pathways.

Finally, it is important to study if RanBP2 depletion could also revert Nup mislocalization and or nucleocytoplasmic defects in diseases known to display Nups recruitment to phase separated compartments, such as ALS, FTD and HD (Table 1; (Zhang *et al*, 2015; Grima *et al*, 2017; Eftekharzadeh *et al*, 2018). To this end, Nup localization and nucleocytoplasmic transport upon RanBP2 depletion could be studied in primary cells from patients suffering from these disorders or animal models of the diseases. Also, aggregation prone proteins characteristic of these diseases such as FUS, Tau or TDP-43, could be overexpressed in HeLa cells in the presence or absence of RanBP2 to observe the aggregate formation and/or Nup recruitment to these compartments. In this context, RanBP2 could emerge as a new target for diseases in which Nups are known to be mislocalized in phase-separated aggregates. However, given the multiple interactions of RanBP2 protein and its importance in basic processes such as cell division and nucleocytoplasmic trafficking, the development of RanBP2-based therapeutics to counteract formation of Nup-containing cellular aggregates may very likely encounter limitations. In fact, it has been shown that conditional ablation of RanBP2 in mouse motoneurons phenocopies prominent pathophysiological ALS traits, such as hindlimb paralysis, weight loss, respiratory distress and disruption of nucleocytoplasmic partitioning of NTRs; which culminate in premature death (Cho *et al*, 2017). Moreover, neurological diseases caused by RanBP2 mutations have also been found (Neilson *et al*, 2009; Denier *et al*, 2014).

While more studies are necessary to understand the precise mechanism by which RanBP2 regulates Nup condensation and fusion, this pathway is likely to contribute to localized assembly of NPCs, nucleocytoplasmic trafficking and therefore cellular homeostasis. Collectively, our data identify a new factor implicated in the spatial regulation of Nups and opens exciting avenues for the further understanding of the regulation of this important protein family.

4. Conclusions

My PhD work was focused on studying the relationship between FXR proteins and Nups, a project that had been initiated by the former post-doc in the team Stephane Schmucker. Mass spectrometry data previously obtained by Stephane identified several Nups as potential FXR1 interactors in HeLa cells. He observed that FXR1 localizes to the NE and also occasionally to small cytoplasmic foci labelled by Nups. Despite FXR1 downregulation did not affect Nup mRNA levels, it led to an increase in the percentage of cells with irregular nuclei and an accumulation of big cytoplasmic Nup granules. Importantly, both aspects could be rescued by ectopic expression of GFP-FXR1 indicating that FXR1 specifically regulates Nup localization and nuclear shape. At this point, I took over the project and based on these results, we decided to further characterize the nature of these big cytoplasmic Nup granules, the physiological relevance of FXR1-Nups interaction and its potential implication in FXS.

We first confirmed the FXR1-Nup interaction by performing IP followed by Western blot experiments. We also observed that FXR1 depletion, in addition to Nup granule formation, leads to a moderate reduction of Nups at the NE. Live video experiments with different GFP-Nup reporter cell lines showed that irregular nuclei and Nup mislocalization could be first observed in early G1 phase of the cell cycle. These results indicate that FXR1 is required for proper Nup localization and nuclear morphology in early G1 phase.

Subsequently, we aimed at further understanding the nature of these Nup granules. Absence of ER markers and G3BP1 or TIA1 failed to identify the granules as ALs or SGs, respectively. However, 1,6-Hexanediol led to the dispersion of small and big cytoplasmic Nup granules indicating that they were made of Nups in a condensate-like state.

In an attempt to understand the underlying mechanism, we identified dynein and its adaptor protein BICD2 as FXR1 interactors. Their absence or microtubule depolymerization also lead to accumulation of big cytoplasmic Nup granules and to the irregular nuclei in HeLa cells, suggesting that transport hindrance leads to Nup granule formation. Live video analysis of Nup granules induced by microtubule depolymerization confirmed their condensate behavior, since they showed fusion and splitting events. These events increased in the absence of FXR1 or dynein. In sum, our observations suggest that microtubule-based transport by the FXR1-dynein complex can decrease local concentrations of cytoplasmic Nups thereby preventing their assembly into condensates.

Our results also showed that all members of the FXR protein family share roles in regulating Nup localization since FXR2 or FMRP depletion also lead to the condensation of cytoplasmic Nups and to nuclear morphology defects in HeLa cells. Similarly, different FXS models (primary fibroblasts, iPSC and Fmr1 KO MEFs) also displayed accumulation of cytoplasmic Nup granules.

Exploring the physiological consequences of Nup mislocalization upon FXR1 depletion, we found that nuclear import was not affected while export was transiently reduced in early G1 phase. We also observed that downregulation of FXR1 led to an increased percentage of cells in S phase and a decreased percentage of cells in G1 phase, suggesting that upon FXR1 downregulation cell cycle progression is perturbed and cells accumulate in S phase

Finally, we identified RanBP2 as a key Nup in regulating condensation of cytoplasmic Nups given that RanBP2 depletion abolished the aberrant Nup condensation induced by FXR1 or dynein downregulation or microtubule depolymerization.

Collectively, our data demonstrate an unexpected role of FXR proteins and dynein in the regulation of Nup condensation in the cytoplasm of human cells. Future studies will be needed to understand the precise mechanism by which FXR proteins and microtubule mediated transport regulate Nup localization and also if and how defects in this pathway contribute to the pathology of FXS.

While the Nup field has achieved big advances in understanding the NPC assembly pathways, very little is known about Nup biogenesis, trajectory and regulation before their incorporation into NPCs. This study brings new findings in the regulation of Nup solubility and transport in human cells, and highlights the need to study these steps in more detail since their misregulation can have implications in human disease.

5. Materials and methodology

5.1. Cell lines and medium

All cell lines were cultured at 37 °C in 5% CO_2 humidified incubator. I used several different cell lines of human origin and cultured them as indicated below.

- **HeLa Kyoto and derived stable cell lines** (GFP, GFP-FXR1, 3xGFP-NUP85, GFP-NUP107, 3xGFP-mNup133) were cultured in Dulbecco's modified Eagle Medium (DMEM) (4.5 g/L glucose, with GLUTAMAX-I) supplemented with 10% FCS, 1% Penicillin, 1% Streptomycin.
- **Human primary fibroblasts** were cultured in DMEM (4.5 g/L glucose) supplemented with 10% FCS and Gentamicin 40 µl/ml.
- Three independent **mouse embryonic fibroblast (MEFs) cell lines** from control and three MEFs from *Fmr1* knockout mice were cultured in DMEM (4.5 g/L glucose) supplemented with 10% FCS, 1% Penicillin and 1% Streptomycin.
- **HEK293T cells** were cultured asynchronously in Dulbecco's modified Eagle Medium (DMEM) (1 g/L glucose) supplemented with 10% FCS and 1% Penicillin and 1% Streptomycin.
- **U2OS (human U-2 osteosarcoma) cells** were cultured asynchronously in DMEM (4.5 g/L glucose, with GLUTAMAX-I) supplemented with 10% FCS, 1% Penicillin and 1% Streptomycin.
- **Mouse myoblasts (C2C12)** were cultured asynchronously in DMEM (1 g/L glucose) supplemented with 20% FCS and gentamicin.
- **Human iPSCs** derived from a FXS patient (FXS-iPSCs) and the isogenic rescue cells (C1_2-iPSCs) were grown asynchronously as indicated by (Xie *et al*, 2016a).

5.2. Cell seeding

Cells were trypsinized, counted in a Neubauer chamber (5-10 squares) and the concentration was calculated. For IF experiments cells were seeded on 11 or 18 mm glass coverslips (Menzel-Glaser) in 12- or 24-well tissue culture plates at a density 15 000 or 25 000 cells per well respectively. For live video experiments cells were seeded on 35/10 mm 4 compartment glass bottom dishes (Greiner Bio-One, 627871) at a density 20 000 cells per compartment.

5.3. Cell cycle synchronizations

- **Double Thymidine block and release:** cells were synchronized by two-times addition of Thymidine at 2 mM for 16 hours. Cells were washed out after each Thymidine addition three times with warm medium to allow for synchronous progression through cell cycle. Cells were analyzed at desired time points after the release from the second thymidine block.
- **Synchronization with taxol and artificial mitotic exit:** cells were treated with Taxol (paclitaxel) 1 µM for 16 hours which inhibits microtubule depolymerization and mitotic spindle formation arresting the cells in G2/M transition. Cells were subsequently released from the mitotic block by addition of Hesperadin at 100 µM for 2 hours.
- **Monastrol release:** cells were synchronized in mitosis with 100 µM Monastrol (Sigma, M8515) for 16 hours that inhibits the kinesin Eg5 which is necessary to maintain spindle bipolarity. Then, cells were washed five times with warm medium and released into fresh medium for 2 hours.

5.4. Immunofluorescence (IF) microscopy and sample preparation

- **Standard IF protocol:** this protocol was used for experiments with human fibroblasts and MEFs and experiments with nocodazole or 1,6-Hexanediol treatments. Cells were fixed with 4% paraformaldehyde (PFA, Electron Microscopy Sciences 15710) for 17 min, washed 3 times in Phosphate buffered saline (PBS) and permeabilized with 0.5% NP-40 in PBS for 5 min. Cells were then washed 3 times with PBS-T and blocked in 3% BSA (Millipore, 160069) in PBS-T for 1 hour at RT or overnight at 4 °C. Cells were incubated with primary antibodies for 90 min in blocking buffer, washed 3 times in PBS-T for 10 min and incubated with secondary antibodies for 1 hour. Cells were washed 3 times in PBS-T for 10 min and mounted as previously described.
- **Nup staining IF protocol:** at the end of the experiments cells were washed twice with PBS and fixed for 10 min with 1% PFA in PBS at RT. The coverslips were rinsed two times with PBS and permeabilized with 0.1% Triton X-100 (Sigma, T8787) and 0.02% SDS (Euromedex, EU0660) in PBS for 5 min at RT, washed two times with PBS and blocked in blocking buffer 3% BSA/PBS-T (0.01% Triton X-100) overnight at 4 °C. Coverslips were subsequently incubated with primary antibodies in blocking buffer for 1 hour at RT, washed three times for 5 min with blocking buffer and incubated with secondary antibodies in blocking buffer for 30 min at RT in the dark. After incubation,

coverslips were washed three times for 5 min with blocking buffer, incubated with 0.1% Triton X-100 and 0.02% SDS in PBS for 1 min and post-fixed for 10 min with 1% PFA in PBS at RT. Then coverslips were washed in PBS and mounted on glass slides using Mowiol (Calbiochem) or Prolong Gold reagent (Invitrogen) with 0.75 µg/µl DAPI and imaged with a 100X, 63X or 40X objectives using Zeiss epifluorescence microscope or confocal microscope Leica Spinning Disk Andor/Yokogawa.

- **For digitonin permeabilization experiments,** cells with treated as indicated in the standard IF protocol but permeabilized with 0.003% digitonin (Sigma, D-141) in PBS for 5 min and subsequent steps were performed without detergent.
- **To induce formation of the cytoplasmic Nup aggregates by microtubule depolymerization,** cells were incubated with 10 µM nocodazole (Sigma-Aldrich M-1404) or vehicle (DMSO, 1:330 dilution) in culture media for 90 min at 37 °C. Subsequently, nocodazole was washed five times in warm media, and 1 hour after washout IF protocol for Nups was performed as previously described.
- **For 1,6-Hexanediol experiments,** coverslips were previously coated during 1 hour with fibronectin 2 ug/mL (Sigma, F1141) and collagen 20 ug/mL (Millipore, 08115) in PBS at 37 °C. Subsequently, coverslips were rinsed three times with PBS before seeding cells. At the end of the experiment, cells were incubated in 10% 1,6-Hexanediol (Sigma, 88571) in medium for 70 seconds, washed once with PBS and the standard IF protocol was performed as previously described.
- **For translational inhibition experiments,** HeLa K cells were seeded on glass coverslips, synchronized by double thymidine block and released from the second G1/S arrest. Cells were observed every hour on a table top microscope to follow cell progression through mitosis. 9 hours after release, when cells had reached anaphase (and no mote Cyclin B needed to be translated for mitosis to progress), translational inhibitors cycloheximide (CHX, 100 µg/mL, Sigma-Aldrich C4859) or the vehicle (DMSO, 1:1000 dilution), puromycin (200 µg/mL, Gibco A1113803) or the vehicle (H_20, 1:50 dilution) were added to the media. Cells were further incubated for 5 hours 30 to allow translational inhibitors to act and subsequently big cytoplasmic Nup granules were induced by the addition of nocodazole 10 µM or the vehicle (DMSO, 1:330 dilution) while keeping the translational inhibitors in the media. Cells were

further incubated for 90 min before IF protocol for Nups was performed as previously described.

- **Super-resolution microscopy** was performed using API OMX "Blaze" with GE DeltaVision OMX stand and analyzed with DeltaVision OMX softWoRx. Cells were grown on #1.5 High Precision Coverslips, fixed, permeabilized and stained according to the Nup staining IF protocol (see above). Coverslips were mounted onto the microscope slides with Vectashield (Vector Laboratories, H1000) mounting medium (soft setting) and sealed with a nail polish.

5.5. EdU incorporation assay

HeLa K cells were plated on 11 mm glass coverslips (Menzel-Glaser) in 24-well tissue culture plates. At the end of the experiments cells were incubated with 10 µM EdU (Lumiprobe, 20540) for 30 min at 37 °C, washed once with PBS and fixed for 10 min with 4% PFA in PBS at RT. Subsequently, the coverslips were incubated in 100 mM Tris HCl 100 mM pH 7.5 for 5 min at room temperature (RT) and permeabilized with 0.1% Triton X-100 and 0.02% SDS in PBS for 5 min at RT. The coverslips were rinsed three times with PBS and the click reaction was performed in freshly prepared label mix (Sufo-Cy3-Azide 8 µM (Lumiprobe, B1330), CuSO4 2 mM, ascorbic acid 20 mg/mL (Sigma, A4544) in PBS) for 30 min at RT. Coverslips were subsequently washed three times for 5 min with PBS.
When combining EdU incorporation assay with p-Rb staining, after incubation with EdU the immunostaining was performed as for Nup staining (with the difference that post-fixation was carried out in 4% PFA instead of 1% PFA) and then the click reaction was performed as described previously.

5.6. Poly A RNA Fluorescent In Situ Hybridization (FISH)

HeLa K GFP-Nup107 cells were plated on 11 mm glass coverslips in 24-well tissue culture plates. At the end of the experiments cells were washed once with PBS and fixed for 10 min with 4% PFA in PBS at RT. Subsequently, cells were incubated with 100% cold methanol at -20 °C for 10 min. The coverslips were incubated with 70% ethanol at 4 °C overnight. Coverslips were incubated in 1M Tris-HCl pH 8 for 5 min at RT before proceeding to hybridization for 3 hours at 37 °C in hybridization buffer (2x SSC (Saline Sodium Citrate buffer), 1 mg/mL yeast tRNA, 0.005% BSA, 10% dextran sulfate, 25% formamide, 1 ng/uL oligo(dT_{30}) fluorescent probes fused to Atto-565 or Atto-488 (Sigma)) protected from light.

After hybridization, cells were washed once with 4x SSC, and 2 times with 2x SSC. Coverslips were mounted and imaged as indicated previously.
For RNase treatment experiments, cells were washed 3 times with PBS and permeabilized with or without RNase A/T1 (0.2 mg/mL, 500 u/mL) in 0.003% digitonin PBS for 5 min, before performing the FISH protocol as described previously. All buffers were DEPC treated before use.

5.7. Live video microscopy

For live-cell microscopy, HeLa cells stably expressing indicated proteins tagged with GFP or mCherry, were grown on 35/10 mm glass bottom four compartment dishes (Greiner Bio-One, 627871). Before filming, cells were treated with SiR-DNA or SiR-tubulin (Spirochrome) probes following manufacturer's instructions when indicated. Live-cell microscopy was carried out using 63X objective of Leica CSU-W1 spinning disk or Nikon PFS spinning disk confocal microscopes.

- **For Nup cytoplasmic granule formation assay,** HeLa cells stably expressing GFP-Nup107 were treated with indicated siRNAs, synchronized by double thymidine block, released for 8 hours and analyzed by live video spinning disk confocal microscopy for 7 hours. Z-stacks (10 µm range, 0.5 µm step) were acquired every 5 minutes and movies were made with maximum intensity projection images for every time point shown at speed 7 frames per second.
- **For protein import assay,** HeLa cells were treated with the indicated siRNAs for 72 hours and transfected with the reporter plasmid XRGG-GFP (kindly provided by Jan M. van Deursen) (Hamada *et al*, 2011; Love *et al*, 1998) 30 hours before filming. Cells were synchronized in early G1 phase by 100 µM Monastrol arrest for 16 hours and released for 4 hours. Cells were incubated with full media with SiR-DNA 1:2000 and Verapamil 1:1000 for 2 hours before filming. Then SiR-DNA and verapamil were washed out with media 2 times and cells were incubated in media with 1.25 µM dexamethasone. Dexametahsone-induced nuclear import of XRGG-GFP was recorded by live video spinning disk confocal microscopy for 25 min (1 acquisition every 30 seconds).
- **For protein export assay,** HeLa cells were treated as described for protein import assay and media with 0.25 µM dexamethasone, SiR-DNA 1:2000 and Verapamil 1:1000 was added for 3 hours to induce XRGG-GFP nuclear import. Then

dexamethasone was washed out by washing 2 times with HEPES pH 7.5 and 3 times with full media. After washes media with SiR-DNA 1:2000 and Verapamil 1:1000 was added and the nuclear export of XRGG-GFP was recorded by live video spinning disk confocal microscopy for 2 hours (1 acquisition every 10 min).

- **For Nup granules' dynamics assays,** HeLa cells stably expressing GFP-Nup107 were treated with the indicated siRNAs for 72 hours and synchronized in early G1 phase by 100 μM Monastrol arrest for 16 hours and released for 2 hours. Microtubule depolymerization and Nup granule formation was induced by 10 μM nocodazole addition for 1.5 hours. To observe the behavior of cytoplasmic Nup granules upon microtubule repolymerization five nocodazole washes with warm media were performed during image acquisition and Nups were recorded by live video spinning disk confocal microscopy for 90 min (1 acquisition every minute).

5.8. Microscopy and image analysis

Image quantification analysis was performed using ImageJ, CellProfiler or Metamorph software.

- **For IP followed by Western blot image quantifications** protein of interest signal was normalized to GFP or IgG light chain signal (GFP-IP and endogenous IP respectively). In all cases the same area was used for intensity quantification and background values were substracted.
- **For nuclear protein intensity and nuclear area quantifications**, I generated a pipeline in CellProfiler software that automatically recognizes cell nuclei based on the DAPI fluorescent image. To this end, I enhanced the edges using the Prewit edge-finding method which establishes object edges at those points where the gradient of the image is maximum. This way nuclei were identified and their area and nuclear mean intensity of desired channels among other parameters were measured. In the end, the program exported parameters' measurements to an Excel file.
- **Quantifications of percentage of cells with big cytoplasmic Nup granules and irregular nuclei** were carried out by eye, as well as mitotic stage timing quantifications.
- **For protein import and export experiment quantification**, nuclear and cytoplasmic areas were drawn manually in Fiji using SiR-DNA and GFP channels respectively, and GFP raw intensities were quantified. From these data the % of cytoplasmic or nuclear

signal was calculated and finally delta percentage for each compartment relative to time 0 was calculated.

- **For poly A mRNA FISH experiment quantification,** nuclear and cytoplasmic areas were drawn manually in Fiji using DAPI and oligo(dT) channels respectively, and fluorescent oligo(dT) raw intensities were quantified. From these data the % of nuclear signal was calculated.

5.9. Experimental design, data acquisition, analysis, and statistics

At least three independent biological replicates were performed for each experiment and image quantifications were carried out in a blinded manner. Curves and graphs were made using GraphPad Prism and Adobe illustrator softwares. Models were created using BioRender.com.

All data was verified for normal distribution using Shapiro-Wilk test. Normal data was analyzed using two sample two-tailed T-test or one-sample two-tailed T-test (two-group comparison or folds increase relative to the control, respectively) or One-way ANOVA with Dunnett's or Sidak's correction, in case of multiple group analysis. For non-normally distributed data, Mann-Whitney's or non-parametric one-way ANOVA (Kruskal-wallis test with Dunn's correction) tests were done respectively. Data from the human iPSCs derived from a FXS patient (FXS-iPSCs) and the isogenic rescue cells (C1_2-iPSCs) were analyzed using paired T-test. Error bars represent Standard Deviation (SD) except for live video experiments where bars represent Standard Error of the Mean (SEM). In all cases, significance was *p < 0.05; **P < 0.01; ***P < 0.001, ****P < 0.0001. Details for each graph are listed in figure legends.

5.10. Plasmid and siRNA transfections

Lipofectamine 2000 (Invitrogen) was used to deliver XRGG plasmid (kindly provided by Jan M. van Deursen) (Hamada *et al*, 2011; Love *et al*, 1998) according to the manufacturer's instructions. Oligofectamine (Invitrogen) was used to deliver siRNAs for gene knockdown according to the manufacturer's instructions at a final concentration of 40-100 nM siRNA. When transfecting two different siRNAs simultaneously, the concentration of each one was divided by two to maintain a constant concentration of total siRNA in all conditions. The following siRNA oligonucleotides were used:

siRNA oligonucleotide	Sequence	Manufacturer
siGENOME Non-targeting individual siRNA-2 (Ctrl siRNA)	5'-UAAGGCUAUGAAGAGAUAC-3'	Dharmacon
BICD2 siRNA-1	5'-GGA GCU GUC ACA CUA CAU G-3'	Eurogentec
BICD2 siRNA-2	5'-GGU GGA CUA UGA GGC UAU C-3'	Eurogentec
Dynein HC siRNA-1	5'-CGUACUCCCGUGAUUGAUG-3'	Eurogentec
Dynein HC siRNA-2	5'-GGAUCAAACAUGACGGAAU-3'	Eurogentec
ELYS siRNA	5'-AUU AUC UAC AUA AUU GCU CUU TT-3'	Eurogentec
FMRP	5'-AAAGCUAUGUGACUGAUGA-3'	Dharmacon
FXR1 siRNA-1	5'-AAACGGAAUCUGAGCGUAA-3'	Dharmacon
FXR1 siRNA-2	5'-CCAUACAGCUUACUUGAUA-3'	Dharmacon
FXR2	5'-CGACAAGGCUGGAUAUAGC-3'	Dharmacon
Nup133 siRNA	5'-GUCGAUGACCAGCUGACCA-3'	Eurogentec
RanBP2 siRNA-1	5'-GGACAGUGGGAUUGUAGUGdTdT-3'	Eurogentec
RanBP2 siRNA-2	5'-CACAGACAAAGCCGUUGAAdTdT-3'	Eurogentec

For ER observation experiments, cells were incubated with CellLight ER-RFP BacMam 2.0 (ThermoFischer, C10591) for 24h before following the manufacturer's instructions.

5.11. Quantitative Real-Time PCR

RNA of cultured cells was isolated using TRIzol reagent (Sigma) according to manufacturer's instructions. Reverse transcription was performed with random hexamer or oligodT primers using the SuperScript III First Strand cDNA Synthesis kit (Invitrogen). SYBR Green (Roche Diagnostics) based Real-time PCR was carried out on the LightCycler 480 (Roche Diagnostics) using gene specific primer pairs:

Target gene	Forward / Reverse	Sequence
GAPDH	Forward	5'-ACCCAGAAGACTGTGGATGG-3'
GAPDH	Reverse	5'-TTCTAGACGGCAGGTCAGGT-3'
Nup85	Forward	5'-GACTGAACAAGTTCGCAGCA-3'
Nup85	Reverse	5'-TCAGTCGGTCACTGAGCATC-3'
Nup133	Forward	5'- TGGAGCATGAGGAGCAAGTC-3'
Nup133	Reverse	5'-ACTTGTTGCCGTCCATGGAA-3'
PO	Forward	5'-GTGATGTGCAGCTGATCAAGACT-3'
PO	Reverse	5'-GATGACCAGCCCAAAGGAGA-3'
RanBP2	Forward	5'-CAGGAAGCTCAAAAATCTCAGACA-3'
RanBP2	Reverse	5'- GAGCCCTGTGCTACTTCCAA-3'

5.12. Primers and molecular cloning

Cloning was performed using New England Biolabs (NEB) restriction enzymes, Taq polymerase (NEB) or Fusion High-Fidelity DNA polymerase (Thermo Scientific) according to the manufacturers' instructions. To clone GFP-FXR1, FXR1 was amplified from HeLa total cDNAs with primers 5'- ttattaCTCGAGCCATGGCGGAGCTGACGGTGGAGG-3' (forward) and 5'- tattatGAATTCTTATGAAACACCATTCAGGACTGC-3' (reverse). FXR1 cDNA was cloned into the pEGFPC1 vector using EcoRI/XhoI restriction enzymes. To obtain the plasmid used in rescue experiment expressing GFP-FXR1-MUT-siRNA1, primers 5'-CTTTCCGTTCGCTCTCTGTCTCAGAGGGGTTAGACAGCTCAGAATTTG-3' (forward) and 5'- TGAGACAGAGAGCGAACGGAAAGACGAGCTGAGTGATTGGTCATTGGC-3' (reverse) to mutate pEGFPC1-FXR1 vector in the region targeted by the FXR1 siRNA1. The pEGFPC1-NUP85 was kindly provided by Valérie Doye. For live video microscopy experiements, cDNAs were cloned into a pVITRO-blasticidin vector (Invivogen). mCherry-H2B was amplified with primers 5'-AATAATGCTAGCATGCCAGAGCCAGCGAAGTCTGC-3' (forward) and 5'-TAATAATCTAGATTACTTGTACAGCTCGTCCATGC-3' (reverse). cDNA was cloned into the pVITRO in the multi cloning site 1 using NheI/XbaI restriction enzymes. GFP-NUP85 was amplified with primers 5'-aataatGCTAGCGCCATCATGGTGAGCAAGGGCGAGGAGCTG-3' (forward) and 5'-

tattatGCTAGCTCAGGAACCTTCCAGTGAGCCTTCTC-3' (reverse). cDNA was cloned into the pVITRO in the multi cloning site 2 using the NheI restriction enzyme. DNA purifications were performed using commercial kits from Macherey-Nagel according to the manufacturer's instructions.

5.13. Generation or acquisition of stable cell lines

Hela cells were transfected with pVITRO or pEGFPC1-derived constructs using Lipofectamine 2000 according to manufacturer's instructions. Transfected cells were selected for 2-3 weeks in medium supplemented by antibiotics, either G418 (400 µg/ml) or blasticidin (5 µg/ml). Transgene-expressing clones were then isolated by FACS (FACS ARIA, BD Biosciences). Expression was validated by Western blot and IF analysis. GFP-NUP107 stable cell line was purchased from CLS cell bank. HeLa Kyoto cells stably expressing 3xGFP-mNup133 were kindly provided by Valérie Doye.

5.14. Western blotting

To isolate proteins, cells were scraped from the culture dish, pelleted by centrifugation at 4 ºC and washed twice with PBS. HeLa cell extracts were prepared using lysis buffer (50 mM Tris HCl pH 7.5, 150 mM NaCl, 1% Triton X-100, 1 mM EDTA 0.25% Sodium Deoxycholate, 1mM PMSF, protease inhibitor cocktail Complete). Cells were lysed on ice by mechanical disruption with a needle (26G brown) or by pipetting 10 times up and down. After, samples were centrifuged at 10 000 g for 30 minutes at 4 ºC, transferred the supernatant to a clean tube a protein concentration was measured using Bradford assay (BioRad, 500-0006) in 1 mL cuvettes. Samples were boiled 15 minutes at 96 °C in Laemmli buffer with β-Mercaptoethanol (BioRad, 1610747), resolved on 10% polyacrylamide gels or pre-cast 4-12% Bis-Tris gradient gels (Thermo Scientific, NW04120BOX) or pre-cast NuPAGE™ 3-8% Tris-Acetate gradient Gels (Thermo Scientific, EA0378BOX) and transferred to a PVDF (polyvinylidene difluoride) membrane (Millipore, IPFL00010) using semi-dry transfer unit (Amersham) or wet transfer modules (Mini Blot Module, Invitrogen, B1000).

Membranes were blocked in 5% non-fat milk powder resuspended in TBS-T (Tris-buffered saline-T: 25mM Tris-HCl, pH 7.5, 150mM NaCl 0.05% Tween) for 1 hour at RT or overnight at 4 °C, followed by incubation with antibodies diluted in TBS-T. TBS-T was used for washing the membranes. Membranes were developed with Luminata Forte Western HRP substrate

(Millipore, WBLUF0500) or ECL Western Blotting substrate (Thermo Scientific, 32209) chemiluminescent substrate (Thermo Scientific).

5.15. Immunoprecipitations (IPs)

- **For GFP-IP experiments**, cell extracts from HeLa K stably expressing GFP, GFP-FXR1, 3xGFP-Nup85 from six to seven 10cm dishes per cell line were prepared as indicated in the Western blotting section. For GFP IP, GFP-fused proteins were immunoprecipitated using GFP-Trap A agarose or magnetic beads (Chromotek, gta-20 and gtma-20). Beads were washed 3 times under rotation for 10 minutes with 0.5 mL washing buffer (10 mM Tris HCl pH 7.5, 150 mM NaCl, 0.5 mM EDTA, protease inhibitor cocktail) and then incubated with cell extracts for 90 minutes at 4 °C under constant rotation to allow interaction with GFP constructs. Before elution, beads were washed 3 times under rotation for 10 minutes with 1 mL washing buffer 0.1% Tween-20, boiled at 96 °C in Laemmli SDS sample buffer for 15 minutes and subjected to SDS-PAGE followed by Western blotting.
- **For endogenous IP experiments,** protein G sepharose 4 Fast Flow beads (GE Healthcare Life Sciences) were washed three times for 1 minute in washing buffer (Tris HCl 50 mM pH 7.5, NaCl 150 mM, EDTA 1 mM, protease inhibitor cocktail). FXR1 protein from HEK293T cell extracts from six 10 cm dishes were incubated with the beads and FXR1 antibody or rabbit IgG (1.5 µL per mg of protein) for 3 hours at 4 °C under constant rotation. Before elution, beads were washed 7 times with 1 mL of washing buffer 0.1% Tween-20 (2 quick washes, 3 long washes of 30 minutes under constant rotation, and 2 quick washes), boiled in Laemmli SDS sample buffer and subjected to SDS-PAGE followed by Western blotting.

5.16. Electron microscopy

HeLa cells stably expressing 3xGFP-Nup85 were grown on carbon-coated sapphire disks and synchronized by double thymidine block and 12 hour release. After synchronization, cells were high pressure frozen (HPM010, AbraFluid) and freeze substituted with 0.1% Uranyl acetate in acetone for 15 hours. The temperature was then raised to - 45 °C at 5 °C /hour and cells were further incubated for 5 hours. After rinsing in acetone, the samples were finally embedded in Lowicryl HM20 (Polysciences Inc.). Thick sections (300nm) were cut from the UV-polymerized resin block and picked up on carbon coated mesh grids. After post-staining, 2D

montages and tilt series of the areas of interest were acquired using a FEI TECNAI F30 TEM. Tomograms were reconstructed using the software package IMOD (Kremer *et al*, 1996).

5.17. Antibodies

The following antibodies were used:

Antibody	Host specie	IF Dilution	WB Dilution	Manufacturer	Reference
α-tubulin	Mouse	1:4000	1:20000	Sigma	T5169
α-BICD2	Rabbit	1:250	1:1000	Sigma	HPA023013
Cyclin B1 clone GSN1	Mouse	/	1:2000	Santa Cruz	sc-245
α-Cyclin A	Rabbit	/	1:1000	Santa Cruz	sc-751
α-CRM1	Rabbit	1:250	/	Novus	NB100-79802
α-Cyclin D1 (M-20)	Rabbit	/	1:1000	Santa Cruz	sc-718
α-Dynein IC	Mouse	1:500	/	Merck	MAB1618
α-ELYS	Rabbit	1:250	/	Bethyl	A300-166A
α-Emerin	Rabbit	1:1000	/	Abcam	ab40688
α-FG-Nups (mAb414)	Mouse	1:4000	/	Abcam	ab24609
α-FMRP	Mouse	1:250	1:1000	IGBMC antibody facility (clone 1C3)	
α-FMRP	Rabbit	1:250	1:1000	Abcam	ab17722
α-FXR1+2	Mouse	1:1000	1:1000	IGBMC antibody facility (clone 2B12)	
α-FXR1	Rabbit	1:800	1:1000	Sigma	HPA018246
α-FXR1	Mouse	1:800	1:1000	Millipore	03-176
α-GAPDH	Rabbit	/	1:20000	Sigma	G9545
α-GAPDH	Mouse	/	1:20000	Genetex	gtx627408
GFP	Rabbit	/	1:20000	Abcam	ab290
α-G3BP1	Rabbit	1:500	/	Genetex	GTX112191
α-LaminA	Rabbit	1:500	/	Sigma	L1293
α-Lamin B1	Rabbit	1:500	/	Abcam	ab16048
α-Lap2β	Mouse	1:500	/	BD biosciences	611000
α-LBR	Rabbit	1:500	/	Abcam	ab35535
α-Nup85	Rabbit	1:100	/	Bethyl	A303-977A
α-Nup98	Rabbit	1:100	/	Cell Signalling	2598S
α-Nup133 (E-6)	Mouse	/	1:1000	Santa Cruz	sc-37673
α-Nup133	Rat	1:250	/	Kindly provided by Valérie Doye	

α-Nup153	Rabbit	1:500	1:1000	Abcam	ab84872
α-Pericentrin-1 (NUP85) (D-4)	Mouse	/	1:1000	Santa Cruz	sc-376111
α-PLK1	Mouse	/	1:1000	Santa cruz	sc-17783
α-POM121	Rabbit	1:200	/	Genetex	GTX102128
α-p-Rb	Rabbit	1:1600	/	Cell Signaling	8516
p-62	Guinea pig	1:500	1:1000	Interchim	GP62-C
α-p150^{glued}	Mouse	1:1000	/	BD biosciences	610473
α-RanBP2	Goat	1:2000	/	Kindly provided by Frauke Melchior	
α-RanBP2	Rabbit		1:2000	Abcam	ab64276
α-RanGAP1	Mouse	1:250	/	Cell Signalling	2365
α-SUMO1	Rabbit	1:500	/	Cell signaling	4930
α-TIA-1 (G-3)	Mouse	1:500	/	Santa Cruz	sc-166247

6. List of publications and communications

Publications:

- Agote-Arán, A.*, Schmucker, A.*, Jerabkova, K., Jmel Boyer, I., Berto, A., Pacini, L., Ronchi, P., Kleiss, C., Guerard, L., Schwab, Y., Moine, H., Mandel, J.L., Jacquemont. S., Bagni, C. and Sumara, I., **"Spatial control of nucleoporin condensation by fragile X-related proteins"**. *EMBO J.* 2020; e104467. doi:10.15252/embj.2020104467

- Jerabkova, K.†, Liao, Y.†, Kleiss, C., Fournane, S., Durik, M., Agote-Arán, A., Brino, L., Sedlacek, R.,* and Sumara, I.*, **"Deubiquitylase UCHL3 regulates bi-orientation and segregation of chromosomes during mitosis"**. *FASEB J.* 2020; 10.1096/fj.202000769R. doi:10.1096/fj.202000769R

- Bielska, O., Pangou, E., Schmucker, S., Agote-Arán, A., Ye, T., Liu, Y., Compe, E., Puig-Gamez, M., Zhang, Z., Aebersold, R., Sumara, I., Ricci, R., **"Control of mitosis by MFF-dependent mitochondrial fission"**. *Under revision in Cell Reports.*

Oral communications and posters:

- **Fragile X proteins control postmitotic nucleoporin assembly.** IGBMC, April 2017. (INTERNAL SEMINAR).

- **Ubiquitin receptor protein NICE-4 links ubiquitin signaling to Fragile X Syndrome**. Arantxa Agote Arán, Stephane Schmucker, Katerina Jerabkova, Sushil Awal, Charlotte Kleiss, Alessandro Berto, Hervé Moine, Jean-Louis Mandel, Claudia Bagni, Valérie Doye and Izabela Sumara. EMBO meeting: Ubiquitin and SUMO: From molecular mechanisms to system-wide responses. Cavtat, Croatia, September 2017. (POSTER)

- **Control of nucleoporin localization by Fragile X-related proteins**. Arantxa Agote-Arán*, Stephane Schmucker*, Katerina Jerabkova, Alessandro Berto, Charlotte Kleiss, Laura Pacini, Sushil Awal, Laurent Guerard, Hervé Moine, Jean-Louis Mandel, Sebastien Jacquemont, Claudia Bagni and Izabela Sumara. Protein Homeostasis in Health and Disease CSH meeting. Cold Spring Harbor, NY, April 2018. (POSTER and FLASH TALK)

- **Control of nucleoporin localization by Fragile X-related proteins**. Arantxa Agote-Arán*, Stephane Schmucker*, Katerina Jerabkova, Alessandro Berto, Charlotte Kleiss, Laura Pacini, Sushil Awal, Laurent Guerard, Hervé Moine, Jean-Louis Mandel, Sebastien Jacquemont, Claudia Bagni and Izabela Sumara. Israel-Unistra-Academie Symposium des Sciences. October 2018. (POSTER and FLASH TALK)

- **Fragile X syndrome proteins control localization of nucleoporins**. Arantxa Agote-Arán*, Stephane Schmucker*, Katerina Jerabkova, Alessandro Berto, Charlotte Kleiss, Laura Pacini, Sushil Awal, Laurent Guerard, Hervé Moine, Jean-Louis Mandel, Sebastien Jacquemont, Claudia Bagni and Izabela Sumara. Department Retreat Poster session. March 2019. (POSTER and FLASH TALK)

- **Control of nucleoporin localization by Fragile X-related proteins**. Arantxa Agote-Arán*, Stephane Schmucker*, Katerina Jerabkova, Inès Jmel Boyer, Alessandro Berto, Laura Pacini, Paolo Ronchi, Charlotte Kleiss, Laurent Guerard, Yannick Schwab, Hervé Moine, Jean-Louis Mandel, Sebastien Jacquemont, Claudia Bagni and Izabela Sumara. Department Poster session. IGBMC, France. June 2019. (POSTER)

- **Control of nucleoporin localization by Fragile X-related proteins**. Arantxa Agote-Arán*, Stephane Schmucker*, Katerina Jerabkova, Inès Jmel Boyer, Alessandro Berto, Laura Pacini, Paolo Ronchi, Charlotte Kleiss, Laurent Guerard, Yannick Schwab, Hervé Moine, Jean-Louis Mandel, Sebastien Jacquemont, Claudia Bagni and Izabela Sumara. Genome Organization and Nuclear Function CSH meeting. Virtual meeting. April 2020. (POSTER)

7. References

Adams-Cioaba MA, Guo Y, Bian C, Amaya MF, Lam R, Wasney GA, Vedadi M, Xu C & Min J (2010) Structural Studies of the Tandem Tudor Domains of Fragile X Mental Retardation Related Proteins FXR1 and FXR2. *PLoS ONE* 5: e13559

Ader C, Frey S, Maas W, Schmidt HB, Gorlich D & Baldus M (2010) Amyloid-like interactions within nucleoporin FG hydrogels. *Proc Natl Acad Sci* 107: 6281–6285

Agote-Aran A, Schmucker S, Jerabkova K, Jmel Boyer I, Berto A, Pacini L, Ronchi P, Kleiss C, Guerard L, Schwab Y, *et al* (2020) Spatial control of nucleoporin condensation by fragile X-related proteins. *EMBO J*

Agulhon C, Blanchet P, Kobetz A, Marchant D, Faucon N, Sarda P, Moraine C, Sittler A, Biancalana V, Malafosse A, *et al* (1999) Expression of FMR1 FXR1 and FXR2 genes in human prenatal tissues. [PREPRINT]

Alpatov R, Lesch BJ, Nakamoto-Kinoshita M, Blanco A, Chen S, Stützer A, Armache KJ, Simon MD, Xu C, Ali M, *et al* (2014) A Chromatin-Dependent Role of the Fragile X Mental Retardation Protein FMRP in the DNA Damage Response. *Cell* 157: 869–881

Ambadipudi S, Biernat J, Riedel D, Mandelkow E & Zweckstetter M (2017) Liquid–liquid phase separation of the microtubule-binding repeats of the Alzheimer-related protein Tau. *Nat Commun* 8: 275

Arnaoutov A, Azuma Y, Ribbeck K, Joseph J, Boyarchuk Y, Karpova T, McNally J & Dasso M (2005) Crm1 is a mitotic effector of Ran-GTP in somatic cells. *Nat Cell Biol* 7: 626–632

Ascano M, Mukherjee N, Bandaru P, Miller JB, Nusbaum JD, Corcoran DL, Langlois C, Munschauer M, Dewell S, Hafner M, *et al* (2012) FMRP targets distinct mRNA sequence elements to regulate protein expression. *Nature* 492: 382–386

Ashley CT, Sutcliffe JS, Kunst CB, Leiner HA, Eichler EE, Nelson DL & Warren ST (1993) Human and murine FMR-1: alternative splicing and translational initiation downstream of the CGG–repeat. *Nat Genet* 4: 244–251

Aumiller WM & Keating CD (2016) Phosphorylation-mediated RNA/peptide complex coacervation as a model for intracellular liquid organelles. *Nat Chem* 8: 129–137

Azuma Y & Dasso M (2002) A New Clue at the Nuclear Pore RanBP2 Is an E3 Enzyme for SUMO1. [PREPRINT]

Bagni C & Zukin RS (2019) A Synaptic Perspective of Fragile X Syndrome and Autism Spectrum Disorders. *Neuron* 101: 1070–1088

Bakker CE, de Diego Otero Y, Bontekoe C, Raghoe P, Luteijn T, Hoogeveen AT, Oostra BA & Willemsen R (2000) Immunocytochemical and Biochemical Characterization of FMRP, FXR1P, and FXR2P in the Mouse. *Exp Cell Res* 258: 162–170

Bakker CE & Reyniers E (1994) Fmr1 knockout mice: a model to study fragile X mental retardation. *Cell* 78: 23–33

Banani SF, Rice AM, Peeples WB, Lin Y, Jain S, Parker R & Rosen MK (2016) Compositional Control of Phase-Separated Cellular Bodies. *Cell* 166: 651–663

Bear MF, Huber KM & Warren ST (2004) The mGluR theory of fragile X mental retardation. *Trends Neurosci* 27: 370–377

Beaudouin J, Gerlich D, Daigle N, Eils R & Ellenberg J (2002) Nuclear Envelope Breakdown Proceeds by Microtubule-Induced Tearing of the Lamina. *Cell* 108: 83–96

Beck M & Hurt E (2017) The nuclear pore complex: understanding its function through structural insight. *Nat Rev Mol Cell Biol* 18: 73–89

Biancalana M & Koide S (2010) Molecular mechanism of Thioflavin-T binding to amyloid fibrils. *Biochim Biophys Acta BBA - Proteins Proteomics* 1804: 1405–1412

Bianco A, Dienstbier M, Salter HK, Gatto G & Bullock SL (2010) Bicaudal-D regulates fragile X mental retardation protein levels, motility, and function during neuronal morphogenesis. *Curr Biol CB* 20: 1487–1492

Bischoff R, Krebber H, Smirnova E, Dong W & Ponstingl H (1995) Co-activation of RanGTPase and inhibition of GTP dissociation by Ran-GTP binding protein RanBP1. *EMBO J* 14: 705–715

Blackwell E, Zhang X & Ceman S (2010) Arginines of the RGG box regulate FMRP association with polyribosomes and mRNA. *Hum Mol Genet* 19: 1314–1323

Bodea L-G, Eckert A, Ittner LM, Piguet O & Götz J (2016) Tau physiology and pathomechanisms in frontotemporal lobar degeneration. *J Neurochem* 138: 71–94

Boehmer T, Enninga J, Dales S & Zhong H (2002) Depletion of a single nucleoporin, Nup107, prevents the assembly of a subset of nucleoporins into the nuclear pore complex. *PNAS* 100: 981–985

Boeynaems S, Alberti S, Fawzi NL, Mittag T, Polymenidou M, Rousseau F, Schymkowitz J, Shorter J, Wolozin B, Van Den Bosch L, *et al* (2018) Protein Phase Separation: A New Phase in Cell Biology. *Trends Cell Biol* 28: 420–435

Boeynaems S, Bogaert E, Kovacs D, Konijnenberg A, Timmerman E, Volkov A, Guharoy M, De Decker M, Jaspers T, Ryan VH, *et al* (2017) Phase Separation of C9orf72 Dipeptide Repeats Perturbs Stress Granule Dynamics. *Mol Cell* 65: 1044-1055.e5

Bolduc FV, Bell K, Cox H, Broadie KS & Tully T (2008) Excess protein synthesis in Drosophila Fragile X mutants impairs long-term memory. *Nat Neurosci* 11: 1143–1145

Bolhy S, Bouhlel I, Dultz E, Nayak T, Zuccolo M, Gatti X, Vallee R, Ellenberg J & Doye V (2011) A Nup133-dependent NPC-anchored network tethers centrosomes to the nuclear envelope in prophase. *J Cell Biol* 192: 855–871

Bontekoe CJM (2002) Knockout mouse model for Fxr2: a model for mental retardation. *Hum Mol Genet* 11: 487–498

Bouzid T, Kim E, Riehl BD, Esfahani AM, Rosenbohm J, Yang R, Duan B & Lim JY (2019) The LINC complex, mechanotransduction, and mesenchymal stem cell function and fate. *J Biol Eng* 13: 68

Brangwynne CP, Eckmann CR, Courson DS, Rybarska A, Hoege C, Gharakhani J, Julicher F & Hyman AA (2009) Germline P Granules Are Liquid Droplets That Localize by Controlled Dissolution/Condensation. *Science* 324: 1729–1732

Brohawn S, Leksa NC, Schwartz TU & Rajashankar KR (2008) Structural Evidence for Common ancestry of the NPc and vesicle coats. *Science* 322: 1369–1373

Brown V, Jin P, Ceman S, Darnell JC, O'Donnell WT, Tenenbaum SA, Jin X, Feng Y, Wilkinson KD, Keene JD, *et al* (2001) Microarray Identification of FMRP-Associated Brain mRNAs and Altered mRNA Translational Profiles in Fragile X Syndrome. *Cell* 107: 477–487

Bui KH, von Appen A, DiGuilio AL, Ori A, Sparks L, Mackmull M-T, Bock T, Hagen W, Andrés-Pons A, Glavy JS, *et al* (2013) Integrated Structural Analysis of the Human Nuclear Pore Complex Scaffold. *Cell* 155: 1233–1243

Burke B & Stewart CL (2013) The nuclear lamins: flexibility in function. *Nat Rev Mol Cell Biol* 14: 13–24

Cai Y, Singh BB, Aslanukov A, Zhao H & Ferreira PA (2001) The Docking of Kinesins, KIF5B and KIF5C, to Ran-binding Protein 2 (RanBP2) Is Mediated via a Novel RanBP2 Domain. *J Biol Chem* 276: 41594–41602

Callan HG, Randall JT & Tomlin SG (1949) An electron microscopy study of the nuclear membrane. *Nature* 163: 1949

Cao H, Gao R, Yu C, Chen L & Feng Y (2019) The RNA-binding protein FXR1 modulates prostate cancer progression by regulating FBXO4. *Funct Integr Genomics* 19: 487–496

Capell BC & Collins FS (2006) Human laminopathies: nuclei gone genetically awry. *Nat Rev Genet* 7: 940–952

Chakraborty P, Wang Y, Wei J-H, van Deursen J, Yu H, Malureanu L, Dasso M, Forbes DJ, Levy DE, Seemann J, *et al* (2008) Nucleoporin levels regulate cell cycle progression and phase-specific gene expression. *Dev Cell* 15: 657–667

Chen E & Joseph S (2015) Fragile X mental retardation protein: A paradigm for translational control by RNA-binding proteins. *Biochimie* 114: 147–154

Chen E, Sharma MR, Shi X, Agrawal RK & Joseph S (2014) Fragile X Mental Retardation Protein Regulates Translation by Binding Directly to the Ribosome. *Mol Cell* 54: 407–417

Cherkasov V, Hofmann S, Druffel-Augustin S, Mogk A, Tyedmers J, Stoecklin G & Bukau B (2013) Coordination of Translational Control and Protein Homeostasis during Severe Heat Stress. *Curr Biol* 23: 2452–2462

Cho K, Yoon D, Qiu S, Danziger Z, Grill WM, Wetsel WC & Ferreira PA (2017) Loss of Ranbp2 in motoneurons causes disruption of nucleocytoplasmic and chemokine signaling, proteostasis of hnRNPH3 and Mmp28, and development of amyotrophic lateral sclerosis-like syndromes. *Dis Model Mech* 10: 559–579

Chou C-C, Zhang Y, Umoh ME, Vaughan SW, Lorenzini I, Liu F, Sayegh M, Donlin-Asp PG, Chen YH, Duong DM, *et al* (2018) TDP-43 pathology disrupts nuclear pore complexes and nucleocytoplasmic transport in ALS/FTD. *Nat Neurosci* 21: 228–239

Chow K-H, Elgort S, Dasso M, Powers MA & Ullman KS (2014) The SUMO proteases SENP1 and SENP2 play a critical role in nucleoporin homeostasis and nuclear pore complex function. *Mol Biol Cell* 25: 160–168

Chow K-H, Elgort S, Dasso M & Ullman KS (2012) Two distinct sites in Nup153 mediate interaction with the SUMO proteases SENP1 and SENP2. *Nucleus* 3: 349–358

Chug H, Trakhanov S, Hülsmann BB, Pleiner T & Görlich D Crystal structure of the metazoan Nup62•Nup58•Nup54 nucleoporin complex. *Science* 350: 106–10

Coffee B, Ikeda M, Budimirovic DB, Hjelm LN, Kaufmann WE & Warren ST (2008) MosaicFMR1 deletion causes fragile X syndrome and can lead to molecular misdiagnosis: A case report and review of the literature. *Am J Med Genet A* 146A: 1358–1367

Comery TA, Harris JB, Willems PJ, Oostra BA, Irwin SA, Weiler IJ & Greenough WT (1997) Abnormal dendritic spines in fragile X knockout mice: Maturation and pruning deficits. *Proc Natl Acad Sci* 94: 5401–5404

Comtesse N, Keller A, Diesinger I, Bauer C, Kayser K, Huwer H, Lenhof H-P & Meese E (2007) Frequent overexpression of the genes *FXR1* , *CLAPM1* and *EIF4G* located on amplicon 3q26-27 in squamous cell carcinoma of the lung. *Int J Cancer* 120: 2538–2544

Cornelison GL, Levy SA, Jenson T & Frost B (2019) Tau-induced nuclear envelope invagination causes a toxic accumulation of mRNA in *Drosophila*. *Aging Cell* 18: e12847

Courchaine EM, Lu A & Neugebauer KM (2016) Droplet organelles? *EMBO J* 35: 1603–1612

Coyle JH, Bor Y-C, Rekosh D & Hammarskjold M-L (2011) The Tpr protein regulates export of mRNAs with retained introns that traffic through the Nxf1 pathway. *RNA* 17: 1344–1356

D'Angelo MA, Anderson DJ, Richard E & Hetzer MW (2006a) Nuclear Pores Form de Novo from Both Sides of the Nuclear Envelope. *Science* 312: 440–443

D'Angelo MA, Anderson DJ, Richard E & Hetzer MW (2006b) Nuclear pores form de novo from both sides of the nuclear envelope. *Science* 312: 440–443

D'Angelo MA, Raices M, Panowski SH & Hetzer MW (2009) Age-Dependent Deterioration of Nuclear Pore Complexes Causes a Loss of Nuclear Integrity in Postmitotic Cells. *Cell* 136: 284–295

Darnell JC (2005) Kissing complex RNAs mediate interaction between the Fragile-X mental retardation protein KH2 domain and brain polyribosomes. *Genes Dev* 19: 903–918

Darnell JC, Fraser CE, Mostovetsky O & Darnell RB (2009) Discrimination of common and unique RNA-binding activities among Fragile X mental retardation protein paralogs. *Hum Mol Genet* 18: 3164–3177

Darnell JC, Jensen KB, Jin P, Brown V, Warren ST & Darnell RB (2001) Fragile X Mental Retardation Protein Targets G Quartet mRNAs Important for Neuronal Function. *Cell* 107: 489–499

Darnell JC, Van Driesche SJ, Zhang C, Hung KYS, Mele A, Fraser CE, Stone EF, Chen C, Fak JJ, Chi SW, *et al* (2011) FMRP Stalls Ribosomal Translocation on mRNAs Linked to Synaptic Function and Autism. *Cell* 146: 247–261

Davidovic L, Durand N, Khalfallah O, Tabet R, Barbry P, Mari B, Sacconi S, Moine H & Bardoni B (2013) A novel role for the RNA-binding protein FXR1P in myoblasts cell-cycle progression by modulating p21/Cdkn1a/Cip1/Waf1 mRNA stability. *PLoS Genet* 9: e1003367

Davis LI & Blobel G (1987) Nuclear pore complex contains a family of glycoproteins that includes p62: glycosylation through a previously unidentified cellular pathway. *Proc Natl Acad Sci U S A* 84: 7552–7556

Dawlaty M, Malureanu L, Jeganathan KB, kao E, Sustmann C, Tahk S, Shuai K, Grosschedl R & van Deursen JM (2008) Resolution of Sister Centromeres Requires RanBP2-Mediated SUMOylation of Topoisomerase IIα. *Cell* 133: 103–115

De Boulle K, Verkerk AJMH, Reyniers E, Vits L, Hendrickx J, Van Roy B, Van Den Bos F, de Graaff E, Oostra BA & Willems PJ (1993) A point mutation in the FMR-1 gene associated with fragile X mental retardation. *Nat Genet* 3: 31–35

De Diego Otero Y, Severijnen L-A, van Cappellen G, Schrier M, Oostra B & Willemsen R (2002) Transport of Fragile X Mental Retardation Protein via Granules in Neurites of PC12 Cells. *Mol Cell Biol* 22: 8332–8341

De Vries BBA, Halley DJJ, Oostra BA & Niermeijer MF (1997) The fragil X syndrome. [PREPRINT]

DeJesus-Hernandez M, Mackenzie IR, Boeve BF, Boxer AL, Baker M, Rutherford NJ, Nicholson AM, Finch NA, Flynn H, Adamson J, *et al* (2011) Expanded GGGGCC Hexanucleotide Repeat in Noncoding Region of C9ORF72 Causes Chromosome 9p-Linked FTD and ALS. *Neuron* 72: 245–256

Denier C, Balu L, Husson B, Nasser G, Burglen L, Rodriguez D, Labauge P & Chevret L (2014) Familial acute necrotizing encephalopathy due to mutation in the RANBP2 gene. *J Neurol Sci* 345: 236–238

Denning DP, Patel SS, Uversky V, Fink AL & Rexach M (2003) Disorder in the nuclear pore complex: The FG repeat regions of nucleoporins are natively unfolded. *Proc Natl Acad Sci* 100: 2450–2455

Devos D, Dokudovskaya S, Alber F, Williams R, Chait BT, Sali A & Rout MP (2004) Components of Coated Vesicles and Nuclear Pore Complexes Share a Common Molecular Architecture. *PLoS Biol* 2: e380

Devys D, Lutz Y, Rouyer N & Mandel JL (1993) The FMR1 protein is cytoplasmic most abundant in neurons and appears normal in carriers of a fragile X premutation. *Nat Genet* 4: 335340

Dictenberg JB, Swanger SA, Antar LN, Singer RH & Bassell GJ (2008) A Direct Role for FMRP in Activity-Dependent Dendritic mRNA Transport Links Filopodial-Spine Morphogenesis to Fragile X Syndrome. *Dev Cell* 14: 926–939

Didiot M-C, Subramanian M, Flatter E, Mandel J-L & Moine H (2009) Cells Lacking the Fragile X Mental Retardation Protein (FMRP) have Normal RISC Activity but Exhibit Altered Stress Granule Assembly. *Mol Biol Cell* 20: 428–437

Dockendorff TC, Su HS, McBride SMJ, Yang Z, Choi CH, Siwicki KK, Sehgal A & Jongens TA (2002) Drosophila Lacking dfmr1 Activity Show Defects in Circadian Output and Fail to Maintain Courtship Interest. *Neuron* 34: 973–984

Dormann D, Rodde R, Edbauer D, Bentmann E, Fischer I, Hruscha A, Than ME, Mackenzie IRA, Capell A, Schmid B, *et al* (2010) ALS-associated fused in sarcoma (FUS) mutations disrupt Transportin-mediated nuclear import. *EMBO J* 29: 2841–2857

Doucet CM, Talamas JA & Hetzer MW (2010) Cell Cycle-Dependent Differences in Nuclear Pore Complex Assembly in Metazoa. *Cell* 141: 1030–1041

Drin G, Casella J-F, Gautier R, Boehmer T, Schwartz TU & Antonny B (2007) A general amphipathic α-helical motif for sensing membrane curvature. *Nat Struct Mol Biol* 14: 138–146

Drozd M, Bardoni B & Capovilla M (2018) Modeling Fragile X Syndrome in Drosophila. *Front Mol Neurosci* 11: 124

Dultz E & Ellenberg J (2010) Live imaging of single nuclear pores reveals unique assembly kinetics and mechanism in interphase. *J Cell Biol* 191: 15–22

Dultz E, Huet S & Ellenberg J (2009) Formation of the Nuclear Envelope Permeability Barrier Studied by Sequential Photoswitching and Flux Analysis. *Biophys J* 97: 1891–1897

Dultz E, Zanin E, Wurzenberger C, Braun M, Rabut G, Sironi L & Ellenberg J (2008) Systematic kinetic analysis of mitotic dis- and reassembly of the nuclear pore in living cells. *J Cell Biol* 180: 857–865

Eftekharzadeh B, Daigle JG, Kapinos LE, Coyne A, Schiantarelli J, Carlomagno Y, Cook C, Miller SJ, Dujardin S, Amaral AS, *et al* (2018) Tau Protein Disrupts Nucleocytoplasmic Transport in Alzheimer's Disease. *Neuron* 99: 925-940.e7

Erickson CA, Davenport MH, Schaefer TL, Wink LK, Pedapati EV, Sweeney JA, Fitzpatrick SE, Brown WT, Budimirovic D, Hagerman RJ, *et al* (2017) Fragile X targeted pharmacotherapy: lessons learned and future directions. *J Neurodev Disord* 9: 7

Fan Y, Yue J, Xiao M, Han-Zhang H, Wang YV, Ma C, Deng Z, Li Y, Yu Y, Wang X, *et al* (2017) FXR1 regulates transcription and is required for growth of human cancer cells with TP53/FXR2 homozygous deletion. *eLife* 6: e26129

Feng Y, Gutekunst C-A, Eberhart DE, Yi H, Warren ST & Hersch SM (1997) Fragile X Mental Retardation Protein: Nucleocytoplasmic Shuttling and Association with Somatodendritic Ribosomes. *J Neurosci* 17: 1539–1547

Feng Z, Chen X, Wu X & Zhang M (2019) Formation of biological condensates via phase separation: Characteristics, analytical methods, and physiological implications. *J Biol Chem*

Finlay DR, Meier E, Bradley P, Horecka J & Forbes DJ (1991) A Complex of Nuclear Pore Proteins Required for Fore Function. *J Cell Biol* 114: 15

Floer M & Blobel G (1999) Putative Reaction Intermediates in Crm1-mediated Nuclear Protein Export. *J Biol Chem* 274: 16279–16286

Flotho A & Werner A (2012) The RanBP2/RanGAP1*SUMO1/Ubc9 complex: A multisubunit E3 ligase at the intersection of sumoylation and the RanGTPase cycle. *Nucleus* 3: 429–432

Folz H, Niño CA, Taranum S, Caesar S, Latta L, Waharte F, Salamero J, Schlenstedt G & Dargemont C (2019) SUMOylation of the nuclear pore complex basket is involved in sensing cellular stresses. *J Cell Sci* 132: jcs224279

Fox AH & Lamond AI (2010) Paraspeckles. *Cold Spring Harb Perspect Biol* 2: a000687–a000687

Franz C, Walczak R, Yavuz S, Santarella R, Gentzel M, Askjaer P, Galy V, Hetzer M, Mattaj IW & Antonin W (2007) MEL-28/ELYS is required for the recruitment of nucleoporins to chromatin and postmitotic nuclear pore complex assembly. *EMBO Rep* 8: 165–172

Freibaum BD, Lu Y, Lopez-Gonzalez R, Kim NC, Almeida S, Lee K-H, Badders N, Valentine M, Miller BL, Wong PC, *et al* (2015) GGGGCC repeat expansion in C9orf72 compromises nucleocytoplasmic transport. *Nature* 525: 129–133

Frey S & Görlich D (2007) A Saturated FG-Repeat Hydrogel Can Reproduce the Permeability Properties of Nuclear Pore Complexes. *Cell* 130: 512–523

Frey S, Richter RP & Gorlich D (2006) FG-Rich Repeats of Nuclear Pore Proteins Form a Three-Dimensional Meshwork with Hydrogel-Like Properties. *Science* 314: 815–817

Frosst P, Guan T, Subauste C, Hahn K & Gerace L (2002) Tpr is localized within the nuclear basket of the pore complex and has a role in nuclear protein export. *J Cell Biol* 156: 617–630

Frost B, Bardai FH & Feany MB (2016) Lamin Dysfunction Mediates Neurodegeneration in Tauopathies. *Curr Biol* 26: 129–136

Garnon J, Lachance C, Di Marco S, Hel Z, Marion D, Ruiz MC, Newkirk MM, Khandjian EW & Radzioch D (2005) Fragile X-related Protein FXR1P Regulates Proinflammatory Cytokine Tumor Necrosis Factor Expression at the Post-transcriptional Level. *J Biol Chem* 280: 5750–5763

Gasset-Rosa F, Chillon-Marinas C, Goginashvili A, Atwal RS, Artates JW, Tabet R, Wheeler VC, Bang AG, Cleveland DW & Lagier-Tourenne C (2017) Polyglutamine-Expanded Huntingtin Exacerbates Age-Related Disruption of Nuclear Integrity and Nucleocytoplasmic Transport. *Neuron* 94: 48-57.e4

Gautam M, Jara JH, Kocak N, Rylaarsdam LE, Kim KD, Bigio EH & Hande Özdinler P (2019) Mitochondria, ER, and nuclear membrane defects reveal early mechanisms for upper motor neuron vulnerability with respect to TDP-43 pathology. *Acta Neuropathol (Berl)* 137: 47–69

Grima JC, Daigle JG, Arbez N, Cunningham KC, Zhang K, Ochaba J, Geater C, Morozko E, Stocksdale J, Glatzer JC, *et al* (2017) Mutant Huntingtin Disrupts the Nuclear Pore Complex. *Neuron* 94: 93-107.e6

Grossman E, Medalia O & Zwerger M (2012) Functional Architecture of the Nuclear Pore Complex. *Annu Rev Biophys* 41: 557–584

Guo L, Fare CM & Shorter J (2019) Therapeutic Dissolution of Aberrant Phases by Nuclear-Import Receptors. *Trends Cell Biol* 29: 308–322

Guo W, Polich ED, Su J, Gao Y, Christopher DM, Allan AM, Wang M, Wang F, Wang G & Zhao X (2015) Fragile X Proteins FMRP and FXR2P Control Synaptic GluA1 Expression and Neuronal Maturation via Distinct Mechanisms. *Cell Rep* 11: 1651–1666

Güttinger S, Laurell E & Kutay U (2009) Orchestrating nuclear envelope disassembly and reassembly during mitosis. *Nat Rev Mol Cell Biol* 10: 178–191

Hagerman RJ, Berry-Kravis E, Kaufmann WE, Ono MY, Tartaglia N, Lachiewicz A, Kronk R, Delahunty C, Hessl D, Visootsak J, *et al* (2009) Advances in the Treatment of Fragile X Syndrome. *PEDIATRICS* 123: 378–390

Hagerman RJ & Hagerman PJ (2002) The fragile X premutation: into the phenotypic fold. *Curr Opin Genet Dev* 12: 278–283

Halfmann R, Wright JR, Alberti S, Lindquist S & Rexach M (2012) Prion formation by a yeast GLFG nucleoporin. *Prion* 6: 391–399

Hamada M, Haeger A, Jeganathan KB, van Ree JH, Malureanu L, Wälde S, Joseph J, Kehlenbach RH & van Deursen JM (2011) Ran-dependent docking of importin-beta to RanBP2/Nup358 filaments is essential for protein import and cell viability. *J Cell Biol* 194: 597–612

Hampoelz B, Andres-Pons A, Kastritis P & Beck M (2019a) Structure and Assembly of the Nuclear Pore Complex. *Annu Rev Biophys* 48: 515–536

Hampoelz B, Mackmull M-T, Machado P, Ronchi P, Bui KH, Schieber N, Santarella-Mellwig R, Necakov A, Andrés-Pons A, Philippe JM, *et al* (2016) Pre-assembled Nuclear Pores Insert into the Nuclear Envelope during Early Development. *Cell* 166: 664–678

Hampoelz B, Schwarz A, Ronchi P, Bragulat-Teixidor H, Tischer C, Gaspar I, Ephrussi A, Schwab Y & Beck M (2019b) Nuclear Pores Assemble from Nucleoporin Condensates During Oogenesis. *Cell* 179: 671-686.e17

Haraguchi T, Kojidani T, Koujin T, Shimi T, Osakada H, Mori C, Yamamoto A & Hiraoka Y (2008) Live cell imaging and electron microscopy reveal dynamic processes of BAF-directed nuclear envelope assembly. *J Cell Sci* 121: 2540–2554

Harel A, Chan RC, Lachish-Zalait A, Zimmerman E, Elbaum M & Forbes DJ (2003) Importin $^{N}_{L}$ Negatively Regulates Nuclear Membrane Fusion and Nuclear Pore Complex Assembly. *Mol Biol Cell* 14: 10

Harrison AF & Shorter J (2017) RNA-binding proteins with prion-like domains in health and disease. *Biochem J* 474: 1417–1438

He Q & Ge W (2017) The tandem Agenet domain of fragile X mental retardation protein interacts with FUS. *Sci Rep* 7: 962

He X, Riceberg J, Soucy T, Koenig E, Minissale J, Gallery M, Bernard H, Yang X, Liao H, Rabino C, *et al* (2017) Probing the roles of SUMOylation in cancer cell biology by using a selective SAE inhibitor. *Nat Chem Biol* 13: 1164–1171

Hetzer MW & Wente SR (2009) Border control at the nucleus: biogenesis and organization of the nuclear membrane and pore complexes. *Dev Cell* 17: 606–616

Hofweber M & Dormann D (2019) Friend or foe—Post-translational modifications as regulators of phase separation and RNP granule dynamics. *J Biol Chem* 294: 7137–7150

Holmer L & Worman HJ (2001) Inner nuclear membrane proteins: functions and targeting: *Cell Mol Life Sci* 58: 1741–1747

Hoogeveen AT, Willemsen R & Oostra BA (2002) Fragile X syndrome, the Fragile X related proteins, and animal models. *Microsc Res Tech* 57: 148–155

Hutten S & Dormann D (2020) Nucleocytoplasmic transport defects in neurodegeneration Cause or consequence? *Semin Cell Dev Biol* 99: 151–162

Hutten S, Flotho A, Melchior F & Kehlenbach RH (2008) The Nup358-RanGAP Complex Is Required for Efficient Importin α β-dependent Nuclear Import. *Mol Biol Cell* 19: 2300–2310

Hutten S & Kehlenbach RH (2006) Nup214 Is Required for CRM1-Dependent Nuclear Protein Export In Vivo. *Mol Cell Biol* 26: 6772–6785

Hutten S, Walde S, Spillner C, Hauber J & Kehlenbach RH (2009) The nuclear pore component Nup358 promotes transportin-dependent nuclear import. *J Cell Sci* 122: 1100–1110

Jimenez-Sanchez M, Licitra F, Underwood BR & Rubinsztein DC (2017) Huntington's Disease: Mechanisms of Pathogenesis and Therapeutic Strategies. *Cold Spring Harb Perspect Med* 7: a024240

Jin X, Zhai B, Fang T, Guo X & Xu L (2016) FXR1 is elevated in colorectal cancer and acts as an oncogene. *Tumor Biol* 37: 2683–2690

Jongjitwimol J, Baldock RA, Morley SJ & Watts FZ (2016) Sumoylation of eIF4A2 affects stress granule formation. *J Cell Sci* 129: 2407–2415

Joseph J & Dasso M (2008) The nucleoporin Nup358 associates with and regulates interphase microtubules. *FEBS Lett* 582: 190–196

Joseph J, Liu S-T, Jablonski SA, Yen TJ & Dasso M (2004) The RanGAP1-RanBP2 Complex Is Essential for Microtubule-Kinetochore Interactions In Vivo. *Curr Biol* 14: 611–617

Joseph J, Tan S-H, Karpova TS, McNally JG & Dasso M (2002) SUMO-1 targets RanGAP1 to kinetochores and mitotic spindles. *J Cell Biol* 156: 595–602

Jul-Larsen A, Grudic A, Bjerkvig R & Ove Boe S (2009) Cell-cycle regulation and dynamics of cytoplasmic compartments containing the promyelocytic leukemia protein and nucleoporins. *J Cell Sci* 122: 1201–1210

Kato M, Han TW, Xie S, Shi K, Du X, Wu LC, Mirzaei H, Goldsmith EJ, Longgood J, Pei J, *et al* (2012) Cell-free Formation of RNA Granules: Low Complexity Sequence Domains Form Dynamic Fibers within Hydrogels. *Cell* 149: 753–767

Kaufmann WE & Moser HW Dendritic Anomalies in Disorders Associated with Mental Retardation. *Dev Neuropsychol* 16: 369–371

Kazdoba TM, Leach PT, Silverman JL & Crawley JN (2014) Modeling fragile X syndrome in the Fmr1 knockout mouse. *Intractable Rare Res* 3: 118–133

Kedersha N, Cho MR, Li W, Yacono PW, Chen S, Gilks N, Golan DE & Anderson P (2000) Dynamic Shuttling of Tia-1 Accompanies the Recruitment of mRNA to Mammalian Stress Granules. *J Cell Biol* 151: 1257–1268

Kedersha N, Ivanov P & Anderson P (2013) Stress granules and cell signaling: more than just a passing phase? *Trends Biochem Sci* 38: 494–506

Kessel RG (1992) Annulate Lamellae: A Last Frontier in Cellular Organelles. In *International Review of Cytology* pp 43–120. Elsevier

Khandjian E (1998) Novel isoforms of the fragile X related protein FXR1P are expressed during myogenesis. *Hum Mol Genet* 7: 2121–2128

Khayachi A, Gwizdek C, Poupon G, Alcor D, Chafai M, Cassé F, Maurin T, Prieto M, Folci A, De Graeve F, *et al* (2018) Sumoylation regulates FMRP-mediated dendritic spine elimination and maturation. *Nat Commun* 9: 757

Khlghatyan J, Evstratova A, Chamberland S, Marakhovskaia A, Bahremand A, Toth K & Beaulieu J-M (2018) Mental Illnesses-Associated Fxr1 and Its Negative Regulator Gsk3β Are Modulators of Anxiety and Glutamatergic Neurotransmission. *Front Mol Neurosci* 11: 119

Kinoshita Y, Ito H, Hirano A, Fujita K, Wate R, Nakamura M, Kaneko S, Nakano S & Kusaka H (2009) Nuclear Contour Irregularity and Abnormal Transporter Protein Distribution in Anterior Horn Cells in Amyotrophic Lateral Sclerosis: *J Neuropathol Exp Neurol* 68: 1184–1192

Kirkpatrick LL, McIlwain KA & Nelson DL (1999) Alternative Splicing in the Murine and Human FXR1 Genes. *Genomics* 59: 193–202

Knockenhauer KE & Schwartz TU (2016) The Nuclear Pore Complex as a Flexible and Dynamic Gate. *Cell* 164: 1162–1171

Kooy RF, D'Hooge R, Reyniers E, Bakker CE, Nagels G, Boulle KD, Storm K, Clincke G, Deyn PPD, Oostra BA, *et al* (1996) Transgenic mouse model for the fragile X syndrome. *Am J Med Genet* 2: 5

Kosinski J, Mosalaganti S, von Appen A, Teimer R, DiGuilio AL, Wan W, Bui KH, Hagen WJH, Briggs JAG, Glavy JS, *et al* (2016) Molecular architecture of the inner ring scaffold of the human nuclear pore complex. *Science* 352: 363–365

Kremer JR, Mastronarde DN & McIntosh JR (1996) Computer visualization of three-dimensional image data using IMOD. *J Struct Biol* 116: 71–76

Kroschwald S, Maharana S, Mateju D, Malinovska L, Nüske E, Poser I, Richter D & Alberti S (2015) Promiscuous interactions and protein disaggregases determine the material state of stress-inducible RNP granules. *eLife* 4: e06807

Kumar A, Sharma P, Gomar-Alba M, Shcheprova Z, Daulny A, Sanmartín T, Matucci I, Funaya C, Beato M & Mendoza M (2018) Daughter-cell-specific modulation of nuclear pore complexes controls cell cycle entry during asymmetric division. *Nat Cell Biol* 20: 432–442

Labokha AA, Gradmann S, Frey S, Hülsmann BB, Urlaub H, Baldus M & Görlich D (2012) Systematic analysis of barrier-forming FG hydrogels from Xenopus nuclear pore complexes. *EMBO J* 32: 204–218

Le Tonqueze O, Kollu S, Lee S, Al-Salah M, Truesdell SS & Vasudevan S (2016) Regulation of monocyte induced cell migration by the RNA binding protein, FXR1. *Cell Cycle* 15: 1874–1882

Lee YL & Burke B (2018) LINC complexes and nuclear positioning. *Semin Cell Dev Biol* 82: 67–76

Lemke EA (2016) The Multiple Faces of Disordered Nucleoporins. *J Mol Biol* 428: 2011–2024

Li C, Goryaynov A & Yang W (2016) The selective permeability barrier in the nuclear pore complex. *Nucleus* 7: 430–446

Li C, Peng Q, Wan X, Sun H & Tang J (2017) C-terminal motifs in promyelocytic leukemia protein isoforms critically regulate PML nuclear body formation. *J Cell Sci* 130: 3496–3506

Li N & Lagier-Tourenne C (2018) Nuclear pores: the gate to neurodegeneration. *Nat Neurosci* 21: 156–158

Li Y & Zhao X (2014) Concise review: Fragile X proteins in stem cell maintenance and differentiation. *Stem Cells Dayt Ohio* 32: 1724–1733

Lin Y, Protter DSW, Rosen MK & Parker R (2015) Formation and Maturation of Phase-Separated Liquid Droplets by RNA-Binding Proteins. *Mol Cell* 60: 208–219

Ling S-C, Fahrner PS, Greenough WT & Gelfand VI (2004) Transport of Drosophila fragile X mental retardation protein-containing ribonucleoprotein granules by kinesin-1 and cytoplasmic dynein. *Proc Natl Acad Sci U S A* 101: 17428–17433

Liu K-Y, Shyu Y-C, Barbaro BA, Lin Y-T, Chern Y, Thompson LM, James Shen C-K & Marsh JL (2015) Disruption of the nuclear membrane by perinuclear inclusions of mutant huntingtin causes cell-cycle re-entry and striatal cell death in mouse and cell models of Huntington's disease. *Hum Mol Genet* 24: 1602–1616

Liu S, Kwon M, Mannino M, Yang N, Renda F, Khodjakov A & Pellman D (2018) Nuclear envelope assembly defects link mitotic errors to chromothripsis. *Nature* 561: 551–555

Love DC, Sweitzer TD & Hanover JA (1998) Reconstitution of HIV-1 rev nuclear export: independent requirements for nuclear import and export. *Proc Natl Acad Sci U S A* 95: 10608–10613

Lucá R, Averna M, Zalfa F, Vecchi M, Bianchi F, La Fata G, Del Nonno F, Nardacci R, Bianchi M, Nuciforo P, *et al* (2013) The fragile X protein binds mRNAs involved in cancer progression and modulates metastasis formation. *EMBO Mol Med* 5: 1523–1536

Lunde BM, Moore C & Varani G (2007) RNA-binding proteins: modular design for efficient function. *Nat Rev Mol Cell Biol* 8: 479–490

Mackenzie IR, Rademakers R & Neumann M (2010) TDP-43 and FUS in amyotrophic lateral sclerosis and frontotemporal dementia. *Lancet Neurol* 9: 995–1007

Mateju D, Franzmann TM, Patel A, Kopach A, Boczek EE, Maharana S, Lee HO, Carra S, Hyman AA & Alberti S (2017) An aberrant phase transition of stress granules triggered by misfolded protein and prevented by chaperone function. *EMBO J* 36: 1669–1687

Matunis MJ, Coutavas E & Blobel G (1996) A novel ubiquitin-like modification modulates the partitioning of the Ran-GTPase-activating protein RanGAP1 between the cytosol and the nuclear pore complex. *J Cell Biol* 135: 1457–1470

Maul GG, Price JW & Lieberman MW (1971) FORMATION AND DISTRIBUTION OF NUCLEAR PORE COMPLEXES IN INTERPHASE. *J Cell Biol* 51: 405–418

Maurer-Stroh S, Dickens NJ, Hughes-Davies L, Kouzarides T, Eisenhaber F & Ponting CP (2003) The Tudor domain 'Royal Family': Tudor, plant Agenet, Chromo, PWWP and MBT domains. *Trends Biochem Sci* 28: 69–74

Mazroui R (2002) Trapping of messenger RNA by Fragile X Mental Retardation protein into cytoplasmic granules induces translation repression. *Hum Mol Genet* 11: 3007–3017

Merisko EM (1989) Annulate lamellae: an organelle in search of a function. *Tissue Cell* 21: 343–354

Mientjes EJ (2004) Fxr1 knockout mice show a striated muscle phenotype: implications for Fxr1p function in vivo. *Hum Mol Genet* 13: 1291–1302

Milles S & Lemke EA (2011) Single Molecule Study of the Intrinsically Disordered FG-Repeat Nucleoporin 153. *Biophys J* 101: 1710–1719

Mitchell JM, Mansfeld J, Capitanio J, Kutay U & Wozniak RW (2010) Pom121 links two essential subcomplexes of the nuclear pore complex core to the membrane. *J Cell Biol* 191: 505–521

Monahan Z, Ryan VH, Janke AM, Burke KA, Rhoads SN, Zerze GH, O'Meally R, Dignon GL, Conicella AE, Zheng W, *et al* (2017) Phosphorylation of the FUS low-complexity domain disrupts phase separation, aggregation, and toxicity. *EMBO J* 36: 2951–2967

Morales J, Hiesinger PR, Schroeder AJ, Kume K, Verstreken P, Jackson FR, Nelson DL & Hassan BA (2002) Drosophila Fragile X Protein, DFXR, Regulates Neuronal Morphology and Function in the Brain. *Neuron* 34: 961–972

Mossaid I & Fahrenkrog B (2015) Complex Commingling: Nucleoporins and the Spindle Assembly Checkpoint. *Cells* 4: 706–725

Muddashetty RS, Nalavadi VC, Gross C, Yao X, Xing L, Laur O, Warren ST & Bassell GJ (2011) Reversible Inhibition of PSD-95 mRNA Translation by miR-125a, FMRP Phosphorylation, and mGluR Signaling. *Mol Cell* 42: 673–688

Mullard A (2015) Fragile X disappointments upset autism ambitions. *Nat Rev Drug Discov* 14: 151–153

Myrick LK, Hashimoto H, Cheng X & Warren ST (2015) Human FMRP contains an integral tandem Agenet (Tudor) and KH motif in the amino terminal domain. *Hum Mol Genet* 24: 1733–1740

Myrick LK, Nakamoto-Kinoshita M, Lindor NM, Kirmani S, Cheng X & Warren ST (2014) Fragile X syndrome due to a missense mutation. *Eur J Hum Genet* 22: 1185–1189

Nagai M, Moriyama T, Mehmood R, Tokuhiro K, Ikawa M, Okabe M, Tanaka H & Yoneda Y (2011) Mice lacking Ran binding protein 1 are viable and show male infertility. *FEBS Lett* 585: 791–796

Nakamoto M, Nalavadi V, Epstein MP, Narayanan U, Bassell GJ & Warren ST (2007) Fragile X mental retardation protein deficiency leads to excessive mGluR5-dependent internalization of AMPA receptors. *Proc Natl Acad Sci* 104: 15537–15542

Napoli I, Mercaldo V, Boyl PP, Eleuteri B, Zalfa F, De Rubeis S, Di Marino D, Mohr E, Massimi M, Falconi M, *et al* (2008) The Fragile X Syndrome Protein Represses Activity-Dependent Translation through CYFIP1, a New 4E-BP. *Cell* 134: 1042–1054

Natalizio BJ & Wente SR (2013) Postage for the messenger: designating routes for nuclear mRNA export. *Trends Cell Biol* 23: 365–373

Neilson DE, Adams MD, Orr CMD, Schelling DK, Eiben RM, Kerr DS, Anderson J, Bassuk AG, Bye AM, Childs A-M, *et al* (2009) Infection-Triggered Familial or Recurrent Cases of Acute Necrotizing Encephalopathy Caused by Mutations in a Component of the Nuclear Pore, RANBP2. *Am J Hum Genet* 84: 44–51

Oberlé I, Rousseau F, Heitz D, Kretz C, Devys D, Hanauer A, Boué J, Bertheas MF & Mandel JL (1991) Instability of a 550-Base Pair DNA Segment and Abnormal Methylation in Fragile X Syndrome. *Sci New Ser* 252: 1097–1102

Oldenburg AR, Delbarre E, Thiede B, Vigouroux C & Collas P (2014) Deregulation of Fragile X-related protein 1 by the lipodystrophic lamin A p.R482W mutation elicits a myogenic gene expression program in preadipocytes. *Hum Mol Genet* 23: 1151–1162

Onischenko E, Tang JH, Andersen KR, Knockenhauer KE, Vallotton P, Derrer CP, Kralt A, Mugler CF, Chan LY, Schwartz TU, *et al* (2017) Natively Unfolded FG Repeats Stabilize the Structure of the Nuclear Pore Complex. *Cell* 171: 904-917.e19

Onischenko EA, Gubanova NV, Kieselbach T, Kiseleva EV & Hallberg E (2004) Annulate lamellae play only a minor role in the storage of excess nucleoporins in Drosophila embryos. *Traffic Cph Den* 5: 152–164

Ori A, Banterle N, Iskar M, Andrés-Pons A, Escher C, Khanh Bui H, Sparks L, Solis-Mezarino V, Rinner O, Bork P, *et al* (2013) Cell type-specific nuclear pores: a case in point for context-dependent stoichiometry of molecular machines. *Mol Syst Biol* 9: 648

Otsuka S, Bui KH, Schorb M, Hossain MJ, Politi AZ, Koch B, Eltsov M, Beck M & Ellenberg J (2016) Nuclear pore assembly proceeds by an inside-out extrusion of the nuclear envelope. *eLife* 5: e19071

Otsuka S & Ellenberg J (2018) Mechanisms of nuclear pore complex assembly – two different ways of building one molecular machine. *FEBS Lett* 592: 475–488

Otsuka S, Steyer AM, Schorb M, Hériché J-K, Hossain MJ, Sethi S, Kueblbeck M, Schwab Y, Beck M & Ellenberg J (2018) Postmitotic nuclear pore assembly proceeds by radial dilation of small membrane openings. *Nat Struct Mol Biol* 25: 21–28

Owen I & Shewmaker F (2019) The Role of Post-Translational Modifications in the Phase Transitions of Intrinsically Disordered Proteins. *Int J Mol Sci* 20: 5501

Palancade B & Doye V (2008) Sumoylating and desumoylating enzymes at nuclear pores: underpinning their unexpected duties? *Trends Cell Biol* 18: 174–183

Paonessa F, Evans LD, Solanki R, Larrieu D, Wray S, Hardy J, Jackson SP & Livesey FJ (2019) Microtubules Deform the Nuclear Membrane and Disrupt Nucleocytoplasmic Transport in Tau-Mediated Frontotemporal Dementia. *Cell Rep* 26: 582-593.e5

Patel SS, Belmont BJ, Sante JM & Rexach MF (2007) Natively Unfolded Nucleoporins Gate Protein Diffusion across the Nuclear Pore Complex. *Cell* 129: 83–96

Patzlaff NE, Shen M & Zhao X (2018) Regulation of Adult Neurogenesis by the Fragile X Family of RNA Binding Proteins. *Brain Plast* 3: 205–223

Pichler A, Gast A, Seeler JS, Dejean A & Melchior F (2002) The Nucleoporin RanBP2 Has SUMO1 E3 Ligase Activity. *Cell* 108: 109–120

Pieretti M, Warren T, Thomas C & Nelson' DL (1991) Absence of Expression of the HIM-7 Gene in Fragile X Syndrome. *Cell* 66: 817–822

Polychronidou M & Großhans J (2011) Determining nuclear shape: The role of farnesylated nuclear membrane proteins. *Nucleus* 2: 17–23

Qian J, Hassanein M, Hoeksema MD, Harris BK, Zou Y, Chen H, Lu P, Eisenberg R, Wang J, Espinosa A, *et al* (2015) The RNA binding protein FXR1 is a new driver in the 3q26-29 amplicon and predicts poor prognosis in human cancers. *Proc Natl Acad Sci* 112: 3469–3474

Rabut G, Doye V & Ellenberg J (2004) Mapping the dynamic organization of the nuclear pore complex inside single living cells. *Nat Cell Biol* 6: 1114–1121

Raghunayakula S, Subramonian D, Dasso M, Kumar R & Zhang X-D (2015) Molecular Characterization and Functional Analysis of Annulate Lamellae Pore Complexes in Nuclear Transport in Mammalian Cells. *PLOS ONE* 10: e0144508

Ramos A (2003) G-quartet-dependent recognition between the FMRP RGG box and RNA. *RNA* 9: 1198–1207

Rampello AJ, Laudermilch E, Vishnoi N, Prophet SM, Shao L, Zhao C, Lusk CP & Schlieker C (2020) Torsin ATPase deficiency leads to defects in nuclear pore biogenesis and sequestration of MLF2. *J Cell Biol* 219: e201910185

Ribbeck K & Görlich D (2001) Kinetic analysis of translocation through nuclear pore complexes. *EMBO J* 20: 1320–1330

Ribbeck K & Görlich D (2002) The permeability barrier of nuclear pore complexes appears to operate via hydrophobic exclusion. *EMBO J* 21: 2664–2671

Ritterhoff T, Das H, Hofhaus G, Schröder RR, Flotho A & Melchior F (2016) The RanBP2/RanGAP1*SUMO1/Ubc9 SUMO E3 ligase is a disassembly machine for Crm1-dependent nuclear export complexes. *Nat Commun* 7: 11482

Roscioli E, Di Francesco L, Bolognesi, A, Giubettini M, Orlando S, Harel A, Schininà ME & Lavia P (2012) Importin-β negatively regulates multiple aspects of mitosis including RanGAP1. *JCB* 196: 435–450

Rotem A, Gruber R, Shorer H, Shaulov L, Klein E & Harel A (2009) Importin $^{N}_{L}$ Regulates the Seeding of Chromatin with Initiation Sites for Nuclear Pore Assembly. *Mol Biol Cell* 20: 12

Rouvière JO, Bulfoni M, Tuck A, Cosson B, Devaux F & Palancade B (2018) A SUMO-dependent feedback loop senses and controls the biogenesis of nuclear pore subunits. *Nat Commun* 9: 1665

Sachdev R, Sieverding C, Flötenmeyer M & Antonin W (2012) The C-terminal domain of Nup93 is essential for assembly of the structural backbone of nuclear pore complexes. *Mol Biol Cell* 23: 740–749

Saitoh H, Pu R, Cavenagh M & Dasso M (1997) RanBP2 associates with Ubc9p and a modified form of RanGAP1. *Proc Natl Acad Sci* 94: 3736–3741

Sakuma S & D'Angelo MA (2017) The roles of the nuclear pore complex in cellular dysfunction, aging and disease. *Semin Cell Dev Biol* 68: 72–84

Salina D, Bodoor K, Eckley DM, Schroer TA, Rattner JB & Burke B (2002) Cytoplasmic Dynein as a Facilitator of Nuclear Envelope Breakdown. *Cell* 108: 97–107

Salina D, Enarson P, Rattner JB & Burke B (2003) Nup358 integrates nuclear envelope breakdown with kinetochore assembly. *J Cell Biol* 162: 991–1001

Santoro MR, Bray SM & Warren ST (2012) Molecular mechanisms of fragile X syndrome: a twenty-year perspective. *Annu Rev Pathol* 7: 219–245

Schmidt HB & Görlich D (2015) Nup98 FG domains from diverse species spontaneously phase-separate into particles with nuclear pore-like permselectivity. *eLife* 4: e04251

Schmidt HB & Görlich D (2016) Transport Selectivity of Nuclear Pores, Phase Separation, and Membraneless Organelles. *Trends Biochem Sci* 41: 46–61

Sellier C, Buijsen RAM, He F, Natla S, Jung L, Tropel P, Gaucherot A, Jacobs H, Meziane H, Vincent A, *et al* (2017) Translation of Expanded CGG Repeats into FMRpolyG Is Pathogenic and May Contribute to Fragile X Tremor Ataxia Syndrome. *Neuron* 93: 331–347

Sheffield LG, Miskiewicz HB, Tannenbaum LB & Mirra SS (2006) Nuclear Pore Complex Proteins in Alzheimer Disease: *J Neuropathol Exp Neurol* 65: 45–54

Shen TH, Lin H-K, Scaglioni PP, Yung TM & Pandolfi PP (2006) The Mechanisms of PML-Nuclear Body Formation. *Mol Cell* 24: 331–339

Shin Y & Brangwynne CP (2017) Liquid phase condensation in cell physiology and disease. *Science* 357

Shorter J (2019) Phase separation of RNA-binding proteins in physiology and disease: An introduction to the JBC Reviews thematic series. *J Biol Chem* 294: 7113–7114

Singh BB, Patel HH, Roepman R, Schick D & Ferreira PA (1999) The Zinc Finger Cluster Domain of RanBP2 Is a Specific Docking Site for the Nuclear Export Factor, Exportin-1. *J Biol Chem* 274: 37370–37378

Siomi MC, Siomi H, Sauer WH, Srinivasan S, Nussbaum RL & Dreyfuss G (1995) FXR1, an autosomal homolog of the fragile X mental retardation gene. *EMBO J* 14: 2401–2408

Siomi MC, Zhang Y, Siomi H & Dreyfuss G (1996) Specific sequences in the fragile X syndrome protein FMR1 and the FXR proteins mediate their binding to 60S ribosomal subunits and the interactions among them. *Mol Cell Biol* 16: 3825–3832

Smythe C, Jenkins HE & Hutchison CJ (2000) Incorporation of the nuclear pore basket protein Nup153 into nuclear pore structures is dependent upon lamina assembly: evidence from cell-free extracts of *Xenopus* eggs. *EMBO J* 19: 3918–3931

Snead WT & Gladfelter AS (2019) The Control Centers of Biomolecular Phase Separation: How Membrane Surfaces, PTMs, and Active Processes Regulate Condensation. *Mol Cell* 76: 295–305

Spencer CM, Serysheva E, Yuva-Paylor LA, Oostra BA, Nelson DL & Paylor R (2006) Exaggerated behavioral phenotypes in Fmr1/Fxr2 double knockout mice reveal a functional genetic interaction between Fragile X-related proteins. *Hum Mol Genet* 15: 1984–1994

Splinter D, Tanenbaum ME, Lindqvist A, Jaarsma D, Flotho A, Yu KL, Grigoriev I, Engelsma D, Haasdijk ED, Keijzer N, *et al* (2010) Bicaudal D2, dynein, and kinesin-1 associate with nuclear pore complexes and regulate centrosome and nuclear positioning during mitotic entry. *PLoS Biol* 8: e1000350

Springhower CE, Rosen MK & Chook YM (2020) Karyopherins and condensates. *Curr Opin Cell Biol* 64: 112–123

Stefani G (2004) Fragile X Mental Retardation Protein Is Associated with Translating Polyribosomes in Neuronal Cells. *J Neurosci* 24: 7272–7276

Tabet R, Moutin E, Becker JAJ, Heintz D, Fouillen L, Flatter E, Krężel W, Alunni V, Koebel P, Dembélé D, *et al* (2016) Fragile X Mental Retardation Protein (FMRP) controls diacylglycerol kinase activity in neurons. *Proc Natl Acad Sci* 113: E3619–E3628

Talamas JA & Hetzer MW (2011) POM121 and Sun1 play a role in early steps of interphase NPC assembly. *J Cell Biol* 194: 27–37

Tamanini F (1997) Differential expression of FMR1, FXR1 and FXR2 proteins in human brain and testis. *Hum Mol Genet* 6: 1315–1322

Tamanini F (2000) The fragile X-related proteins FXR1P and FXR2P contain a functional nucleolar-targeting signal equivalent to the HIV-1 regulatory proteins. *Hum Mol Genet* 9: 1487–1493

Tamanini F, Bontekoe C, Bakker CE, van Unen L, Anar B, Willemsen R, Yoshida M, Galjaard H, Oostra BA & Hoogeveen AT (1999a) Different targets for the fragile X-related proteins revealed by their distinct nuclear localizations. *Hum Mol Genet* 8: 863–869

Tamanini F, van Unen L, Bakker CE, Sacchi N, Galjaard H, Oostra B & Hoogeveen AT (1999b) Oligomerization properties of fragile X mental retardation protein FMRP and the fragile x related proteins FXR1P and FXR2P. *Biochem J* 1: 517–523

Tsang B, Arsenault J, Vernon RM, Lin H, Sonenberg N, Wang L-Y, Bah A & Forman-Kay JD (2019) Phosphoregulated FMRP phase separation models activity-dependent

translation through bidirectional control of mRNA granule formation. *Proc Natl Acad Sci* 116: 4218–4227

Tucker B, Richards R & Lardelli M (2004) Expression of three zebrafish orthologs of human FMR1-related genes and their phylogenetic relationships. *Dev Genes Evol* 214: 567–574

Ungricht R, Klann M, Horvath P & Kutay U (2015) Diffusion and retention are major determinants of protein targeting to the inner nuclear membrane. *J Cell Biol* 209: 687–703

Ungricht R & Kutay U (2017) Mechanisms and functions of nuclear envelope remodelling. *Nat Rev Mol Cell Biol* 18: 229–245

Uversky VN, Gillespie JR & Fink AL Why are 'natively unfolded' proteins unstructured under physiologic conditions? *Proteins Struct Funct Bioinforma* 41: 415–427

Van Driesche SJ, Sawicka K, Zhang C, Hung SKY, Park CY, Fak JJ, Yang C, Darnell RB & Darnell JC (2019) FMRP binding to a ranked subset of long genes is revealed by coupled CLIP and TRAP in specific neuronal cell types Neuroscience

Van Treeck B, Protter DSW, Matheny T, Khong A, Link CD & Parker R (2018) RNA self-assembly contributes to stress granule formation and defining the stress granule transcriptome. *Proc Natl Acad Sci* 115: 2734–2739

Verheij C, Bakker CE, de Graaff E, Keulemans J, Willemsen R, Verkerk AJMH, Galjaard H, Reuser AJJ, Hoogeveen AT & Oostra BA (1993) Characterization and localization of the FMR-1 gene product associated with fragile X syndrome. *Nature* 363: 722–724

Vollmer B, Lorenz M, Moreno-Andrés D, Bodenhöfer M, De Magistris P, Astrinidis SA, Schooley A, Flötenmeyer M, Leptihn S & Antonin W (2015) Nup153 Recruits the Nup107-160 Complex to the Inner Nuclear Membrane for Interphasic Nuclear Pore Complex Assembly. *Dev Cell* 33: 717–728

Vollmer B, Schooley A, Sachdev R, Eisenhardt N, Schneider AM, Sieverding C, Madlung J, Gerken U, Macek B & Antonin W (2012) Dimerization and direct membrane interaction of Nup53 contribute to nuclear pore complex assembly: Nup53 membrane binding promotes NPC assembly. *EMBO J* 31: 4072–4084

de Vrij FMS, Levenga J, van der Linde HC, Koekkoek SK, De Zeeuw CI, Nelson DL, Oostra BA & Willemsen R (2008) Rescue of behavioral phenotype and neuronal protrusion morphology in Fmr1 KO mice. *Neurobiol Dis* 31: 127–132

Wälde S, Thakar K, Hutten S, Spillner C, Nath A, Rothbauer U, Wiemann S & Kehlenbach RH (2012) The Nucleoporin Nup358/RanBP2 Promotes Nuclear Import in a Cargo- and Transport Receptor-Specific Manner: Nup358 in nuclear import. *Traffic* 13: 218–233

Walther TC, Alves A, Pickersgill H, Loïodice I, Hetzer M, Galy V, Hülsmann BB, Köcher T, Wilm M, Allen T, *et al* (2003a) The Conserved Nup107-160 Complex Is Critical for Nuclear Pore Complex Assembly. *Cell* 113: 195–206

Walther TC, Askjaer P, Gentzel M, Habermann A, Griffiths G, Wilm M, Mattaj IW & Hetzer M (2003b) RanGTP mediates nuclear pore complex assembly. *Nature* 424: 689–694

Wang A, Conicella AE, Schmidt HB, Martin EW, Rhoads SN, Reeb AN, Nourse A, Ramirez Montero D, Ryan VH, Rohatgi R, *et al* (2018) A single N-terminal phosphomimic disrupts TDP-43 polymerization, phase separation, and RNA splicing. *EMBO J* 37

Weberruss M & Antonin W (2016) Perforating the nuclear boundary – how nuclear pore complexes assemble. *J Cell Sci* 129: 4439–4447

Wente SR & Rout MP (2010) The Nuclear Pore Complex and Nuclear Transport. *Cold Spring Harb Perspect Biol* 2: a000562–a000562

Wild T, Horvath P, Wyler E, Widmann B, Badertscher L, Zemp I, Kozak K, Csucs G, Lund E & Kutay U (2010) A Protein Inventory of Human Ribosome Biogenesis Reveals an Essential Function of Exportin 5 in 60S Subunit Export. *PLoS Biol* 8: e1000522

Woerner AC, Frottin F, Hornburg D, Feng LR, Meissner F, Patra M, Tatzelt J, Mann M, Winklhofer KF, Hartl FU, *et al* (2016) Cytoplasmic protein aggregates interfere with nucleocytoplasmic transport of protein and RNA. *Science* 351: 173–176

Wu J, Matunis MJ, Kraemer D, Blobel G & Coutavas E (1995) Nup358, a cytoplasmically exposed nucleoporin with peptide repeats, Ran-GTP binding sites, zinc fingers, a cyclophilin A homologous domain, and a leucine-rich region. *J Biol Chem* 270: 14209–14213

Xie N, Gong H, Suhl JA, Chopra P, Wang T & Warren ST (2016a) Reactivation of FMR1 by CRISPR/Cas9-Mediated Deletion of the Expanded CGG-Repeat of the Fragile X Chromosome. *PloS One* 11: e0165499

Xie W, Chojnowski A, Boudier T, Lim JSY, Ahmed S, Ser Z, Stewart C & Burke B (2016b) A-type Lamins Form Distinct Filamentous Networks with Differential Nuclear Pore Complex Associations. *Curr Biol* 26: 2651–2658

Yang W, Gelles J & Musser SM (2004) Imaging of single-molecule translocation through nuclear pore complexes. *Proc Natl Acad Sci* 101: 12887–12892

Yuzwa SA, Shan X, Macauley MS, Clark T, Skorobogatko Y, Vosseller K & Vocadlo DJ (2012) Increasing O-GlcNAc slows neurodegeneration and stabilizes tau against aggregation. *Nat Chem Biol* 8: 393–399

Zalfa F, Panasiti V, Carotti S, Zingariello M, Perrone G, Sancillo L, Pacini L, Luciani F, Roberti V, D'Amico S, *et al* (2017) The fragile X mental retardation protein regulates tumor invasiveness-related pathways in melanoma cells. *Cell Death Dis* 8: e3169

Zhang J, Fang Z, Jud C, Vansteensel MJ, Kaasik K, Lee CC, Albrecht U, Tamanini F, Meijer JH, Oostra BA, *et al* (2008) Fragile X-Related Proteins Regulate Mammalian Circadian Behavioral Rhythms. *Am J Hum Genet* 83: 43–52

Zhang K, Daigle JG, Cunningham KM, Coyne AN, Ruan K, Grima JC, Bowen KE, Wadhwa H, Yang P, Rigo F, *et al* (2018) Stress Granule Assembly Disrupts Nucleocytoplasmic Transport. *Cell* 173: 958-971.e17

Zhang K, Donnelly CJ, Haeusler AR, Grima JC, Machamer JB, Steinwald P, Daley EL, Miller SJ, Cunningham KM, Vidensky S, *et al* (2015) The C9orf72 repeat expansion disrupts nucleocytoplasmic transport. *Nature* 525: 56–61

Zuccolo M, Alves A, Galy V, Bolhy S, Formstecher E, Racine V, Sibarita J-B, Fukagawa T, Shiekhattar R, Yen T, *et al* (2007) The human Nup107–160 nuclear pore subcomplex contributes to proper kinetochore functions. *EMBO J* 26: 1853–1864

Université de Strasbourg

Arantxa AGOTE ARÁN

igbmc institut de génétique et de biologie moléculaire et cellulaire

Spatial control of nucleoporin condensation by Fragile X-related proteins

Résumé

Les nucléoporines (Nups) construisent des complexes de pores nucléaires (NPC) hautement organisés au niveau de l'enveloppe nucléaire (NE). Dans le cytoplasme, les Nups solubles existent, mais on ignore pour l'instant comment leur assemblage se limite à la NE. Nous montrons ici que la protéine 1 liée au X fragile (FXR1) peut interagir avec plusieurs Nups et faciliter leur localisation vers NE pendant l'interphase par un mécanisme dépendant des microtubules. La régulation négative de la FXR1 ou des paralogues FXR2 et la protéine de retard mental du X fragile (FMRP) conduit à l'accumulation de condensats de Nups cytoplasmiques. De même, les modèles du syndrome du X fragile (SXF), caractérisés par une perte de FMRP, accumulent des granules de Nups. Les cellules contenant des granules de Nups présentent des défauts dans l'exportation des protéines, la morphologie nucléaire et la progression du cycle cellulaire. Ces résultats révèlent un rôle inattendu pour la famille des protéines FXR dans la régulation spatiale de la condensation des Nups.

Mots clé: FXR1 ; dynéine, syndrome de l'X fragile ; nucléoporines ; séparation de phases

Summary

Nucleoporins (Nups) build highly organized Nuclear Pore Complexes (NPCs) at the nuclear envelope (NE). Several Nups assemble into a sieve-like hydrogel within the central channel of the NPCs. In the cytoplasm, the soluble Nups exist, but how their assembly is restricted to the NE is currently unknown. Here we show that Fragile X-related protein 1 (FXR1) can interact with several Nups and facilitate their localization to the NE during interphase through a microtubule-dependent mechanism. Downregulation of FXR1 or closely related paralogs FXR2 and Fragile X mental retardation protein (FMRP) leads to the accumulation of cytoplasmic Nup condensates. Likewise, models of Fragile X syndrome (FXS), characterized by a loss of FMRP, accumulate Nup granules. The Nup granules-containing cells show defects in protein export, nuclear morphology and cell cycle progression. These results reveal an unexpected role for the FXR protein family in the spatial regulation of Nup condensation.

Key words: FXR1; dynein; fragile X syndrome; nucleoporins; phase separation